NUREG/CR-1561
SAND80-1495
R3

THE BEHAVIOR OF HYDROGEN DURING ACCIDENTS IN LIGHT WATER REACTORS

Martin P. Sherman
Marshall Berman
John C. Cummings
George W. Perkins
Dana A. Powers

Peter P. Bieniarz
Owen R. Green

Energy Incorporated
Albuquerque, New Mexico

Date Published: August 1980

Sandia National Laboratories
Albuquerque, New Mexico 87185
operated by
Sandia Corporation
for the
U. S. Department of Energy

Prepared for
Division of Reactor Safety Research
Office of Nuclear Regulatory Research
U. S. Nuclear Regulatory Commission
Washington, D. C. 20555
Under Memorandum of Understanding DOE 40-550-75
NRC FIN No. A1051

ABSTRACT

A compendium of information concerning the possible behavior of hydrogen during hypothetical accidents in light water reactors has been compiled. The report addresses the questions of hydrogen generation, solubility, detection, combustion and recombiners. The report is intended for use for reactor operator training and as a reference during emergencies as well as for individuals interested in the general state of knowledge concerning the behavior of hydrogen in LWR accidents. The hydrogen sources considered include the metal-steam reaction, radiolysis, corrosion of paints and galvanized material and the interaction of core materials with concrete. Conditions which may lead to hydrogen combustion and containment damage are also discussed.

Table of Contents

ACKNOWLEDGEMENTS

The authors would like to thank the many individuals at Sandia National Laboratories who contributed their time and effort to review and criticize this document. Their expertise and support were freely given, and we acknowledge the importance of their contributions. We would also like to thank the library personnel who provided valuable assistance during the literature search, and Martha Tenorio, without whose support, the report could not have been completed.

SUMMARY

The accident at Three Mile Island (TMI) and the occurrence of a combustion highlighted not only the real possibility that hydrogen might pose a threat to public safety, but also the importance of readily available knowledge concerning the nature of such a threat. This manual attempts to present, in a simple and understandable way, information concerning the generation, transport, detection and combustion of hydrogen which might occur during serious accidents in light water reactors. More than a thousand documents were surveyed by several individuals over a three month period. Of these, several hundred documents were extensively reviewed. This manual summarizes this review as well as presents some additional ideas and calculations pertinent to hydrogen behavior. Because of the limited time and effort involved, the manual is necessarily limited. Our goal was to produce a comprehensive document as soon as possible which would be of significant utility to reactor operators and to the Nuclear Regulatory Commission. Subsequent editions of this manual are expected to be more detailed and comprehensive.

The manual is divided into four major sections covering hydrogen generation, detection, combustion, and existing schemes for mitigating the effects of combustion. Sources of hydrogen which are discussed include the zircaloy-steam and steel-steam reactions, radiolytic decomposition of water, corrosion of zinc-based paints and coatings and the interaction of molten core materials with concrete. The section on hydrogen detection briefly discusses requirements and existing instrumentation. Topics addressed in the combustion section

include deflagrations, detonations, limits of flammability and detonability, flame stability and ignition sources. A description of existing recombiners is provided in the last section.

In the event of significant core uncovery, the primary source of hydrogen during the early phases of a serious accident would be oxidation of the zircaloy cladding by steam. Radiolytic generation of hydrogen, although orders of magnitude slower than this metal-steam reaction, could, nevertheless, produce large quantities of hydrogen over an extended period of time. In a reactor like TMI, complete reaction of the zirconium inventory would produce about 1000 kg of hydrogen. A comparable BWR could produce nearly 2000 kg of hydrogen. The burning of all this hydrogen would produce pressures well in excess of the design pressures of the strongest existing containments (see discussion in introduction).

The oxidation of zirconium is a complex process involving the decomposition of the water molecule, the diffusion of steam and oxygen into the metal, the solution and dissolution of oxygen in the various phases of the metal, the physical state and possible mechanical motion (downflow) of the metal and its eutectics if melting occurs. Although uncertainties exist about the rates of each of these chemical and physical reactions, the process is fairly well understood from the reactor safety point of view with the exception of mechanical motion, i.e., the melting, downflow and refreezing which might occur. This clad melting and migration behavior is not adequately understood at present and probably depends strongly on accident scenario. At temperatures approaching the melting point of steel, the production of iron oxides and

2 -

and chromium oxides by steel-steam reaction can be a significant source of hydrogen. The production of hydrogen from steel oxidation is probably small for most accident scenarios, but the possibility cannot be ruled out.

Although radiolysis produces hydrogen much more slowly than the metal-water reaction, its contribution can be important for long term accidents. It seems unlikely that a sufficient mixture of hydrogen and oxygen could be evolved by radiolysis to cause a detonation within the primary system but further study is needed. Threats to containment might be met with existing low flow rate hydrogen recombiners or with chemical additives, such as sodium metavanadate, which suppress or reduce the net yield of gases from radiolysis.

Another possible source of hydrogen could be the zinc-based paints and galvanized coatings in containment which have been subjected to environments containing high temperature steam, corrosive sprays, fission products, and radioactivity. Crude calculations indicate maximum hydrogen yields from this source of approximately 150 kg. Experiments to address the rates and magnitude of this possible source are presently being contemplated by the NRC.

If an accident results in core melt and vessel penetration, substantial quantities of hydrogen and other combustible gases could be generated by core-concrete interactions. Experiments have shown that molten steel in the "corium" melt chemically reduces the vast quantities of water and carbon dioxide liberated from the concrete to hydrogen, carbon monoxide, and sometimes methane. It is possible that this interaction of core materials

with concrete could produce a quantity of combustible gases of the same order of magnitude as the metal-water reaction. Further experimentation and code development should provide quantitative estimates of the magnitude of this source in the near future.

The transport of hydrogen is important in both the primary system and in containment. In the primary system, the hydrogen could accumulate at high points and interfere with or completely block natural circulation. The pressure dependence of the solubility of hydrogen was an important factor in the strategy to reduce the hydrogen bubble size at TMI. Although the solubility of hydrogen in pure water is well known, its solubility in water containing boric acid and other impurities has not been measured. Literature on the rates of solution and dissolution of hydrogen in water appears to be absent. Transport in containment is a problem involving both gas diffusion and convection. Whether the hydrogen is homogeneously distributed throughout containment or can be trapped in local regions for short periods of time could determine the probability of a detonation.

The detection of hydrogen in the primary system and in containment is extremely important. Since reactor operators will be making decisions affecting accident mitigation, knowledge of gas concentrations and distributions would be imperative. If hydrogen control features are eventually employed, the reliability and survivability of such detectors would need to be high. Further instrumentation development may be required to improve the existing state of hydrogen detection.

Given the presence of hydrogen and oxygen within containment,

the possibility of a deflagration exists if the volumetric concentration of hydrogen is above 4% and an ignition source exists. A detonation (supersonic burn speed in unburned gas) is possible if the concentration of hydrogen in air exceeds 18%. These flammability and detonability limits also depend on the concentrations of other substances including nitrogen, steam, liquid water, etc., as well as the initial conditions of pressure and temperature.

Estimates of the final pressures resulting from the slow and complete burning (deflagration) of hydrogen can be made, employing only simple thermodynamic approximations. Rapid deflagrations can produce dynamic pressures which exceed the quasi-static calculations, but are less severe than detonations. The transition from deflagration to detonation is not well understood. Even when concentrations are within detonability limits, detonations might not occur unless strong ignition sources are present or the geometry is favorable. Calculations of "pseudo-detonations" (rapid burning of non-detonable mixtures) have been performed which predicted dynamic loads several times larger than quasi-static pressures lasting for tens of milliseconds. The pressure histories generated by simple analysis (static) or computer codes (dynamic) can be used to estimate structural loads and the possibility of component damage or containment failure.

In the course of this literature search, it became obvious to us that hydrogen could pose a threat to the containment. Several methods could be employed to control or eliminate this danger. The primary existing control method has been the hydrogen

recombiner, marketed in several different forms by different manufacturers. These recombiners are generally made to operate at hydrogen concentrations of less than 4% with flow rates limited to approximately 100 cubic feet per minute. That is, the recombiners operate in non-flammable mixtures at very low rates. They are primarily intended to handle the radiolytic generation of hydrogen. For accidents in which the core has been uncovered and metal-water reactions are occurring, the recombiners would be inadequate. Most chemical gettering schemes also appear to be flow rate limited.

Several hydrogen control schemes have been proposed for possible future incorporation into reactors. These include deliberate ignition at low hydrogen concentrations, water droplet fogging, Halon injection, etc. Research in these areas is presently being considered.

INTRODUCTION

The accident at Three Mile Island produced about 400 to 500 kg of hydrogen, well in excess of previous release guidelines. Approximately 270 kg of this was burned in the containment resulting in a 28 psi pressure rise at about 10 hours into the accident. Although the TMI containment apparently survived the burn without incurring severe damage, the events emphasized the real possibility of generating large quantities of hydrogen during LWR accidents. During the TMI accident, many questions arose concerning the rates and quantities of hydrogen which could be generated, the transport and solubility of hydrogen, the possibility of deflagrations or detonations within the vessel or in containment, and the structural damage which might occur as a result of combustion. Although much of this information was available, it was widely scattered in various references and among researchers at several laboratories. It was very difficult to gather the information and to reach a consensus for making decisions in the "real time" accident environment.

The primary purpose of this document is to provide information and data which may be of value to operators and NRC staff during hydrogen emergencies. The volume also provides an introduction to the various subjects involved with hydrogen behavior and indicates the state of present understanding in these areas. Over a thousand documents were surveyed and several hundred of these were extensively reviewed. This report presents the major results of that literature search, supplemented by additional analysis and calculations where appropriate.

To illustrate the potential hydrogen threat, consider Figures 1-3. Figure 1 illustrates the approximate net free containment volumes and associated design pressures for typical BWR and PWR plants. Figure 2 shows the volumetric concentration of hydrogen in containment which would result from a given percent of zircaloy-steam reaction within the core. Note that even for the largest PWR dry containments, 100% metal-water reaction would result in concentrations above the downward propagation limit of 9% hydrogen in air. In terms of reactor safety, this concentration limit is probably more important than the accepted lower flammability limit for upward propagation of 4.1%, because nearly complete combustion and significant overpressures usually don't occur unless concentrations are 9% or greater. Figure 3 shows the temperatures and pressures which would result from the complete, isochoric (constant volume), adiabatic deflagration* of various concentrations of hydrogen. (Actual pressures and temperatures do not approach these theoretical values until concentrations are 9% or greater.) Comparing all three figures, we see that 100% metal-water reaction can result in combustion pressures which exceed the design pressures for all existing containments.

The amount of hydrogen generated is of major importance in assessing the potential threat. The first section, therefore, addresses the generation of hydrogen from the various possible

*The word "explosion" is so commonly used that it is no longer meaningful in a technical sense. We have therefore defined combustion to include both deflagrations and detonations. Deflagrations are burned fronts which move subsonically, while detonation fronts are supersonic in the unburned gas.

FIGURE 1

COMPARISON OF CONTAINMENT
VOLUMES AND DESIGN PRESSURES
(TYPICAL 1200 MWE PLANTS)

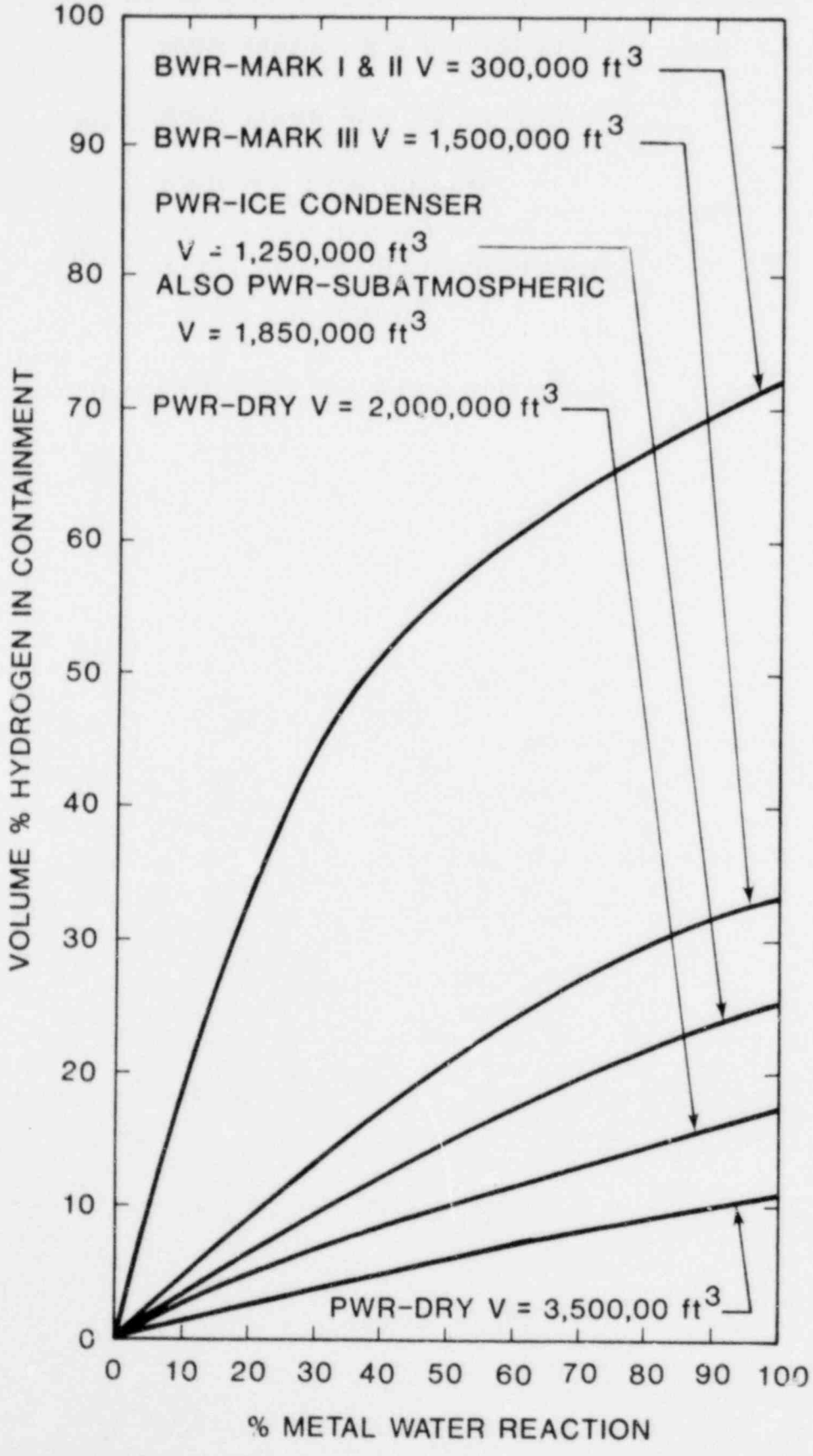

FIGURE 2
VOLUME % HYDROGEN IN CONTAINMENT
VS % METAL-WATER REACTION

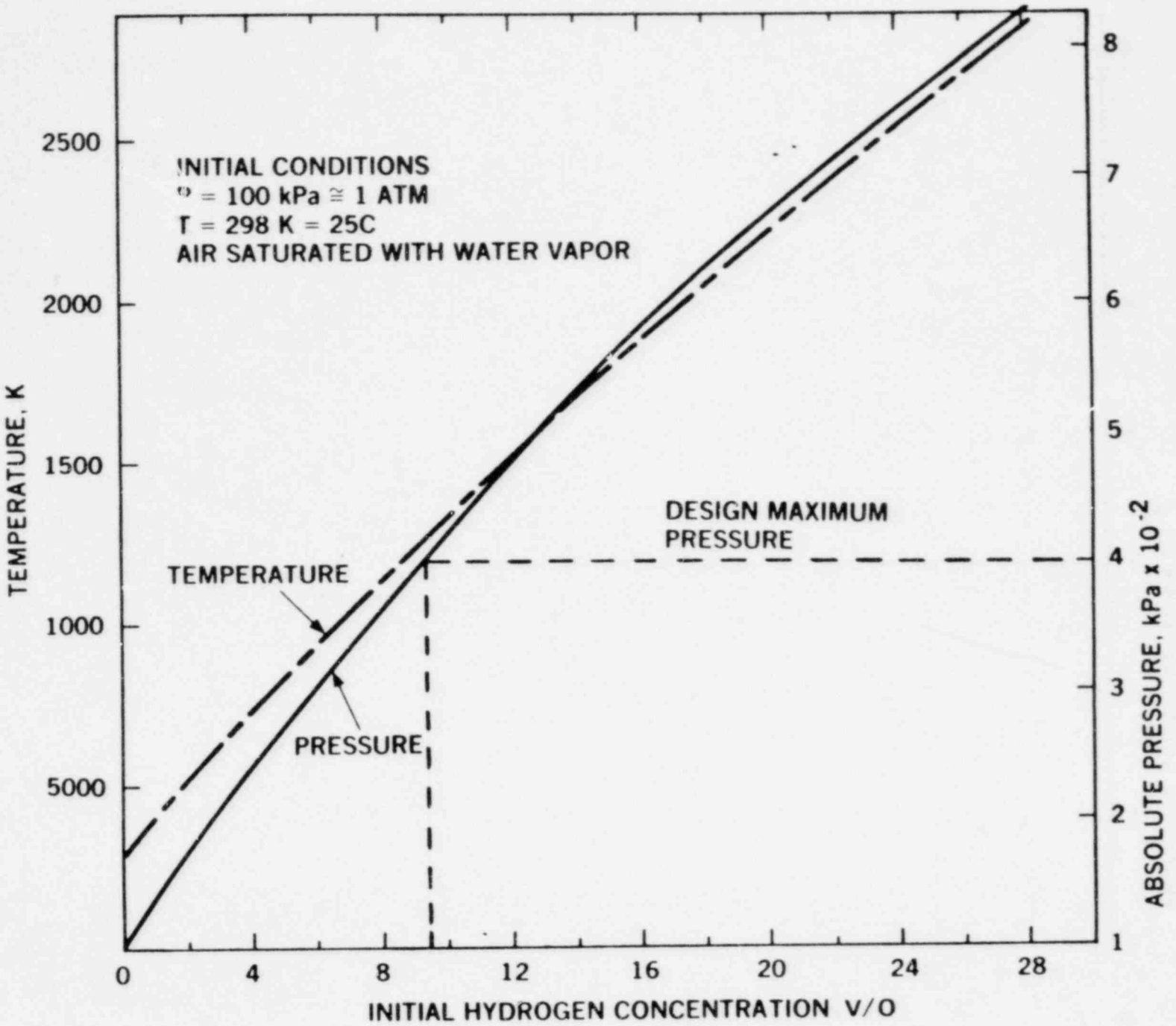

FIG. 3. PRESSURE AND TEMPERATURE AFTER HYDROGEN-AIR COMBUSTION, CONSTANT VOLUME AND ADIABATIC

sources including the zirconium-steam and steel-steam reactions, radiolysis, corrosion of zinc-based paints and coatings, and the interaction of core materials with concrete in the event of vessel melt-through. Although the transport of hydrogen throughout the primary system and containment can affect the accident evolution, transport is not specifically treated here. The solubility of hydrogen in pure water, however, is discussed extensively.

The measurement of hydrogen in the primary system and containment is important, since the knowledge of the concentrations can assist the operator in taking control measures. Existing detectors are briefly discussed in section II.

The combustion of hydrogen will determine the nature and extent of the threat to containment. The subject is introduced in section III. Deflagration, detonation, ignition, flammability and detonability limits, and the effects of diluents are addressed.

The types and characteristics of hydrogen recombiners are discussed in detail in the last section.

Because of time and manpower constraints, the scope of this document is limited. Later editions are anticipated which will expand and update the present discussions and introduce new material. Since this manual may contain errors, we welcome review and constructive criticism by readers. If any serious errors are found, please notify the authors as soon as possible.

I. HYDROGEN GENERATION AND SOLUBILITY

Hydrogen is generated during normal plant operation as well as during and following an accident. During normal operation, hydrogen is generated by radiolytic decomposition of the reactor coolant. The handling of this hydrogen source varies, depending upon the type of reactor. In a PWR, hydrogen is purposely dissolved into the primary system in order to effectively stop the net yield of radiolytic gases. In a BWR, it is removed from the main condenser as a noncondensible by the air ejectors and moved to the off-gas system where it is recombined.

If a loss-of-coolant accident (LOCA) occurs involving core uncovery and heat-up, a large quantity of hydrogen can be generated by the reaction of the hot zirconium cladding with the surrounding steam. In addition, radiolytic decomposition of the reactor coolant and steam will continue to produce hydrogen. This radiolytic decomposition can take place as a result of radiation from fission products released to the coolant and from fission products remaining in the fuel. Another product of radiolysis is oxygen and it will be generated in a stoichiometric ratio to radiolytically-produced hydrogen. The rate of production of hydrogen from radiolysis is much smaller than that from the zirconium-steam reaction; nevertheless it can become the controlling source of hydrogen if the zirconium-steam reaction lasts only for a short period of time. Moreover, this source of hydrogen deserves attention to ascertain whether formation of potentially dangerous "pockets" of hydrogen and oxygen in the primary system are possible.

If the accident progresses until clad temperatures reach 1400-1900°C, steam temperatures will be high enough to heat the upper grid structure and other steel reactor vessel internals to the point at which the steel-steam reaction may become a major source of hydrogen. Another potential post-accident source of hydrogen is the decomposition of paint coatings and the reaction of galvanized surfaces in the containment with containment spray solutions or steam. Finally, if the core melts and penetrates the reactor vessel the decomposition of the concrete base mat will result in the generation of large amounts of hydrogen and other gases.

This section examines the different sources of hydrogen produced during and after an accident. The primary emphasis of this section is to examine the sources of hydrogen associated with a core which has not melted. Therefore, concrete decomposition in the reactor cavity and the associated gas generation will not be examined in the same manner as the rest of the sources.

The examination of the sources of hydrogen is presented in order of the expected magnitude, production rate, and potential importance of each.

- Zirconium - Steam Reaction
- Steel-Steam Reaction
- Radiolytic Decomposition of Water
- Decomposition of Paints and Galvanized Material

Finally, concrete decomposition by a molten core and the resultant gas generation will be discussed.

The solubility and transport of hydrogen can exert important influences on the evolution of an accident. In this compendium, however, only solubility will be discussed.

I.1. Zirconium-Steam Reaction

I.1.1 Physical/Chemical Nature of the Reaction

The complete reaction of zirconium with steam can be characterized by the following:

$$Zr + 2\ H_2O \rightarrow ZrO_2 + 2H_2 + 140\ kcal/mol \qquad (1)$$

Thus for every mole of zirconium reacted, one mole of zirconium dioxide and two moles of hydrogen are produced. Moreover, for each mole of zirconium reacted, two moles of steam are required. The reaction is exothermic, i.e., net energy (heat) is released.

Oxidation of zirconium by steam is a complex process consisting of several steps. The first step involves diffusion of steam through a layer of hydrogen which is present on the surface of the oxidizing clad. Initially, that layer will be very thin, because the reaction rate is very slow at normal operating temperatures. The supply of steam would therefore be essentially unimpeded. As the reaction rate increases and more hydrogen is evolved, the thickness of the hydrogen layer increases and the density of steam traveling up along a fuel channel decreases as the hydrogen gas mixes with it. Several models representing steam limiting conditions have been proposed,[1-4] all of which use, as a parameter, the diffusion coefficient or mass-transfer coefficient of steam through hydrogen. Virtually no data exist for the diffusion rate of steam through hydrogen at high temperatures and so mass-transfer rates are usually estimated. These estimates are conservative, and thus result in underpredictions of the effect of "steam limiting," i.e., overpredictions of the production rate of hydrogen.

The next step involves the dissociation of the H_2O molecule at the oxide/steam interface. This step is endothermic (i.e., requires the addition of heat) by about 58 kcal/mol. The oxygen moves through the oxide layer and into the metal by a diffusion process involving an interstitial mechanism. Growth of the oxide layer is thought[5] to occur by an anion diffusion mechanism (bulk, interstitial, and/or grain boundary). The chemical formation of the oxide, ZrO_2, is an exothermic reaction with a heat release of roughly 255 kcal/mol. In order to understand the metal/oxide transformation, reference is made to Fig. 1 which shows a phase diagram for the zirconium-oxygen system. It should be recognized that Zircaloy 2 and 4 contain small quantities of other metals such as tin; however, their effect on the Zr-O phase diagram is small.[6] For the purpose of this discussion it is assumed that the Zr-O phase diagram is applicable to either Zircaloy 2 or 4.

The phase diagram shows that at temperatures below approximately 870°C and for oxygen concentrations between 0 and about 30 atomic %, the metal will exist in only one phase (α). Each phase represented on Fig. 1 has a characteristic crystallographic description. If a sample of zirconium is raised to temperatures above 870°C (the $\alpha \rightarrow \beta$ transus temperature), several metal and oxide phases are possible depending on the oxygen concentration. As shown in Fig. 1, β-phase zirconium exists at low oxygen concentrations, followed by a mixture of α and β, then α-phase zirconium, then a mixture of α-phase metal and the oxide (ZrO_2), and finally only the oxide exists at high oxygen concentrations. The crystalline structure of the oxide changes from monoclinic to tetragonal to cubic

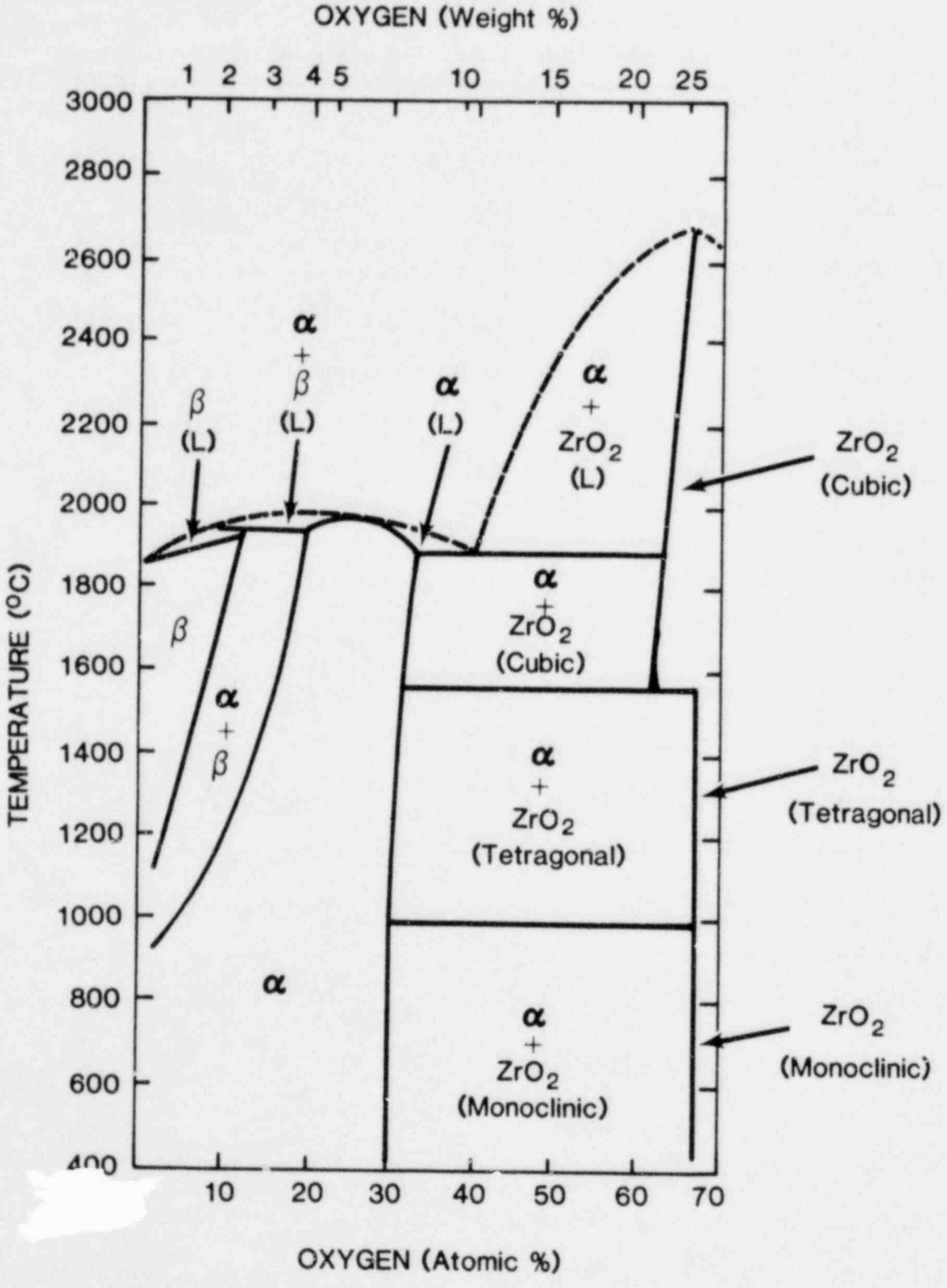

FIG. 1. ZIRCONIUM - OXYGEN PHASE DIAGRAM

as the temperature increases. Both the monoclinic and the tetragonal oxide, when initially formed, are slightly substoichiometric; i.e, their chemical representation is more like $ZrO_{2-\delta}$ where δ is the extent of substoichiometry. It should be pointed out that the actual thickness of the material associated with the $\alpha + \beta$ phase and the $\alpha + ZrO_2$ phase is extremely small and therefore these mixed phases are not represented on the figures which will be discussed next.

The normal operating temperature of the cladding is much below the 870°C point at which α zirconium changes crystalline structure. Therefore, a typical cladding cross section of an operating fuel rod will look as represented in Fig. 2A. The cladding is composed entirely of α zirconium except for a very thin film of oxide on the surface. Typical thicknesses of oxide film, at the time of fuel unloading, range from about 15-20 μm for PWR fuel to about 10 μm for BWR fuel, although localized thicknesses of up to 100 μm for BWR fuel are possible. If measurements of oxygen concentration throughout the cladding were taken and represented graphically, results would look as illustrated in Fig. 2A. The steep gradient of oxygen concentration is due to the very slow diffusion of oxygen at normal operating temperatures.

Following core uncovery, heat-up of the fuel cladding will begin and the temperature will rapidly approach 870°C. Since this temperature is considerably higher than the normal operating temperature a cross section of the cladding would show a slightly thicker oxide film and oxygen concentration measurements would reveal a changed oxygen concentration profile as shown in Figs. 2B

and 2B'. The change in the oxygen concentration gradient is due to the faster oxygen diffusion at this higher temperature.

After the temperature exceeds 870°C (and for the purpose of illustration reaches 1200°C), the cladding and the oxygen concentration profile can be illustrated by Figs. 2C and 2C'. Note that the oxide layer must expand in order to compensate for the difference in specific volume between the oxide and the zirconium. The sharp gradients in oxygen concentration between oxide and α and between α and β are due to the extreme thinness of the $\alpha + ZrO_2$ mixture and the $\alpha + \beta$ mixture, respectively.

If the heat-up rate is very slow or the temperature is kept constant, the diffusion of oxygen into the α and β phases will result in continuous growth of the oxide layer and the α layer. Assuming that it takes a long time to reach 1400°C, the cladding cross section and oxygen concentration profile are shown in Figs. 2D and 2D'. Continued heating of the fuel cladding will result in the conversion of the remainder of the β zirconium into α by oxygen diffusion. In other words, every portion of the cladding will have oxygen concentrations in excess of $\sim$15 atomic % at 1400°C. The cladding cross section and oxygen profile at 1450°C are shown in Figs. 2E and 2E'. Oxygen diffusion into the α zirconium will continue and eventually all of the α zirconium will be converted into oxide.

The conversion of the α zirconium into oxide is also a complicated process. Simply stated it involves the dissolution of oxygen into the α zirconium and a chemical reaction of zirconium with this oxygen. In actuality, the oxide thus formed

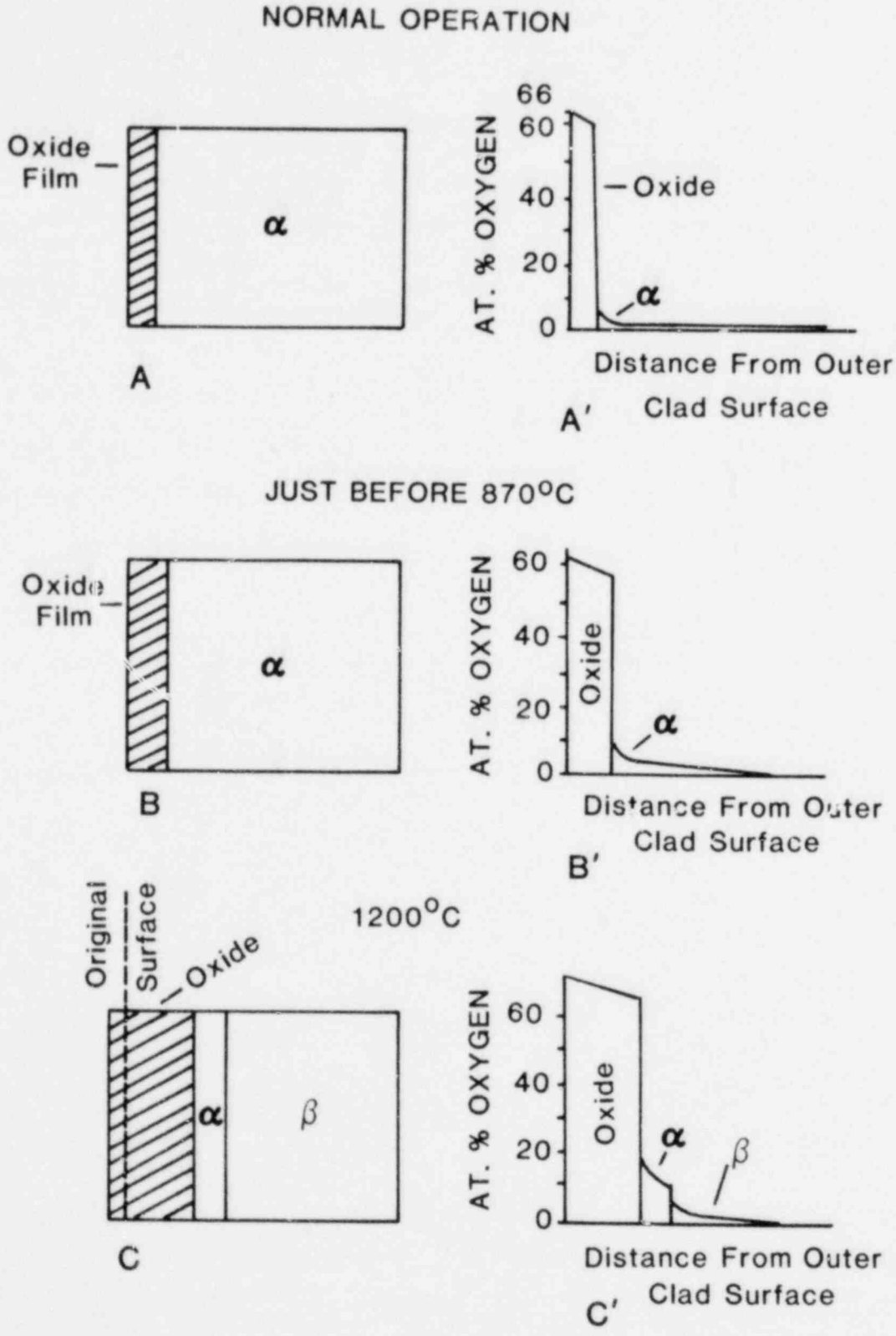

FIG. 2. CLADDING CROSS SECTIONS AND OXYGEN CONCENTRATION PROFILES FOR NORMAL AND HEAT-UP CONDITIONS

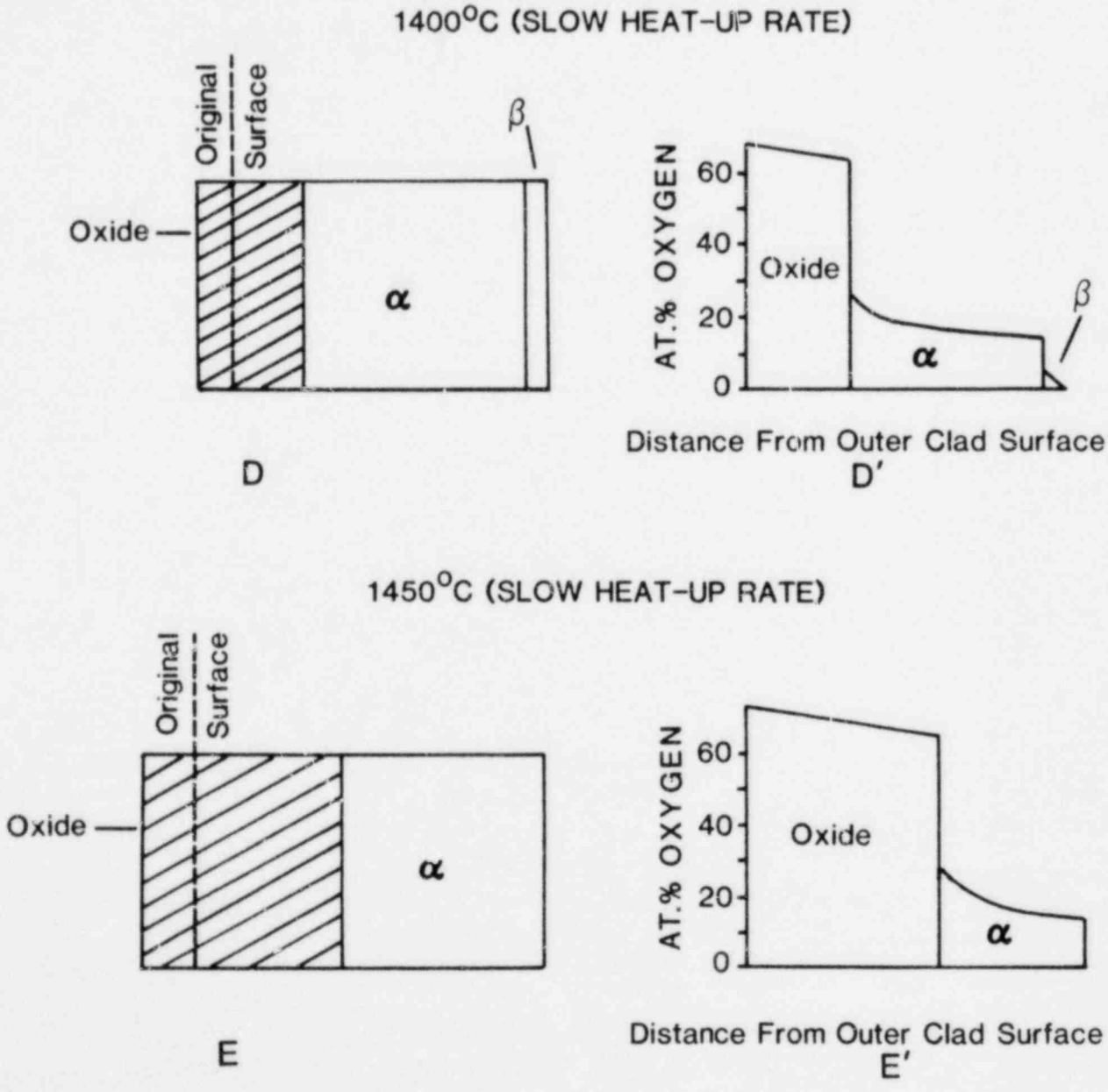

FIG. 2. (CONTINUED)

is substoichiometric. The diffusing oxygen fills the oxygen vacancies and thus converts the oxide into its stoichiometric form. From the above discussion it may be concluded that given an abundant steam supply the rate of zirconium oxidation is dominated by oxygen diffusion through the oxide layer. Therefore, the processes occurring in the metal phases do not influence the oxidation rate.

The heat-up rate of the fuel cladding plays an important role in the extent of oxidation. At high and moderate heat-up rates the temperature of the cladding can reach the melting temperature of α or β zirconium before either complete conversion of β into α or α into oxide takes place. The melting temperatures of α and β zirconium vary with oxygen concentration as is shown by the highest solid lines in Fig. 1. At low heat-up rates, complete clad oxidation would be expected before melting temperatures are achieved. Since the oxidation of zirconium is an exothermic reaction, heat would be added to the cladding in addition to the radioactive decay heat. The effect of this added heat is to increase the temperature of the cladding. Figures 3 and 4 show results of heat-up calculations performed on TMI-2* which illustrate the effect of the heat release due to oxidation. The heat-up rate curves (Fig. 3) indicate a slow rise in temperature for the first 20-40 minutes due to the reactor decay heat. As each region of the core reaches $\sim$1000°C (see Fig. 4) the heat-up rate begins to increase dramatically. This rapid temperature increase is due to heat released by the Zr/H_2O reaction.

*These calculations were performed utilizing a modified version of the code BOIL in support of the Rogovin Study Review Group formed by Sandia Laboratories.

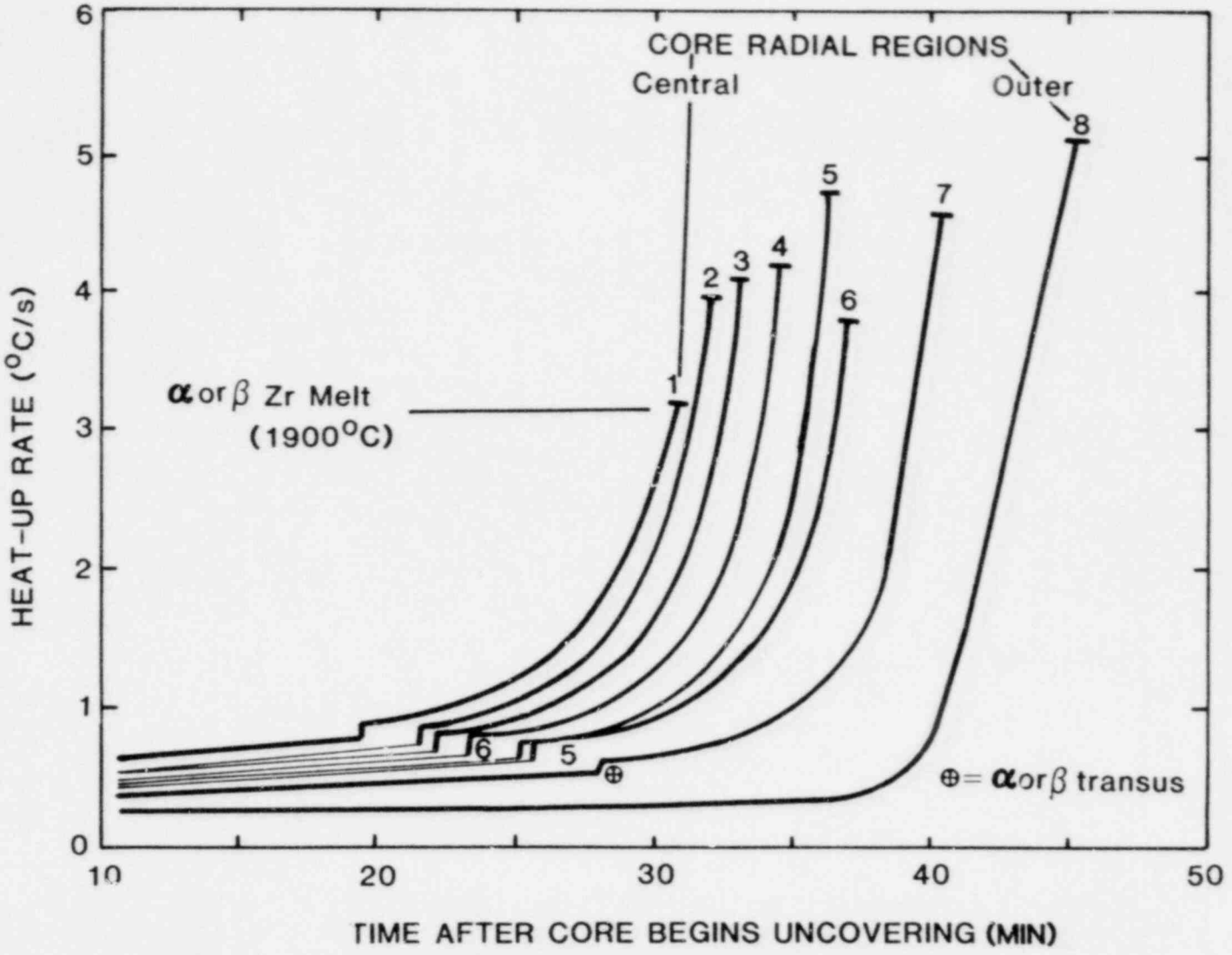

FIG. 3. TMI-2 CORE : HEAT-UP RATE AS A FUNCTION OF TIME AFTER UNCOVERING

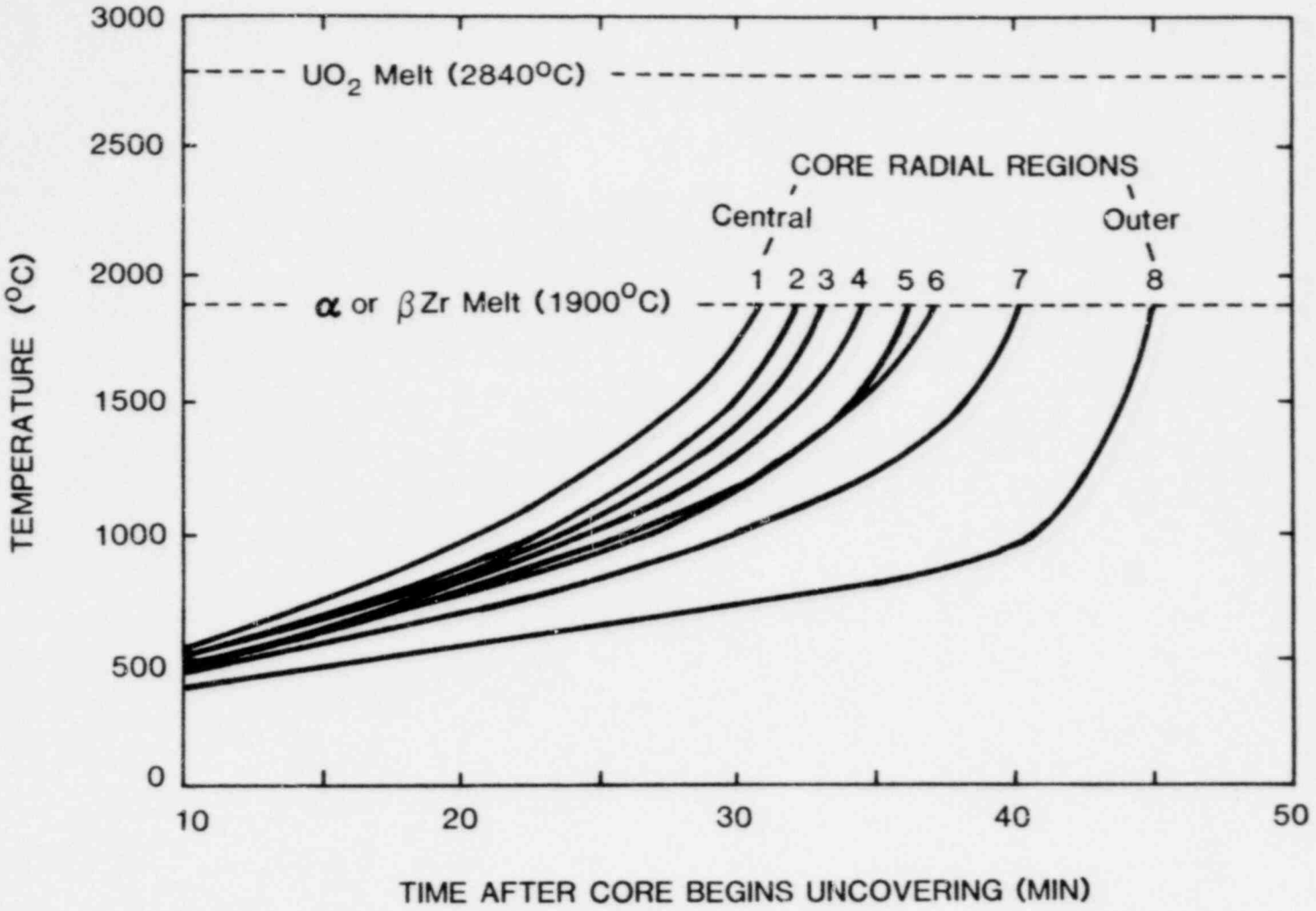

FIG. 4. TMI-2 CORE : TEMPERATURE AS A FUNCTION OF TIME AFTER UNCOVERING

It is evident that for even the lowest radial-power regions of the core, heat released by the zirconium-steam reaction dominates the heat-up rates of the fuel. Thus for a power reactor experiencing prolonged core uncovery, once the fuel reaches ∿1000°C the heat released by the oxidation reaction will dominate the heat-up, and the melting temperature of α and β zirconium will be reached quickly. It should be noted that the fuel clad temperatures are highly uncertain after the melting of α and β phases of zirconium. Consequently, calculations were not performed beyond 1900°C.

This idealized description of hydrogen generation and core heat-up from the Zr/H_2O reaction does not consider several phenomena that may be important in an actual LOCA. Microfissuring and/or spallation of the oxide layer of the cladding will tend to increase the Zr/H_2O reaction rate by eliminating all or part of the oxide layer through which the oxygen must diffuse. Limiting of the amount of steam available to react, as discussed previously, will slow down or stop the Zr/H_2O reaction (but this will eventually lead to core melt). Finally, when the cladding temperature reaches ∿1900°C the clad may begin to melt or rupture. If this occurs, the physical and chemical processes that may ensue are not clear.

I.1.2 Rate of Hydrogen Generation by the Zirconium/Steam Reaction

The amount of zirconium consumed by the reaction with steam, as a function of temperature and time, can be calculated from the following expression:

$$W_{Zr}^2 = K(T)\ t \qquad (2)$$

where:

W_{Zr} = the mass (mg) of metal reacted per unit (cm^2) of Zr surface

$K(T)$ = the experimentally determined parabolic rate constant, $(mg/cm^2)^2/sec$

T = the temperature, °K

t = the time, sec

This parabolic-growth law accurately describes the Zr/H_2O reaction over the temperature range from 1300-1800°K.[5] The parabolic rate constant is a function of temperature, obtained from consumption plots such as those shown in Fig. 5. This function is expressed in the following form:

$$K(T) = A \exp [-B/RT] \qquad (3)$$

where:

A = a constant, $(mg/cm^2)^2/sec$

B = the activation energy, cal/mole

R = the gas constant, cal/mole °K

Knowing the value of K as a function of temperature, the weight of the reacted metal at any time can be computed from Eq. 2. By noting from Eq. 1 that for every mole of zirconium there are two moles of hydrogen produced, the amount of hydrogen

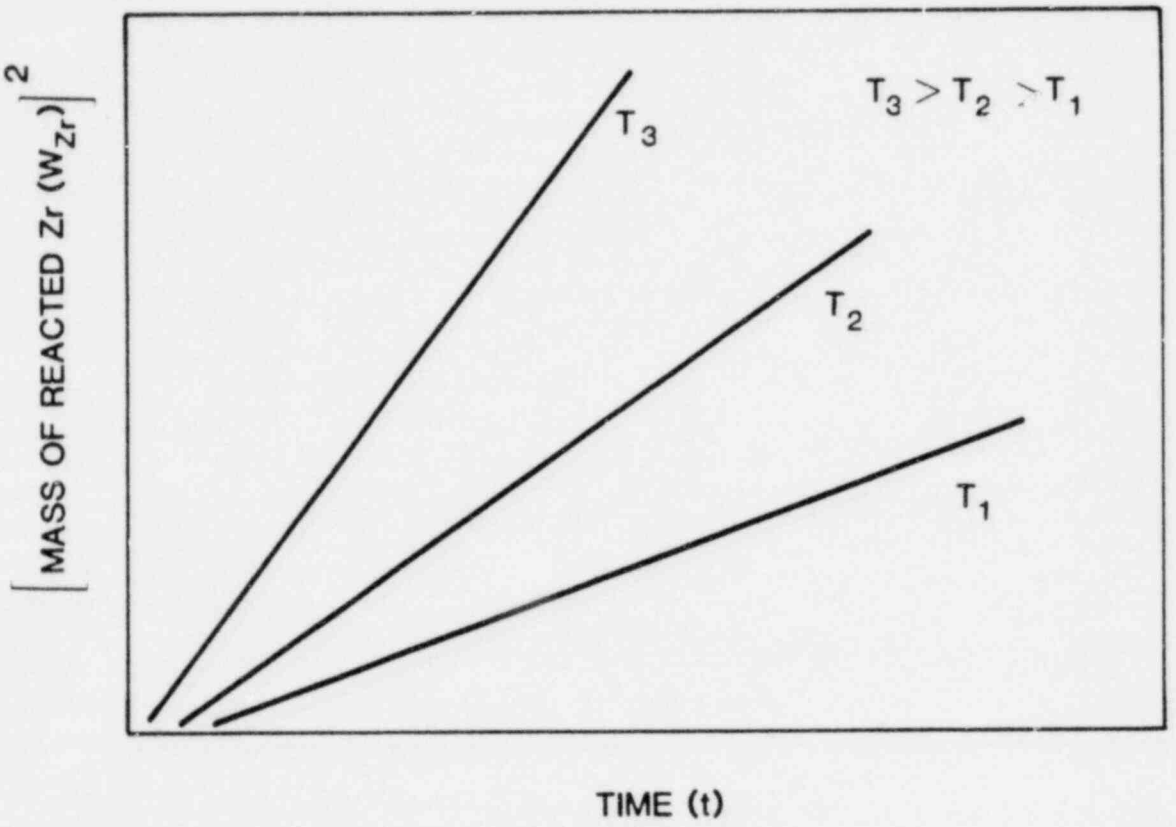

FIG. 5. TYPICAL RESULTS OF PARABOLIC-RATE MEASUREMENTS

produced at any time can be expressed as below:

$$W_{H_2} = 2 \frac{M_{H_2}}{M_{Zr}} \sqrt{Kt} \qquad (4)$$

where:

W_{H_2} = the mass (mg) of hydrogen produced per unit (cm^2) of Zr surface

M_{H_2} = the molecular weight of H_2(2.002), mg/mg-mole

M_{Zr} = the molecular weight of zirconium (91.22), mg/mg-mole

2 = the number of moles of hydrogen produced per mole of zirconium consumed.

The amount of heat released can be calculated from the following expression:

$$E = \frac{\sqrt{Kt}}{M_{Zr}} \frac{\Delta H}{4184} \qquad (5)$$

where:

E = the heat released, J/cm^2

ΔH = the heat of reaction, kcal/mole

4184 = the number of J in one kcal

The above expressions indicate that, as the temperature of the cladding (T) increases, the reaction rate increases. That, in turn, increases the temperature of the cladding. Such a reaction is said to be self-sustaining and unless the heat release is removed by external cooling, clad melting temperatures will be reached.

The above discussion assumes that adequate amounts of steam will be available to sustain the reaction at all times. However, there may be regions of the core which are blocked, or regions of

a fuel channel in which adequate amounts of steam are not available. The reaction is then said to be "steam limited" and its rate is governed by the supply of steam. "Steam limiting" is a localized phenomenon and it may play an important role in controlling the rate of oxidation in areas of low steam flow.

I.1.3 Sample Calculation of H_2 Generation

At this point it is useful to carry out a sample calculation that will illustrate several features of the Zr/H_2O reaction. We begin the calculation by selecting a value for the parabolic rate constant (Eq.3). Numerous values exist in the literature[7-16] but a good "average" of these is the Cathcart-Pawel[14] rate:

$$K(T) = A \exp[-B/RT]$$

where:

$$A = 2.94 \times 10^6 (mg/cm^2)^2/sec$$

$$B = 39,940 \text{ cal/mole}$$

$$R = 1.987 \text{ cal/mole-°K}$$

Using this rate in Eq. 4, we can calculate the mass of H_2 generated (per unit area of clad) in a time t:

$$W_{H_2} = .0439 \sqrt{t\ K(T)}$$

The total area of cladding in a TMI-size reactor is roughly 4.9×10^3 m^2 (40,000 rods, each 3.66 m in length, with a rod outer radius of 5.36×10^{-3} m). This area was used with the above expression for W_{H_2} to compute the parabolic rate of hydrogen evolution ($W_{H_2}/\sqrt{t}$) and the time required to produce 100 kg of H_2 (roughly 10% of the maximum available from the Zr/H_2O reaction) as a function of clad temperature. Results are shown in Table I-1 (recall that the parabolic growth rate model has been proven accurate only for the 1300-1800°K temperature range[5]). The exponential nature of of the hydrogen production is clearly demonstrated by these results. Once a reactor core attains a temperature in excess of 1400°K, only

minutes remain before significant quantities of hydrogen are produced.

As a further illustration of the exponential rate of hydrogen production, we can apply our tabulated rates to the TMI-2 temperature history shown previously (Fig. 4). To simplify our calculations, we will approximate the temperature history of core region #6 by 4 discrete temperature-time blocks as shown in Fig. 6. The result of this exercise is summarized below:

- 800°K for 20.5 minutes → 0.42 kg H_2 evolved
- 1200°K for 8.5 minutes → 18.7 kg H_2 evolved
- 1600°K for 5.5 minutes → 124 kg H_2 evolved
- 2000°K for 2.5 minutes → 295 kg H_2 evolved
- total H_2 evolved in 37 minutes → 438 kg

The heat released by the Zr/H_2O reaction during these 37 minutes can be computed from Eq. 5. For a heat of reaction of 140 kcal/mole-Zr the total heat release for this example is 6.4×10^7 J. As indicated in Fig. 6, this reaction heat is sufficient to increase the temperature of the entire core by ~1000°K.

TABLE I-1

H_2 Generation from the Zr/H_2O Reaction

T(°K)	$W_{H_2}/\sqrt{t}$ (kg/s$^{1/2}$)	Time to Produce 100 kg of H_2 t(s)
800	.012	6.5×10^7 (2 yrs)
1000	.15	4.4×10^5 (5 days)
1200	.83	1.5×10^4 (4 hrs)
1400	2.8	1.3×10^3 (21 min)
1600	6.8	216
1800	13.9	52
2000	24.1	17
2200	37.0	7.3

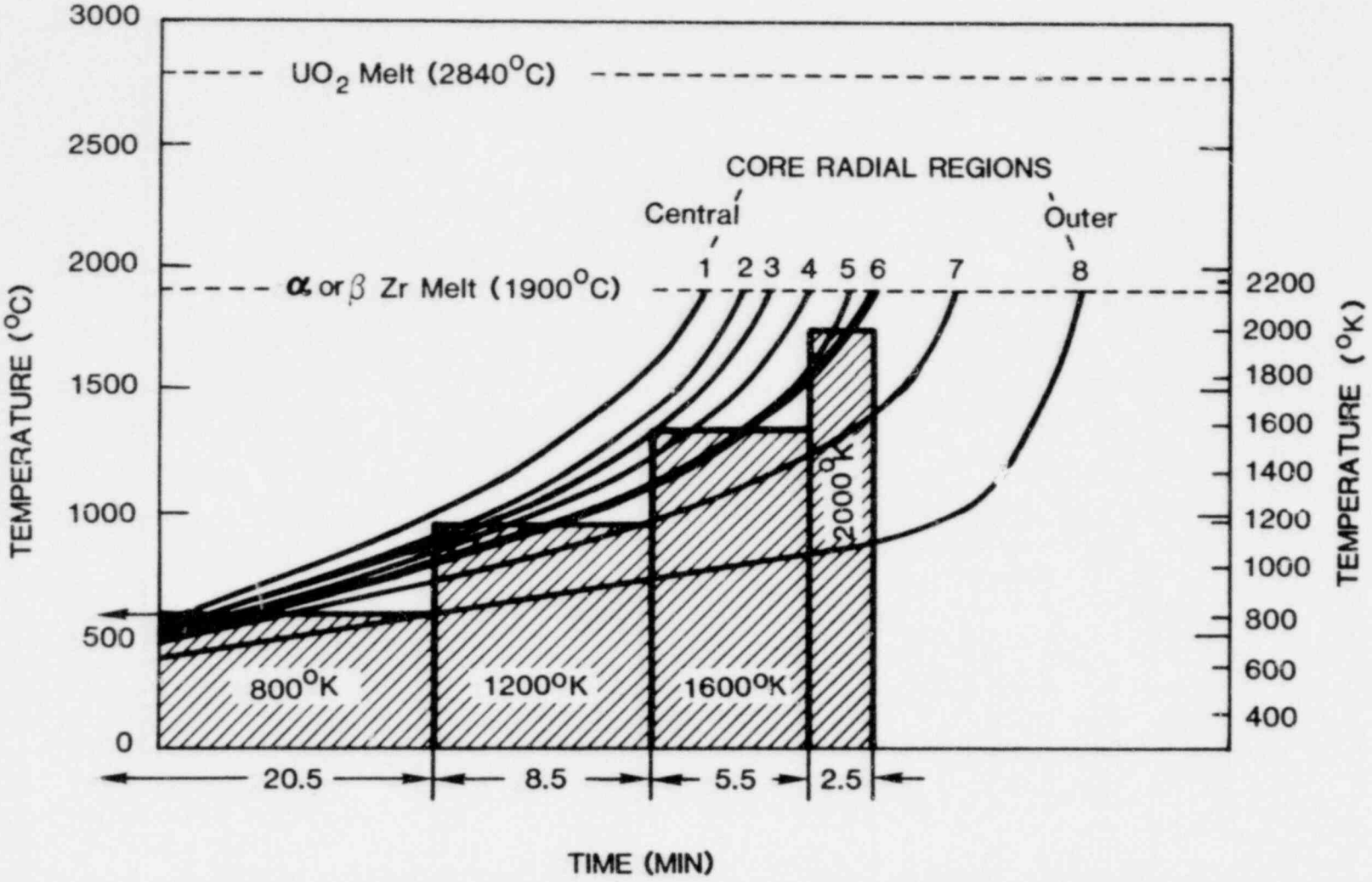

FIG. 6. SIMPLIFIED TEMPERATURE HISTORY OF CORE REGION 6 USED FOR HYDROGEN-GENERATION CALCULATIONS (SEE TEXT)

I.1.4 Conclusions and Recommendations

A large effort was expended in assessing the state-of-the art as applied to zirconium oxidation during long periods of core uncovery. From this work several conclusions may be drawn.

- The parabolic oxidation rate expression is valid for most of the temperature range of interest provided an adequate supply of steam is available.

- The accuracy of the modelling of steam-limited conditions is very uncertain, yet steam limiting may play a significant role in limiting the rate of hydrogen generation.

- Microfissures in the clad and/or spallation of the oxide layer may significantly increase the oxidation rate.

- The effects of radiolytically-produced species and fission products is not well understood.

- Above 1900°C the physical and chemical processes that can occur are not well understood. In the absence of further research, worst-case assumptions must be made for the condition of the core.

- The existing state of knowledge, as applied to modelling of core heat-up is capable of providing rough estimates of hydrogen generation up to temperatures of ~1900°C. These idealized calculations depend on many factors such as plant power level, operating history (both of which determine the decay heat generation), and the type of

accident (which determines the water level time history). Also each plant has its own design characteristics which are important in heat-up calculations. Knowing the water level in the reactor vessel at any time, rough estimates of hydrogen generation can be obtained.

I.2 STEEL-STEAM REACTION

I.2.1 Background

The presence of large amounts of stainless steel in a reactor vessel makes further consideration of the oxidation of steel by high temperature steam advisable. The mechanism of oxidation of steel is highly complex and several oxide forms are possible. As in the case of zirconium the reaction results in the generation of hydrogen and heat. The rate of reaction is described in a manner similar to that described in the discussion of zirconium oxidation, i.e., by a parabolic rate expression. The rate of oxidation of stainless steel is low at temperatures below approximately 1000°C but it becomes larger than that of zirconium at temperatures approaching the melting point of steel (1370-1500°C).

During an accident which involves long periods of core uncovery, steam temperatures at the top of the core would be expected to approximate the temperatures of the cladding and could be in excess of 1900°C. When this steam comes in contact with the steel in the upper grid structure and elsewhere in the upper vessel, the temperature of the vessel wall will increase. Hydrogen will be released at a very fast rate if the wall t perature approaches the melting temperature of steel.

The following section discusses the current state of knowledge on the oxidation of steel at very high temperatures. An estimate of the amount of hydrogen which could be produced from this source is made.

I.2.2 Discussion and Sample Calculation of H_2 Generation

The oxidation of stainless steel proceeds according to the following types of reactions:

$$aFe + bCr + cNi + dH_2O \longrightarrow Fe_a\ Cr_b\ Ni_c O_d + dH_2 + \text{heat}$$

As represented by the above reactions, several forms of oxidation car take place. A major fraction is represented by Fe_3O_4 and other spinel-type or inverse spinel compounds.[17] The heat release is calculated to be 155 kcal/mole if the products are spinel-type compounds. In steam environments steel oxidizes to form a duplex scale consisting of an outer layer which has a well developed columnar crystalline structure of approximately uniform thickness and an inner oxide layer which tightly adheres to the metal. The outer scale readily exfoliates.

The oxidation kinetics of steel have been well researched for temperatures below 650°C.[18] Oxidation of steel at temperatures approaching the melting point was investigated when stainless steel was being considered for use as fuel rod cladding material. The results of these investigations[19] indicated that two stages of oxidation exist. The oxidation is characterized initially (5-30 minutes) by linear kinetics:

$$\Delta W_{steel} = [1.1 \times 10^5 \exp(-44350/RT)]t \qquad (6)$$

where:

ΔW_{steel} = the mass (mg) gained per unit (cm^2) of steel surface

R = the gas constant, cal/mole °K

T = the temperature, °K

t = time, sec

The second stage of steel oxidation is characterized by parabolic kinetics:

$$\Delta W_{steel} = [2.4 \times 10^{12} \exp(-84300/RT)]^{1/2} t^{1/2} \quad (7)$$

To obtain the quantity of hydrogen generated by steel oxidation, the following expression should be used:

$$W_{H_2} = 2 \frac{M_{H_2}}{M_{O_2}} \Delta W_{steel} \quad (8)$$

where:

W_{H_2} = the mass (mg) of hydrogen produced per unit (cm^2) of steel surface

M_{H_2} = the molecular weight of hydrogen (2.002), gm/gm-mole

M_{O_2} = the molecular weight of oxygen (31.998), gm/gm-mole

2 = the number of hydrogen moles produced for each mole of oxygen absorbed.

Figure 7 shows a comparison of the parabolic rate constants for stainless steel and zircaloy. Below approximately 1000°C the rate of steel oxidation is much smaller than that for zirconium. When the temperature approaches the melting point of stainless steel, ∿1400°C, the rate of steel oxidation is higher than that of zircaloy.

In order to calculate the amount and rate of hydrogen production from the steel/steam reaction we need to estimate the surface area of stainless steel in a reactor that would be exposed to steam during a LOCA. For purposes of illustration we can compute the surface area of stainless steel above the lower core plate in a 1000 MW PWR. The result of this computation is ∿600 m^2 of stainless

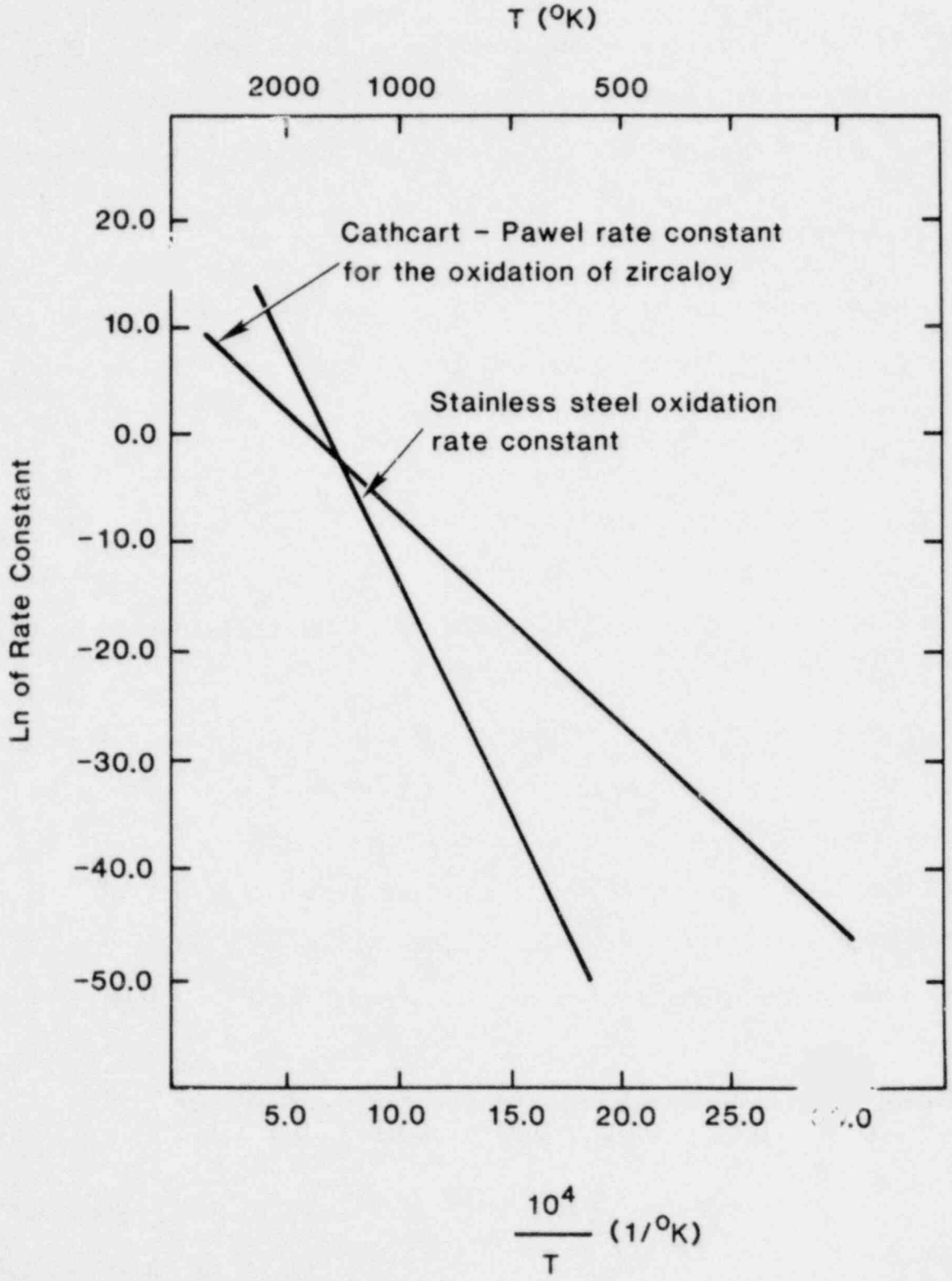

FIG. 7. COMPARISON OF REACTION RATES FOR STEAM OXIDATION OF ZIRCALOY AND STAINLESS STEEL AS A FUNCTION OF TEMPERATURE

steel if we include the following: control-rod cladding, baffle, upper-core barrel, control-rod guide tubes, control-rod drive shafts, upper-core plate, and upper support plate. Using these 600 m^2 as the total stainless steel surface area that can react with steam, we can calculate the rate of hydrogen production and the time required to produce 100 kg of hydrogen as a function of the surface temperature. The results of this calculation are shown in Table I-2 for both the linear and parabolic oxidation stages. The parabolic rate probably yields a better estimate of H_2 production for a realistic LOCA. Note that for temperatures above 1600°K the amount of H_2 produced from stainless steel oxidation is not negligible compared to that produced from zircaloy oxidation (see Table I-1).

When steel melts it does not flow easily because of the presence of oxide scales. In addition, steel foams during the melting process thus increasing the area exposed to steam. It is reasonable to assume that the melting steel would continue to oxidize, especially for vertical surfaces. On the other hand, at high reaction rates the oxidation process might be limited by steam availability. The issue of steam-limited reactions is important when considering stainless steel oxidation, since much of the available steel lies in regions above the core and even above the coolant outlet nozzles. No detailed temperature profiles have been computed for the regions above the core at TMI-2 and so the extent of stainless steel oxidation at TMI cannot be assessed at present.

TABLE I-2. HYDROGEN PRODUCTION FROM THE STAINLESS STEEL/STEAM REACTION

Temperature T(°K)	Linear Stage[a]		Parabolic Stage[b]	
	Linear Rate W_{H_2}/t (kg/s)	Time to Produce 100 kg H_2 t(s)	Parabolic Rate $W_{H_2}/t^{1/2}$ (kg/$s^{1/2}$)	Time to Produce 100 kg H_2 t (s)
1000	1.5×10^{-5}	6.5×10^{6} (75 da)	6.6×10^{-4}	2.3×10^{10} (730 yrs)
1200	6.5×10^{-4}	1.6×10^{5} (1.8 da)	2.3×10^{-2}	1.9×10^{7} (220 da)
1400	9.3×10^{-3}	1.1×10^{4} (3 hrs)	2.9×10^{-1}	1.2×10^{5} (33 hrs)
1600	6.9×10^{-2}	1.5×10^{3} (24 min)	1.9	2.8×10^{3} (46 min)
1800	3.3×10^{-1}	3.1×10^{2} (5 min)	8.5	1.4×10^{2} (2.3 min)

a) Based on Eqs. 6 and 8 with 600 m^2 of steel surface
b) Based on Eqs. 7 and 8 with 600 m^2 of steel surface

I.2.3 Conclusions and Recommendations

The steel-steam reaction is an identified source of hydrogen. However, for this process to become of real significance, the temperature of the steel has to approach the melting point. High steam temperatures are possible during long term core uncovery. To assess the potential of the steel as a serious source of hydrogen an estimate was performed of the amount of hydrogen which could be generated by this source. This estimate indicated that the hydrogen generated by steel oxidation could be comparable to that generated by the zirconium-steam reaction. It is concluded that the steel-steam reaction can play an important role in hydrogen production during accidents involving prolonged core uncovery.

It is recommended that detailed temperature histories be computed for the stainless steel surfaces above the core. The questions related to steam-limited reactions should be addressed in similar research for the zirconium-steam oxidation.

I.3 RADIOLYTIC DECOMPOSITION OF WATER

I.3.1 Background

Radiolytic decomposition of water is a phenomenon associated with both normal plant operation and accidents. In both cases it involves the decomposition of the water molecule by radiation. During normal operation of a PWR, an excess of hydrogen is intentionally dissolved in the primary system coolant in order to limit the net yield of hydrogen and oxygen. In BWR's, however, the radiolytic gases are swept out of the reactor by the steam and collected in the condenser. The noncondensable gases in the condenser are then swept by vacuum-maintaining systems into the off-gas system where the hydrogen and oxygen are burned in a recombiner. It should be noted that spontaneous deflagrations or detonations have occurred in off-gas systems at a number of BWR power plants (Cooper, 1975, 76; Brown's Ferry 3, 1977; Millstone 1, 1977).

During an accident involving fuel-cladding rupture, fission products may be released from the fuel into the coolant system and the containment (if coolant was released). In a BWR containment the fission products could also be transported to the steam suppression chamber, commonly referred to as the wet-well. These fission products emit β and γ radiation that will decompose the water with which they are mixed. The fission products remaining in the fuel also emit β and γ radiation; however, β radiation is significantly attenuated by the fuel and its cladding. The amount of fission products released from the fuel and their distribution throughout the plant are very strongly dependent on the type of

accident. Predictions of the released fraction of fission products associated with each such accident scenario are highly uncertain. Regardless of these uncertainties, it is clear that radiolytic decomposition of water will occur following an accident and hydrogen and oxygen can be generated in both the reactor vessel and the containment.

The rate of hydrogen and oxygen generation is controlled by three factors; 1) the decay energy, 2) the fraction of this energy that is absorbed by the water, and 3) the effective rate of hydrogen and oxygen production per unit of energy absorbed by the water. The first two factors are well understood and can be calculated with a reasonable degree of certainty. The last factor, however, is highly uncertain. The uncertainty stems from a number of parameters which influence the production rate, such as the effect of impurities, motion of the water, pressure, temperature, pH, etc.

The objective of the following discussion is to examine the radiolysis process and ascertain its importance to nuclear-reactor safety.

1.3.2 Radiolysis of Pure Water

The radiolytic decomposition of reactor coolant water is of interest because the hydrogen and oxygen evolved could combust within the primary system or containment for PWRs and BWRs (even with inerted containments).

The mechanisms involved in the radiolytic decomposition of water have been studied by numerous investigators. Allen[20] presents a summary of the fundamental theory of these processes. Basically, radiolytic decomposition involves the production of solvated electrons (e^-_{aq}), radicals, and molecules as illustrated by Eq. 9.[21]

$$H_2O \rightarrow e^-_{aq},\ OH,\ H,\ HO_2,\ H_2,\ H_2O_2. \qquad (9)$$

These initial products of water decomposition are formed heterogeneously in the track (spur) along which energy is being deposited. Once these species are formed they can react with each other or they can diffuse into the solution where they may react either with each other or with other molecules in the solution. Table I-3[22] lists the principal reactions of the products as they diffuse into the solution (pure water only). The ultimate result of these reactions is the formation of molecular products H_2, H_2O_2, O_2 and the reformatio of H_2O.

The yield of a product species due to the radiolysis of water is generally expressed as that product's "G" value (molecules of product formed per 100 eV of energy absorbed). Distinction must be made between the primary or direct radiolytic yield of a species and the net yield of the same species. The direct or primary yield is usually

Table I-3 - Interactions of Radiolytic Products of Water.[22]

Reaction No.	Reaction
* 8	$e^-_{aq,} + O_2 \rightarrow O_2^-$
* 9	$e^-_{aq.} + H_2O_2 \rightarrow OH + OH^-$
*11	$H + O_2 \rightarrow HO_2$
*12	$H_2 + OH \rightarrow H + H_2O$
*14	$H_2O_2 + OH \rightarrow HO_2 + H_2O$
15	$HO_2 + H_2O_2 \rightarrow OH + H_2O + O_2$
*16	$2HO_2 \rightarrow H_2O_2 + O_2$
16b	$O_2^- + O_2^- \xrightarrow{2\ H_2O} H_2O_2 + O_2 + 2OH^-$
*18	$OH + HO_2 \rightarrow H_2O + O_2$
18b	$OH + HO_2 \rightarrow H_2O_3$
20	$OH + OH \rightarrow H_2O_2$
21	$H + H_2O_2 \rightarrow H_2O + OH$
22	$e_{aq}^- + H \rightarrow H$
23a	$e_{aq}^- + HO_2 \rightarrow H_2O_2$
23	$H + HO_2 \rightarrow H_2O_2$
26	$e_{aq}^- + e_{aq}^- \xrightarrow{2\ H_2O} H_2 + 2OH^-$
27	$e_{aq}^- + OH \rightarrow OH^-$
28	$H + H \rightarrow H_2$
29	$H + OH \rightarrow H_2O$
30	$e_{aq}^- + H \xrightarrow{H_2O} H_2 + OH^-$

* - Defines the principal reaction route

expressed as a subscript to G while the net or actual yield is written as a parenthetical notation. Thus, G_{H_2} is the hydrogen formed directly from the water by radiation, while $G(H_2)$ is the net hydrogen formed directly by radiation and indirectly by all subsequent chemical reactions. The G(x) value can be larger or smaller than G_x due to secondary reactions taking place between the various radiolytic species and the solutes. Typical values[23] of G_{H_2} in pure water are 0.44 for $\beta + \gamma$ radiation, 1.12 for reactor fast neutrons, and 1.70 for the recoil nuclei from the reaction $^{10}B(n,\alpha)\rightarrow{}^{7}Li$. Since molecular oxygen is not produced directly by radiolysis, $G_{O_2} = 0$.

A closed water/gas system will eventually attain equilibrium with respect to radiolytic decomposition of the water. The concentration of gaseous products at equilibrium will be a function of the reactor power density, the water pH and temperature, and the impurity (solute) type and concentration. Once equilibrium is attained, $G(H_2) = G(O_2) = 0$ (although the concentrations of H_2 and O_2 will not be zero). It is well established that small quantities of hydrogen (less than 10^{-3} moles/liter) dissolved in pure water or boric acid solutions will effectively limit the equilibrium condition to one in which negligible O_2 is generated. This technique is employed routinely in PWR nuclear plants.

An open water/gas system will not attain an equilibrium condition because the product species are being continuously removed. A typical BWR power plant operates in such a manner. If the water is boiling vigorously, H_2 and O_2 will be produced in stoichiometric portions and $G(O_2) = 1/2\ G(H_2) = 1/2\ G_{H_2}$. For pure water exposed

to $\beta + \gamma$ radiation, this would result in the production of $\sim$ 22 molecules of O_2 and 44 molecules of H_2 for each 10^4 eV of radiation energy. Experimental confirmation of such production rates has been attained using the action of CO_2 bubbling in pure water to continuously remove the gaseous products of radiolytic decomposition.(23)

I.3.3 Radiolysis of Water in a Severe Accident

One of the key questions associated with the accident at TMI-2 concerned radiolytic decomposition of the reactor coolant water and the possibility that a combustible mixture of H_2 and O_2 might exist inside the reactor. Armed with our present understanding of the TMI-2 accident scenario, it can be stated that the probability of such an occurrence was small. It cannot be stated, however, that the probability was zero (or would be zero for all conceivable accidents) due to the boiling of the reactor coolant. Radiolytic decomposition of water in the containment building has been recognized for years as a potential combustion hazard and several analyses have been conducted previously to estimate the severity of the threat.[22,24-26]

The impact of radiolytic decomposition of water with respect to hydrogen combustion in an accident is difficult to assess at present for a number of reasons. The specific accident scenario can have a major effect of the relative importance of radiolytic production of H_2 and O_2. In order to realistically estimate the effects of radiolysis, it is necessary to know the extent and distribution of fission-product release, the water temperature and pH, the degree of bubbling and turbulence of the water, and the types and quantities of impuritie dissolved in the water. Presently we cannot assess the effect of simultaneous variations in several of these parameters. We can state, however, that the rate of production of combustibles from radiolysis is slow compared to that from the high-temperature Zr/steam and steel/steam reactions (sample caluclations for radiolytic production of combustibles are presented in Section I.3.4).

The rate of radiolytic decomposition of pure water increases linearly with the reactor decay power but the equilibrium concentrations of product species in a closed system increase as the square root of the power. Variations in pH have little effect on α-irradiated water, but not much is known about the effect of pH variations with other forms of radiation. It has been speculated that pH variation may have a significant effect when combined with solutes.[23] Increasing temperature will tend to decrease equilibrium concentrations of product species in pure water, but it has been suggested that increasing temperature will enhance solute effects due to increased reaction rates between solute molecules and radiolytically-produced radicals.[23]

As discussed previously, the effect of vigorous boiling or bubbling of the water can be quite significant. The products of radiolysis are constantly removed from the liquid and therefore recombination of the H_2 and O_2 in solution is not possible. Radiolysis of the vapor phase itself has not been studied extensively but this may become an important issue in an accident. In order to estimate the rate of production and net yields of various products, more research will be necessary in the radiolysis of turbulent, bubbling, two-phase water systems.

The effects of the many possible solutes, which could be present in the reactor coolant following an accident, on the equilibrium conditions or the net product yields are not well understood. The impurities can react with the radiolytically-produced radicals and upset the chemical balance. Only very small quantities of impurities[22] are necessary to upset this balance.

Researchers in the past have been mostly concerned with the effects of certain solutes which were being used in conjunction with the operation of plant safety systems and would become mixed with the reactor water after an accident. Of particular interest were the effects of boric acid and containment spray additives such as base-borate or base-thiosulphate.[20,27-30] The experiments essentially indicated that while no large departures from the $G(H_2)$ values for pure water were observed, the equilibrium conditions were changed. Both sodium hydroxide and sodium thiosulphate increased the equilibrium hydrogen concentration. Boric acid solutions, however, behaved essentially in the same manner as pure water.

Other experiments were conducted to evaluate the capabilities of several solutes to reduce the radiolytic yield of hydrogen.[31-36] It was found that a number of solutes such as NO_2^-, NO_3^-, H_2O_2, Cu^{2+}, and Ce^{4+} reduce the production of hydrogen. The compound $NaVO_3$ (sodium metavanadate) has been studied extensively[33,36] and found to be very effective in reducing the yield of hydrogen. In general, it can be stated that solutes that react rapidly with e_{aq}^- or H will reduce $G(H_2)$ while those that react with OH will reduce $G(H_2O_2)$ (which in turn reduces $G(O_2)$).

Major uncertainties in an accident include the type and quantity of various impurities that will dissolve in the coolant water. Fission products, oxides, and adsorbed gases (that evolve from surfaces only at high temperatures) may appear as solutes at some stage during an accident and their impact on radiolysis may be significant. As an example, fission products such as Br and I are known to affect the H_2 - O_2 recombination reactions by

electron-transfer processes with the H and OH radicals. Nevertheless, the net effect of Br and I on product yield and production rates has not been predicted.

1.3.4 Sample Calculations of H_2O_2 Production from Radiolytic Decomposition of Water

There are many uncertainties associated with radiolytic decomposition of water in a LOCA. It is most useful to carry out sample calculations as part of a parametric analysis. To do this we can follow the analysis of Turner.[22] He considers the two key parameters to be the net yield G value for hydrogen, $G(H_2)$, and the fraction of reactor-shutdown (decay) radiation absorbed by the water, f. Turner estimates a range of f from 0.07 for a "normal" shutdown (no release of fission products from the fuel rods) to 0.20 for a LOCA involving rupture of fuel rods (based upon the accident postulated in Report TID-14844).[37] The value of $G(H_2)$ can vary with time as well as with the numerous parameters discussed in the previous section. In order to proceed we set the product $G(H_2)\cdot f$ equal to 1.0 and then all results can be scaled with the "correct" value of $G(H_2)\cdot f$. Results of calculations for a 3300 MW(t) reactor are given in Table I-4. While these calculations probably overestimate the yield and rate, there are too many unknowns to say that conclusively. Comparison of Table I-4 to Tables I-1 and I-2 indicates that the threat of a hydrogen combustion due to radiolysis is more long term than that due to the Zr/steam and steel/steam reactions at high temperature.

The issue of combustible mixtures of H_2 and O_2 existing inside the reactor primary will be examined now. The primary can behave like an open water/gas system if there is a LOCA or if pressure-relief valves remain open (as at TMI-2). With this scenario it is clear that significant concentrations of both H_2 and O_2 can exist inside the primary since this system is essentially a BWR. Whether or not the mixture is combustible is not clear due to uncertainties of

the quantities of H_2 and O_2 present in addition to the possible quantities of steam. Detailed flow and combustion calculations will be needed to better assess the problem. The effect of solutes and gas bubbling on the rate of H_2/O_2 production may be critical to this entire issue, but further research on these effects will be necessary before definitive answers appear.

A closed water/gas system can model the radiolytic behavior inside the containment or the primary (after the primary system isolation has been reestablished). The major questions to be addressed here are the final equilibrium condition and the rate of H_2 - O_2 production as the system approaches equilibrium. The effects of temperature, pH, water bubbling, solutes, and initial gas-phase concentrations will control the final equilibrium and the system's approach to that equilibrium. In the scenario of primary pressure relief followed by closure of the primary system, it is possible for significant quantities of H_2 and O_2 to recombine and consequently inert the gas phase, but the rate of approach to equilibrium cannot be predicted adequately at present.

The equilibrium condition within containment has been estimated by various authors as 4-16 volume % H_2 concentration. Once again, factors such as water temperature, pH, bubbling, solutes, and initial gas-phase concentrations will determine the actual equilibrium condition. Using an analysis similar to that presented above, several authors have estimated the time required to reach a 4% H_2 concentration in a typical PWR ($\sim$3300 MW(t), containment gas volume of $\sim 2.6 \times 10^6$ ft^3 and a typical BWR (2500-3500 MW(t), containment gas volume of $\sim 3 \times 10^5$ ft^3. The results of these analyses are summarized in Table I-5.

Table I-4. Conservative Calculation of Radiolysis Yield and Rate for a 3300 MW(t) Reactor with $G(H_2)\cdot f = 1.0$

Time after Shutdown (sec)	Integrated Decay Energy* MJ/MW	Radiolysis Yield and Rate with $G(H_2)\cdot f = 1.0$ for a 3300 MW Reactor		
		Total Yield (moles H_2)	Total Yield (kg H_2)	Average Rate (moles H_2/sec)
10^2 (2 min)	6	2.0×10^3	4	20
10^3 (17 min)	25	8.6×10^3	17	7.3
10^4 (3 hr)	160	5.5×10^4	110	5.2
10^5 (1 day)	800	2.7×10^5	548	2.4
10^6 (12 days)	3500	1.2×10^6	2400	1.0

* Data from Ref. 22

Table I-5. Time Required to Attain a 4% H_2 Concentration in Containment Due to Radiolytic Decomposition of Water

Reference	Time Required for a BWR 3000 MW(t) and 3×10^5 ft^3	Time Required for a PWR 3300 MW(t) and 2.6×10^6 ft^3
22	5.5×10^4 sec (15 hr.)	1.4×10^6 sec (16 days)
24	14 hours	12 days
25	21 hours (worst case) 85 hours (realistic case)	--
26	150 hours (worst case) 300 hours (realistic case)	--

I.4 CORROSION OF PAINTS AND GALVANIZING

I.4.1 Background

The inside surface of a containment building is coated with paint that contains zinc, in order to inhibit corrosion. In addition, extensive use of galvanizing is made for coating of gratings, ductwork, cable trays, and conduits. Following an accident, an environment will exist in the containment which could initiate accelerated corrosion of the zinc contained in the paint and galvanizing. Corrosion of aluminum and other metals can also occur; however, the inventory of these metals in the containment is small.

A number of workers have measured rates of hydrogen evolution from painted galvanized steel coupons under simulated LOCA conditions (high temperatures, saturated steam, immersion in safety-spray solutions). Radiation effects have not been examined. As will be discussed in the following sections, the rate of hydrogen evolution is somewhat uncertain, but apparently it is slow relative to other hydrogen sources, and the total inventory of hydrogen available from paints and galvanizing is limited.

I.4.2 Discussion and State-of-the-Art

The extensive use of zinc-based primers inside containment as well as galvanizing, presents another possible source of hydrogen in the post-accident environment. The corrosion of zinc present in these substances appears to proceed according to the following reaction:

$$Zn + 2H_2O \longrightarrow Zn(OH)_2 + H_2 \qquad (10)$$

Competing reactions may result in products other than hydrogen. For example, a protective coating can be formed by the reaction

$$4Zn + 2O_2 + 3H_2O + CO_2 \longrightarrow Zn_4\,CO_3(OH)_6 \qquad (11)$$

Several factors have been shown to affect the yield and rate of hydrogen generation from corrosion of zinc coatings. These factors are:

- temperature of the coating
- type (and possibly thickness) of topcoat paint
- composition of the coating
- surface area of coating immersed in spray solution
- composition and pH of the spray solution

Spray solutions here refers to those borated water solutions commonly considered for use as pressure suppressants in reactor containments. Examples of sprays that have been used in corrosion tests are: (a) 1 wt % $Na_2S_2O_3$ - 0.15 N NaOH - 3000-ppm B; (b) 0.15 N NaOH - 3000-ppm B; and (c) 3000-ppm B. The first two solutions have pH$\sim$ 9.3 while the latter has pH $\sim$4.7. Apparently, BWR sprays such as

H_3BO_3 have not been tested. In addition, no corrosion tests have been conducted in a radiation environment or on "aged" samples.

Zittel[38] has published the most complete study of corrosion of zinc coatings to date. He tested sample coupons supplied by seven major paint vendors as well as coupons of galvanized steel (ASTM A525). Spray solutions relevant to a PWR (listed above) were used. Tests were generally conducted at 130°C for 24 hours or with the temperature history of a design-basis accident (5 min at 149°C; 105 min at 140°C; 22.25 hours at 107°C). Zittel summarized his findings as follows:

- for a containment with 10^5 ft^2 of surface coated with one of the paints tested, H_2 evolution could amount to an atmospheric concentration of >0.5% H_2.
- topcoat paints can reduce or enhance the hydrogen generation
- spray-solution pH has little effect
- visual condition of the coated surface after testing does not correlate to hydrogen generation.
- for all samples tested at 130°C, the quantity of H_2 evolved was a considerable fraction of the theoretical maximum (calculated on the basis that all zinc present was converted to hydrogen)

Van Rooyen[39] used data from several workers[40-42] to estimate the rate of hydrogen production from zinc corrosion.

While these data are characterized primarily by a lack of consistency, van Rooyen suggests that a rate expression may be developed in the form

$$V_{H_2} = A\, e^{-B/RT} \qquad (1)$$

where V_{H_2} = rate of hydrogen production, $SCF/ft^2 \cdot hr$

A = a constant factor, $SCF/ft^2 \cdot hr$

B = an activation energy, cal/mole

R = the gas constant, 1.987 cal/mole - °K

T = surface temperature, °K

Zittel did not measure directly the rate of H_2 production, but rather the net yield following a 24-hour test. Consequently the maximum rate during the tests probably exceeded the average rate over the 24 hours. Nevertheless, Zittel's 24-hour average rates are somewhat higher than rates observed by others[40-41], so it may be conservative to use values for A and B appropriate to the highest rates observed by Zittel. Van Rooyen characterizes these values for Zittel's highest average rates as:

$$A = 4.7 \times 10^5 \ SCF/ft^2 \cdot hr$$

$$B = 14{,}500 \ cal/mole$$

Zittel's average rate for a 100-hour corrosion test on galvanized steel was somewhat lower than the highest rate for painted steel. Zittel also observed that the net yield did not increase significantly with increased exposure time (from 24 to 48 hours) for several of the samples he tested. This may indicate that, for some paints, the

reaction will not reach completion (i.e., the maximum quantity of H_2 evolved may be less than the theoretical yield based on the quantity of zinc present).

I.4.3 Sample Calculation of Hydrogen Generation from Corrosion of Paints and Galvanizing

The calculation of the rate and yield of H_2 generated by corrosion will proceed as with the metal/steam reactions. The total area of surfaces in a PWR containment painted with zinc-based primers is of the order of 1.5×10^5 ft^2.[34,43] If we use this value for the surface area and convert from SCF to kg we obtain the following form of Eq. 12,

$$W_{H_2} = 1.8 \times 10^8 \left[\exp\left(-\frac{7323}{T}\right)\right] t \qquad (13)$$

where

W_{H_2} = the quantity of H_2 released by the paint, kg

t = the elapsed time, hours

The maximum quantity of H_2 that can be generated by the corrosion of paints and galvanizing is equal to the theoretical yield based upon the quantity of zinc. For our purposes, we will use the largest value from Zittel[38] for a 3.5-mil primer coat (8.5 cm^3/cm^2 (STP)). Converting this value to kg/ft^2 we obtain a theoretical yield of 7.1×10^{-4} kg/ft^2 or 106 kg of H_2 for the entire painted surface of 150,000 ft^2.

Lopata[43] has estimated the surface area of galvanized steel in a containment to be of the order of 30,000 ft^2. If we use this value of surface area in Eq. 12 and convert units as before, we obtain,

$$W_{H_2} = 3.6 \times 10^7 \left[\exp\left(-\frac{7323}{T}\right)\right] t \qquad (14)$$

where W_{H_2} = the quantity of H_2 released by the galvanizing, kg

The theoretical hydrogen yield of the galvanizing can be calculated based upon the amount of zinc present (2 oz/ft^2). Converting units we obtain a theoretical yield of 1.7 x 10^{-3} kg/ ft^2 or 52 kg of H_2 for the entire galvanized surface of 30,000 ft^2.

For the sake of completeness we will discuss Lopata's[43] estimate of rate and yield of H_2 due to aluminum corrosion. Lopata estimates the surface area of aluminum to be 475 ft^2 and the total amount of aluminum to be 1250 lbs. The rate of aluminum corrosion is cited as 200 mils/yr under normal conditions and as 10,000 mils/yr under LOCA conditions at 300°F. Using the value under accident conditions results in a hydrogen generation rate of 0.4 kg/hr. The maximum quantity of hydrogen that can be produced from 1250 lbs. of aluminum is 63 kg. Consequently, all of the aluminum will be corroded within a time on the order of 7 days following an accident.

In order to compare to other sources of H_2, we have calculated evolution rates and times to attain total yield for zinc corrosion. Table I-6 presents the results for paints and galvanizing at several different temperatures. Compared to the metal/steam reactions at high temperature (Tables I-1 and I-2) the rates and yields of H_2 production due to zinc corrosion are small. The maximum quantity of H_2 available from corrosion of zinc and aluminum is 220 kg. This amount of hydrogen in a large dry PWR (2.5 x 10^6 ft^3 containment air volume) would result in a 3.5% H_2 concentration. Apparently these sources, by themselves, do not represent a significant threat to those PWR containments.

Table I-6. Sample Calculation of Zinc-Corrosion Yield and Rate for Paints and Galvanizing

Temperature °K	Zinc-Based Paint 150,000 ft^2		Zinc Galvanizing 30,000 ft^2	
	H_2 Production Rate (kg/hr)	Time to Attain Total Yield[a] (hrs)	H_2 Production Rate (kg/hr)	Time to Attain Total Yield[b] (hrs)
422 (300°F)	5.2	20	1.1	50 (2 days)
413 (285°F)	3.6	30	0.72	73 (3 days)
380 (225°F)	0.77	138 (6 days)	0.15	338 (14 days)
339 (150°F)	0.07	1420 (59 days)	0.02	3480 (145 days)

a) Total yield from painted surfaces is 106 kg H_2

b) Total yield from galvanized surfaces is 52 kg H_2

7.5 GAS GENERATION DURING CORE MELT INTERACTION WITH CONCRETE

In the unlikely event that a reactor accident progresses to the point of gross fuel melting, the reactor pressure vessel may be penetrated. Collapse of the molten reactor core materials into the reactor cavity would initiate vigorous gas generation as this high temperature melt attacked the concrete basemat of the reactor.

The three stages of gas generation during the interaction of molten fuel, cladding, and steel with concrete are:

1) thermal decomposition of the concrete to yield gaseous products,
2) passage of these gases up through the melt, and
3) chemical evolution of the gases as they emerge from the melt.

The general topic of core melt interactions with concrete is the subject of ongoing research both in the United States and in the Federal Republic of Germany. The many processes and phenomena associated with melt/concrete interactions that relate to questions of nuclear reactor safety are tightly interrelated. Only those processes directly connected to generation of permanent gases are described below. References in the bibliography at the end of this document provide more detailed discussions of this and other features of melt interactions with concrete.

The discussions below will concentrate on the generation of permanent gases heated directly by hot core materials. It should be remembered, however, that radiant or convective heating of concrete not in contact with the melt will also lead to concrete decomposition and gas generation.

I.5.1 Thermal Decomposition of Concrete

The structural concrete encountered in reactor installations consists of a heterogeneous mixture of cementitious material binding together both fine and coarse aggregate. The cementitious material is nearly always Type II or Type I and II Portland cement. A nominal composition of Type II Portland cement before it is used to make concrete is:

Ca_3SiO_5 (alite)	47 weight %
Ca_2SiO_4	32 weight %
$Ca_3Al_2O_6$	3 weight %
$Ca_4Fe_2Al_2O_{10}$	12 weight %
$CaSO_4 \cdot 2H_2O$ (gypsum)	4 weight %

When mixed with water and aggregate, Portland cement hydrates to form an adherent mass that bonds to the aggregate. Some of the chemical reactions that are believed[44] to occur during hydration of the cement are listed in Table I-7. The hydration reactions involve participation of both a solid and a liquid phase. Initially the reactions are fairly rapid. The solid products of reaction retard the reaction rate. Hydration of the Portland cement is usually taken to be complete for engineering purposes after 7-90 days. Actual completion of the hydration process may require decades if, in fact, it ever is complete.

The products of hydration contain water in the form of hydroxides and molecular water coordinated to metal ions.

Table I-7. Some Hydration Reactions in Portland Cement

$$2\ (Ca_3SiO_5) + 6H_2O \rightarrow Ca_3SiO_3(OH)\cdot 3H_2O + 3Ca(OH)_2$$

$$2\ (Ca_2SiO_4) + 4H_2O \rightarrow Ca_3SiO_3(OH)\cdot 3H_2O + Ca(OH)_2$$

$$Ca_4Fe_2Al_2O_{10} + 2Ca(OH)_2 + 10H_2O \rightarrow Ca_6Fe_2Al_2O_{12}\cdot 10H_2O \rightarrow$$

$$\rightarrow Ca_3\ [Al\ (OH)_6]_2 + 3Ca_3Fe_2O_6\cdot 4H_2O$$

$$Ca_3Al_2O_6 + 6H_2O \rightarrow Ca_3\ [Al(OH)_6]_2$$

$$2Ca_3Al_2O_6 + 6CaSO_4\cdot 2H_2O + 50H_2O \rightarrow$$

$$\rightarrow Ca_{12}Al_4\ (OH)_{24}\ (SO_4)_6\cdot 50H_2O \rightarrow$$

$$\rightarrow 4CaSO_4\cdot 2H_2O + 30H_2O + 2(3CaO\cdot Al_2O_3\cdot CaSO_4\cdot 12H_2O)$$

$$3CaO\cdot Al_2O_3\cdot CaSO_4\cdot 12H_2O \rightarrow Ca_3[Al(OH)_6]_2 + CaSO_4\cdot 2H_2O + 4H_2O$$

The chemically constituted water, in the form of hydroxide groups, amounts to 1.5-2 percent based on the weight of the concrete. Molecular water, bound to ions, is about 1.6 to 2 percent of the concrete weight. The solid products of cement hydration have gelatinous, porous structures that physically entrap water. The amount of water physically held in this form within the concrete is between 1 and 5.5 weight percent, depending on the relative humidity of the ambient atmosphere surrounding the concrete and the age of the concrete.

Concrete found in reactor cavities that are purposely kept wet will contain a total of 7-9 percent water by weight. Dry reactor cavities will contain little physically-bound water. Water in the form of hydroxides, coordinated molecular water, as well as modest amounts of physically-held water will amount to about 4-5 weight percent of such dry concrete.

Aggregate used for reactor concretes is much less standardized than the cementitious material. Criteria for the selection of aggregate are provided in guides published by the American Concrete Institute and the American Society for Testing and Materials. These criteria focus on the strength and serviceability of concrete and do not refer to its ability to withstand high temperatures. Choice of aggregate at any given site is usually dictated by cost and supply. Aggregates found at existing reactors may be categorized as:

<u>siliceous</u> - basalt, granite, gneiss

<u>calcareous</u> - calcite ($CACO_3$), dolomite ($MgCa[CO_3]_2$)

<u>heavy aggregates</u> - magnetite, baryite.

Heavy aggregates are little used at light-water reactor sites because of their cost and the difficulty in handling dense solids. Concrete made with the heavy aggregates is used in areas requiring critical shielding from radiation.

Siliceous aggregate contains little material that may be thermally vaporized to form permanent gases. Water present in these aggregates is usually in the form of coordinated molecular water or water physically adsorbed on the aggregate surface and seldom amount to 1 weight percent.

Calcareous aggregate, on the other hand, readily decomposes at elevated temperatures to yield carbon dioxide. Concrete made with these aggregates will contain 20-45 percent carbon dioxide by weight

Weight losses incurred when a sample of powdered limestone concrete was heated at a linear rate are plotted versus temperature in Figure 8. Over the temperature interval of 30 to 1000°C there is continuous loss in sample weight. Three particularly abrupt weight losses occur.

These occasions of rapid loss in sample weight may be attributed to the rapid loss of:

1) molecular and physically-entrapped water between 30 and 230°C,

2) water chemically constituted as hydroxides in the concrete over the interval 350 to 500°C, and

3) carbon dioxide from aggregate and the cementitious phases over the interval 600 to 1000°C.

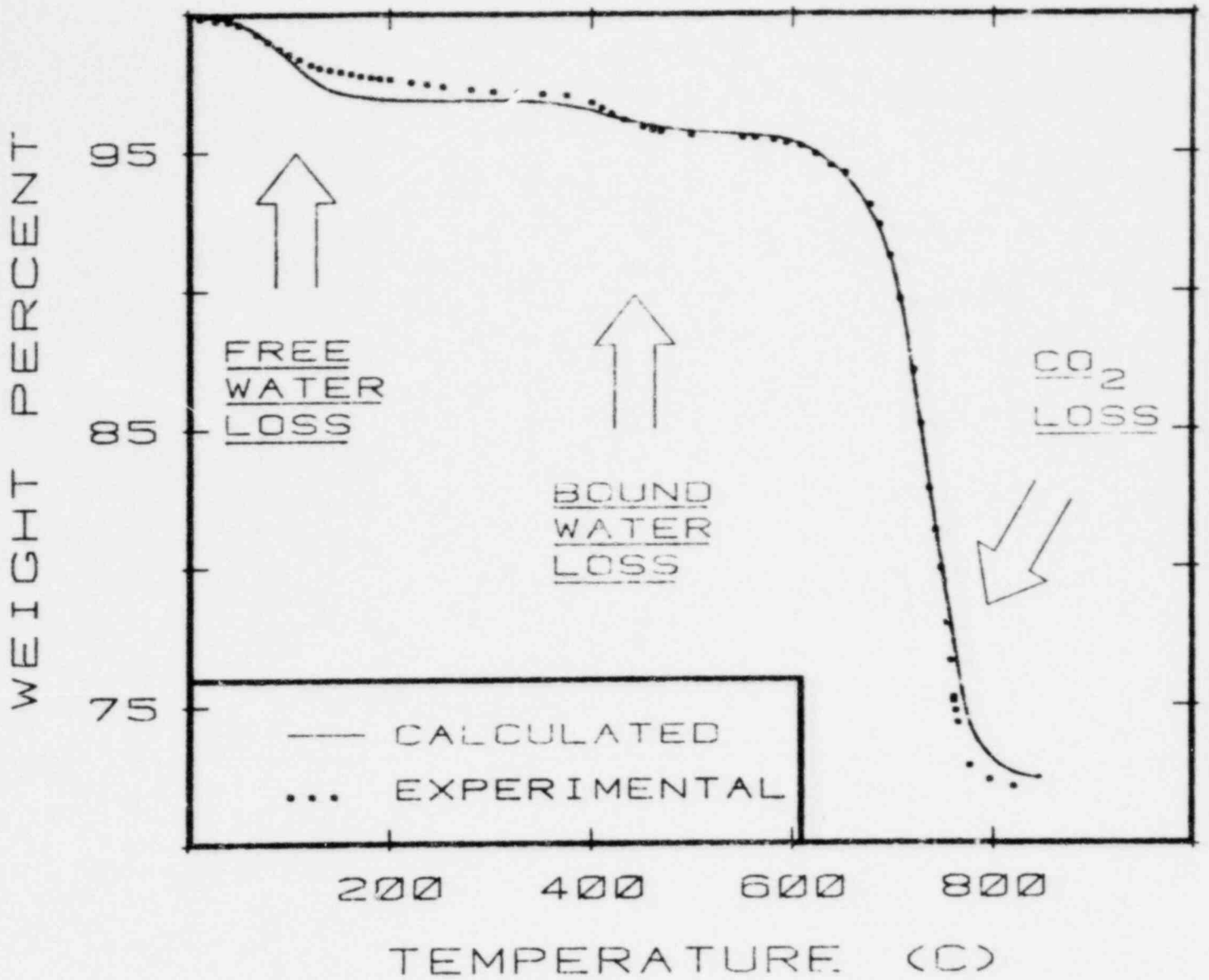

FIG. 8. COMPARISON OF MEASURED AND CALCULATED WEIGHT LOSSES FROM LIMESTONE CONCRETE HEATED AT 10 C / MIN
(note that the volumes of H_2O and CO_2 released are similar)

This pattern of three sudden weight losses is observed in similar experiments with other concretes, though the magnitude of the events do vary with concrete composition. Even siliceous concretes show weight losses of about 1 percent in the range of 600-1000°C due to decomposition of carbonates. These carbonates are probably formed by the reaction of cement constituents, such as calcium hydroxide ($Ca[OH_2]$), with CO_2 in the air during concrete manufacture and curing. At high heating rates, loss of physically bound water and coordinated water can produce distinguishable weight loss events.

Decomposition of the concrete to yield volatile products is a kinetic process. The rates of each of the three principal weight-loss events may be described by the rate equation:[45]

$$\frac{d\alpha}{dt} = K \exp(-E/RT)(1 - \alpha)^n \qquad (15)$$

where

α = fraction of decomposing species lost

t = time

R = gas constant

T = absolute temperature .

Values of the constants K, E, and n found for the three major decomposition events in several concretes are shown in Table I-8. A comparison of weight losses predicted by Eq. (15) and those determined experimentally is made in Fig. 8.

The microscopic description provided by Eq. (15) shows that gas generation during heating of concrete depends on the heating rate and the past thermal history of the concrete as well as temperature. Heat transfer from a melt to concrete is still not well understood.

It is complicated by the decomposition reactions themselves which are endothermic. Heats required for these reactions are:

Reaction	Heat (kJ/mole)
Loss of physically bound water	41
Loss of coordinated molecular water	45-64

Reaction	Heat (kJ/mole)
Loss of chemically-constituted water	99-110
Loss of carbon dioxide	160-180

The decomposition reactions also produce changes in the porosity and thermal behavior of the concrete.

Additional complications in the analysis of gas generation from heating bulk concrete arise because mass transfer within the concrete cannot be neglected. Two effects due to mass transfer are especially important:

a) the porosity of concrete is sufficiently low that gaseous products of reaction build up pressure in the concrete and retard the rate of decomposition, and

b) steam produced by the decomposition reactions condenses in the cooler regions of the concrete.

The first of these mass-transfer effects gives rise to high gas pressures within the concrete. Some data on this pressurization are shown in Fig. 9. Pressurization of the concrete can cause spallation and consequent increases in the surface area of concrete exposed to heating. Spallation does not appear to be an important process during melt attack on concrete, but it is important for concrete heated by radiant or convective processes.

Condensation of vaporized water produces a flux of water away from the heated surfaces of concrete. Especially when the concrete is cracked, the water participating in this flux is lost and does not contribute to gas generation. This effect is important during melt/concrete interactions (see Fig. 10).

Three attempts have been made to construct models that will predict gas generation during intense heating of concrete. The three computer models (WATRE, Produced at the Hanford Engineering and Development Laboratory;[46] COWAR-2, produced by General Electric Corp.;[47] and USINT, produced at Sandia National Laboratories[48] are currently being evaluated at General Electric-Sunnyvale. Unfortunately, the dearth of definitive experimental data may preclude detailed verification of these models. Experimental studies have concentrated on determination of temperatures within heated concrete. Determinations of pressure and mass transfer, especially water migration, are more difficult and typically have been made under conditions that are not representative of conditions during core meltdown accidents.

A) TEST WARD - 2

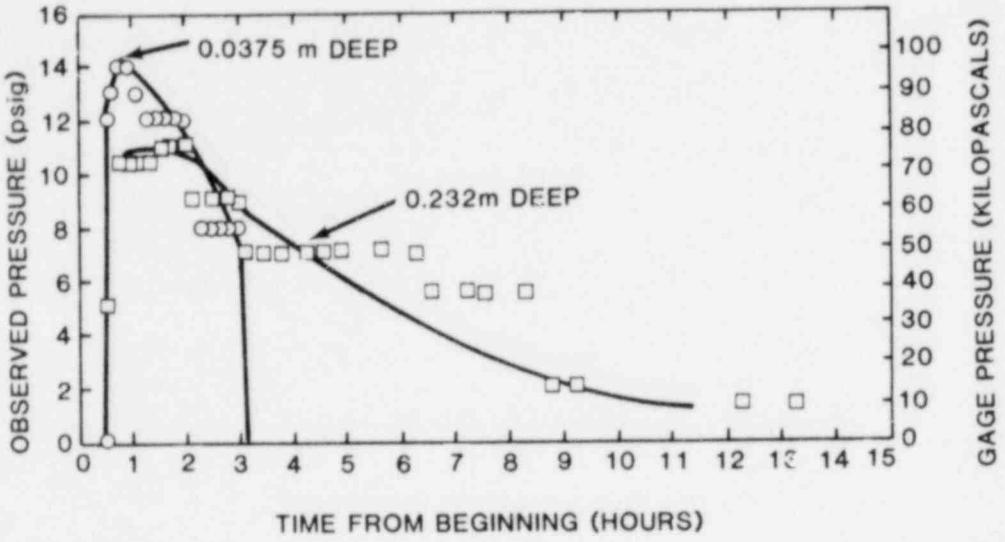

B) TEST WARD - 1

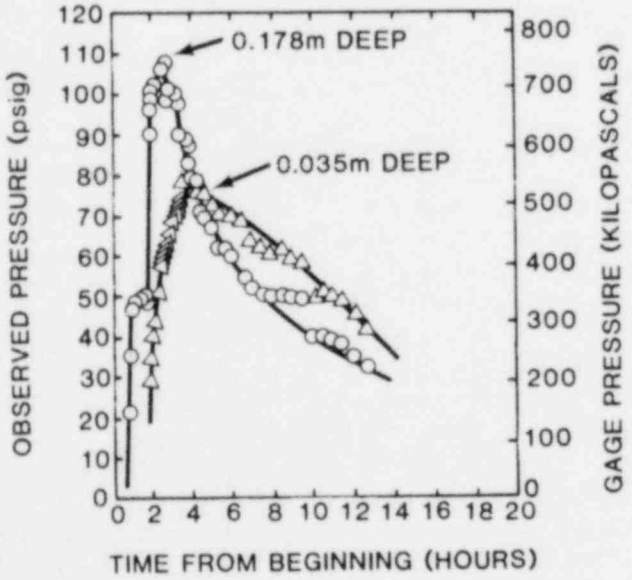

FIG. 9. PRESSURE WITHIN HEATED CONCRETE DETERMINED IN EXPERIMENTS AT THE HANFORD ENGINEERING AND DEVELOPMENT LABORATORY

FIG. 10. WATER, DRIVEN FROM THE HEATED CONCRETE, FLOWS THROUGH CRACKS THAT DEVELOPED DURING A MELT/CONCRETE INTERACTION

Table I-8. Kinetic Parameters for Concrete Decomposition*,≠

Reaction	Basaltic Concrete	Limestone-Common Sand Concrete	Generic Southeastern United States Concrete
Loss of evaporable water (n = 1)	E = 11.6 K = 4.4×10^{6}	E = 11.0 K = 1.29×10^{6}	E = 11.0 K = 1.29×10^{6}
Loss of chemical water (n = 1)	E = 41.9 K = 2.8×10^{12}	E = 40.8 K = 1.96×10^{12}	E = 40.8 K = 1.96×10^{12}
Decarboxylation (n = 1)	E = 42.6 K = 3.6×10^{9}	E = 38.5 K = 1.98×10^{7}	E = 45.8 K = 1.73×10^{9}
Decarboxylation (n = 2/3)	--- ---	E = 37.0 K = 3.6×10^{7}	E = 44.9 K = 1.94×10^{6}

*E in units of Kcal/mole; K in units of minutes $^{-1}$
≠Standard errors in E ∿ 10%; standard errors in K ∿ 30 to 50%

Prediction of gas generation during heating of concrete by melts has also been attempted.[49-51] The models used to make these predictions, as yet, do not include detailed descriptions of the concrete decomposition process. The simplified descriptions that are used are:

1) gas generation is defined by the stoichiometry of concrete eroded by the melt, or

2) decomposition of the concrete is determined by the propagation of isotherms into the concrete ahead of the melt and by thermodynamic criteria for gas release.

To date, the models consider gas generation only from concrete under attack by molten core materials. This feature, and the simplified descriptions of concrete, mean that the melt/concrete interaction models will yield predictions of gas generation that are lower bounds on the true gas generation during a reactor accident. Even the crude models of melt interaction with concrete that are currently available have shown that gases liberated during the interaction will eventually over-pressurize the reactor containment. The most serious uncertainty concerning these estimates is the time required for the generation of sufficient gas to cause over-pressurization.

Accurate estimates of the gas released from concrete during a meltdown accident cannot be made at present. Without adequate coupling between models of melt/concrete interactions and models of the concrete itself, estimates of the rates of gas release during reactor accidents are extremely speculative. The magnitude of the gas release can be illustrated by simplified calculations. Assume the following:

a) gas release is due solely to melt attack on concrete,

b) the complexities of the melt attack are neglected and the melt erodes a cylindrical cavity of uniform diameter,

c) the basemat is 3 meters thick and the containment volume is 5×10^4 m^3,

d) condensation of steam released from the concrete is neglected.

Using these assumptions, the pressure increase in containment may be computed as a function of cavity diameter, concrete type, and the mean temperature of the containment. Results are summarized below.

Cavity Diameter (ft)	Mean Containment Temperature (°C)	Increase in Containment Pressure Due to Attack On: Basaltic Concrete (psi)	Increase in Containment Pressure Due to Attack On: Limestone Concrete (psi)
20	27	6.9	15.8
25	27	10.8	24.7
30	27	15.6	35.6
20	100	8.6	19.6
20	140	9.5	21.8
20	200	10.9	24.9

These calculated increases in pressure are lower bounds on the amount of gas released. Significant radial erosion of the concrete or significant radiant or convective heating of concrete not in contact with the melt would increase the amount of gas release by factors of 2 or 3. Conduction of heat into concrete surrounding the melt could produce further increases in the gas release.

The pressure that actually develops in containment will depend on the composition of the gas (described in the following sections). If the gas contains significant amounts of steam which condenses, or if carbon monoxide and hydrogen react to form methane and coke, pressurization of the containment will be reduced.

I.5.2 Passage of Gases Through the Melt

Gases generated by the attack of the molten core material on concrete will enter the melt and react with it. The molten material will consist of fuel, fuel cladding, structural steel, and the condensed products of concrete decomposition. Water and carbon dioxide released from the concrete will readily oxidize metallic constituents of the melt. Some of the idealized reactions that can take place are listed in Table I-9. The gaseous products of these reactions are hydrogen and carbon monoxide. The feasibility of such oxidation reactions is demonstrated by the data plotted in Fig. 11. Equilibrium partial-pressure ratios (P_{H_2}/P_{H_2O}) and P_{CO}/P_{CO_2}), produced in the reaction of water and carbon dioxide with the major metallic constituents of the core melt, are plotted in this figure against temperature. If solution effects are neglected, zirconium will be preferentially oxidized from the melt. Once the zirconium has been depleted, chromium, iron, and nickel will be oxidized in that order. Both zirconium and chromium will completely convert carbon dioxide and water to carbon monoxide and hydrogen, respectively, if only thermodynamic factors control the reaction. As the amounts of CO and H_2 build in the gas stream, oxidation of iron and nickel will be inhibited. Moderately-reducing gas mixtures will reduce iron and nickel oxides to the respective metals.

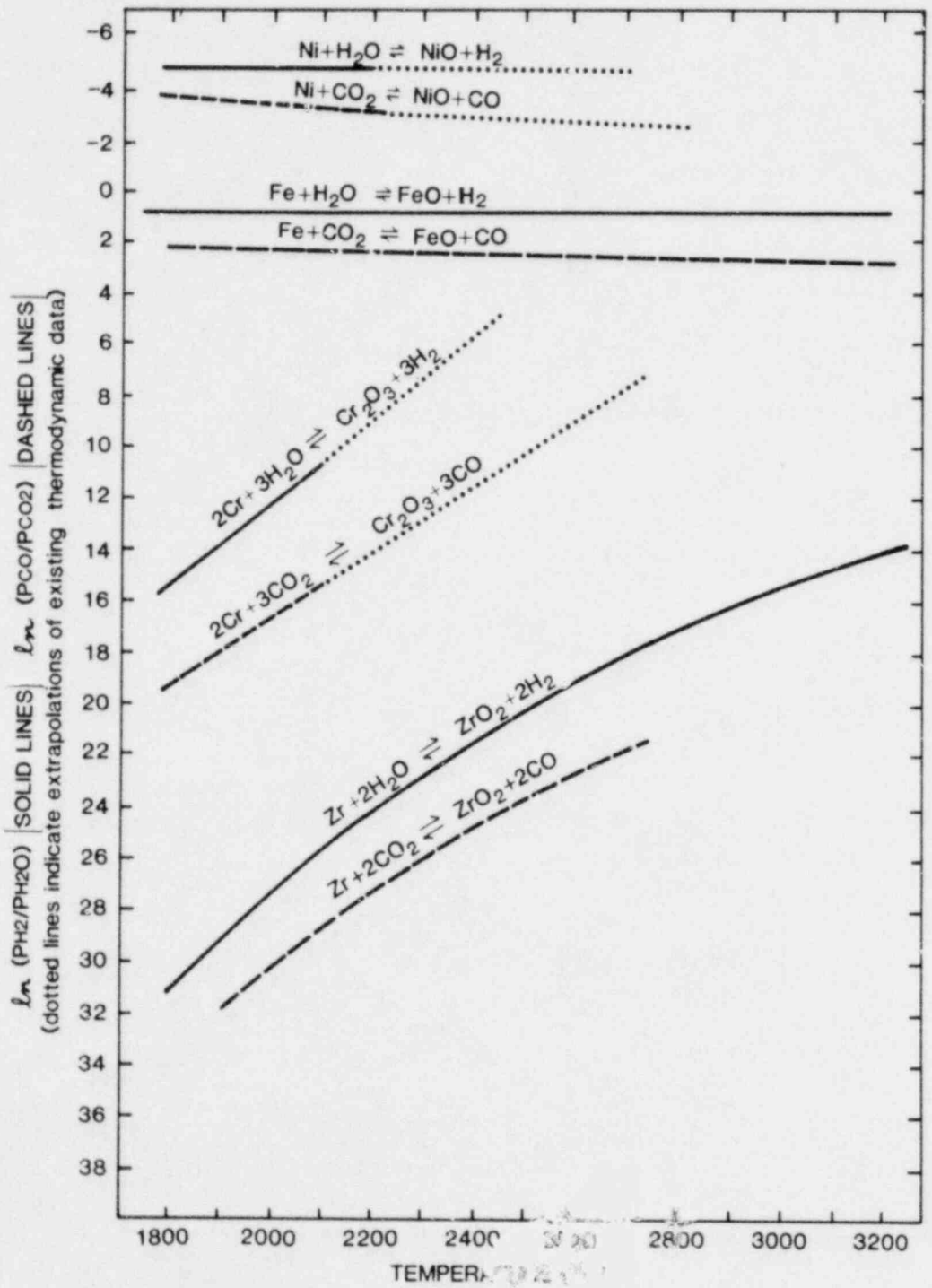

FIG. 11. EQUILIBRIUM GAS COMPOSITIONS FOR BINARY METAL / METAL - OXIDE PAIRS

Table I-9. Reactions of Gases with Metallic Melt Constituents

$$Zr(c) + 2H_2O(g) \longrightarrow ZrO_2(c) + 2H_2(g)$$

$$Zr(c) + 2CO_2(g) \longrightarrow ZrO_2(c) + 2CO(g)$$

$$2Cr(c) + 3H_2O(g) \longrightarrow Cr_2O_3(c) + 3H_2(g)$$

$$2Cr(c) + 3CO_2(g) \longrightarrow Cr_2O_3(c) + 3CO(g)$$

$$Fe(c) + xH_2O(g) \longrightarrow FeO_x(c) + xH_2O(g)$$

$$Fe(c) + xCO_2(g) \longrightarrow FeO_x(c) + xCO(g) \qquad x = 1 - 1.5$$

$$Ni(c) + H_2O(g) \longrightarrow NiO(c) + H_2(g)$$

$$Ni(c) + CO_2(g) \longrightarrow NiO(c) + CO(g)$$

$$Mo(c) + H_2O(g) \longrightarrow MoO_3(g) + 3H_2(g)$$

$$Mo(c) + 3CO_2(g) \longrightarrow MoO_3(g) + 3CO(g)$$

$$Ru(c) + yH_2O(g) \longrightarrow RuO_y + yH_2(g)$$

$$Ru(c) + yCO_2(g) \longrightarrow RuO_y + yCO(g) \qquad y = 1, 2, \text{ or } 4$$

$$Mn(c) + zH_2O(g) \longrightarrow MnO_z(c) + zH_2(g)$$

$$Mn(c) + zCO_2(g) \longrightarrow MnO_z(c) + zCO(g) \qquad z = 1 \text{ or } 2$$

Within the thermodynamic formalism and the assumption that alloy and solution effects on condensed-phase activities may be neglected, it is apparent that virtually complete conversion of CO_2 and H_2O to CO and H_2 will occur early in a core melt/concrete interaction. As the accident progresses, and if the H_2 and CO are not burned, the extent of CO_2 and H_2O reduction will decline. More sophisticated analysis including solution and alloy effects will result in similar conclusions, though the variation in CO and H_2 production over the course of the melt/concrete interaction will be much smoother.

Where the metallic phases are completely absent from the melt, some reduction of evolved CO_2 and H_2O to CO and H_2 would still occur. Evidence from studies of aerosol release during melt/concrete interactions[52] suggests that reactions such as:

$$UO_2(c) + H_2O(g) \longrightarrow UO_3(g) + H_2(g)$$

$$1/2Cr_2O_3(c) + 3/2H_2O(g) \longrightarrow CrO_3(g) + 3/2H_2(g)$$

will occur in the oxidic phases of a core melt. The thermodynamic favorability of these reactions is not nearly so strong as for gas reactions with metallic species. Consequently, the extent of reduction of the evolved gases would be less.

Note that none of the reactions cited above decrease the molecular amounts of gas. The less significant reactions in which both products of reaction are volatile (i.e., $Mo + 3H_2O \longrightarrow MoO_3 + 3H_2$) are not especially important for considerations here. Not only is there little of the condensed phase reactant present, but the oxidized product will condense when it emerges from the melt. More exotic

species that can form in the gas phase at the high temperatures of core melt such as OH, H, and C_2O have been neglected since they will disappear with only modest cooling of the gas. These reactions of gases, liberated from the concrete with the melt, preserve molecular amounts of the gas, but greatly increase its flammability.

Kinetics of gas reaction with the melt are indeed complex. They depend on gas generation rate, melt geometry, contact time, gas and melt composition, as well as temperature and pressure. No in-depth study of these kinetic factors, for specific application to reactor safety considerations, has yet appeared. Considerable analysis of similar processes has been conducted for metallurgical and chemical applications.[53] Considerations have been given to rate control by the following processes:

1) mass transfer in the melt,

2) chemical reaction at the melt/gas interface, and

3) mass transfer within the gas.

All these studies have been for slow flow of gas into a melt where each gas bubble is largely unaffected by neighboring bubbles. Unfortunately, gases enter the melt during melt/concrete interactions as streams of bubbles or even as jets of gas. These situations are formidable analytical and experimental problems.

To date there have been no experimental determinations of the real-time compositions of gases emerging from the melt during melt interactions with concrete. Gas compositions determined in experiments with such interactions have all been made after the gases have cooled or otherwise had the opportunity to chemically evolve. The compositions of these "aged" gas samples strongly suggest that the

extent of gas reaction with metallic species is largely controlled by the thermodynamics of the reactions. Composition data for gases that have passed through melts of varying depths, shown in Table I-10, suggest that the kinetic features of the reactions are not important except when the melt depth is less than 1-2 cm. These results are, however, not definitive. They may simply reflect similar equilibration of the gas with hot structures above the melt prior to or following sampling of the gas.

Table I-10. Experimentally Measured Gas Composition At Various Melt Depths

	Melt Depth				
SPECIES	1.9 cm	3.8 cm	3.8 cm	22 cm	22 cm
H_2 (v/o)	52	34.6	33.3	34.0	26.6
H_2O (v/o)*	ND	0.8	0.6	ND	ND
CO (v/o)	24	29.1	45.9	59.7	69.3
CO_2 (v/o)	24	35.5	20.8	6.3	5.2
CO/CO_2	1.0	0.82	2.21	9.48	13.3
H_2/C (observed)	1.08	0.54	0.50	0.52	0.36
H_2/C (calculated from concrete composition)	0.52	0.52	0.52	0.28	0.28

*Water content could not be detected in some samples of gas.

5.3 Evolution of Gases Above the Melt

When the gases from the concrete emerge from the melt they can continue to react. The critical feature of gas reaction above the melt is ignition. When the atmosphere above the melt is sufficiently oxidizing the hydrogen and carbon monoxide formed by reaction with the melt can burn as diffusional flames. Ignition limits for such diffusional flames have not been studied as much as have the limits of well-mixed flames. Noughton[54] investigated ignition of diffusional mixtures of helium and hydrogen. The ignition limits he found are shown in Fig. 12. Ignition was dependent on the temperature of the orifice used to dispense the gas mixture into the oxidizing medium. The ignition limits were insensitive to gas flow for flow rates between 200 and 470 cm^3/min.

These diffusional flammability limits suggest that prompt ignition of gases emerging from a melt is likely. This suggestion has been amply verified in tests of melt/concrete interactions conducted in the open air. However, tests of melt/concrete interactions have also shown that if gases evolved at higher flow rates are protected from the air until they have cooled to less than 150°C, they will not spontaneously ignite. Artificial ignition will, however, still lead to sustained flames.

Ignition of gases formed during interactions of core melt with concrete is likely when there is unrestricted access of air to the reactor cavity. The burning of the gases will reduce the molar content of gases in the reeactor containment due to the consumption of oxygen. Consumption of oxygen is no guarantee that pressure

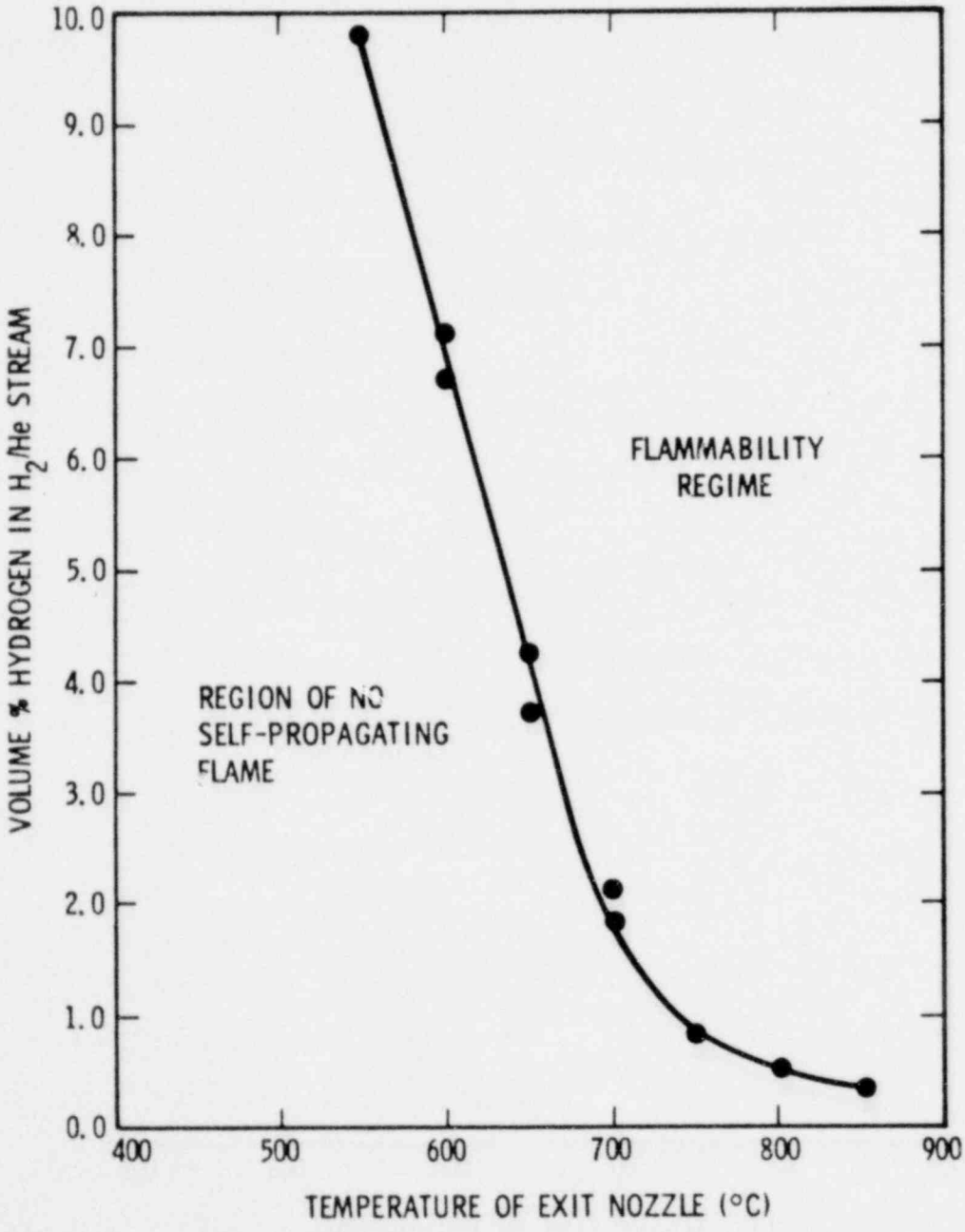

FIG. 12. LOWER FLAMMABILITY LIMITS OF HYDROGEN DIFFUSION FLAMES IN AIR

within containment will be less than in the unburned case, because the burning of the gases is quite exothermic.

When ignition is suppressed, the gases will still react though in a much less dramatic fashion. The nature of the reaction is determined both by thermodynamic and kinetic considerations. Gases, liberated at very high temperatures, will re-equilibrate as they cool according to the reaction:

$$H_2 + CO_2 \rightleftharpoons H_2O + CO \quad .$$

A critical observation in experimental studies of melt/concrete interaction is the tendency for this re-equilibration to proceed so that the fugacity of oxygen in the gas is buffered by the iron-Wustite (FeO_x) equilibrium. Note that at temperatures high enough to prevent condensation of water, re-equilibration according to this reaction does not change the molar amounts of gaseous species. When other reactions become important, reduction in the molar amounts of gaseous species can occur.

The calculated variations in gas composition with temperature, for two systems of varying elemental composition, are shown in Table I-11. As the gas cools, the hydrogen and carbon dioxide content of the gases increases at the expense of carbon monoxide and residual water vapor.* Experimental verification of this trend is at best

*At very high temperatures, exotic chemical species such as H, OH, O, C_2O, as well as ionized species develop in the gas phase. These species were neglected in the calculations.

inferential at present. Nevertheless, it seems likely that a thermodynamic analysis of gas composition is at least approximately correct for temperatures above 1500°C. Reaction kinetics in the gas phase at these temperatures are typically quite rapid.

As temperatures fall below 1000°K, additional reactions (coking and hydrogenation) become thermodynamically feasible. Coking is the precipitation of solid carbon from the gas. Hydrogenation is the reaction of gas constituents to form methane and even higher hydrocarbons. The effects of these reactions on the gas composition, as estimated from thermodynamic considerations, are also shown in Table I-11. Hydrogenation and coking sharply reduce the molar amounts of gas-phase species at temperatures less than 800°K. Coking can be significant only for gas having high initial concentrations of carbonaceous species such as gases produced in melt attack on calcareous concretes. Hydrogenation reactions were considered in the calculations only to the extent of methane formation. At low temperatures, methane becomes a significant constituent of the gas. Cooling of gases having high carbonaceous contents at high temperatures results in very nearly complete conversion of gaseous hydrogen to gaseous methane.

The coking and hydrogenation reactions should be quite sensitive to the pressure of the gas. Because these reactions reduce the molar amount of gas, the reactions should increase in significance with increases in pressure.

The above discussion of coking and hydrogenation has been based on the presumption that reactions in the gas phase are controlled

Table I-11. Variation in the Equilibrium Composition of Gases with Temperature

TEMPERATURE K	VOLUME % OF*					Moles Coke per Mole Carbon in the Initial Gas
	H_2	H_2O	CO	CO_2	CH_4	
300	- (93.3)	--- (-)	--- (-)	--- (-)	100 (6.7)	0.797 (-)
500	2.1	---	---	---	97.9	0.799
700	6.3	2.1	---	---	91.6	0.806
800	56.7	5.2	0.5	0.25	37.3	0.887
900	43.8 (82.7)	5.8 (11.0)	41.0 (1.6)	1.3 (0.5)	8.1 (4.4)	0.689 (-)
1200	23.4	8.3	58.7	11.2	---	---
1500	22.2 (66.9)	8.2 (27.3)	60.1 (5.1)	9.6 (0.8)	--- (-)	---
1800	20.0 (65.4)	8.8 (28.8)	63.7 (5.2)	7.4 (0.6)	--- (-)	--- (-)
2000	19.8	9.0	64.6	6.5	---	---

*Calculations were made by minimizing the free-energy of the gas mixture at 0.83 atms in contact with a large excess of iron and "FeO." Species that could develop in the system aside from Fe and FeO were C, CO, CO_2, CH_4, H_2, H_2O, and H. Atomic hydrogen did not become a significant constituent of the gas at any temperature.

Compositions listed without parentheses are for a gas with an H_2/C ratio of 0.406. Composition data listed within parentheses are for a gas with an H_2/C ratio of 16.0. A dash entry means the species constituted less than 0.1% of the gas.

solely by thermodynamic considerations. These reactions are known to be kinetically sluggish. Hydrogenation especially can occur at a significant rate only in the presence of a catalyst. Research on catalytic hydrogenation of carbon oxides is an active field. It is well known that nickel, cobalt, and iron will assist the hydrogenation reaction. Investigation of the catalytic activities of these metals in alloys present in a nuclear reactor has not been conducted. Methane and the higher hydrocarbons ethylene (C_2H_4) and ethane (C_2H_6) have been observed in tests of high-temperature melt/concrete interactions. Some evidence of coking has been observed in tests of melt interactions with calcareous concrete when the melts had temperatures in excess of 2400 K. Melts of temperatures below 2000 K do not seem to yield carbon precipitates during interaction with concrete.

I.5.4 Summary

The interaction of molten core materials with concrete in the reactor cavity will yield large quantities of gas. The gases liberated from the concrete are principally water and, especially for calcareous concretes, carbon dioxide. These gases will also be liberated from concrete not in contact with the melt by radiant or convective heating. Gases liberated from the concrete that pass through the melt will chemically react to form hydrogen and carbon monoxide. When these reduced gases emerge from the melt they may spontaneously ignite if sufficient oxygen is present. If the gases do not burn, they will continue to chemically evolve as they cool. If conditions suitable with respect to both kinetic and thermodynami considerations are reached, the chemical evolution of the gases will lead to the formation of hydrocarbons and possibly the precipitation of carbon from the gas.

I.6 SOLUBILITY OF HYDROGEN IN WATER

I.6.1 Introduction

The solubility of hydrogen in water is a simplified case of the more general problem of vapor-liquid equilibrium.[55,56] We will first present the simple theory that is valid when the gas phase can be considered as ideal (a mixture of perfect gases). Then we will introduce the more general thermodynamic theory of phase equilibrium that is needed to consider imperfect-gas effects.

Hydrogen is one of the least soluble gases. The concentration of dissolved hydrogen molecules will always be low compared to the concentration of liquid water molecules. Because of the low concentration of dissolved hydrogen and lack of chemical reaction between the dissolved hydrogen and the water, it is not surprising that the liquid solution is found to be "ideal." The concentration of dissolved hydrogen is linearly proportional to the partial pressure of hydrogen in the gas phase, if the gas phase is also ideal. A more general definition of an ideal solution, valid when the gas is not ideal, is found in the later section on the thermodynamics of phase equilibrium.

I.6.2 Simple Theory of Hydrogen Solubility

We assume that the liquid solution is ideal and that the gas phase is ideal. The mole fraction of hydrogen in the liquid obeys Henry's law,

$$P_{H_2} = H(T,P)X_{H_2} \qquad (16)$$

where P_{H_2} is the partial pressure of hydrogen in the gas, X_{H_2} is the mole fraction of hydrogen in the liquid, and H(T,P) is the Henry "constant." The Henry constant is a function of temperature and a weak function of pressure, but not a function of hydrogen concentration. For our simple-theory calculations we will ignore the effect of pressure on the Henry constant.

The total pressure, P, will be the sum of the hydrogen partial pressure, P_{H_2}, and the steam partial pressure, P_{H_2O}. To first approximation the steam partial pressure can be taken as equal to the saturation vapor pressure of water at the mixture temperature. The saturation vapor pressure of water can be found in nearly all thermodynamics books and in "Steam Tables." The hydrogen mole fraction in the liquid is then obtained using the equation

$$X_{H_2} = (P - P_{H_2O})/H(T) \ . \qquad (17)$$

I.6.3 The Henry Constant

The Henry constant for hydrogen dissolved in water has been measured over a wide range of temperature, and the agreement among several works reviewed by Anderson[57] is very good.[58-60] In Figures 13 and 14, the Henry constant is shown versus the reciprocal of the absolute temperature. As the temperature increases from room temperature, the solubility of hydrogen in water decreases up to a temperature of about 327 K (54°C). Note that decreasing solubility means increasing Henry constant, and vice versa. The solubility increases above 327 K. Himmelblau[58] developed curve fits for the Henry constant as a function of temperature. One very complex fit covered the entire temperature range. However, two linear fits given below cover a good part of the entire range. At low temperatures, between 0 and 25°C,

$$H = 21.13 \times 10^4 - 4.20 \times 10^7/T \qquad (18)$$

where H is in units of atm/mole fraction and T is in degrees Kelvin. Between 151 and 374°C, a similar curve fit applies,

$$H = -9.01 \times 10^4 + 5.83 \times 10^7/T \quad . \qquad (19)$$

Between 25 and 151°C, the relation between H and 1/T is not linear.

The Henry constant is a weak function of pressure. The Henry constants presented in Figs. 13 and 14 are presumably at the saturation pressure of water. At constant temperature but higher overall pressure, the Henry coefficient decreases. The relation is fairly accurately given by the Krichevsky-Kararnovsky equation,[55]

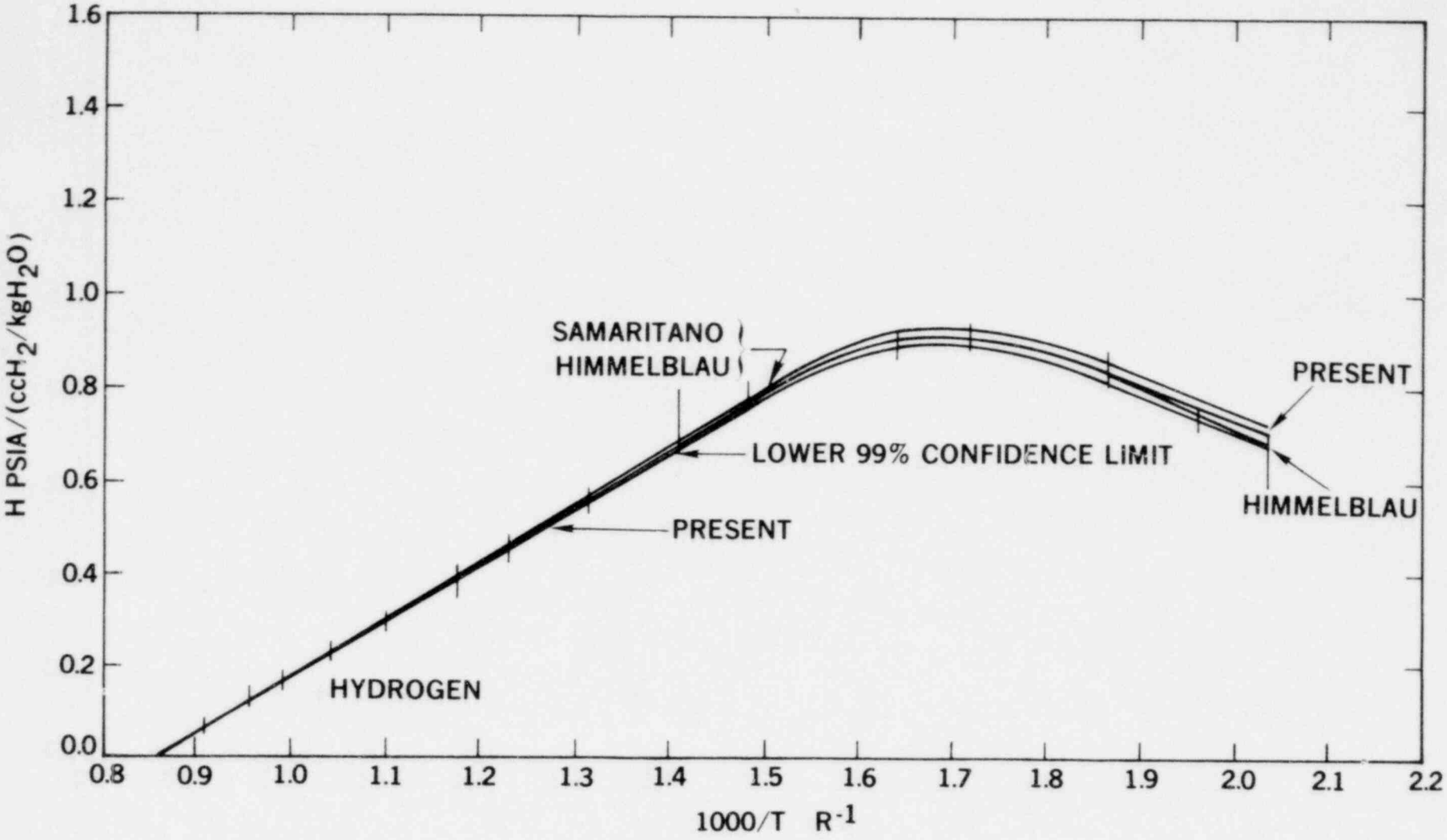

FIG. 13. COMPARISON OF HENRY CONSTANT VALUES FOR HYDROGEN IN WATER [57]

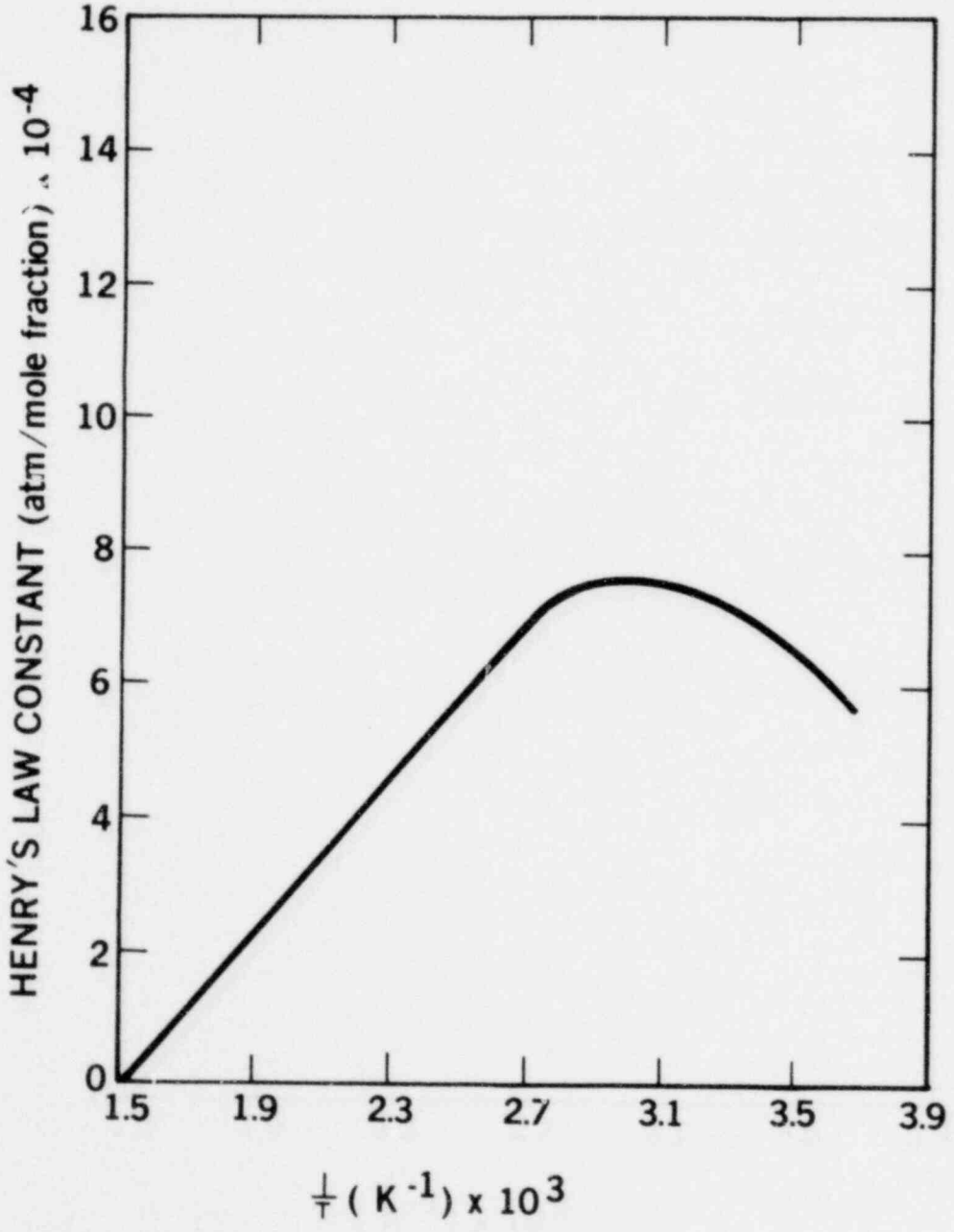

FIG. 14. HENRY CONSTANT FOR HYDROGEN IN WATER[58]

$$H(T,P) = H(T,P_s)\ \exp(v[P-P_s]/RT) \qquad (20)$$

where P_s is the vapor pressure of water, R is the universal gas constant, and v is the partial molar volume of hydrogen in water at infinite dilution. The partial molar volume at infinite dilution is the increase in volume of a water-hydrogen liquid solution, per mole of hydrogen added, when the hydrogen is very dilute in the mixture, so that each hydrogen molecule is surrounded by water molecules. Some representative values of v were obtained from measuring the slopes of the lines of Figure 15, taken from Reference 55. We have

$$\ln(f_{H_2}/X_{H_2}) = \ln(H[T,P]) = \ln H(T,P_s) + v(P - P_s)/RT \qquad (21)$$

Table I-12. Partial Molar Volume of Hydrogen in Water at Infinite Dilution

Temperature, °C	v cm^3/gm-mole
25	19.5
50	20.0
100	21.1

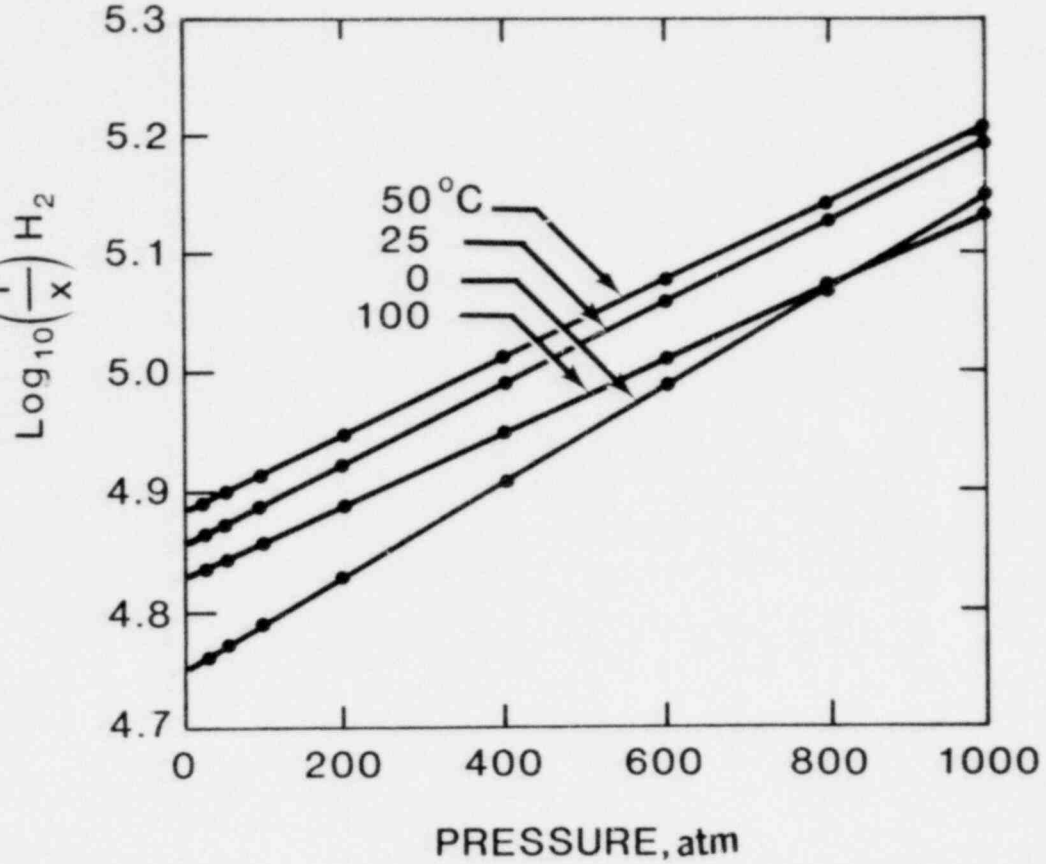

FIG. 15. FUGACITY OF HYDROGEN IN WATER[55]

I.6.4 General Thermodynamic Theory of Solubility

When either the gas or liquid phase is nonideal, the more general thermodynamic theory of phase equilibrium must be considered. Since all measurements indicate that the liquid phase solution of hydrogen in water is ideal, we need only consider the effects of gas nonideality. The details of the general theory are presented in the Appendix. Here we present a very short summary.

Most modern presentations of phase-equilibrium theory make use of the concept of fugacity. The fugacity has units of pressure. For an ideal gas, the fugacity of a component is equal to its partial pressure. The fugacity is the "escaping tendency" of a component to go from one phase to the other. At equilibrium the fugacity of each component in the gas must equal the fugacity of the component in the liquid,

$$f_i^L = f_i^V \tag{22}$$

where L indicates liquid and V vapor or gas. The fugacity of the gas component can be written in the form

$$f_i^V = Y_i P \phi_i \tag{23}$$

where Y_i is the mole fraction of component i in the gas, and ϕ_i is the fugacity coefficient. For an ideal gas, all the $\phi_i = 1$, and the partial pressures $P_i = Y_i P$. The deviation from unity of ϕ_i is an indication of imperfect-gas effects on phase equilibrium. The more general definition of an ideal solution is one in which the mole fractions in the liquid, X_i, are proportional to the gas-phase fugacities, f_i^V, rather than the partial pressures. P_i.

We have made a series of calculations of the results of the simple theory of solubility and the more general theory discussed above. The results are shown in Table I-13. The differences in the mole fraction of dissolved hydrogen predicted by the two theories are shown to be small. The agreement is surprising in view of the comparatively large deviations of the fugacity coefficient from unity. Himmelblau[58] commented that imperfect-gas effects could be neglected up to 1500-2000 psia (10 - 13 MPa). He stated that simply computing the fugacities without simultaneously considering the effect of pressure on the Henry constant would overestimate the imperfect-gas effects. Our results are in accord with Himmelblau's comments. Compensating effects make the simple theory valid over a wider range than a simple look at the values of fugacity coefficients would indicate.

Table I-13. Comparison of Hydrogen Solubility Computed by the Simple Theory and General Thermodynamic Theory

5 MPa (735 psia)

T,K	ϕH_2	ϕH_2O	General Theory $X_{H_2} \times 10^3$	Simple Theory $X_{H_2} \times 10^3$
300	1.029	.904	.718	.71
350	1.027	.929	.66	.66
400	1.026	.911	.83	.83
450	1.037	.854	1.02	1.02
500	1.117	.800	.89	.82

10 MPa (1470 psia)

T,K	ϕH_2	ϕH_2O	General Theory $X_{H_2} \times 10^3$	Simple Theory $X_{H_2} \times 10^3$
300	1.059	.824	1.40	1.43
350	1.053	.899	1.30	1.33
400	1.050	.882	1.68	1.71
450	1.052	.834	2.25	2.27
500	1.087	.767	2.74	2.67

Table I-13 (Continued)

20 MPa (2940 psia)

T,K	ϕH_2	ϕH_2O	General Theory $X_{H_2} \times 10^3$	Simple Theory $X_{H_2} \times 10^3$
300	1.117	.694	2.72	2.86
350	1.107	.796	2.56	2.66
400	1.099	.830	3.35	3.47
450	1.093	.803	4.62	4.77
500	1.105	.741	6.30	6.37

I.6.5 Useful Results of Hydrogen Solubility in Water

In Figures 16 and 17 we present calculated values of hydrogen solubility in water, based on the simple theory, as functions of temperature and pressure. They were obtained by first subtracting the vapor pressure of steam from the total pressure, Eq. 17. The mole fraction of hydrogen in the liquid shown in Figure 16 was obtained using Eq. 16 with the Henry constant obtained from Fig. 14. Hydrogen concentration in water is often reported in the form of cc hydrogen (at standard temperature and pressure) per kilogram of water. We obtained results in this form in Fig. 17 by use of Fig. 13.

Figures 4 and 5 show hydrogen solubility at constant pressure versus temperature as a series of curved lines. The solubility at constant pressure goes to zero at high temperatures because the vapor pressure of the steam approaches the total pressure, and there is no hydrogen left in the gas phase. The low-temperature minimum in the curves is due to the maximum in the Henry coefficient.

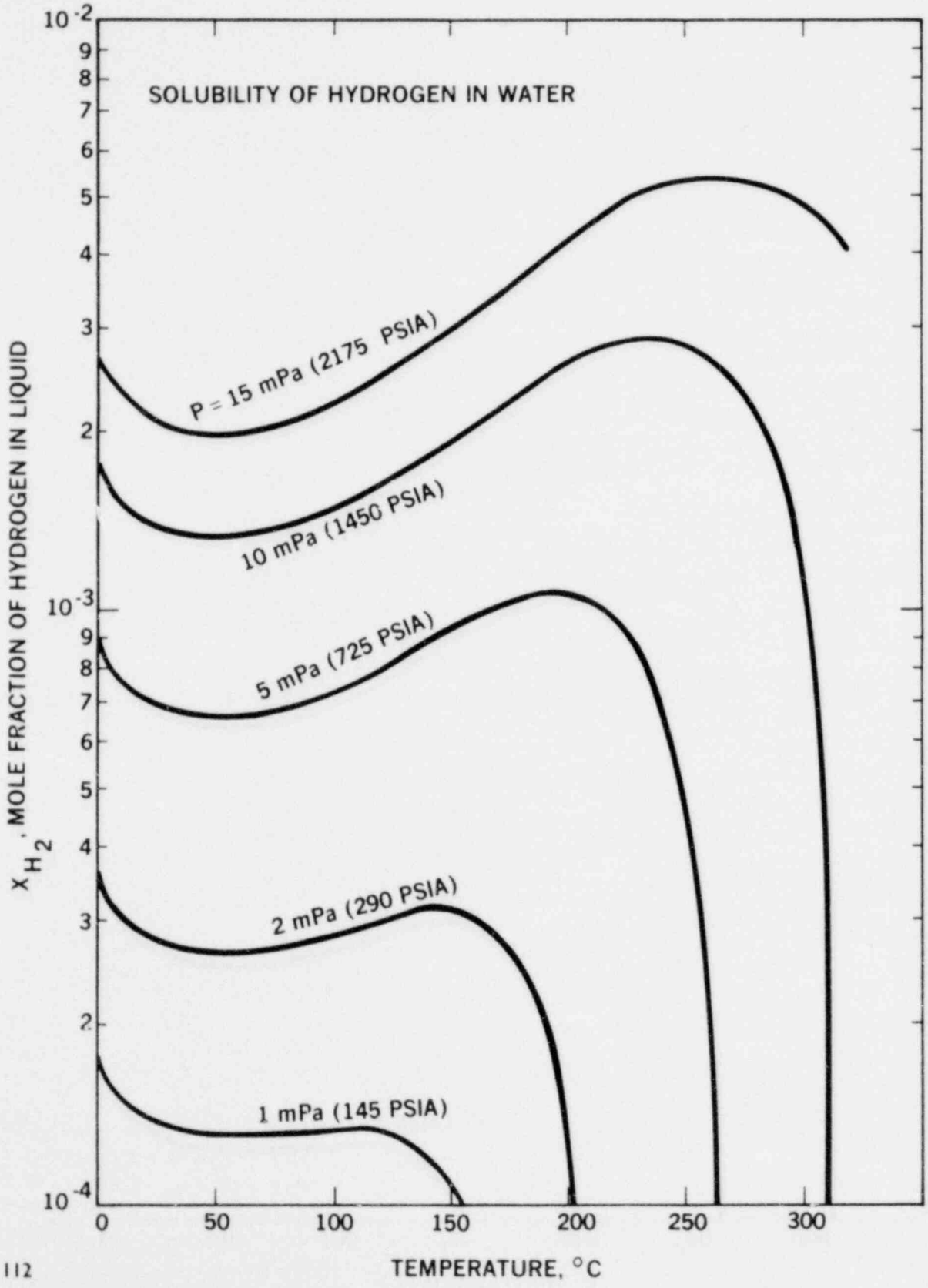
SOLUBILITY OF HYDROGEN IN WATER
P = 15 mPa (2175 PSIA)
10 mPa (1450 PSIA)
5 mPa (725 PSIA)
2 mPa (290 PSIA)
1 mPa (145 PSIA)
X_{H_2}, MOLE FRACTION OF HYDROGEN IN LIQUID
TEMPERATURE, °C
10^{-2}
10^{-3}
10^{-4}
0
50
100
150
200
250
300

FIG. 16.

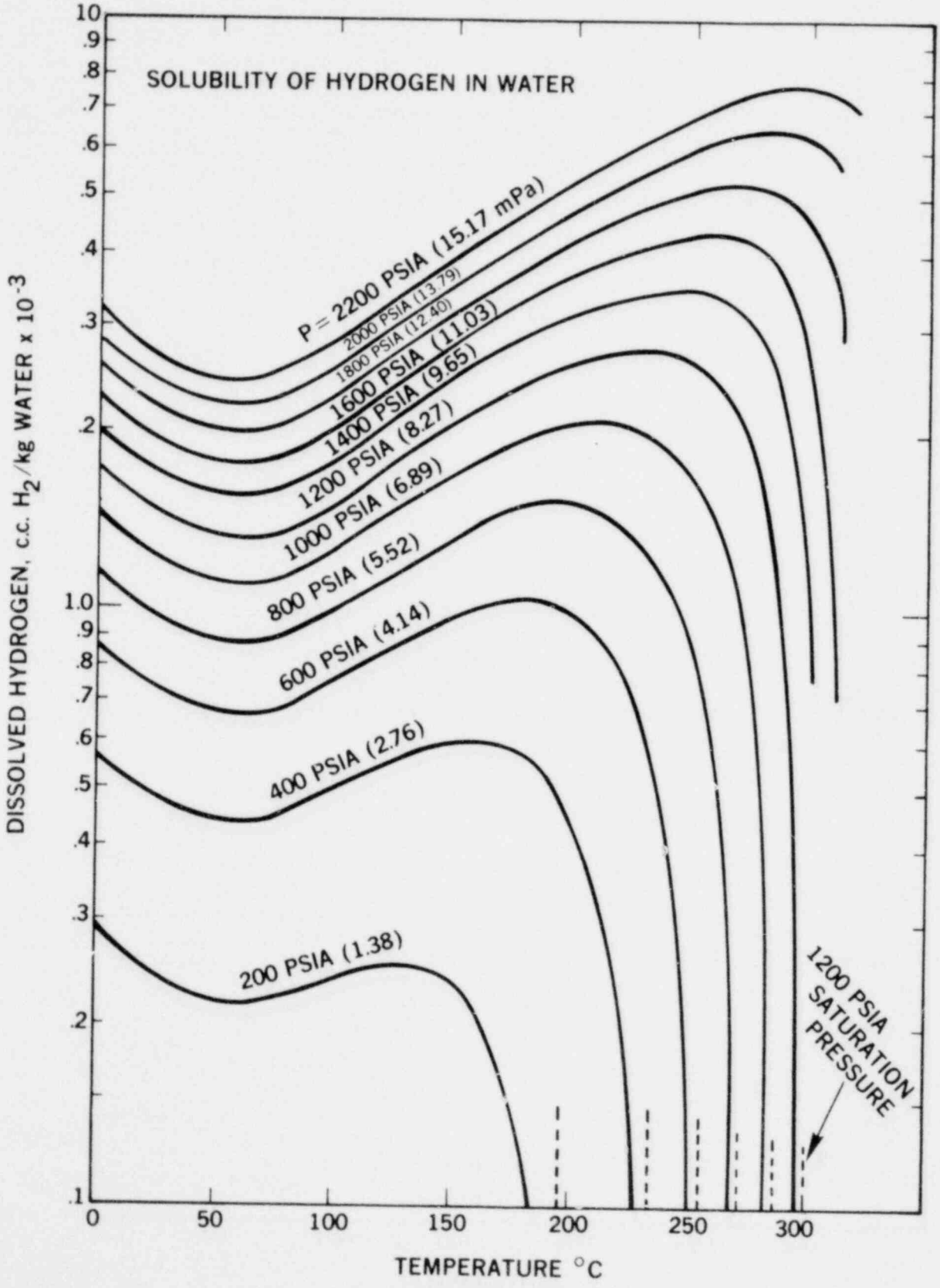
SOLUBILITY OF HYDROGEN IN WATER
DISSOLVED HYDROGEN, c.c. H_2/kg WATER x 10^{-3}
TEMPERATURE °C
P = 2200 PSIA (15.17 mPa)
2000 PSIA (13.79)
1800 PSIA (12.40)
1600 PSIA (11.03)
1400 PSIA (9.65)
1200 PSIA (8.27)
1000 PSIA (6.89)
800 PSIA (5.52)
600 PSIA (4.14)
400 PSIA (2.76)
200 PSIA (1.38)
1200 PSIA SATURATION PRESSURE
10
.9
.8
.7
.6
.5
.4
.3
.2
1.0
.9
.8
.7
.6
.5
.4
.3
.2
.1
0
50
100
150
200
250
300

FIG. 17.

I.6.6 Solubility of Hydrogen in Borated Water

Boric acid is used as a chemical shim in PWRs. In an accident, the concentration of boric acid might be increased to over 3000 ppm, corresponding to a mole fraction of about .001. In this section we will show that the presence of boric acid at 3000 ppm can be expected to give a small reduction in the solubility of hydrogen.

We have failed to find any reference dealing with the solubility of hydrogen in borated water. However, we can estimate the effect of boric acid on the solubility by a study of the effects of other dissolved electrolytes. There are data on the solubility of hydrogen in uranyl sulphate and uranyl fluoride solutions, presumably for application to homogeneous salt reactors.[61,62] Collections of data on solubility can be found in References 63 and 64. Most useful is the collection and organization of data on the effects of dissolved electrolytes on hydrogen solubility by Matzuka, Tanaka, and Majima.[65]

For many electrolytes the reduction in the hydrogen solubility is nearly linear with increasing electrolyte concentration at the low concentrations of interest.[65] The data on uranyl sulphate and uranyl fluoride show a nonlinear decrease in solubility, the reduction being most rapid for very low concentrations. We will examine the concentration required to cause a ten percent reduction in solubility. The concentrations required to cause other reductions in solubility can be inferred if the effect is assumed linear.

Matzuka, Tanaka, and Majima[65] have correlated the hydrogen solubility with the ionic size of the electrolyte cation and anion and with the concentration of ions. In Figures 18, 19, and 20 are shown the effects of the diameter of the cation on the solubility of

hydrogen in sulfate, chloride, and nitrate solutions. In Figure 21 is shown the effect of the diameter of the anion for different acids and sodium electrolytes. In all cases the concentration was 1 mol per liter, a mole fraction of .018, a temperature of 50°C, and a pressure of about 10 atmospheres. If boric acid, H_3BO_3, is similar in effect to sulfuric acid, then a mole fraction of about .02 gives a ten percent reduction in solubility. For uranyl sulphate a mole fraction of only .0007 gives a ten percent reduction in solubility. However, the ionic size of the UO_2^{2+} is large, and hence the small amount of electrolyte required to reduce the solubility is not out of line with the results of Figure 20.

Without experimental data on the solubility of hydrogen in borated water, the effect of the boric acid on the solubility of hydrogen is somewhat uncertain. However, it appears that based on the effects of other electrolytes, the reduction in solubility caused by the boric acid will be negligible or at most small.

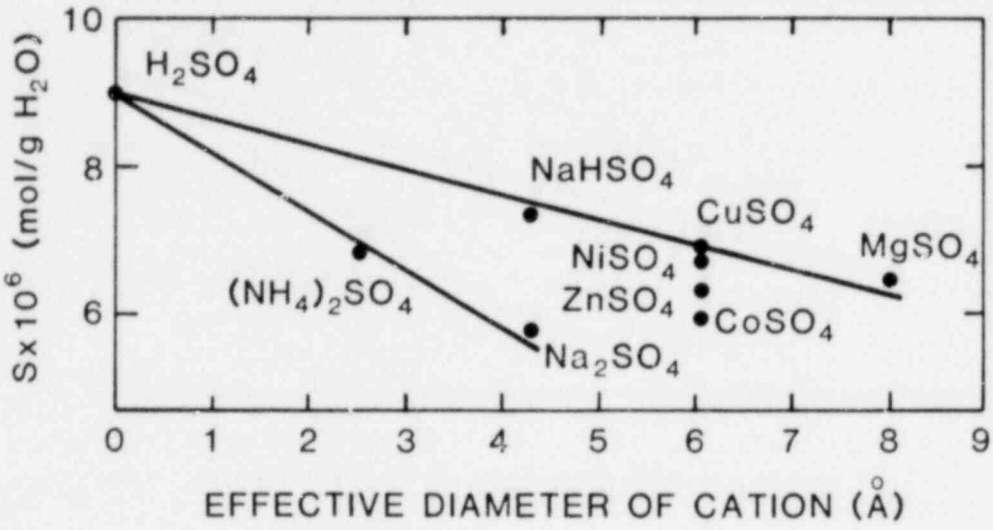

FIG. 18. SOLUBILITY OF HYDROGEN IN SULFATE SOLUTIONS[65]

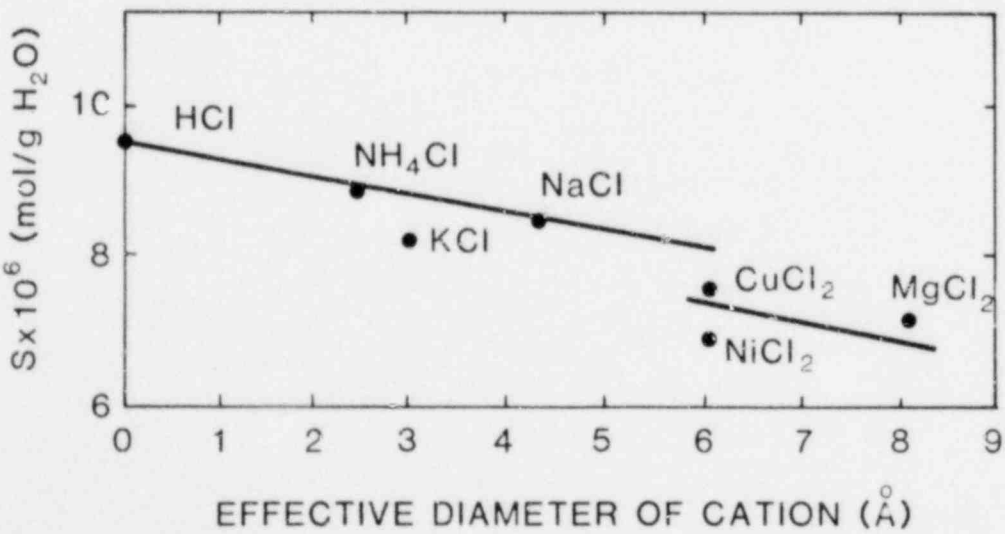

FIG. 19. SOLUBILITY OF HYDROGEN IN CHLORIDE SOLUTIONS[65]

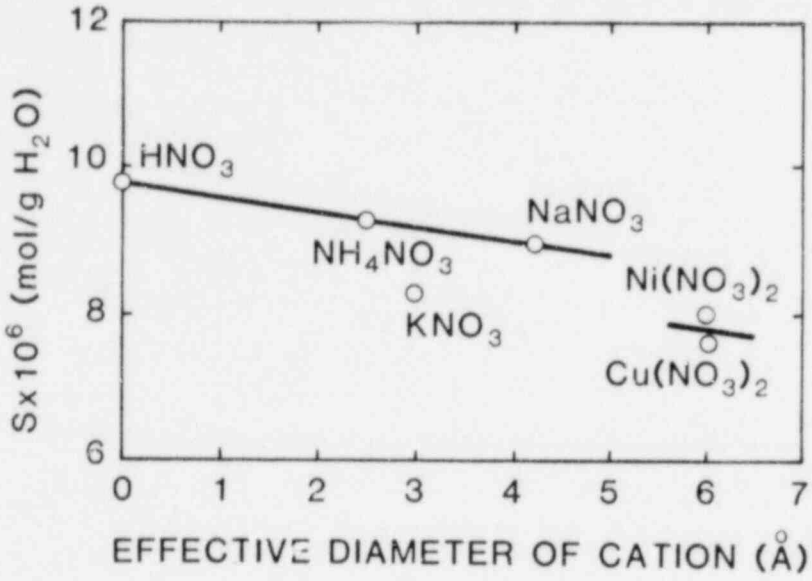

FIG. 20. SOLUBILITY OF HYDROGEN IN NITRATE SOLUTIONS[65]

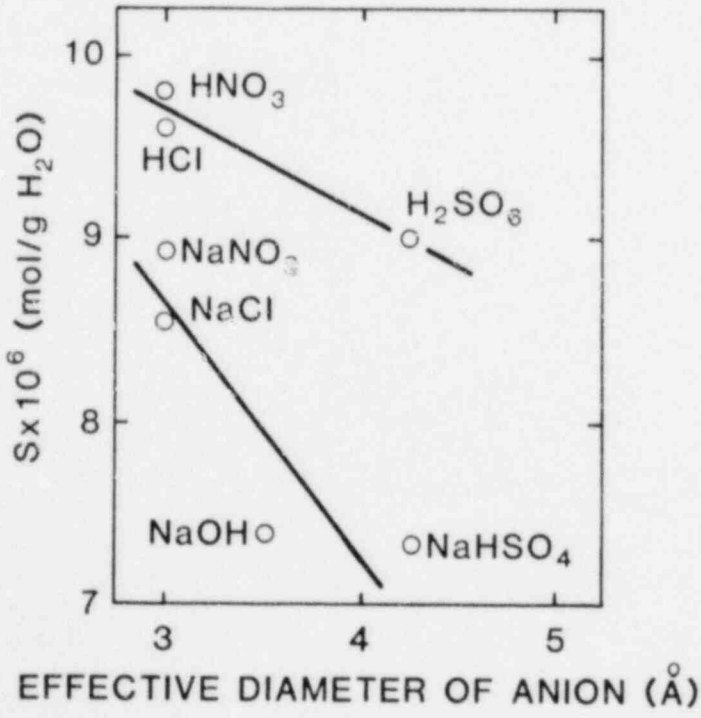

FIG. 21. DEPENDENCE OF HYDROGEN SOLUBILITY UPON ANION DIAMETER[65]

I.6.7 Kinetics of Solubility

Equilibrium saturation is usually obtained in solubility measurements by shaking the closed container of gas and liquid, or by bubbling the gas through the liquid. There appears to be an absence of literature on the rates of solubility applicable to reactor accident conditions. In the event of a hydrogen bubble in the reactor pressure vessel, as at TMI-2, we cannot estimate at what rate the coolant water in the reactor will become saturated with hydrogen. It is widely believed that because of the turbulent mixing between the cooling water and the hydrogen bubble,[66] equilibrium saturation will be attained. We have found no analysis or experiment to confirm this belief. In a scale model testing of the transport of hydrogen in a reactor coolant system, equilibrium saturation was not obtained.[67]

APPENDIX

General Thermodynamic Theory of Solubility

Consider a vapor-liquid mixture of n components. For thermal, mechanical, and component diffusive equilibrium between the two phases, we require

$$T^L = T^V \tag{9}$$

$$p^L = p^V \tag{10}$$

$$\mu_i^L = \mu_i^V \quad , \quad i = 1,\ldots,n \tag{11}$$

where the superscripts L and V indicate liquid and vapor (gas) respectively, T is the temperature, P is the pressure, and μ_i the chemical potential of component i. The chemical potential is defined in terms of the partical derivative of the Gibbs function (G = H - TS) with respect to the number of moles of component i (n_i), that is

$$\mu_i = \frac{\partial G}{\partial n_i}\Bigg|_{T,P,n_j,j \neq i} \quad . \tag{12}$$

It has become common with most chemists and chemical engineers to use the related idea of fugacity in place of chemical potential.

$$\mu_i - \mu_i^o = RT \ln(f_i/f_i^o) \quad . \tag{13}$$

The superscript o indicates the value at the standard state and the same temperature. It is easily shown[55] that Eqn. (9) becomes

$$f_i^L = f_i^V \quad . \tag{14}$$

The fugacity has units of pressure. In a mixture of perfect gases, the fugacity f_i^V is equal to the partial pressure of component i in the gas. We can think of fugacity as an "effective partial pressure" or "escaping tendency" of a component in a phase. Hence equality of fugacity in both phases means no net tendency of a component to move from one phase to the other.

In the liquid phase we write

$$f_i^L = X_i \lambda_i f_i^{oL} \tag{14}$$

where λ_i is the activity coefficient and f_i^{oL} is the fugacity of i in a standard state. For a solvent such as water, the standard state is taken to be pure water at the mixture temperature and pressure. For a solute such as hydrogen that cannot exist as a pure liquid at the liquid temperature, the standard state is that of infinite dilution,

$$f_{H_2}^{oL} = \lim_{X_{H_2} \to 0} \left[\frac{f_{H_2}^L}{X_{H_2}} \right] . \tag{15}$$

In ideal solution, in the general theory, is one in which all the activity coefficients are independent of composition of the liquid. For hydrogen this gives Henry's law,

$$f_{H_2}^L = H(T,P) X_{H_2} , \tag{16}$$

as a generalization of Eq. (1) which applies only when the gas is ideal.

In the gas phase we write

$$f_i^V = Y_i \phi_i P_i \qquad (17)$$

where Y_i is the mole fraction of component i in the gas, ϕ_i is the fugacity coefficient of i, and P_i is the partial pressure of i. For an ideal mixture all the fugacity coefficients are unity. Our computation of the effects of imperfect gas mixtures on the solubility mostly means computation of the fugacity coefficient of hydrogen and steam as a function of temperature and pressure. Given the temperature and gas composition, we can determine the pressure and liquid composition from the solution of Eqs. 10, 12, 13, and an equation of state for the gas.

Computation of the Fugacity Coefficients

There is no completely satisfactory way to compute the fugacity coefficients. The use of the truncated virial equation of state is recommended for cases in which the gas is not too far from perfect,[55,56]

$$PV/RT = Z = 1 + B/V \qquad (18)$$

where $B = \sum_i^N \sum_j^N Y_i Y_j B_{ij}$ and V is the molar volume.

The coefficients for the pure components, the B_{ii}, can be determined fairly accurately by the methods of Reference 56. The cross coefficients, the B_{ij} if $i \neq j$, are less accurately computed by other methods of Reference 56. The fugacity coefficients and compressibility are expressed in terms of the virial coefficients as follows,

$$\ell n\phi_i = \frac{2}{V} \sum_{j=1}^{N} Y_j B_{ij} - \ell nZ \qquad (19)$$

$$Z = 1 + \frac{1}{V} \sum_{i}^{N} \sum_{j}^{N} Y_i Y_j B_{ij} \qquad (20)$$

Method of Computation Using the General Thermodynamic Theory

The computations for Table I-13 were carried out for a given set of temperature values. At a given temperature, the coefficients in the virial equation were computed. The mole fraction of hydrogen and steam in the gas were selected to be equal to that in the simple theory calculations. The computation then involves finding the presure nd liquid mole fractions of water and hydrogen corresponding to the given temperature and gas mole fractions.

The following two equations were solved iteratively for P and X_2,

$$\phi_2 Y_2 P = X_2 H(T) \exp[V_2(P-P_s)/RT] \qquad (21)$$

$$\phi_1 Y_1 P = (1-X_2) P_s \phi_1 \exp[V_1(P-P_s)/RT] \qquad (22)$$

where the subscript 2 indicates hydrogen and the subscript 1 indicates water (steam). To obtain a solution at a given pressure, the gas phase mole fraction was varied until the solution of the above two equations for P was close to the desired value.

REFERENCES FOR SECTION I

1. A. S. Benjamin, D. J. McCloskey, D. A. Powers, S. A. Dupree, "Spent Fuel Heatup Following Loss of Water During Storage," NUREG/CR0649 SAND77-1371, March 1979.

2. C. T. Walters, J. M. Genco, "NURLOC-1.0 A Digital Computer Program for Thermal Analysis of a Nuclear Reactor Loss of Coolant Accident," BMI-1807, July 6, 1967.

3. S. S. Iyer, "ECCSA-I: A Digital Computer Program for Thermal and Hydraulic Analysis of Core Channels in the Event of a Nuclear Reactor Loss-of-Coolant Accident," BMI-1832, (1968).

4. P. Cybulskis, W. A. Carbuiner, R. E. Holmes, R. A. Cudmip, "Application of the ECCSA-4 and MUCHA Computer Codes to Emergency Core Cooling Analysis" Trans. Am. Nucl. Soc. 12, 353 (1969).

5. R. E. Pawel, J. Electro Chem. Soc. 126, 1111-1118 (1979).

6. R. R. Biderman, et al., "A Study of Zircaloy-4-Steam Oxidation Reaction Kinetics, "EPEI NP-734, April 1972.

7. R. E. Westerman, G. M. Hesson and C. R. Hann, "Zircaloy Cladding ID/OD Oxidation Studies," Final Report, EPRI NP-525 November 1977.

8. R. G. Ballinger, W. G. Dobson, and R. R. Biederman, "Oxidation Reaction Kinetics of Zircaloy-4 in an Unlimited Steam Environment," J. of Nucl. Matls. 62:213-220, 1976.

9. High Temperature Material Progress Report, No. 54, Part A, GE-NMPO, GEMP-54A. High temperature oxidation results reported by G. J. Scatena, "Fuel Cladding Embrittlement During a Loss-of-Coolant-Accident," NEDO-10, 674, October 1972.

10. L. Baker and L. C. Just, "Studies of Metal-Water Reactions at High Temperatures. III. Experimental and Theoretical Studies of the Zirconium-Water Reaction," ANL-6548, May 1962.

11. S. Leistikow, H. V. Berg, and D. Jennert, "Comparative Studies of Zircaloy-4 High Temperature Steam Oxidation Under Isothermal and Temperature Transient Conditions," CNSI Specialist Meeting on Behavior of Light Water Reactor Fuel Elements under Accident Conditions, Spating, Norway, September 13-16, 1976.

12. S. Kawasaki, R. Furuta, and K. Honma, "Inner Surface Oxidation of a Fuel Cladding for LWR under a LOCA," CNSI Specialist Meeting on Behavior of Light Water Reactor Fuel Elements under Accident Conditions, Spating, Norway, September 13-16, 1976.

13. Brown, A. F. and Healy, R., "The Kinetics of Total Oxygen Uptake in Steam Oxidized Zircaloy-2 between 1000°C-1400°C," RD/B/N4117, Central Electricity Generating Board, Berkeley, United Kingdom, September 197.

14. Cathcart, J. V. Pawel, R. E., McKee, R. A., Druschel, R. E., Yurek, G. J., Campbell, J. J., and S. H., "Zirconium Metal-Water Oxidation Kinetics IV. Reaction Rate Studies," ORNL/NUREG-17, Oak Ridge National Laboratory, Oak Ridge, Tennessee, August 1977.

15. Suzuki, M., Kawasaki, S., and Furuta, T., "Zircaloy Steam Reaction and Embrittlement of the Oxidized Zircaloy Tube Under Postulated Loss-of-Coolant Accident Conditions," JAERI-M 6879, Japanese Atomic Energy Research Institute, Tokai, Japan (NUREG-tr-0014), January 1977.

16. Urbanic, V. F. and Heidrick, T. R., "High Temperature Oxidation of Zircaloy-2 and Zircaloy-4 in Steam," Journal of Nuclear Materials, Vol. 75, 1978, pp. 251-261.

17. R. E. Wilson, et al., Isothermal Studies of the Stainless Steel-Steam Reaction, pp. 150-153 in Chem. Eng. Div. Semi-Annual Progress Rept., July-Dec. 1965, USAEC Rept. ANL-7125, Argonne National Laboratory, May 1966.

18. G. F. Lien (ed), "Superheater Alloys in High Temperature High Pressure Steam," ASME, N.Y. (1968).

19. J. T. Bittle, L. H. Sjodahl, J. F. White, "Oxidation of 304L Stainless Steel by Steam and by Air," Corrosion NACE Vol. 25, No. 1 January 1969.

20. A. O. Allen, The Radiation Chemistry of Water and Aqueous Solutions, Van Nostrand-Reinhold, New York 1961.

21. T. H. Row, L. F. Parsly, and H. E. Zittel, "Design Considerations of Reactor Containment Spray Systems" - Part I, ORNL-TM-2412, Oak Ridge National Laboratory, April 1969.

22. S. E. Turner, "Radiolytic Decomposition of Water in Water-Moderated Reactors Under Accident Conditions," Reactor and Fuel-Processing Technology, 12(1), Winter 1968-1969: 6679.

23. P. Cohen, Water Coolant Technology of Power Reactors (Chapter 4), Gordon and Breach, New York 1969.

24. P. Rodder and H. Geiser, Kerntechnik 19. Jahrgang, No. 11, 473-477 (1977).

25. R. M. Wilson and B. C. Slifer, "Hydrogen Generation and the General Electric Boiling Water Reactor," NEDO-10723 (Licensing Topical Report), Feb. 1973.

26. Dresden Nuclear Power Station Unit 3, Amendment 23, "Hydrogen Generation in a Boiling Water Reactor," Commonwealth Edison Company (post 1970).

27. M. Koike, E. Tachikawa, and T. Matsui, "Gamma-Radiolysis of Aqueous Boric Acid Solution," Journal of Nuclear Science and Technology, 6(4), April 1969: 163-169.

28. W. B. Cottrell, "Nuclear Safety Program Annual Progress Report for Period Ending December 31, 1967," ORNL-4228, Oak Ridge National Laboratory, April 1968.

29. H. E. Zittel, "Radiation and Thermal Stability of Spray Solutions, in ORNL Nuclear Safety Research and Development Program Bimonthly Report for November-December 1968," ORNL-TM-2479, Oak Ridge National Laboratory, March 1969.

30. M. J. Bell, J. E. Bulkowski, and L. F. Picone, "Investigation of Chemical Additives for Reactor Containment Sprays," WCAP-7153-A, Westinghouse Electric Corporation, April, 1975.

31. E. Hayon and M. Moreau, Reaction Mechanism Leading to the Formation of Molecular Hydrogen in the Radiation Chemistry of Water, The Journal of Physical Chemistry, 69(12) December 1965: 4058-4062.

32. E. Peled and G. Czapski, "Studies on the Molecular Hydrogen Formation $G(H_2)$ in the Radiation Chemistry of Aqueous Solutions," The Journal of Physical Chemistry, 74(15), 1970: 2903-2911.

33. H. E. Zittel, "Radiation and Thermal Stability of Spray Solutions, in ORNL Nuclear Safety Research and Development Program Bimonthly Report for November-December 1970," ORNL-TM-3263, Oak Ridge National Laboratory, March 1971.

34. H. E. Zittel, "Radiation and Thermal Stability of Spray Solutions, in ORNL Nuclear Safety Research and Development Program Bimonthly Report for September-October 1970," ORNL-TM-3212, Oak Ridge National Laboratory.

35. H. E. Zittel, "Radiation and Thermal Stability of Spray Solutions, in ORNL Nuclear Safety Research and Development Program Bimonthly Report for March-April 1971," ORNL-TM-3411, Oak Ridge National Laboratory.

36. H. E. Zittel, "Radiation and Thermal Stability of Spray Solutions, in ORNL Nuclear Safety Research and Development Program Bimonthly Report for January-February 1971," ORNL-TM-3342, Oak Ridge National Laboratory.

37. DiNunno, J. J., et al., "Calculation of Distance Factors for Power and Test Reactors," TID 14844, March 23, 1962.

38. H. E. Zittel, "Post-Accident Hydrogen Generation from Protective Coatings in Power Reactors," Nuclear Technology, February 17, 1973: 143-146.

39. D. Van Rooyen, memorandum, Brookhaven National Laboratory, April 7, 1978.

40. NUS Report; NUS: CD-SET-112, March 1977.

41. Franklin Institute Report: F-C 2928, January 1971 (Wachtell); also F-C 4290, August 1976 (Carfango, et al.).

42. Westinghouse Report: WCAP 8776, Undated, (Burchell and Whyte).

43. J. R. Lopata, "Control of Containment H_2 Levels Evolved from Zinc Primers During a LOCA," in Power Engineering November 1974: 48-51.

44. H. F. W. Taylor (ed.) The Chemistry of Cements, Academic Press, 1964.

45. D. A. Powers, "Empirical Model for the Thermal Decomposition of Concrete," Trans. Amer. Nucl. Soc. 26 400 (1977)

46. J. D. McCormak, A. K. Postma and J. A. Schur, Water Evolution From Heat Concrete, HEDL-TME-78-87, February 1979.

47. A. Dyan COWAR-2 User's Manual - Thermohydraulic Behavior of Heated Concrete, GE-FBRD-GEFR-00090 (L), May 1977.

48. J. V. Beck and R. L. Knight, User's Manual for USINT - A Program for Calculating Heat and Mass Transfer in Concrete Subjected to High Heat Fluxes, NUREG/CR-1375, SAND75-1694, May 1980.

49. W. B. Murfin, A Preliminary Model for Core/Concrete Inter-Actions, SAND77-0370, July 1977.

50. M. Reimann and W. B. Murfin, "Calculations for the Decomposition of Concrete Structures by a Molten Pool," Proc. Post Accident Heat Removal Information Exchange Meeting, Ispra, Italy, October 10-12, 1978.

51. R. Kumas, L. Baker, Jr. and M. G. Chasanov, "Ex-Vessel Considerations in Post Accident Heat Removal," Chapter 5 ANL/RAS74-29, October 1974.

52. D. A. Powers, "Influence of Gas Generation on Melt/Concrete Interactions," IAEA Symposium on Therm. of Nucl. Matls. Julich, Fed. Rep. of Germany, 1979.

53. F. D. Richardson, Physical Chemistry of Melts in Metallurgy Vol. 2, Academic Press (1974).

54. J. J. Noughton, Geochemica et Cosmochimica Acta 37 1163 (1973).

55. J. M. Prausnitz, Molecular Thermodynamics of Fluid-Phase Equilibria, (Englewood Cliffs; Prentice Hall, 1969).

56. J. M. Prausnitz, C. A. Eckert, R. V. Orye, and J. P. O'Connell, Computer Calculations for Multicomponent Vapor-Liquid Equilibria, (Englewood Cliffs: Prentice Hall, 1967).

57. T. S. Anderson, "Correlation of Solubility Data for Hydrogen and Nitrogen in Water," Trans. Amer. Nuclear Soc., 10:507-508, 1967.

58. D. M. Himmelblau, "Solubilities of Inert Gases in Water," J. Chem. Eng. Data, 5:10-15 (1960).

59. I. J. Samaritano, "Equilibrium Solubility of Hydrogen and Nitrogen in Water at High Temperatures, "KAPL-M-6419, (CSA 33) UC4, Knolls Atomic Power Lab., (Oct. 1964).

60. W. L. Sibbett and A. R. Lyle, The Solubility of Gases in Water, N-3-653, TIO 5883, Los Alamos Sci. Lab.

61. H. A. Pray and E. F. Stephan, The Solubility of Hydrogen in Uranyl Sulphate Solutions at Elevated Temperatures, BMI-870, (Columbus: Battelle Mem. Inst., 1953).

62. H. A. Pray and E. F. Stephan, The Solubility of Oxygen and Hydrogen in Uranyl Fluoride Solutions at Elevated Temperatures, BMI-897, (Columbus: Battelle Mem. Inst., 1954).

63. A. E. Markham and K. A. Kobe, "The Solubility of Gases in Liquids," Chem. Revs., 28:519-588, 1941.

64. R. Battino and H. L. Clever, "The Solubility of Gases in Liquids," Chem. Revs., 66:395-463, 1966.

65. K. Matsuka, T. Nobuhiro and H. Majima, "Dissolution Behavior of Hydrogen Gas in Aqueous Solutions Containing Strong Electrolytes," Nippon Kogyo Kaishi, (J. Min. Metall. Inst. Jpn.) 94:44-48, 1978 (Trans. from Japanese for Sandia National Labs., April 1980).

66. EPRI Meeting on Hydrogen Hazards on Nuclear Reactors, EPRI Hdq., Palo Alto, March 1980.

67. R. E. Billings, et al., Three Mile Island Reactor Simulation Final Report, (Provo: Billings Energy Corp., April 1979).

II. HYDROGEN AND OXYGEN DETECTION SYSTEMS

In order to intelligently control both normal and post-accident operations of nuclear power plants, it is imperative that instrumentation be available to monitor the gas composition in the reactor vessel and the containment building. The purposes of this chapter are:

- to survey the state-of-the-art in gas detection,
- to describe the design characteristics of H_2 and O_2 detection systems, and
- to determine areas for possible additional development.

The gas detection requirements for the reactor vessel and for the containment building in general are sufficiently different to require separate discussion.

II.1 Survey of Existing Hydrogen Detectors

Several excellent surveys of hydrogen detection hardware are already in existence.[1,2] Reference 2 is a monograph which discusses the general principles of gas analysis, while Reference 1 is devoted to a survey of existing (in 1970) methods for analysis of hydrogen in air.

The existing techniques which are most applicable to the problem at hand depend primarily on the physical or chemical properties of hydrogen. These properties include thermal conductivity, density, reactivity with metals, and electrochemical behavior. Each of these is discussed briefly here. A more complete discussion is given in Reference 1 and the literature cited therein.

Thermal conductivity detectors are based on the different rates of cooling of heated wires exposed to air with and without an admixture of hydrogen. These wires may form two legs of a Wheatstone bridge so that very small differences in temperature (and thus resistance) can be detected. Estimates of the sensitivity of these techniques range from 5×10^{-4}% to 0.1% H_2 in the air.

Gas density measurements are based on the use of a mechanical principle in which air with and without hydrogen is used to drive the vanes of an impulse wheel. The difference in torque generated with and without admixed gas is a measure of the density. Under ideal conditions, sensitivities $\sim 5 \times 10^{-3}$ H_2 in air have been measured.

Chemical reactivity tests are based on the fact that hydrogen will react exothermally with palladium or such transition metals as titanium to release heat. The heat released can be measured, for example, by the change in resistance of a wire in a Wheatstone bridge arrangement.

As is well known, the electrical resistance of hydride-forming metals changes as a function of hydrogen concentration and hence of local hydrogen partial pressure. In 1963, the Bendix Corporation fabricated prototypes of a detector based on this principle under NASA contract,[3] but the concept was never commercialized. More recently, the same physical effect has been used to develop metal-insulator-semiconductor (MIS) diodes with a palladium gate.[4] The change in electrical conductivity of the palladium allows this device to provide a signal which is a quantitative measure of H_2 partial pressure in air. Provided that a device can be made which is sufficiently radiation hard, this concept may be very attractive.

Another technique which can generate an electronic signal is based on the electrochemical oxidation of H_2 molecules to two protons. Briefly, the principle of operation is that H_2 gas enters an electrolytic cell via a permeable membrane which is in close contact with a platinum anode. The hydrogen is electrochemically oxidized at the anode, and the current thus generated is a measured of the external H_2 partial pressure.

Table II-1 gives a list of techniques and detectability levels for H_2 in air under laboratory conditions, as taken from Reference 1.

Table II-1

Several H_2 Detection Techniques and Their Sensitivities

Technique	Sensitivity (Mole % in air)
Thermal Conductivity	5×10^{-4}
Gas Density	5×10^{-3}
MIS Gate	?
Electrochemical	0.05

II.2 Desired Characteristics and State of the Art of H_2 and O_2 Detection Systems in the Reactor Vessel

Even during normal operation of water-cooled reactors, radiolysis of water generates some quantities of hydrogen and oxygen. It has long been a standard practice in PWR's to deliberately dissolve hydrogen in the coolant (at $\sim$3 ppm) to provide for rapid recombination of radiolytically-generated, oxygen-bearing species. This procedure prevents the generation of a flammable hydrogen-oxygen mixture during normal reactor operation. Thus, current regulations require only analysis for hydrogen in the reactor vessel. Current practice is to obtain an indirect measurement of hydrogen in the reactor vessel by sampling and analyzing the coolant. A standard measurement technique is to extract a sample of the pressurized coolant, and then to measure the amount of hydrogen that is released from the sample at ambient pressure using, e.g., gas chromatography and thermal conductivity. More recently, another method has been used in which the partial pressure of hydrogen in the gas volume of the hydrogen injection tank is monitored, and the Henry's law solubility for H_2 in water is used to infer the resulting concentration in the primary system. For example, planning in the South Texas Project plant calls for a sufficient partial pressure of hydrogen to be maintained in the volume control tank in order to maintain the specified equilibrium concentration of hydrogen in the reactor coolant. A self-contained pressure control valve maintains a minimum pressure in the vapor space space of the volume control tank. This pressure control can be adjusted to provide the correct equilibrium hydrogen

leaks in the system and that one can be assured that the pressure is due entirely to hydrogen.

Under normal operating conditions, the indirect hydrogen measurement and control technique apparently works satisfactorily, and this technique appears to be the only one in use for reactor-vessel analysis. However, under accident conditions, the generation rates of hydrogen and/cr oxygen may be so much greater than normal that the amount of gas dissolved in water becomes limited by kinetics rather than by the equilibrium constant, and analysis of the coolant may no longer be adequately informative. Serious consideration should be given either to the development of means to sample the reactor-vessel gas composition directly or to an experimental program which will verify the validity of the indirect techniques for both hydrogen and oxygen analyses under severe accident conditions.

II.3 Desired Characteristics and State of the Art of H_2 and O_2 Detection Systems in the Containment Building

In the event of escape of hydrogen into the containment, the formation of a uniform mixture of hydrogen and air will occur over a finite period of time. This period will depend on the rates of natural convection, forced convection, and diffusion processes. It is possible that the hydrogen could be stratified for a period sufficiently long to permit high concentrations to exist locally. Thus, a desirable trait of a hydrogen detection system would be the ability to map the H_2 concentration as a function of position in the containment building. This feature would require either a movable detector or strategic placement of an adequate number of fixed monitors. Although the concept of a movable detector is attractive, it may not be feasible because of the presence of hardware (e.g., overhead cranes, pumps, valves) in the containment building. Most of the discussion below is concerned with concepts that use a fixed detector.

Capability for measuring the concentrations of combustible gases in containment is a standard requirement for nuclear power plants. Since a high concentration (21 vol %) of oxygen is normal for atmospheric containments, only a hydrogen monitoring requirement applies to these during normal operation. Inerted containments must, of course, also verify that the oxygen concentration is sufficiently low (<5 vol %). Prior to the 1979 TMI-2 accident, no standard monitoring arrangements were defined. Currently, the proposed Revision 2 to NRC Regulatory Guide 1.97 requires continuous monitoring and recording of the combustible gas concentrations (identified above) during normal operation. Furthermore, the

systems required to perform these functions must be of high reliability and must be capable of functioning even after exposure to severe environmental disturbances. The Revision also requires that, following an accident, a manual sampling and analysis capability will exist for on-demand monitoring of H_2 and O_2 in both inerted and atmospheric containments.

Monitoring of containment gases requires access to the containment atmosphere and selective measurement of each constituent of interest. Two obvious alternatives are either to place the measuring device in the containment, or to bring a sample of the containment atmosphere to a measuring device outside containment. Both methods have been used, and each method has advantages and disadvantages.

Locating the measuring device within containment requires a device that will operate reliably, unattended, for long intervals, and under adverse conditions; it also requires that the device's output information be transmitted through the containment. Locating the measuring device outside the containment gives greater flexibility in the design and operation of the analytical instrumention, but limits access to the containment atmosphere in terms of response time, and requires the gases to be transported over long distances and through the containment walls. For either arrangement, it is expensive to provide a large number of sampling points.

If the measuring device is located outside containment, samples of the containment atmosphere must be withdrawn at selected ports by a piping and pumping system, and caused to flow past the sampling or analysis points. Some systems allow the flowing gases to enter

directly into analytical instruments. Others require that a "grab-sample" method be used, in which a container is manually attached to the pipe containing the flowing gases, filled, sealed, removed from the sample point, and then carried to the measuring device. The grab-sample method is obviously much slower than the direct-feed method. Plants which were designed to use the manual sampling arrangement may require several hours to obtain a sampling of containment. Since the manual method does not meet the pending requirement for continuous monitoring, it is to be expected that manual sampling will soon be replaced by direct feed.

For the actual measurement of H_2 and O_2 concentrations in samples taken from the containment atmosphere, the classical approach is first to separate the gases in a gas chromatograph and then to measure the concentration of each gas by the method of thermal conductivity. To measure only hydrogen and oxygen concentrations in the presence of nitrogen (as in air, or in nitrogen-inerted containments), Com-Sip, Inc., of Linden, NJ and El Monte, CA markets a system which uses thermal conductivity, but replaces the expensive gas chromatograph with a catalytic reactor. This technique takes advantage of the fact that the thermal conductivity of hydrogen is about seven times that of oxygen and nitrogen (which have almost equal thermal conductivities). In normal gas chromatography, only the carrier gas passes by the reference heat source. In the Com-Sip technique, the thermal conductivity of the containment gas is first measured. Then the gas component to be measured (H_2 or O_2) is completely burned by adding an excess of the complementary gas (O_2 or H_2) to the gas stream. The resulting gas mixture is then passed by the heat source.

The difference in thermal conductivity between the unburned and burned gas provides the information necessary to infer the original concentration.

An entirely different approach to measuring gas concentrations is used in devices developed by the General Electric Company's Space Division and now marketed by Exo-Sensors, Inc., of Laguna, CA. These compact instruments, which can be placed inside containment, employ selective gas-permeable membranes that feed electrochemical sensors. The basis for operation of these sensors is the electrochemical oxidation of H_2 or reduction of O_2, respectively. The measurement of oxygen is performed by an electrochemical cell where the rate of oxygen permeation of the catalytic sensing electrode is controlled with a thin film of FEP Polyarsulfol. This membrane passes oxygen to the cell at a rate directly proportional to the oxygen partial pressure. The oxygen passing through the membrane undergoes an electrochemical reaction which liberates four electrons per oxygen molecule. Thus, the electrical current generated is limited by the amount of oxygen passing through the membrane (or in other words, limited by the oxygen partial pressure in the gas being sampled). Each oxygen sensor has a finite life which is a function of the number of atmosphere-hours of oxygen to which it is exposed. The sensor as designed has sufficient capacity in the counter electrode to withstand 1750 atmosphere hours of operation, or at the normal O_2 levels anticipated in the reactor drywell and suppression chamber, 48 months of operation.

The hydrogen sensor is based on permeation of hydrogen through a membrane and the reaction between hydrogen and gold hydroxide in

a sulfuric acid electrolyte. The electrochemical reaction liberates two electrons per hydrogen molecule oxidized. Therefore, the current generated is directly proportional to the local partial pressure of hydrogen in the atmosphere. The hydrogen sensors are advertised to have a normal-use life of 18 months and a post-LOCA life of 100 days. The life limitation is caused by sulfuric acid attack on rubber seals in the device housing rather than material loss due to electrochemical reactions. In the United States, electrochemical hydrogen sensors have been installed in the General Electric designed reactors at Browns Ferry.

II.4 CONCLUSIONS

The discussion of hydrogen sources established that there are large uncertainties as to the amount and ultimate location of hydrogen and oxygen that will be generated during and following an accident. It is necessary, therefore, to rapidly measure and continuously monitor the concentration of combustible gases in the containment so that effective decisions can be made to control the gases.

Traditional monitoring systems are very expensive, some are unreliable, and some do not give rapid and continuous measurement. The accident at TMI-2 clearly established the need for high reliability and for rapid, continuous monitoring. The effect of the TMI-2 experience has been stricter regulations and scrutiny.

The major requirements which will be placed on present and future hydrogen detection systems will be concerned with sensitivity, accuracy, reliability, and hardness. It would be of considerable value to be able to detect hydrogen at levels substantially below the lower flammability limit, which is ~4 percent H_2 in air. Early detection might allow for strategic use of mitigation schemes at stages early enough to prevent explosion or fire damage entirely. It is also desirable to have a high degree of confidence in the accuracy and reliability of the detectors, primarily to avoid possible false alarms.

Advanced diagnostics, capable of measuring the concentration of H_2, O_2, and other "accident" species, do exist at present. In particular, optical techniques may provide the best diagnostics for monitoring both the primary and containment systems. Optical radar

techniques (LIDAR) can use a variety of back-scattered signals (Rayleigh, Mie, or Raman scattering; absorption, fluorescence, or Doppler measurements) to determine gas concentrations, temperature, particulate size, and gas velocity.[5] Such a system could be located at a single position in containment and scan most of the volume.* It is possible that coolant water from the primary system could be examined on a real-time basis using Raman scattering techniques (spontaneous, CARS, stimulated, or advanced nonlinear) to determine the concentrations of various solutes.[6,7] Other types of advanced diagnostics may also prove beneficial when adapted for use in the nuclear-reactor environment.

Finally, before deployment of any hydrogen detection equipment in operational reactors, due consideration must be paid to its ability to withstand long-term exposure to radiation at levels common to the reactor containment building. It would certainly be inappropriate, for example, to deploy a system which depends on radiation-sensitive electronic components, unless such components can be either hardened or shielded from the environment.

*Difficulties might arise due to steam or particulates in the optical path during an accident--these kinds of problems must be addressed as with any diagnostic technique.

References for Section II

1. B. Rosen, V. H. Dayan, and R. L. Proffit, Hydrogen Leak and Fire Detection, a Survey, NASA, SP-5092, 1970.

2. A Verdin, Gas Analysis Instrumentation, John Wiley and Sons, New York, 1973.

3. P. A. Michaels, "Design, Development, and Fabrication of ar Area Hydrogen Detector," NAS8-5282, Bendix Corp., Southfield, Mich., 1964.

4. M. Plihal, "Field Effect Gas Sensor for Hydrogen," Siemens Forsch.-Entwicklungsber. 6 (1), 53 (1977).

5. P. J. Hargis, Jr., The Remote Measurement of Meteorological Parameters by Optical Radar, Sandia Report: SAND74-0209 (1975).

6. J. P. Hohimer, Laser-Based Analytical Monitoring in Nuclear-Fuel Processing Plants, Sandia Report: SAND78-1522 (1978)

7. A. Owyoung, The Application of Third Order Nonlinear Optical Techniques to the Diagnosis of Combusting Media, Sandia Report: SAND77-0005 (1977).

III. HYDROGEN COMBUSTION

III.1 Introduction

The main concern over hydrogen combustion in nuclear reactor containments is that the high pressure generated might cause a breach of containment and a release of radioactivity. A second concern is that the resultant high temperature or blast might damage important safety-related equipment. The temperature and pressure obtained from the complete combustion of hydrogen in air, adiabatically and at constant volume, is shown in Fig. 1 (see Introduction, p. 8). The initial conditions for the calculation are a temperature of 298 K (25 C), a pressure of 100 kPa (approximately 1 atmosphere), and 100% relative humidity. Details of the calculation are given in Appendix A. At approximately 9% hydrogen by volume, the final pressure is 400 kPa (60 psia), the design maximum pressure of many large dry PWR containments (neglecting safety factors). Furthermore, hydrogen combustion is only one of several mechanisms that can contribute to generating high containment pressures. The release of steam and hydrogen from the reactor coolant system to the containment can also increase the containment pressure substantially.

If the hydrogen has had time to completely mix with the containment atmosphere before combustion, the combustion will be a premixed flame or detonation. The speed of the combustion front may be as low as 1 m/s for a laminar deflagration or as high as 2000 m/s for a detonation. Deflagrations are flames that travel at subsonic speeds relative to the unburned gas, and propagate mainly by thermal conduction from the hot burned gas into the unburned gas, raising its temperature high enough for rapid exothermic chemical reaction

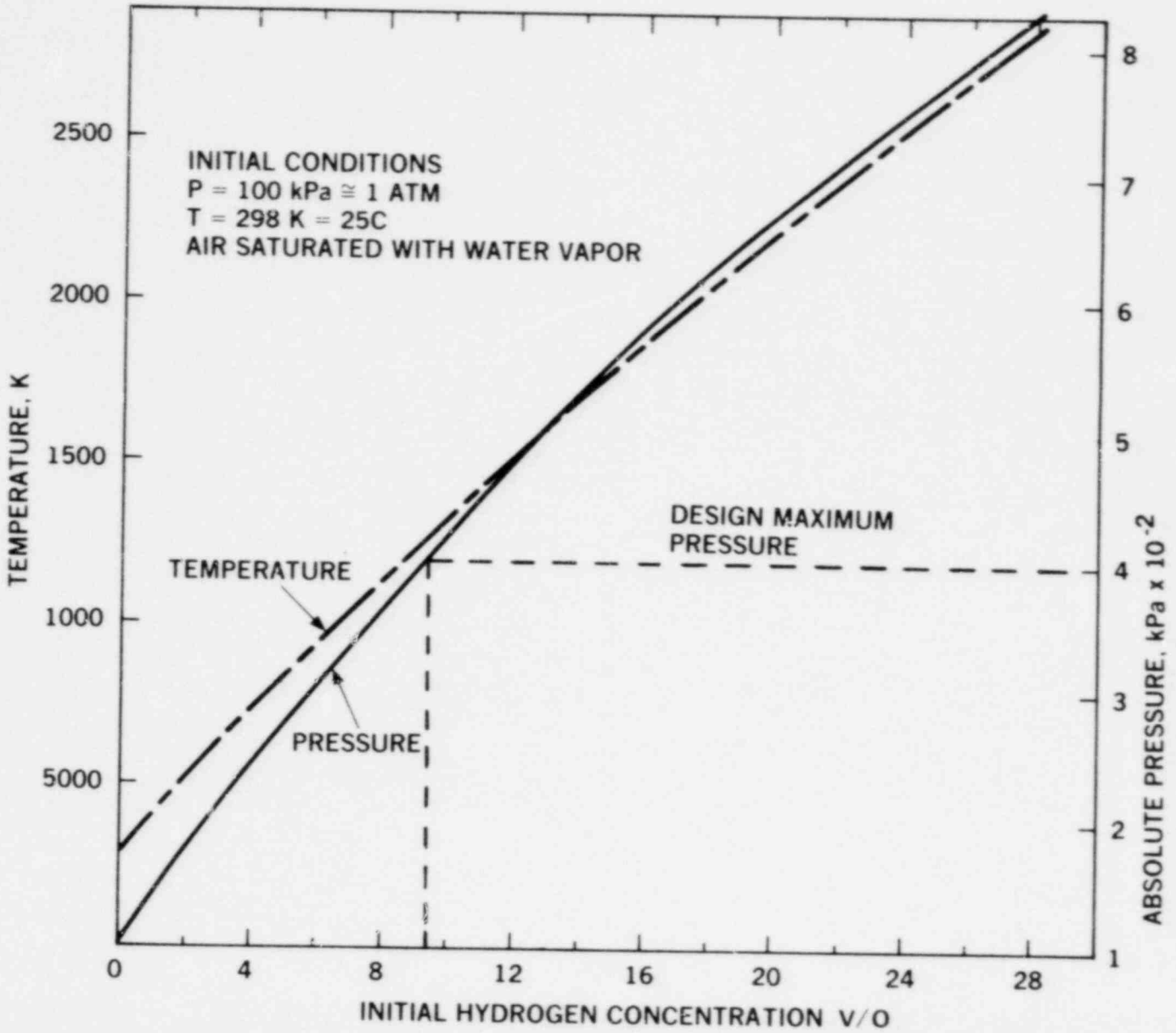

FIG. 1. PRESSURE AND TEMPERATURE AFTER HYDROGEN-AIR COMBUSTION, CONSTANT VOLUME AND ADIABATIC

to take place. Detonations are supersonic relative to the unburned gas and involve unsteady shock wave phenomena in their structure. Unburned gas is heated primarily by shock compression in contrast to heat conduction operating in deflagrations. A discussion of the classical Chapman-Jouguet theory of deflagrations and detonations is presented in Appendix B.

If the speed of the combustion front is low relative to the sound speed, the pressure within containment will rise uniformly throughout the volume of the enclosed gas (unless there are combustion instability effects) in a time of several seconds. The pressure will decay slowly due to heat transfer from the gas to the walls and other surfaces in containment with a time constant of a few minutes. If the water sprays in containment are activated, the decay of gas temperature and pressure will be more rapid. The loads on the structure will be quasi-static.[1,2,3] The structure will respond only to the magnitude of the pressure and transient effects will not be important.

For a detonation, the initial loads on the structure will be large and dynamic, and will be followed by quasi-static loads. The pressure history seen at the wall will be that of an intense pressure pulse followed by a series of reflected pressure pulses due to shock wave reverberations within containment. After the reverberations have decayed, the residual pressure will be equal to that produced by a slow deflagration. Calculations of the pressures caused by a detonation were obtained at various points in a simplified containment geometry using the CSQ wave-propagation program.[4] The detonation was assumed to be initiated at the center of the bottom of containment

The combustion wave was assumed to move at the Chapman-Jouguet detonation speed, even though for the 7.5% hydrogen mixture considered, no detonation could occur. The pressure history at the top of the containment is shown in Fig. 2. It agrees with the description of the loading history as a strong initial pressure pulse followed by other pressure pulses.

If the duration of a pressure pulse is short compared to the period of the lowest relevant mode of vibration of a structure, the load is called impulsive. The severity of the load is mainly governed by the impulse per unit area (the time integral of the pressure pulse) rather than the peak value of pressure. In the other limit, when the variation in pressure is long compared to the period of the structure, the load is called quasi-static. The severity of the load is mainly governed by the peak pressure and the impulse is irrelevant. When the pressure-pulse duration and structure period are of roughly the same magnitude the severity of the load is governed by both the peak pressure and impulse. A short discussion of the effects of dynamic loads can be found in Appendix C. For a large dry PWR containment, the period for the symmetrical expansion mode due to an internal pressure load is of the order of 0.05 seconds. For a detonation in containment, loads will range from impulsive to quasistatic, and each must be investigated for potential damage to the containment structure. In addition, there is the possibility of damage to piping, instrumentation, and control systems in containment from the aerodynamic forces caused by the detonation and shock waves.

In the last decade there has been great interest in mechanisms for the acceleration of deflagrations to high speeds. Such "fast

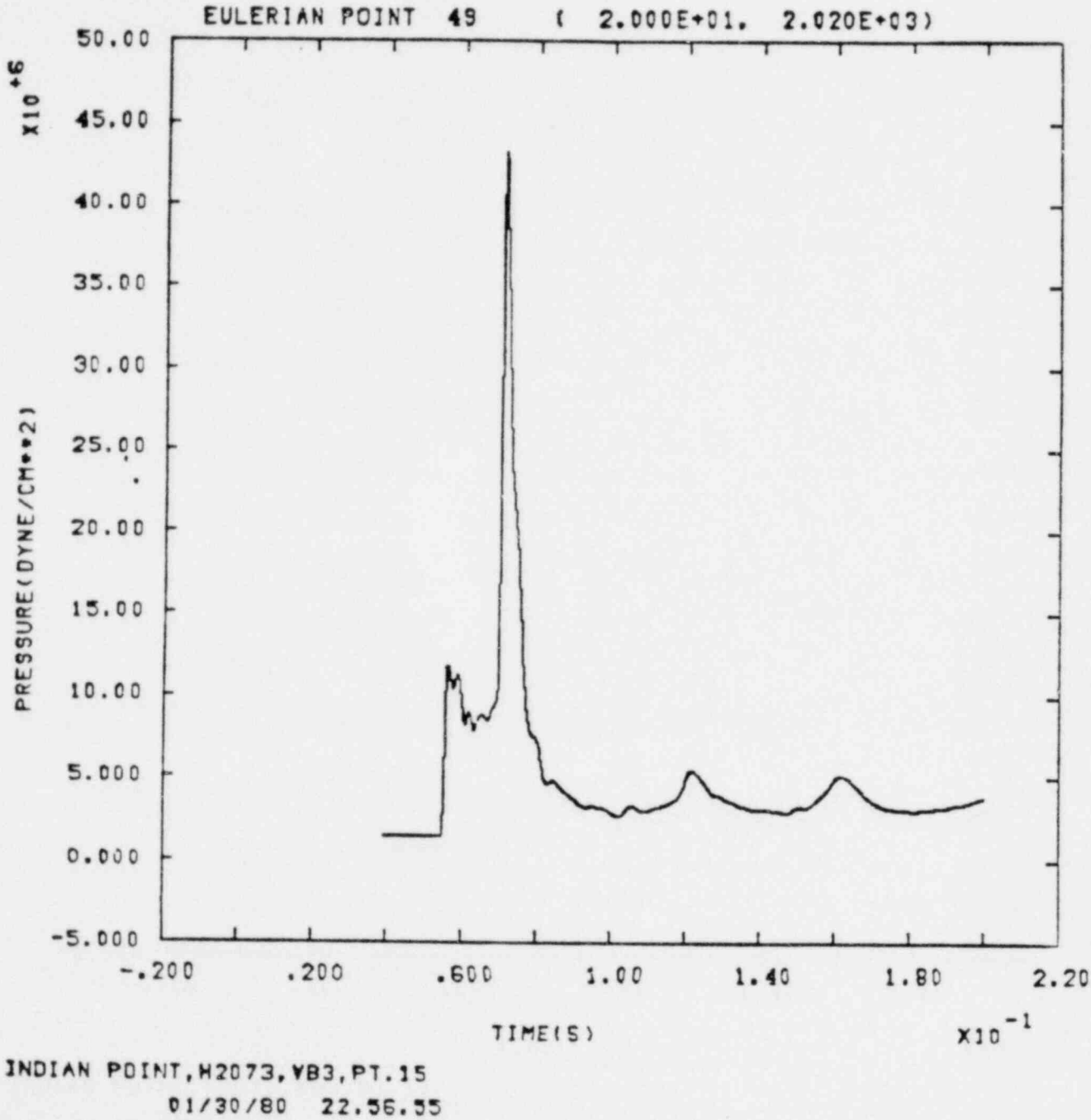

FIG. 2. PRESSURE HISTORY AT THE TOP CENTER OF CONTAINMENT DUE TO A DETONATION INITIATED AT THE BOTTOM CENTER[4]

deflagrations" or "quasi-detonations" will generate shock waves, and produce dynamic loads on the containment structure intermediate between those of detonations and slow deflagrations.[5] The probability of "quasi-detonations" in containment is not known. The uncertainties in this area are a major concern.

Hydrogen released into containment may burn before it has time to mix uniformly. Hydrogen may be released into containment from the reactor coolant system in the form of a steam-hydrogen jet. The jet may burn, giving a large turbulent diffusion flame. If the hydrogen has time to partly mix before ignition, stratified combustion will result.

III.2 Hydrogen Deflagrations

Flammability Limits of Hydrogen

For a mixture of flammable gases such as hydrogen and air, the flammability limits are defined as the limiting concentrations of fuel, at a given temperature and pressure, in which a flame can be propagated indefinitely. The flammability limit is assumed to be independent of (1) the method of ignition, as long as it is sufficiently strong to start a flame, and (2) the enclosure, as long as it is sufficiently large that heat transfer to the walls does not quench the flame. Limits for upward propagation of flames are wider than those for downward propagation. Limits for horizontal propagation are between those for upward and downward propagation.

There is some doubt concerning the applicability of flammability limits, as defined above, to accident conditions. There may be scale effects due to the large size of reactor containments, and variations in flammability due to the ignition source strength. Lovachev[6] discussed possible scale effects. It is known that flames can propagate for short distances using mixtures outside the flammability limits. It has been suggested that, with intense or large ignition sources, one might be able to propagate a flame for a long distance, if not indefinitely, at fuel concentrations outside the accepted flammability limits. Intense ignition sources are often generated in accidents involving combustion. In order to obtain uniformity of data on flammability limits, the work of the Bureau of Mines by Coward and Jones[7] and Zabetakis[8] has standardized flammability measurements using a 5-cm diameter, 150-cm long tube with an electric spark ignition.

Near the flammability limits, the flame temperature is comparatively low and the laminar flame speed is low. The propagation of these limiting mixture flames is dominated by natural convection caused by the presence of hot, low-density, burned gases. Parvenof[9] studied the flame speed of lean hydrogen-oxygen mixtures in a weightless condition by using freely-falling chambers. Thus eliminating natural convection, he obtained spherical deflagrations. Although his work was limited, it seemed to show that if a lower flammability limit exists in zero gravity, it is below the values quoted for ordinary laboratory experiments. Flammability limits are useful guidelines, but do not appear to be fundamental quantities. Having stated our reservations on the significance of flammability limits, we will present the generally accepted results.

The lower flammability limit is the minimum concentration of hydrogen required to propagate a flame, while the upper limit is the maximum concentration. At the lower limit, the hydrogen is in short supply and the oxygen is present in excess. The flame temperature and flame speed for hydrogen-air and hydrogen-oxygen mixtures are nearly the same for the hydrogen-lean case. It is not surprising then that the lower limit of flammability of hydrogen-air and hydrogen-oxygen mixtures is about the same.

At the upper limit of flammability for hydrogen, the oxygen is in short supply, about 5% oxygen by volume. The behavior of the upper limit of flammability of hydrogen with various mixtures such as air-steam is more easily understood if one considers it as the lower flammability limit of oxygen.

In large PWR containments we are usually interested in the lower limit of flammability, there being large amounts of oxygen present. In the much smaller BWR containments, particularly the inerted containments, we may be interested in the upper flammability limit.

For hydrogen-air mixtures, the flammability limits of Coward and Jones[7] are still accepted.[11,12] The best values for hydrogen flammability in air saturated with water vapor at room temperature and pressure are given in Table III-1.

TABLE III-1

HYDROGEN FLAMMABILITY LIMITS IN STEAM-SATURATED AIR[7]

	Lower Limit, Vol. %	Upper Limit, Vol. %
Upward Propagation	4.1	74
Horizontal Propagation	6.0	74
Downward Propagation	9.0	74

In reactor accidents the conditions inside containment prior to hydrogen combustion may be at elevated temperature and pressure with the presence of steam. The flammability limits widen with increasing temperature. At 100°C the lower limit for downward propagation is approximately 8.8% (see Fig. 3). In the temperature range of interest, the widening of the downward propagation limits is small. No data for the widening of the upward or horizontal propagation limits were found. The effect of increasing pressure up to 10 atmospheres, is to narrow the flammability limits. Since an increase in containment temperature leads to an increase in pressure, the net effect of these two opposing small effects should be small.

If the containment atmosphere is altered by the addition of carbon dioxide, steam, nitrogen or other diluent, the lower flammability limit will increase slowly with additional diluent, while the upper flammability limit will drop more rapidly. With continued increase in diluent concentration the two limits approach one another until they meet and the atmosphere is inerted. A flame cannot be propagated indefinitely for any fuel-air ratio in an inerted atmosphere. Figure 4 shows the flammability limits with the addition of excess nitrogen or carbon dioxide. Note that for 75% additional nitrogen, the atmosphere is inert.[7,12] This corresponds to 5% oxygen at the limit of the flammable region, a value very close to that of the upper limit for hydrogen-air combustion. Roughly speaking, hydrogen-oxygen-nitrogen mixtures will be flammable if the hydrogen concentration is above 4% and the oxygen concentration is above 5%. For carbon dioxide, the atmosphere is inerted when

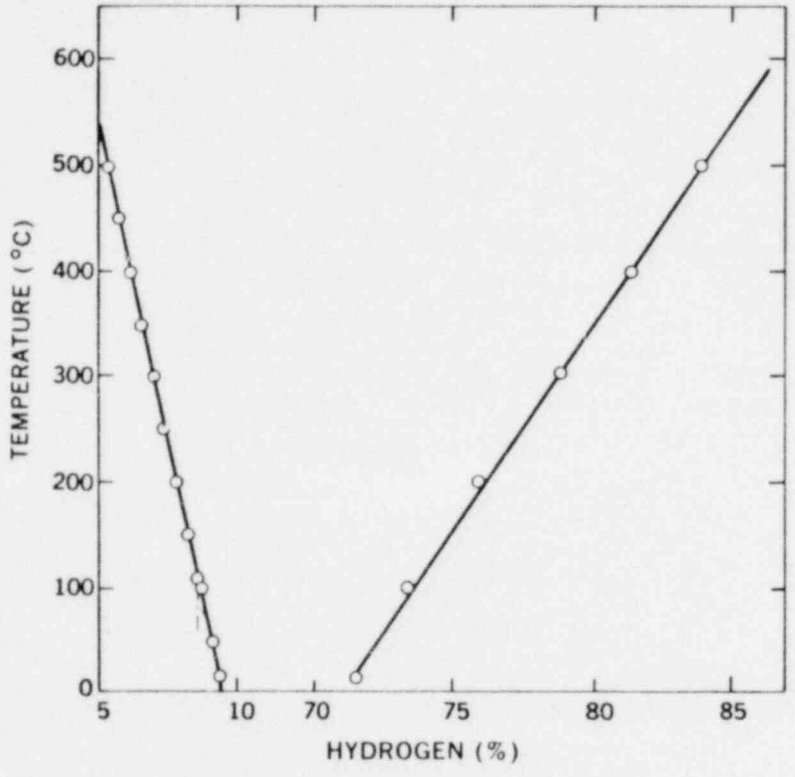

FIG. 3. EFFECT OF INITIAL TEMPERATURE ON DOWNWARD PROPAGATING FLAMMABILITY LIMITS IN HYDROGEN-AIR MIXTURES[7,10]

In reactor accidents the conditions inside containment prior to hydrogen combustion may be at elevated temperature and pressure with the presence of steam. The flammability limits widen with increasing temperature. At 100°C the lower limit for downward propagation is approximately 8.8% (see Fig. 3). In the temperature range of interest, the widening of the downward propagation limits is small. No data for the widening of the upward or horizontal propagation limits were found. The effect of increasing pressure up to 10 atmospheres, is to narrow the flammability limits. Since an increase in containment temperature leads to an increase in pressure, the net effect of these two opposing small effects should be small.

If the containment atmosphere is altered by the addition of carbon dioxide, steam, nitrogen or other diluent, the lower flammability limit will increase slowly with additional diluent, while the upper flammability limit will drop more rapidly. With continued increase in diluent concentration the two limits approach one another until they meet and the atmosphere is inerted. A flame cannot be propagated indefinitely for any fuel-air ratio in an inerted atmosphere. Figure 4 shows the flammability limits with the addition of excess nitrogen or carbon dioxide. Note that for 75% additional nitrogen, the atmosphere is inert.[7,12] This corresponds to 5% oxygen at the limit of the flammable region, a value very close to that of the upper limit for hydrogen-air combustion. Roughly speaking, hydrogen-oxygen-nitrogen mixtures will be flammable if the hydrogen concentration is above 4% and the oxygen concentration is above 5%. For carbon dioxide, the atmosphere is inerted when

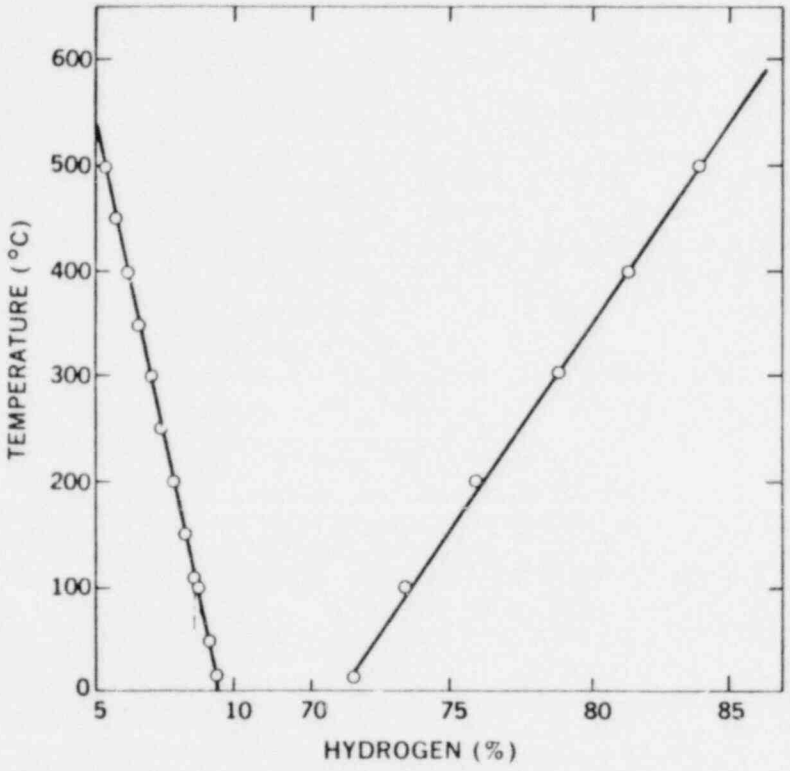

FIG. 3. EFFECT OF INITIAL TEMPERATURE ON DOWNWARD PROPAGATING FLAMMABILITY LIMITS IN HYDROGEN-AIR MIXTURES[7,10]

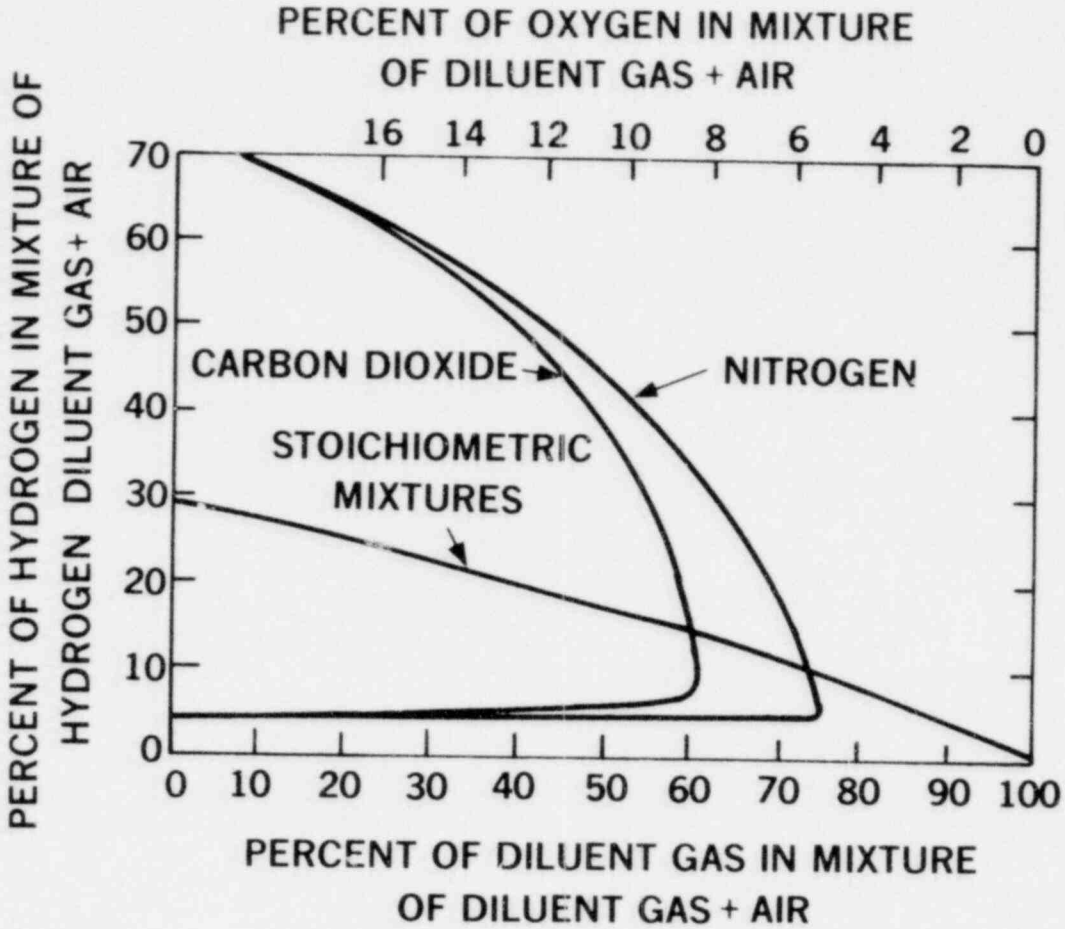

FIG. 4. FLAMMABILITY LIMITS OF HYDROGEN IN AIR DILUTED WITH CO_2 AND N_2 [7]

the carbon dioxide concentration is 60% or above, corresponding to 8% oxygen or less. The larger specific heat of the carbon dioxide reduces the flame temperature and flame velocity, hence carbon dioxide suppresses flammability more than nitrogen. It requires about 60% steam to inert hydrogen-air mixtures. The triangular diagram of Shapiro and Moffette[10] indicates regions of flammability and detonability of hydrogen-air-steam mixtures. It has been widely reproduced[11,2] and appears as Figure 5.

Empirical attempts have been made to correlate the flammability limits to the flame temperature with fair success.[1,14] The effects of adding nitrogen, carbon dioxide and steam are in agreement with this approach. The "Halon" halocarbons are found to inert hydrogen-air atmospheres with much smaller concentrations than would be expected from thermal considerations. These substances interfere with the chemical reactions in the flame, removing active radicals. We will discuss the use of Halon for combustion suppression in a future report.

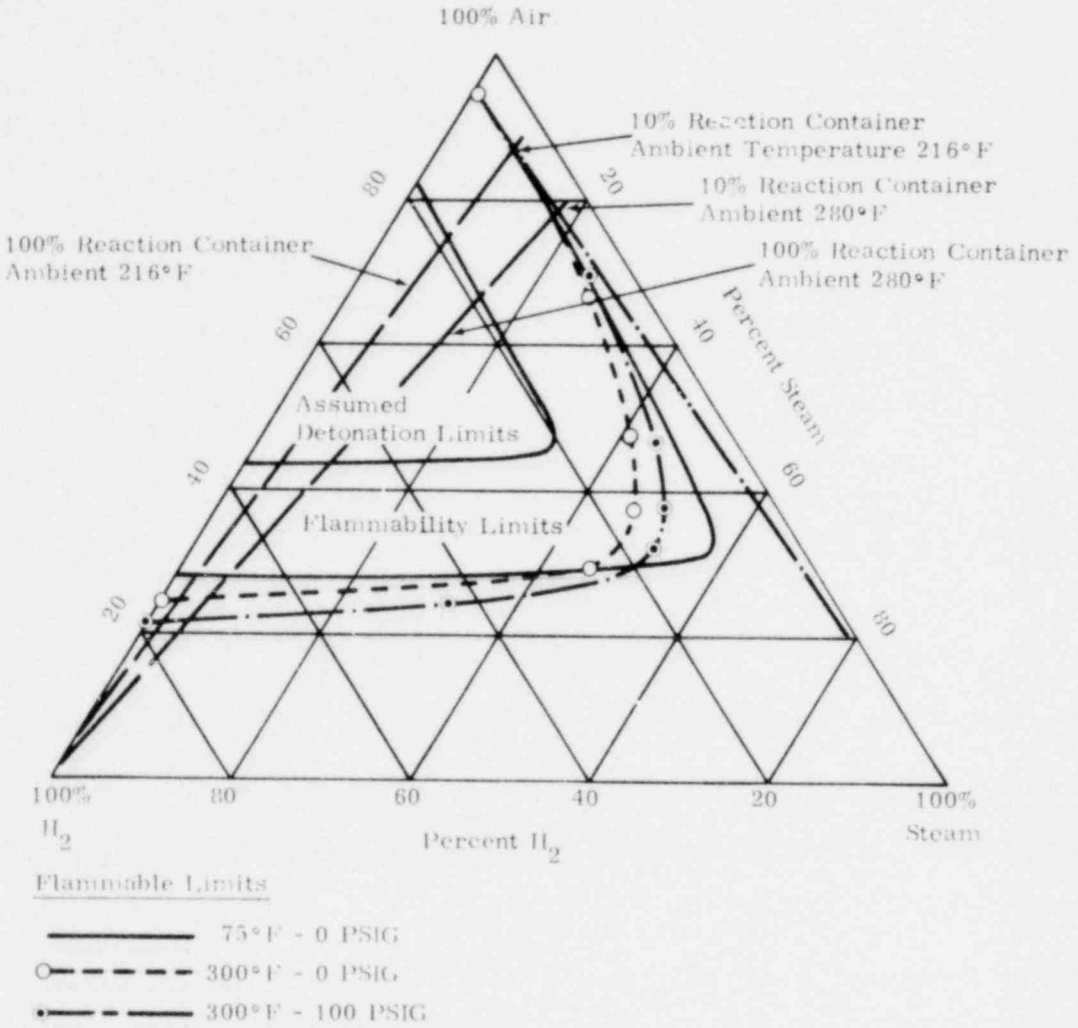

FIG. 5. FLAMMABILITY AND DETONATION LIMITS OF HYDROGEN-AIR-STEAM MIXTURES[10,11,2]

Incomplete Burning of Lean Hydrogen-Air Mixtures

It has been found in several small- and medium-scale laboratory experiments that when hydrogen-air mixtures with hydrogen concentrations in the range 4-8% were ignited with a spark, much of the hydrogen was not burned.[15,16,17] The resultant pressure rise was far below that predicted for complete combustion as shown in Fig. 1. Experimental results with a spark ignition source, shown in Fig. 6, indicate that the completeness of combustion increases with increasing hydrogen concentration, and is nearly complete at about 10% hydrogen. The range of incomplete combustion corresponds to the range in which the mixture is above the upward propagation flammability limit, but below the downward propagation flammability limit. In upward propagation of lean hydrogen-air flames, "separated globules" of flame have been observed.[18] Even when ignition occurs at the bottom of a chamber, the upward propagating flame fails to burn some of the hydrogen.

The phenomenon of incomplete burning of lean hydrogen-air mixtures may be of great importance in reactor safety. If the results of Fig. 6 are valid for combustion in the larger volumes of reactor containments, then combustion of lean mixtures, below 8% hydrogen, appears to be a method of partly eliminating hydrogen without significant pressure rise. We will discuss deliberate ignition as a mitigation scheme in a later report.

The combustion that took place in the TMI-2 containment appears to have been an incomplete burning of a lean hydrogen-air mixture. Using Fig. 6, the 28 psi pressure rise observed at TMI-2 corresponds to combustion of a hydrogen-air mixture containing

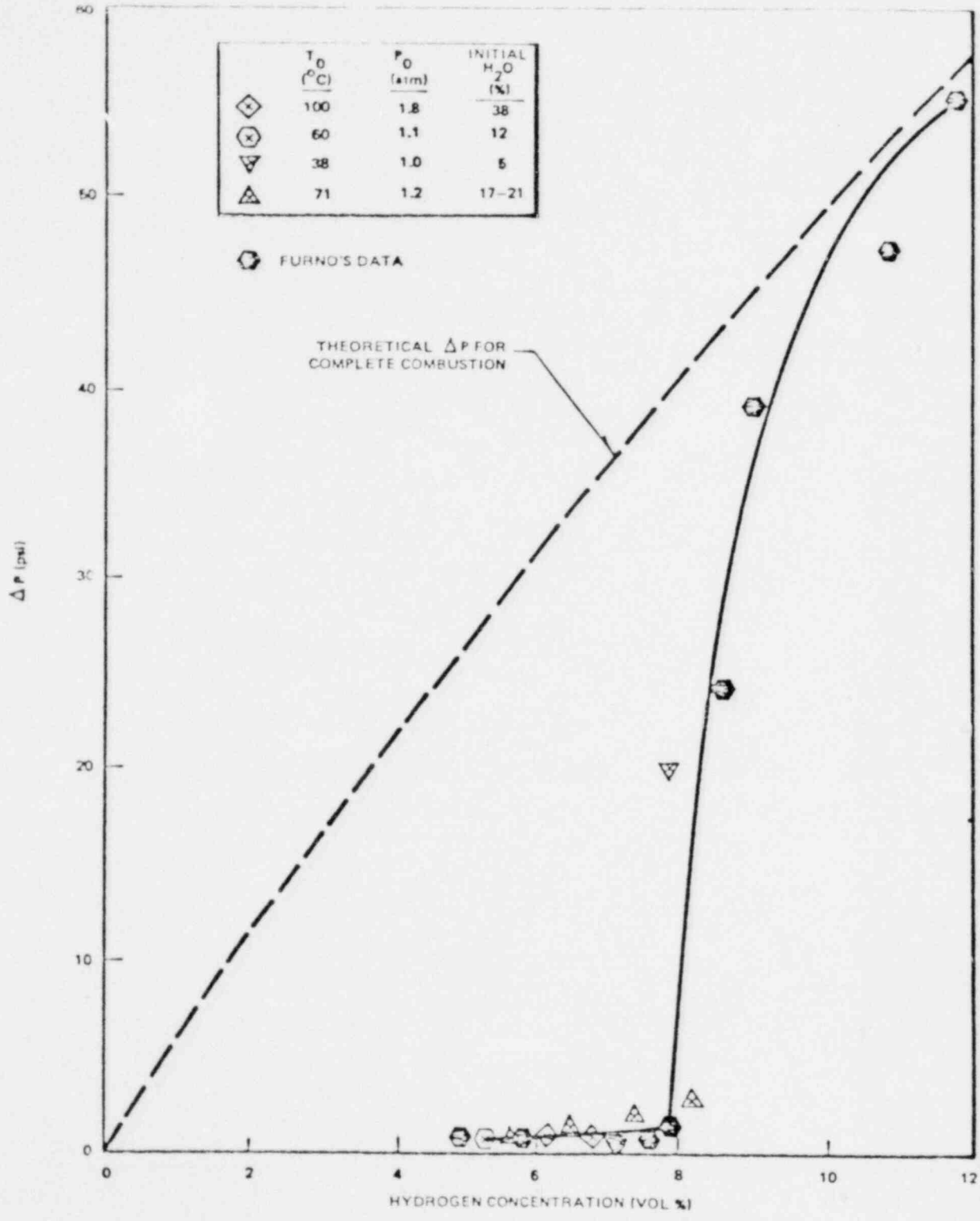

FIG. 6. PRESSURE RISE VERSUS HYDROGEN CONCENTRATION, SPARK IGNITOR[16,15]

about 8.5% hydrogen. Note that the pressure rise increases very rapidly between 8 and 9% hydrogen.

Ignition of Hydrogen Deflagrations

"Ignition of hydrogen-air mixtures, particularly when the mixtures are well within the flammability limits, occurs with an exceedingly small input of energy. A spark that has such a energy as to be invisible in a dark room will ignite such as mixture. Common sources of ignition are sparks from electrical equipment and from the discharge of small static electric charges."[10,18] The minimum energy required from a spark for ignition of a quiescent hydrogen-air mixture is of the order of tenths of a millijoule. The ignition energy required as a function of hydrogen concentration is shown in Fig. 7.[19] For a flammable mixture, the required ignition energy increases as the hydrogen concentration approaches the flammability limits. As mentioned previously, large ignition sources can cause mixtures outside the flammability limits to burn for some distance.

In recent years there has been research on the initiation of fast deflagrations and detonations using very strong ignition sources. One possible strong ignition source is combustion in a semi-confined space, such as the housing of an electric motor or a duct. A jet of hot combustion gases from the semi-confined space can act as a strong ignition source.

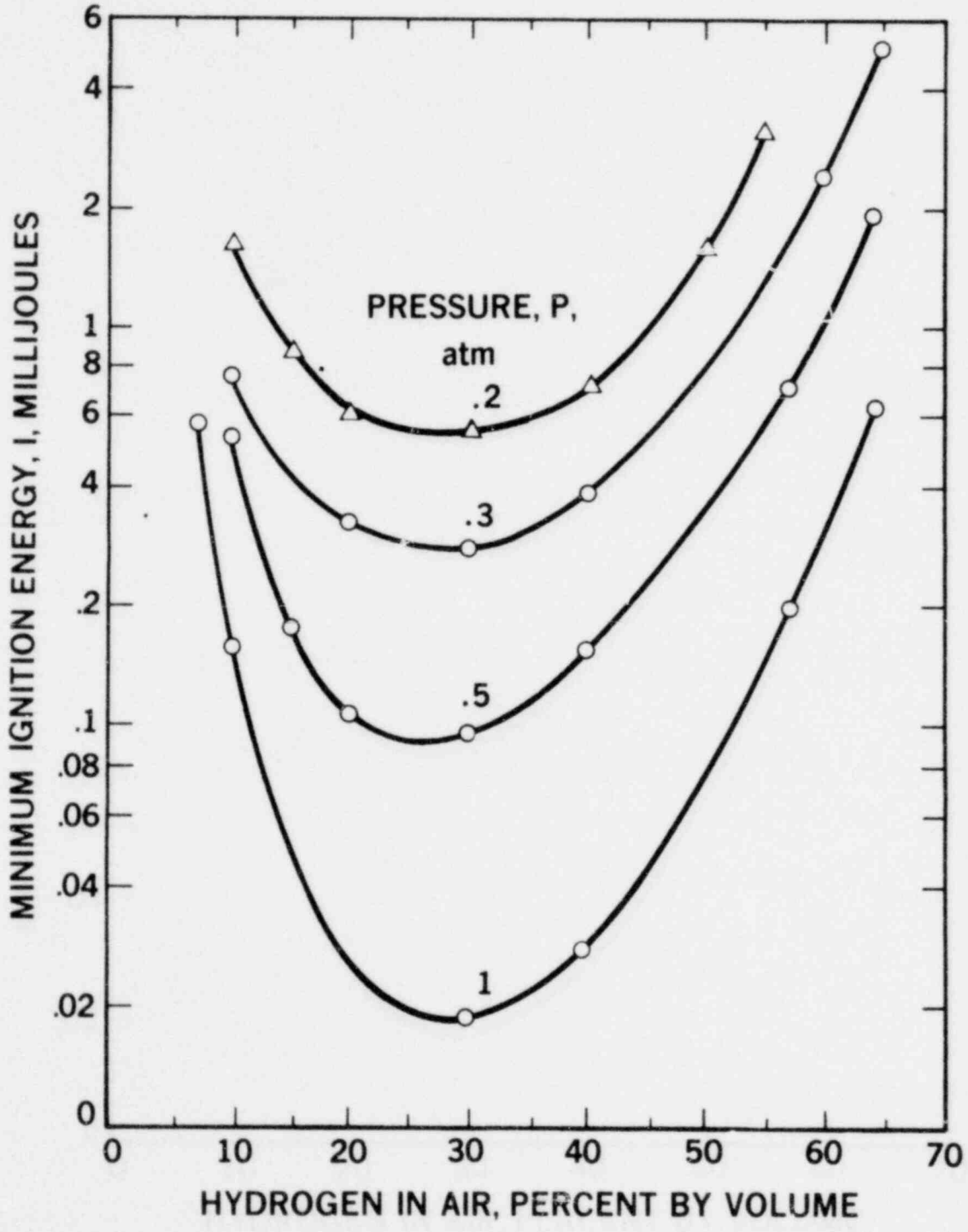

FIG. 7. SPARK IGNITION ENERGIES FOR HYDROGEN-AIR MIXTURES[1,19]

Laminar Flame Speed and Structure

Several techniques are used to measure laminar flame speeds. Each technique has sources of inaccuracy.[1,20,21] The early work of Jahn[22] and Scholte and Vaags[23] on hydrogen flame speed is now considered to have given results 20% too low. The experimental work of Edmondson and Heap,[24] Dixon-Lewis,[25-29] and others is in good agreement with recent theoretical calculations of laminar flame speed using laminar-flame-structure models.[30] The detailed chemical reactions of importance in hydrogen-oxygen combustion are believed known, and the rates of the reactions are fairly well known. The chemistry of the hydrogen combustion is discussed in Appendix D. The thickness of the laminar flame front for hydrogen-air at atmospheric pressure is about 1 mm.

Warnitz[30] computed the laminar flame speed for hydrogen-air mixtures and compared his results with those of several other workers. The results are shown in Fig. 8. After corrections were made to results of some early work believed to be in error, the revised data are in good agreement. The effect on laminar flame speed of different ratios of oxygen to nitrogen concentration is shown in Fig. 9. The results of the work of Jahn[22,1] were multiplied by a factor of 1.2 to agree with Warnitz's results and those of other recent workers.

The maximum laminar flame speed of hydrogen-air mixtures is about 3 m/s near a concentration of about 42% hydrogen. The flame speed becomes much smaller as the flammability limits are approached. The effect of diluents such as nitrogen is to reduce flame speed by reducing flame temperature. Steam also reduces flame speed, but by less than the amount expected from equilibrium flame temperature considerations.[31,32,33]

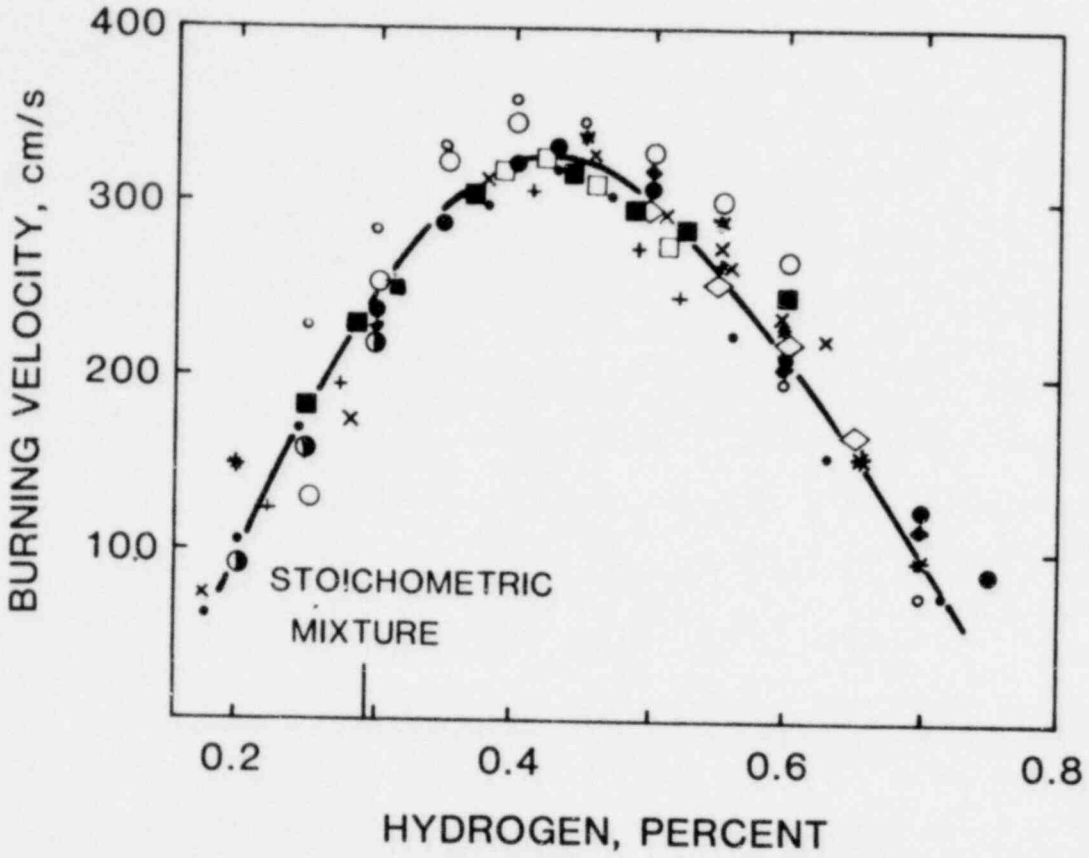

FIG. 8. LAMINAR FLAME VELOCITY OF HYDROGEN-AIR MIXTURES
T = 298 K, P = 100 kPa
Line - Calculated Values, Warnitz[31]
- ● Jahn (x 1.2)[23]
- ◆ Scholte and Vaags (x1.2)[24]
- ◇ Edmondson and Heap[25]
- □ Bartholomé
- ■ Burwasser and Pease
- ◦ Günther and Janisch
- ○ Günther and Janisch
- * Andrews and Bradley
- • Miller, Evers and Skinner (x1.1)
- × Gibbs and Calcote
- + Smith and Pickering (x1.2)
- ◑ Senior (x1.1)

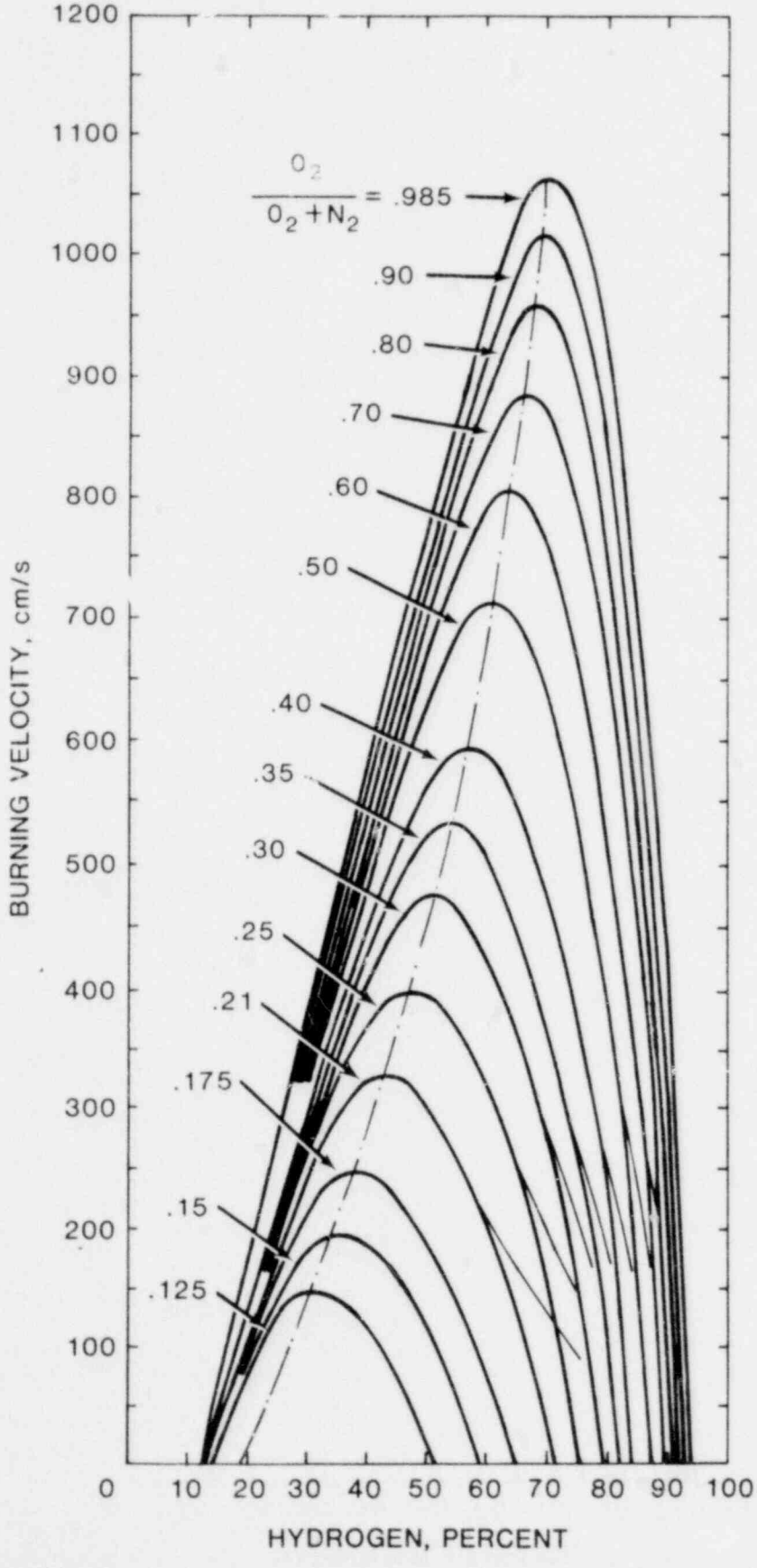

FIG. 9. LAMINAR FLAME VELOCITY OF HYDROGEN-OXYGEN-NITROGEN MIXTURES[23, 31]

The laminar flame speed will only be changed slightly by moderate changes in ambient temperature and pressure.[19] For a 50°C temperature rise above room temperature, the increase in laminar flame speed is less than 0.2 m/s. The variation of hydrogen-air flame speed with pressure is very small for pressure changes in the range of interest for reactor containments.

The plane or spherically expanding laminar flame front has been shown to be unstable. Freely propagating laminar flame fronts, if they do not become turbulent, have complex cellular structure.[34-39] Hydrogen-lean flames tend to form nonsteady cellular structures, and will probably become turbulent. For hydrogen-rich flames, one expects "widespaced wrinkled irregular stationary surfaces."[38] Istratov and Librovish[39] carried out a theoretical analysis of the instabilities of a spherically expanding flame.

The importance of the instability of the flat laminar flame front is that the mean speed of a laminar flame will be somewhat higher than the laminar flame speed. The laminar flame speed is the normal component of velocity of the unburned gas moving into the flame front. If the normal to the flame front is at an angle θ to the direction of flame propagation, then the propagation speed of the front is equal to the laminar flame speed divided by the cosine of θ. In any case, if the front stays laminar, the Mach number of the front will be extremely small. The pressure is then expected to be uniform in containment, and to rise monotonically. The loads imposed on the containment structure will be quasi-static. However, the instability of the laminar flame front can lead to turbulence, flame acceleration and possibly transition to detonation, if the

mixture is within the detonation limits. This was observed in a spherically-expanding deflagration by Struck and Reichenbach.[40]

Turbulent Deflagrations

It is likely that a laminar deflagration in containment will become turbulent. Shivashinsky[38] has discussed the "self-turbulization" of laminar flames. Many turbulent flames have mean flame speeds in the range 2 to 5 times the laminar flame speed. Even at these speeds, the Mach number of the flame front will be very low. The pressure in containment will be nearly spatially uniform, and the pressure will rise monotonically.

Of great concern is the possibility of large flame accelerations, generating a "quasi-detonation." If the turbulent flame speed becomes greater than about one-tenth of the sound speed (Mach number 0.1), shock waves will be formed ahead of the flame front. Dynamic loads in addition to static loads will be created at the containment structure.

One acceleration mechanism under active study is the action of obstacles in the path of flames.[41] The flame front is stretched and turbulence is promoted. Dramatic increases in flame speed have been observed when a flame front passes through a field of obstacles such as the lower sections of PWR containments that contain many pipes, pressure vessels, etc. However, much of the upper portion of such containments is fairly open. There have been no experiments to study flame speed behavior when the flame front leaves an obstacle field and enters an open region. Several researchers suggest that the flame speed might decrease after leaving the obstacle field. A second mechanism for the generation of a quasi-detonation is the presence of a very intense ignition source. As was suggested earlier, this could be a jet of hot combustion

products formed subsequent to ignition in some adjoining semi-confined volume.

The subject of fast deflagrations or quasi-detonations is one of active current research. It is not well understood. Further work will be needed to determine its importance to hydrogen combustion in reactor containments.

III.3 Hydrogen Detonations

Detonation Limits of Hydrogen

For a detonable mixture of gases such as hydrogen and air, the detonation limits are defined as the limiting concentrations of fuel, at a given temperature and pressure, in which a detonation can be propagated indefinitely. If a detonation wave is driven into a region where the mixture is outside the detonation limits, the detonation wave will decay into a blast wave, and finally into an acoustic wave. Since the possibility of propagating a detonation wave in a near-limiting mixture depends on the geometry of the container, there is concern that wider detonation limits might be observed in a more favorable geometry for the detonation.

The generally accepted values of detonation limits of hydrogen-air mixtures at room temperature and pressure are those of Breton[42] quoted by Lewis and Von Elbe:[1] 18.2% and 58.9% hydrogen by volume. The lower detonation limit is somewhat uncertain. A 15% hydrogen mixture was found to support stable detonation when the moisture content was reduced to .005%, but did not support a stable detonation at higher moisture content.[1] For hydrogen-oxygen mixtures, the detonation limits are 15% and 90% hydrogen. Although there is no successful theory of detonation limits, as there is none for flammability limits, the effect of diluents on detonation limits can be estimated by the observation that the temperature behind the limiting mixture detonation of hydrogen is about 2100 K. Consequently, the lower detonation limit of hydrogen-oxygen-nitrogen mixtures, when oxygen is present in excess, is only weakly dependent on the oxygen to nitrogen ratio, since its effect on the detonation temperature is small.

There is not much data on the effect of temperature and pressure on the detonation limits. One expects the detonation limits to widen with increased temperature, as with flammability limits. Heckes[2] presented data from Sokolik[43] attributed to Breton and Laffitte on the effects of temperature and pressure on detonation limits. The data seemed to show a very small widening of the detonation limits with increasing temperature and with increasing pressure. The effect is negligible for the range of pressure and temperature expected in containment during accident conditions.

The effect of steam on detonation limits is more important. As shown in Fig. 6, Shapiro and Moffette[10] indicate that the upper and lower detonation limits merge when the steam concentration is about 35% and consequently they predict that for mixtures with steam concentration above 35%, detonation is impossible. Moore and Gilby[44] computed the detonation limits using the theory of explosion limits and obtained a very different result: detonations were prevented by only about 11% steam. We conclude that hydrogen-air-steam detonation limits are uncertain.

Detonation Speed and Pressure

Detonation waves travel at a speed very close to that corresponding to the Chapman-Jouguet point (see Appendix B), except that "marginal detonations," (detonations in mixtures near the detonation limits) travel at a speed lower than the Chapman-Jouguet speed. For hydrogen-air detonations, the pressure ratio across the detonation wave will be approximately 16, the detonation velocity approximately 2000 m/s, and the temperature behind the detonation wave will be about 2800 K (see Figs. 10 and 11). Shown below in Table III-2 from Ref. 1 giving the pressure, temperature and detonation speed of several hydrogen-oxygen mixtures. Subscript 1 refers to undisturbed conditions, and subscript 2 to post-shock conditions. Notice the close agreement between the measured detonation speed and the speed computed using the Chapman-Jouguet condition.

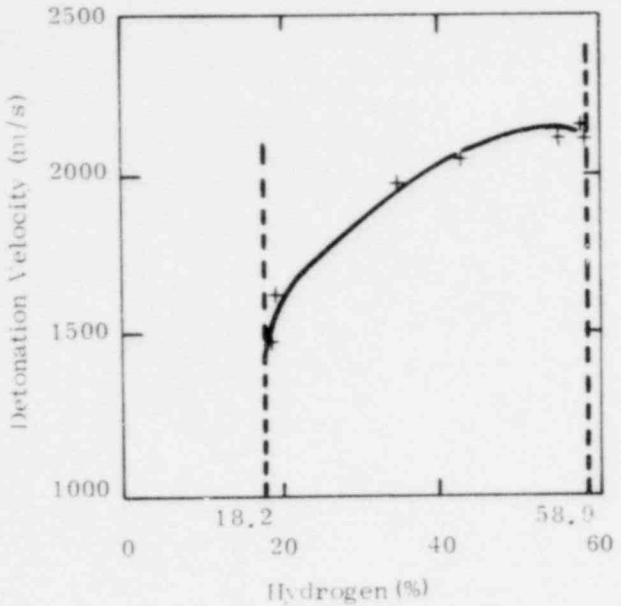

FIG. 10. HYDROGEN-AIR DETONATION VELOCITY [1]

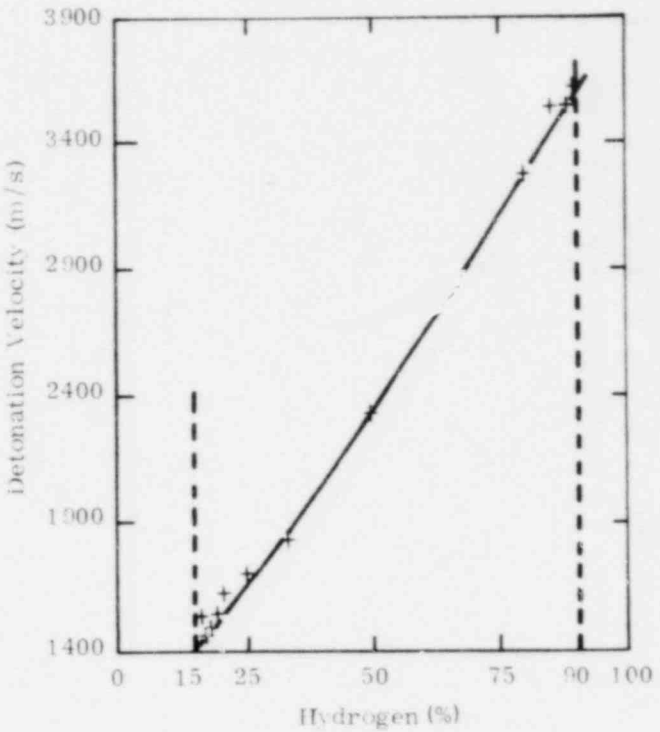

FIG. 11. HYDROGEN-OXYGEN DETONATION VELOCITY [1]

Table III-2[1]

Comparison of Calculated and Experimental Detonation Velocities of Mixtures of Hydrogen, Oxygen, and Nitrogen

Explosive mixture	P_2, atm.	T_2, °K	Detonation Velocity m/sec	
			Calculated	Experimental[15]
$(2H_2 + O_2)$	18.05	3583	2806	2819
$(2H_2 + O_2) + 1O_2$	17.4	3390	2302	2314
$(2H_2 + O_2) + 3O_2$	15.3	2970	1925	1922
$(2H_2 + O_2) + 5O_2$	14.13	2620	1732	1700
$(2H_2 \pm O_2) + 1N_2$	17.37	3367	2378	2407
$(2H_2 + O_2) + 3N_2$	15.63	3003	2033	2055
$(2H_2 + O_2) + 5N_2$	14.30	2685	1850	1822
$(2H_2 + O_2) + 2H_2$	17.25	3314	3354	3273
$(2H_2 + O_2) + 4H_2$	15.97	2976	3627	3527
$(2H_2 + O_2) + 6H_2$	14.18	2650	3749	3532

P_1 = 1 atmosphere; T_1 = 291°K.

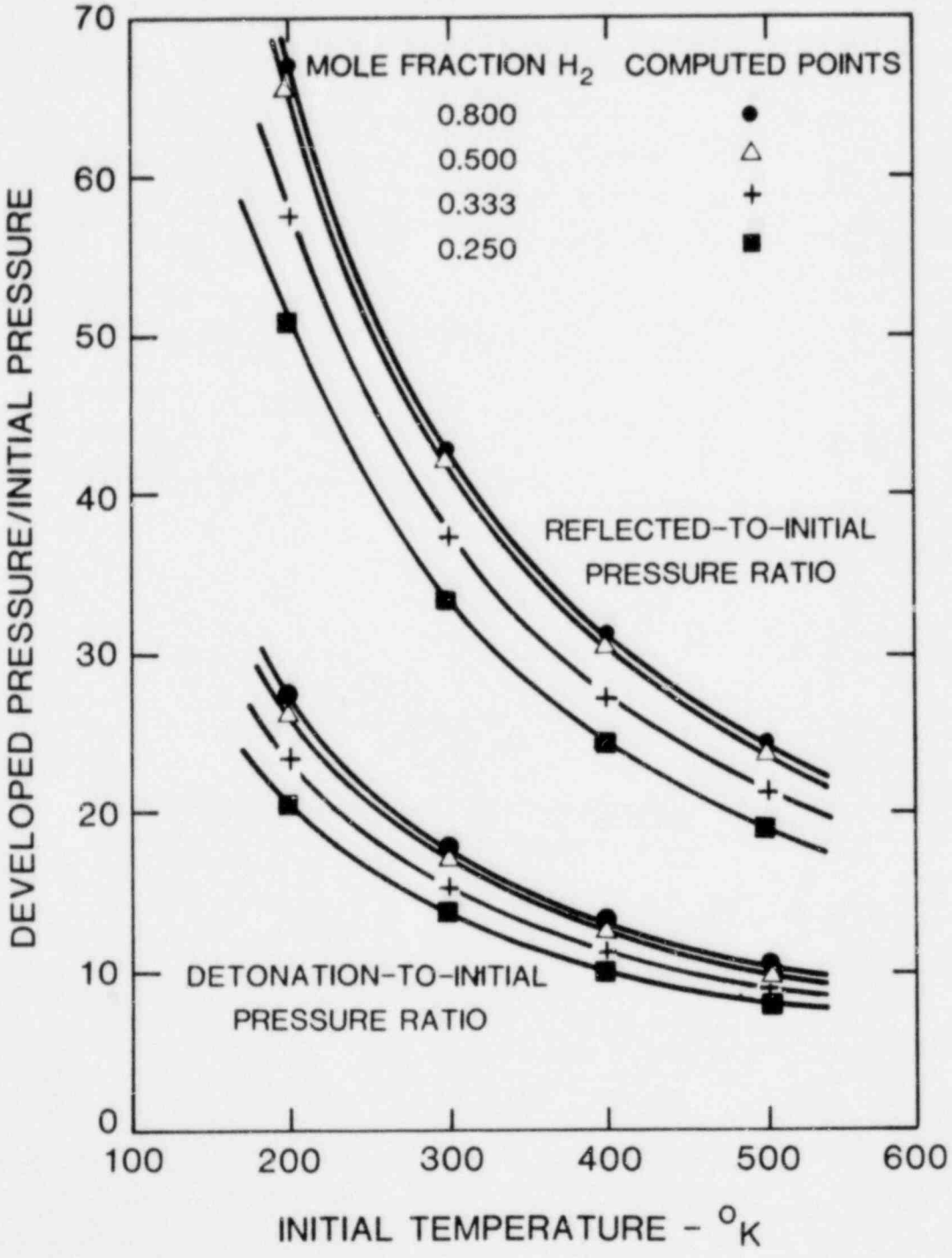

FIG. 12. EFFECT OF INITIAL TEMPERATURE ON DETONATION PRESSURE RATIOS IN HYDROGEN-OXYGEN MIXTURES AT ATMOSPHERIC PRESSURE[78]

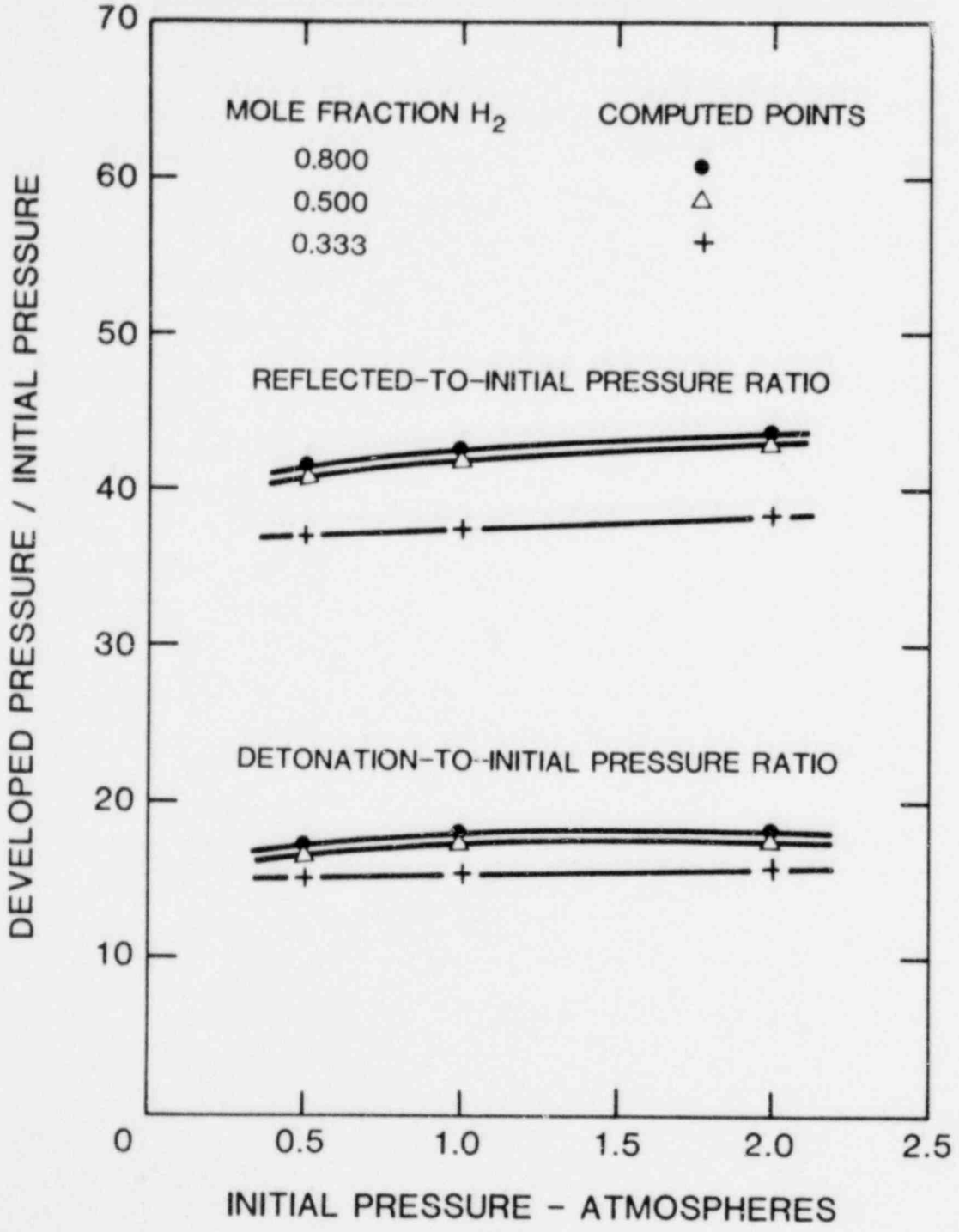

FIG. 13. EFFECT OF INITIAL PRESSURE ON DETONATION PRESSURE RATIOS IN HYDROGEN-OXYGEN MIXTURES AT 298 K [78]

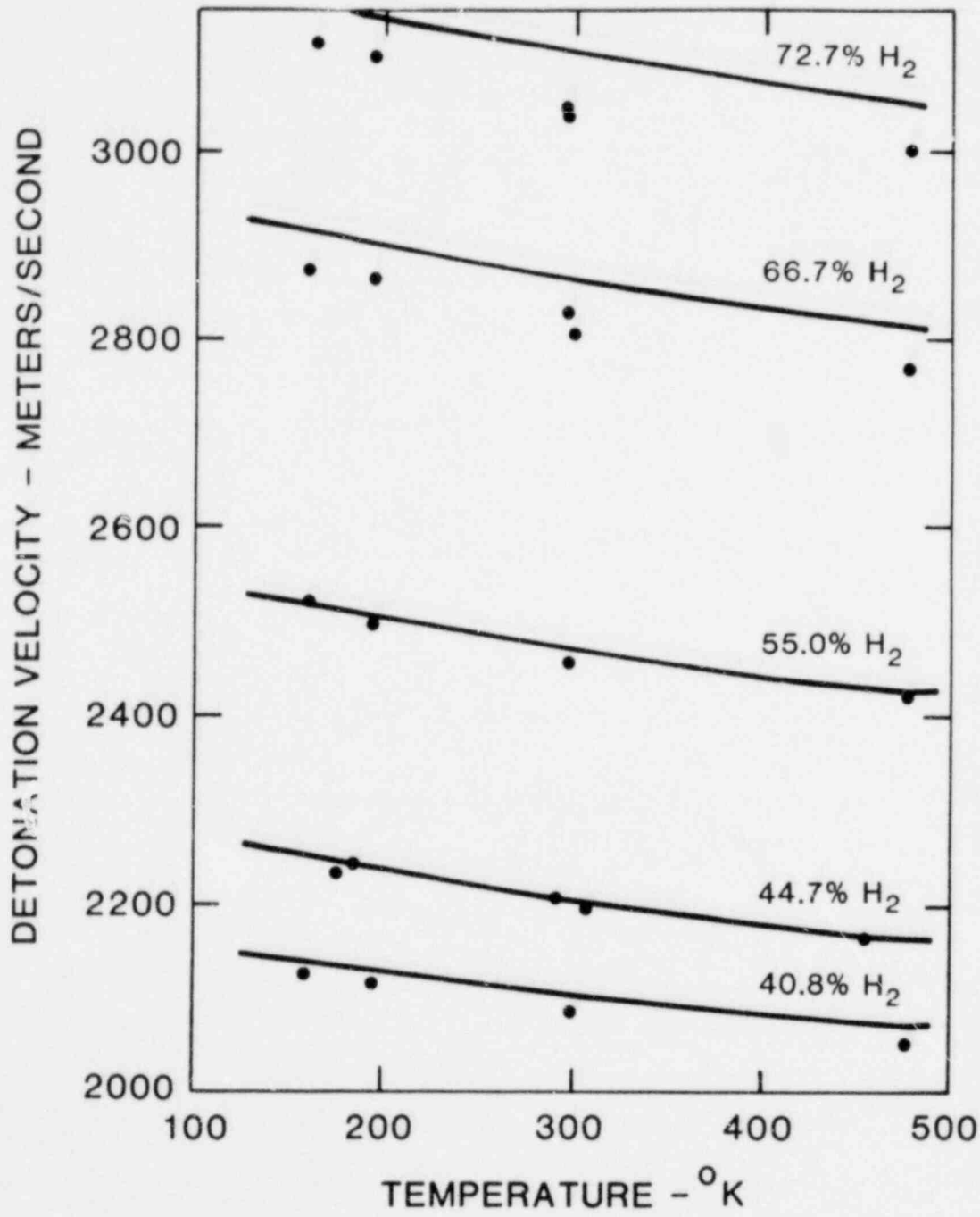

FIG. 14. EFFECT OF INITIAL TEMPERATURE ON DETONATION VELOCITY IN HYDROGEN-OXYGEN MIXTURES AT ATMOSPHERIC PRESSURE[78]

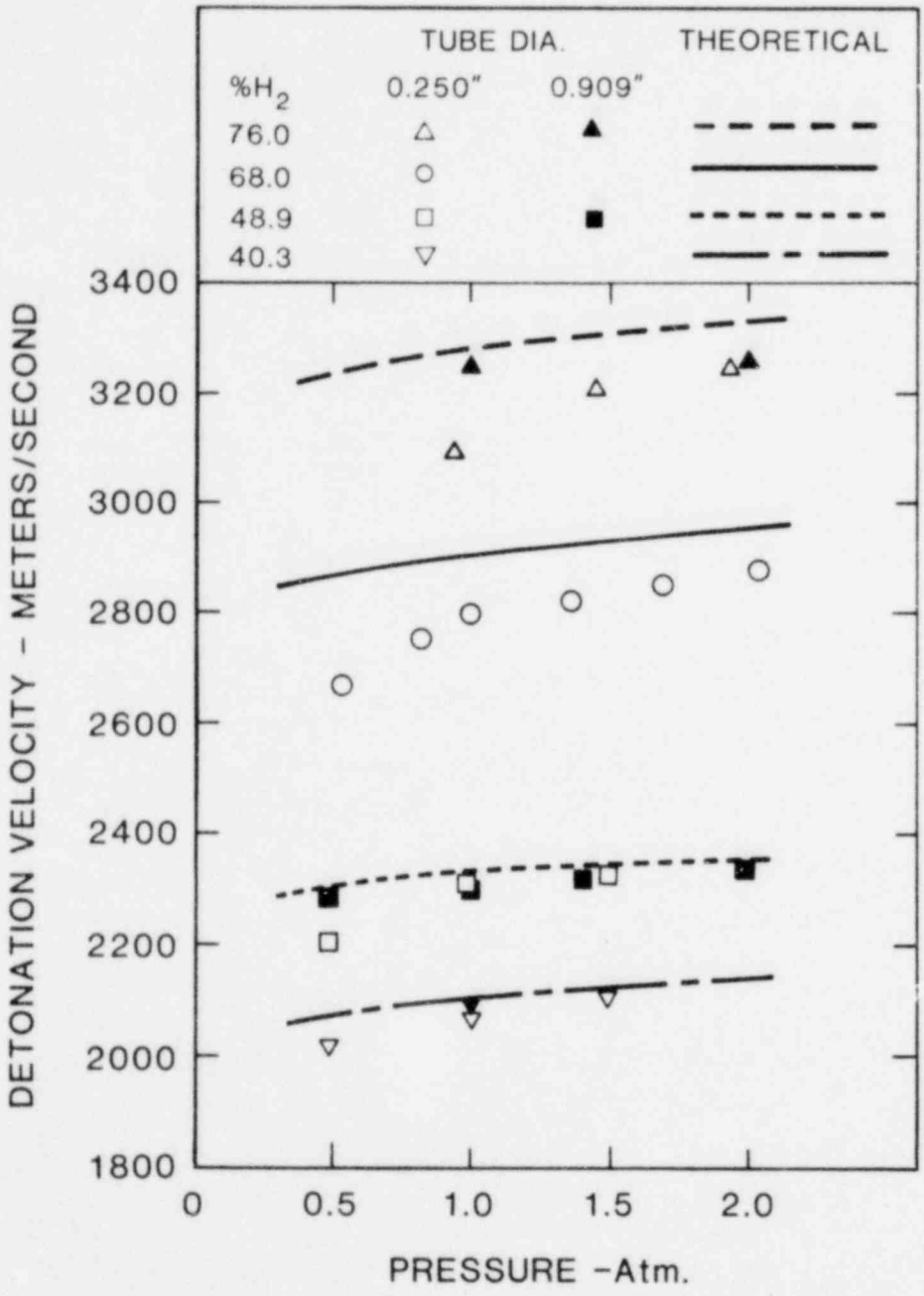

FIG. 15. EFFECT OF INITIAL PRESSURE ON DETONATION VELOCITY IN HYDROGEN-OXYGEN MIXTURES AT 298 K[78]

The effect of small changes in initial temperature and pressure on the detonation pressure ratio is small. Shown in Figs. 12 and 13 are the effects of variations in temperature and pressure on the pressure ratio of hydrogen-oxygen detonations, and in Figs. 14-15 are the effects on the detonation speed. Data on the effects of changes in temperature and pressure for hydrogen-air detonations are not as clearly presented. Sokolik[43] presented data attributed to Breton and Lafitte on the effects of variations in temperature and pressure. These data, presented in Ref. 2, show a very small decrease in the lower detonation limit with increased pressure and temperature. There are no data on the upper detonation limit.

Transition to Detonation

If a hydrogen-air or hydrogen-air-steam mixture is within detonation limits when combustion occurs, a detonation may or may not follow. It is possible to directly initiate a detonation with a strong explosive source.[45,46] In an accident however, it is more likely that combustion will begin as a deflagration. Deflagrations, rather than detonations, are often observed up to hydrogen concentrations of 24% in air.[16,48] There has been a great deal of work on the deflagration-to-detonation transition, DDT, for over 50 years, but the subject is still not understood satisfactorily. Several mechanisms believed to cause the transition have been investigated, but new experimental results have confounded the interpretation of the data.

One mechanism begins with a deflagration occurring in a confined volume. The expansion of hot burned gas causes compression of the gas ahead of the deflagration front. The compressive heating of the unburned gas increases the flame speed, causing further increases in compression until a shock wave is developed. The unburned gas behind the shock wave is heated above its autoignition temperature and a detonation occurs.[49] It is usually accepted today that the above transition mechanism must involve the formation of a turbulent flame and perhaps reflected shock waves.[50-52] The above mechanism has usually been studied in closed tubes. For containment, the nearly spherical expansion of the gas is not as confined as in closed tubes, and this mechanism may not be as important.

A second mechanism for transition to detonation is the acceleration of a flame front by obstacles in its path. Detonations can be produced in some tubes containing obstacles, when no detonation occurs for identical mixtures in the same tubes with no obstacles.

It is important to know not only if detonation will occur, but also how long the transition to detonation will take. The initial deflagration precompresses the containment atmosphere. The pressure behind the detonation wave will be increased by the precompression because the pressure ratio across the detonation wave is not greatly altered by the precompression. If the initial deflagration increases the containment atmosphere from 1 to 4 atmospheres, and the pressure ratio across the detonation is 16, the pressure behind the detonation wave will be 64 atmospheres. When the detonation wave hits the containment wall, it will be reflected as a shock wave. The pressure ratio across the shock wave will be about 2.5. Consequently, the peak pressure seen at the wall could be as great as 4 x 16 x 2.5 = 160 atmospheres (16 MPa, 2350 psia). The damage done to the containment structure by this strong shock wave will depend mainly on the impulse given to the wall (see Appendix C).

Detonation Wave Structure

The first modern theories of detonation wave structure were due to Zeldovich, Doring and von Neumann. The detonation wave model was that of a normal shock wave followed by a deflagration. The detonation was assumed to travel at a speed corresponding to the upper Chapman-Jouguet point. This steady one-dimensional model was used in conjunction with chemical reaction rate data to predict detonation wave structure. Since the pressure drops when passing through a deflagration, one would expect the pressure behind the initial shock wave portion of the detonation to overshoot the final Chapman-Jouguet value. This "von Neumann pressure spike," however, has not been seen experimentally.

It became clear in the late 1950s and early 1960s that detonation waves were unsteady multidimensional flow regions with moving transverse shock waves and cellular structure.[53-60] Modern detonation theory is helpful in interpreting the results of detonation experiments. For estimating overall effects of blast on the containment structure, the simple Chapman-Jouguet model of the detonation wave as a discontinuity is quite adequate[61] and much easier to deal with mathematically.

Mixing of Hydrogen in Containment

The previous sections dealt with the combustion of uniform premixed hydrogen-air or hydrogen-air-steam mixtures. However, the hydrogen from the reactor coolant system could be released into containment in the form of a fast, highly turbulent, steam-hydrogen jet. The hydrogen in the jet may start to burn as a turbulent diffusion flame, or the hydrogen may first partly mix with the surrounding containment atmosphere before it burns. Additional hydrogen may be evolved by radiolysis of water in the reactor or in the containment. Hydrogen could also evolve at numerous locations by oxidation of paints and galvanized coatings. These issues are discussed in detail in section II. In this section we will consider the time required for the hydrogen to mix in the containment atmosphere.

First let us clarify a common misconception. The hydrogen will not separate out from the air and stratify near the top of the containment. Once the gases mix, they will not separate. If hydrogen reaches the top of containment without having mixed, particularly if the top of containment is at a higher temperature than the bottom, the mixing will be slowed.[62] It is expected, however, that the hydrogen will be released into containment near the bottom, and that the bottom will be at a higher temperature than the top.

The mechanisms for mixing are diffusion, natural convection, forced convection caused by the jets that release hydrogen from the reactor coolant system, and forced convection due to fans and sprays. Willicut and Gido[63] investigated the mixing of hydrogen generated by radiolysis from water on the containment floor. Their results can be qualitatively extended to other situations involving hydrogen

mixing. They found that if there were no fluid motion and only diffusive mixing, it would take many days for the hydrogen to completely mix throughout containment. The diffusion coefficient of hydrogen is large compared to those of other gases, but diffusion over a scale of tens of feet is slow, even for hydrogen. However, diffusion over a scale of inches is rapid, of the order of a minute. Willcut and Gido[63] considered what would happen if a bubble of hydrogen were formed at the bottom of containment and began to rise to the top. Considering mixing only by diffusion, and ignoring any instability in the bubble or turbulence, a one-inch-diameter bubble would spread out enough to lower its maximum concentration below the flammability limit if mixing into air.

Since it is expected that the hottest parts of containment will be near the bottom, natural convection currents will be present. For the large distances involved in containment, and the resultant large Grashof numbers, the natural convective flow will be turbulent, promoting mixing. Willcut and Gido[63] predict that for only a 1.4°C temperature difference between the floor and the other walls, in a chamber 20 feet high, the circulation will be about 10 chamber-volumes per hour. Trent[64] carried out a numerical solution of the mixing in a BWR containment. Due to natural convection, flow velocities of several tenths of a foot per second were found for a 2.8°C temperature difference in a 16-foot-high chamber. His results implied a circulation of about 1 chamber-volume per hour.

Detailed calculations or experimental tests are required to predict the time required to obtain mixing of hydrogen in containment.

It appears that natural convection will mix the hydrogen in times of the order of one hour, perhaps less. If fans or sprays are used in containment, mixing will be much faster.

Combustion of a Steam-Hydrogen Jet

If the hydrogen is injected into containment in the form of a steam-hydrogen jet, it is possible that hydrogen may start to burn as a turbulent diffusion flame. A diffusion flame is one in which the burning rate is controlled by the rate of mixing of oxygen and fuel. For the jet to burn, it is necessary that at some locations the hydrogen-air-steam mixture be within flammability limits.

Combustion can begin either because of some outside ignition source, or because the mixture temperature is above the spontaneous ignition temperature. Shapiro and Moffette[10] in 1952 presented experimental results on the spontaneous ignition temperature of hydrogen-air-steam mixtures applicable to stationary gases, or moving gases with obstacles in the path acting as a flame holder (see Fig. 16). The spontaneous ignition temperature is in the range 515-580°C. Using then current computer codes which predicted the steam-hydrogen jet temperatures during a LOCA accident, Shapiro and Moffette predicted it was likely that spontaneous ignition of the jet would occur. We have not found any more recent accident calculations that carry a LOCA accident to the point of predicting steam-hydrogen jet temperatures. However, the onset of hydrogen production and jet temperatures do not appear to agree with more recent work.

If the jet impinges on the floor, pipes, or other obstructions, the shape of the jet and the mixing will be drastically altered. An obstruction such as a pipe can act as a flame holder. If the jet does not impinge on any solid surface, it will be much more difficult to ignite the mixture.[65,66]

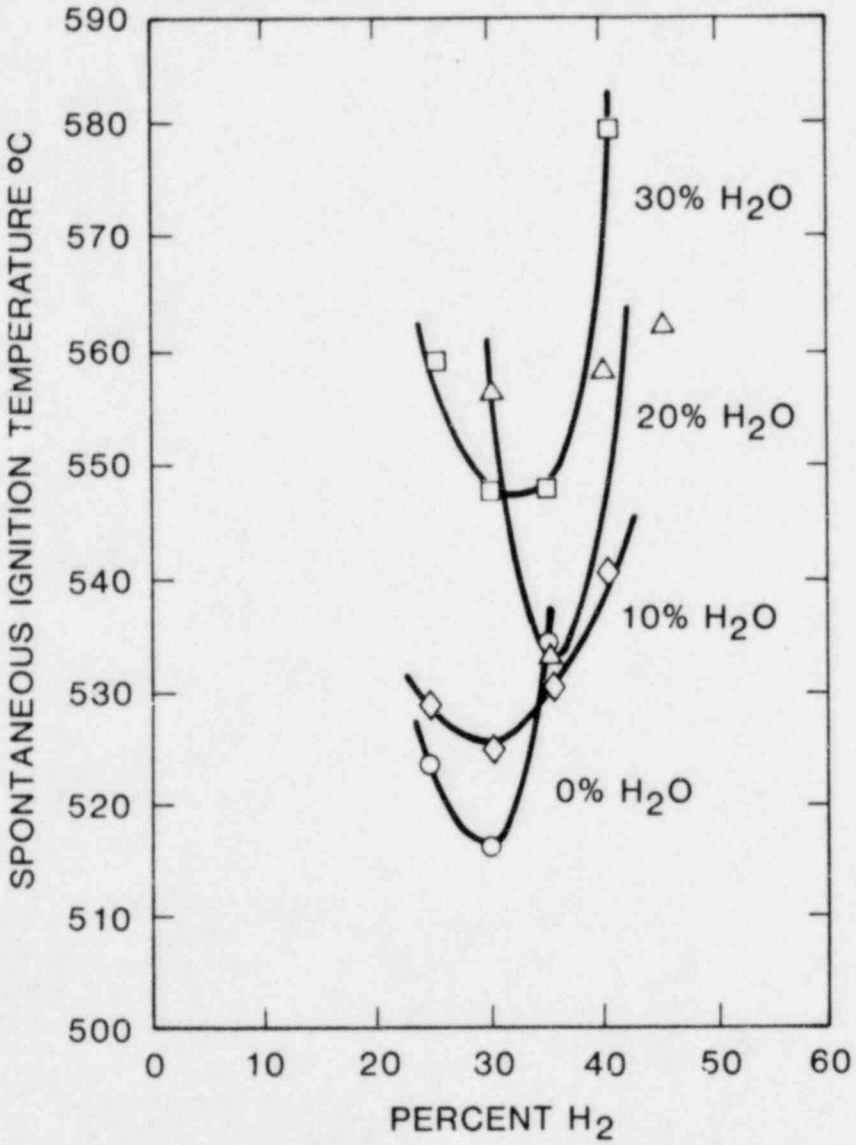

FIG. 16. MINIMUM SPONTANEOUS IGNITION TEMPERATURES OF HYDROGEN-AIR-STEAM MIXTURES AT 100 P.S.I.G.[10]

APPENDIX A

CALCULATION OF FLAME TEMPERATURE AND PRESSURE

In our calculation of hydrogen combustion in containments, we assume that the combustion is adiabatic and at constant volume. The hydrogen is assumed to be completely consumed, and the dissociation of the combustion products is neglected. Consequently, the calculation is meaningful only up to stoichiometric concentrations of hydrogen. The gas is assumed to be a mixture of perfect gases. In all our calculations we assumed that the air was saturated with water vapor.

SI units were used in the calculations. Data on specific heats and heats of formation were taken from Sontag and von Wylan.[67] The various components were identified by the following subscripts: 1 = hydrogen, 2 = nitrogen, 3 = oxygen, 4 = steam. The symbols used used are identified below.

P = pressure, kPa

P_i = partial pressure of component i, kPa

T = temperature, K

V = volume of mixture, taken as 1 m^3

N = mole density of gas, moles/m^3

N_i = mole density of component i, moles/m^3

U_i = internal energy of component i, kJ/mole

C_{pi}, C_{vi} = specific heats of component i, kJ/mole-K, at constant pressure and volume, respectively

R = universal gas constant, 8.31434 kJ/mole-K

H_i = enthalpy of component i, kJ/mole

X_i = mole fraction of component i

θ, θ_o = T/100 and 298/100

The symbols used for the combustion products are distinguished from those for the reactants by the use of a tilde (~).

The calculations were begun by specifying the initial temperature, pressure and oxygen/(oxygen + nitrogen) mole fraction. For initial conditions, we used T = 298 K, P = 100 kPa and $X_3/(X_2 + X_3) = 0.21$, values representative of room temperature air. The partial pressure of steam in the initial mixture was assumed to be that of saturated vapor at the mixture temperature. The hydrogen mole fraction was varied up to the stoichiometric ratio, 28.6%.

Given the pressure and temperature, the number of moles of gas per m^3 was obtained from

1) $$PV = NRT \quad (V = 1\ m^3)$$

The corresponding number of moles of hydrogen was obtained from

2) $$N_1 = X_1 N$$

The number of moles of steam was obtained using

3) $$P_4 V = N_4 RT$$

The number of moles of oxygen and nitrogen was obtained using

4) $$N_3 = \frac{X_3}{X_2 + X_3} (N - N_1 - N_4)$$

5) $$N_2 = N - N_1 - N_3 - N_4$$

For the products of combustion we have

6) $\tilde{N}_1 = 0$

7) $\tilde{N}_2 = N_2$

8) $\tilde{N}_3 = N_3 - N_1/2$

9) $\tilde{N}_4 = N_4 + N_1$

The first law of thermodynamics for the reacting, adiabatic, constant-volume system is

10) $$\sum N_i U_i = \sum \tilde{N}_i \tilde{U}_i$$

An initial estimate of the final temperature was obtained by assuming the specific heats of the components were constant. The temperature above the standard temperature, 298 K, ΔT, was obtained using

11) $$\Delta T = \frac{\sum \tilde{N}_i U_i - \sum \tilde{N}_i U_{if}}{\sum \tilde{N}_i C_{vi}}$$

where U_{if} are the internal energies at the standard temperature, 298 K. The U_{if} were obtained from the heats of formation (enthalpies at the standard temperature) using $U_{if} = H_{if} - 298*R$

12) $U_{1f} = U_{2f} = U_{3f} = -298*R = -2478$ kJ/mole

$U_{4f} = -241,827 - 298*R = -244,305$ kJ/mole

An accurate value of the final temperature was obtained by an iterative Newton-Raphson solution of Eq. 10, using finite-difference approximations for the derivatives and the solution of Eq. 11 as the initial estimate. The iteration was carried out until the temperature was determined to within one degree. Convergence was rapid.

The internal energies were obtained from curve fits of C_{pi} in Ref. 67. using

13) $$C_{vi} = C_{pi} - R$$

14) $$U_i = U_{if} + 100 \int_0^{\theta} C_{vi}(\theta)\, d\theta$$

The results obtained for the internal energy equations are presented below. They were compared with values of enthalpy in tables of Ref. 67 using $U_i = H_i - RT$ and found to differ by no more than 20 kJ/mole, which is negligible compared to values of the order of 50,000 kJ/mole for the enthalpies.

15) $$U_2 = 100\ [-24.7767 + 30.746(\theta - \theta_o) + 2 \times 512.79(\theta^{-.5} - \theta_o^{-.5}) - 1072.7(\theta^{-1} - \theta_o^{-1}) + 820.4/2(\theta^{-2} - \theta_o^{-2})]$$

16) $$U_3 = 100\ [-24.7767 + 29.118(\theta - \theta_o) + (.020102/2.5)(\theta^{2.5} - \theta_o^{2.5}) + 2x178.57(\theta^{-.5} - \theta_o^{-.5}) - 236.88(\theta^{-1} - \theta_o^{-1})]$$

17) $$U_4 = 100\ [-2443.05 + 134.736(\theta - \theta_o) - 1183.54/1.25)(\theta^{1.25} - \theta_o^{1.25}) + (82.751/1.5)(\theta^{1.5} - \theta_o^{1.5}) - (3.6989/2)(\theta^{2} - \theta_o^{2})]$$

After the temperature is known, the final pressure is easily obtained from

18) $$PV = NRT$$

The flame temperature and pressure calculations were carried out for use in this report and for use in a later report on mitigation schemes. For the latter, the initial mixture was assumed to include liquid water drops that were evaporated in combustion. Only minor additions to the above work are required to include the effects of liquid water drops.

APPENDIX B

REVIEW OF THE CLASSICAL CHAPMAN-JOUGUET THEORY

An understanding of the classical Chapman-Jouguet theory is very helpful when discussing deflagrations, detonations and Chapman-Jouguet points. The theory can be found in most works on combustion.[1,20,68,69] It is remarkable that the classical theory remains so useful in view of our present knowledge of the unsteady multidimensional character of detonation and some deflagration fronts.

We ignore the structure of the combustion front and consider it as a discontinuity into which enter unburned combustible gases and out of which exit burned combustion products as depicted below.

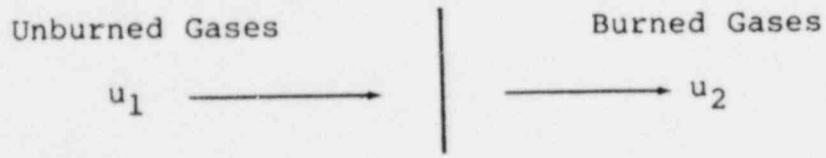

Schematic combustion front

From integration of the conservation of mass, momentum and energy equations we obtain

1) $\rho_1 u_1 = \rho_2 u_2 = \text{constant} = m$

2) $p_1 + \rho_1 u_1^2 = p_2 + \rho_2 u_2^2 = \text{constant} = p_o$

3) $h_1 + u_1^2/2 = h_2 + u_2^2/2 = \text{constant} = h_o$

where the subscript 1 refers to the unburned gas, and the subscript 2 refers to the burned gas. The symbol u is the normal component of velocity relative to the combustion front, ρ is the density, p is the pressure and h is the specific enthalpy. The three constants of integration are m, the mass flow per unit area, p_o, and h_o,

the stagnation enthalpy. In the further development we will use the specific volume, $v = 1/\rho$, in place of the density.

Algebraic manipulation of Eqs. 1-3 gives a form excluding the velocities, the famous Hugoniot relation,

4) $$h_2 - h_1 = 1/2(p_2-p_1)(v_1+v_2)$$

and the important form

5) $$(u_1-u_2)^2 = (p_2-p_1(v_1-v_2) \quad .$$

These two equations show that we can classify combustion fronts into those in which the pressure, density and enthalpy increase (detonations) and those in which the pressure, density and enthalpy decrease (deflagrations). Further analysis shows that detonations are supersonic relative to the unburned gas, while deflagrations are subsonic relative to the unburned gas. The results are most easily shown on a pressure-specific volume diagram, the Hugoniot diagram, Fig. 17. The initial state is represented by point O. The final state is represented by a point on the line A to F, excluding the segment C to D by the arguments previously given. The points of tangency B and E, the Chapman-Jouguet points are of special interest. Detonations are observed to move at speeds corresponding to the upper Chapman-Jouguet point, or near to it.

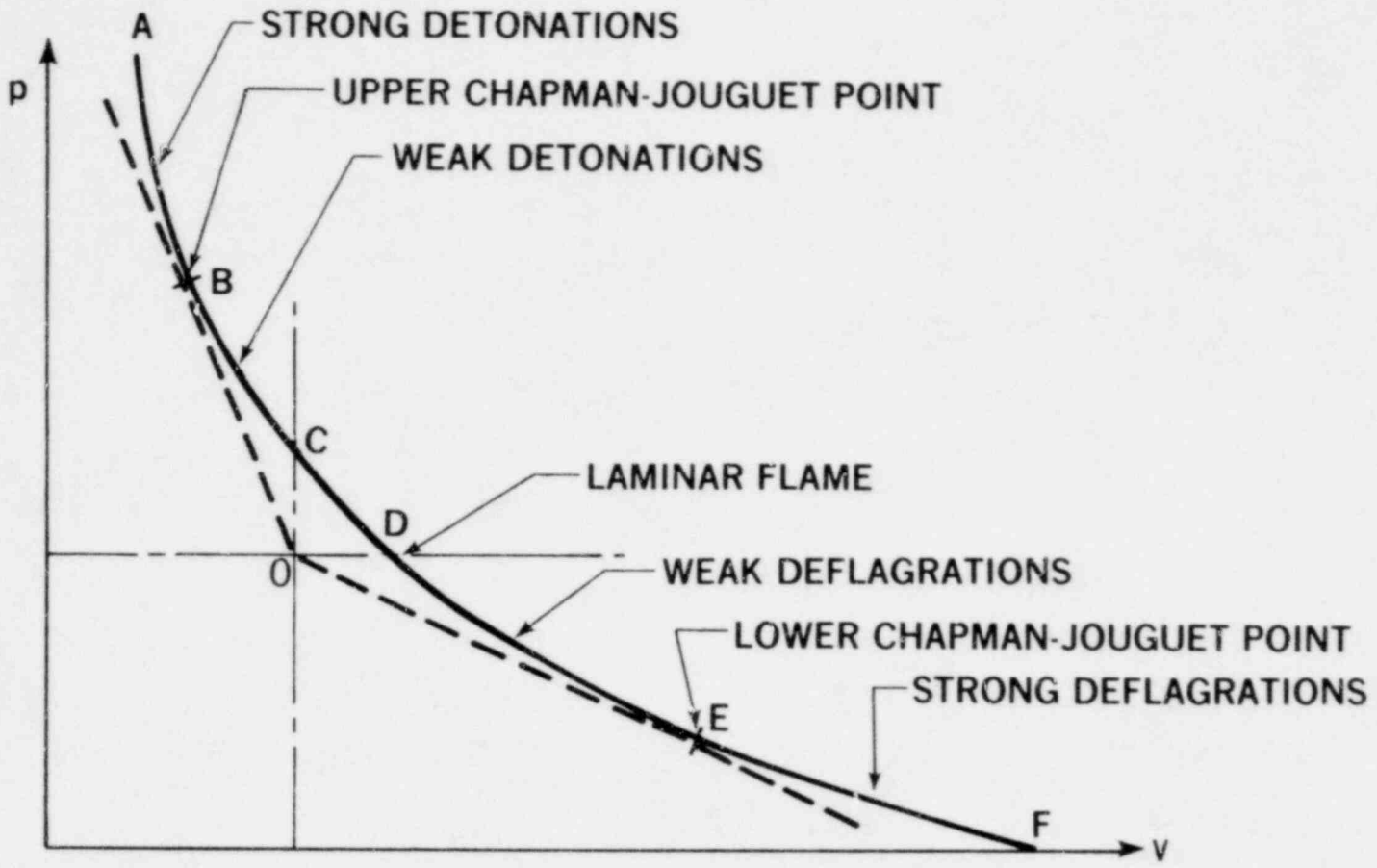

FIG. 17. **HUGONIOT DIAGRAM**

Section on Curve	Name	Speed Relative to Unburned Gas	Speed Relative to Burned Gas	Pressure Change	Comments
A-B	Strong Detonation	Supersonic	Subsonic	Very Large Increase	Decays to C-J point
B	Upper C-J point detonation	Supersonic	Sonic	Large Increase	Observed
B-C	Weak Detonation	Supersonic	Supersonic	Increase	Marginal detonations just below C-J point
Just below D	Laminar flame	Subsonic	Subsonic	Very Small Decrease	Observed
D-E	Weak deflagration	Subsonic	Subsonic	Decrease	
E	Lower C-J point	Subsonic	Sonic	Large Decrease	Not Observed
E-F	Strong Deflagration	Subsonic	Supersonic	Very Large Decrease	Not observed, believed

APPENDIX C

THE EFFECTS OF RAPIDLY APPLIED LOADS ON STRUCTURES

The purpose of this section is to give a qualitative appreciation of the influence of the duration of pressure loads on the containment structure. We will drastically simplify the problem while retaining the essence of the structural response to rapid loading. We will assume that the containment is a spherical shell, the pressure load is spherically symmetric and hence the deformations of the containment are radial and spherically symmetric. We will first consider the structure to be linearly elastic and briefly discuss plastic behavior.

In our highly simplified model there is one mode of vibration, radial "ringing." We have a single degree of freedom system. If allowed to vibrate freely, the structure will undergo a slightly damped sinusoidal radial motion. We will ignore the small damping of the motion. The period of the motion will be proportional to the square root of the ratio of the mass of the structure to the stiffness of the structure, $\sqrt{m/k}$. (Natural frequency is the reciprocal of the period.) The period is the characteristic time for the response of the structure to imposed loads. Loads of duration much less than this period are "impulsive." The period for a large dry PWR containment is of the order of 0.05 seconds.

Let us consider the behavior of a single degree of freedom structure to a load that is applied suddenly and then decays exponentially with time constant T, an approximation to a shock or detonation load. Shown in Fig. 18 is the maximum deformation, X, normalized by the ratio of force to stiffness, P/k, (P is force),

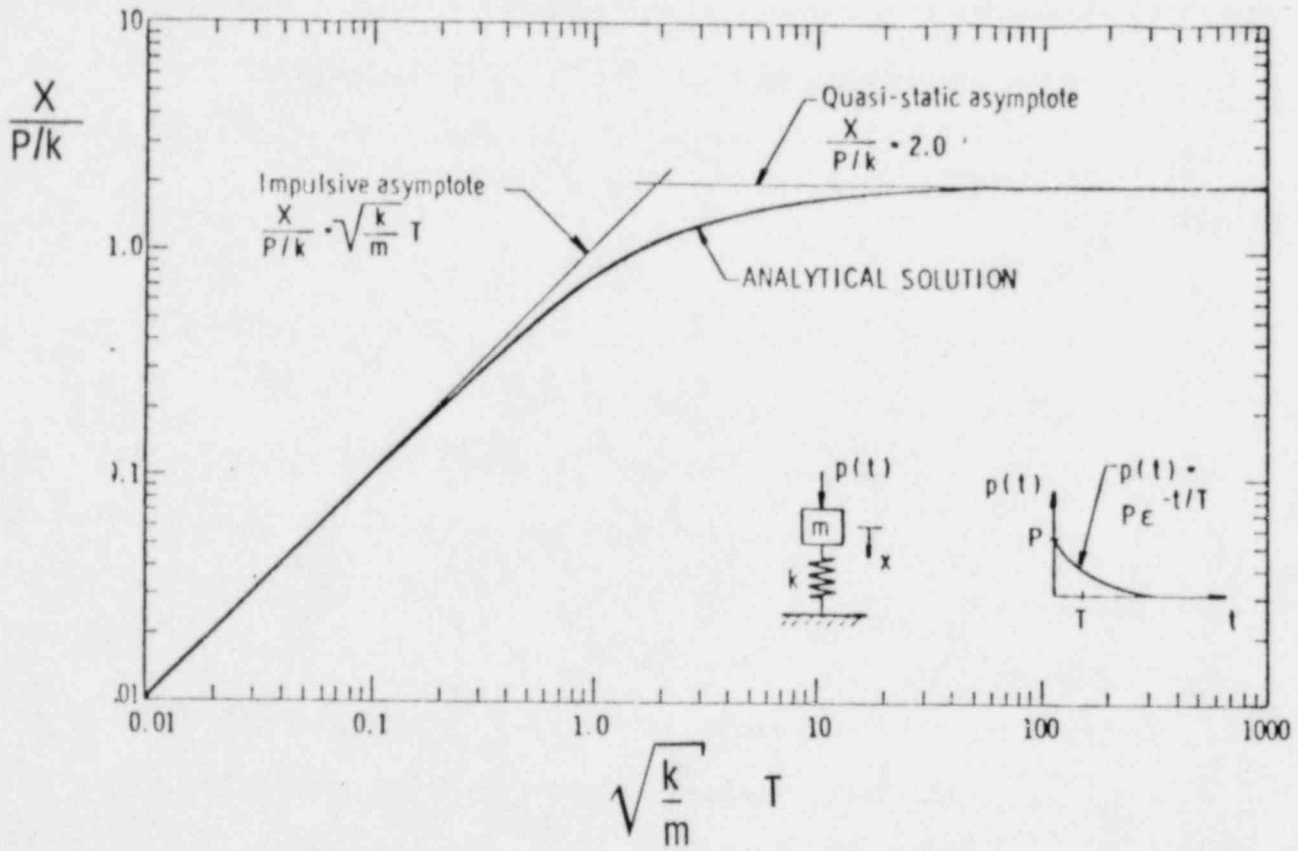

70

FIG. 18. SHOCK RESPONSE FOR BLAST LOADED ELASTIC OSCILLATOR

versus the ratio of load duration to structural period. If the load P had been applied statically, the static deformation of the structure would be $X/(P/k) = 1$. For a suddenly applied constant load P, the structure vibrates with a maximum deformation of $X/(P/k) = 2$. If the time constant for the decay of the load considered is longer than about 40 periods, the maximum deformation will be essentially equal to that of the suddenly applied constant load. This is called the quasi-static asymptote. If the decay of the suddenly applied load is more rapid, the maximum deformation of the structure is reduced. Assuming that the damage to the structure is governed solely by the maximum deformation, short duration loads of the same peak magnitude as long duration loads are less destructive. If the time constant for decay of the suddenly applied load is less than about 0.3 times the period, the load is considered to be impulsive. For impulsive loads, the maximum deformation depends on the impulse, the time integral of the load, and not on the peak load. This is shown more clearly in Fig. 19. This force-impulse diagram shows a curve of constant maximum deflection. The structure is assumed to be damaged if the combination of force and impulse gives a point in the upper righthand region; the structure is assumed undamaged if the point is below and/or to the left of the curve. We see that if the maximum load is below a given value, the structure will not be damaged for any value of impulse. We also see that if the impulse is below a given value, the structure will not be damaged by any value of maximum load. There is an intermediate region in which damage is controlled by both maximum load and impulse.

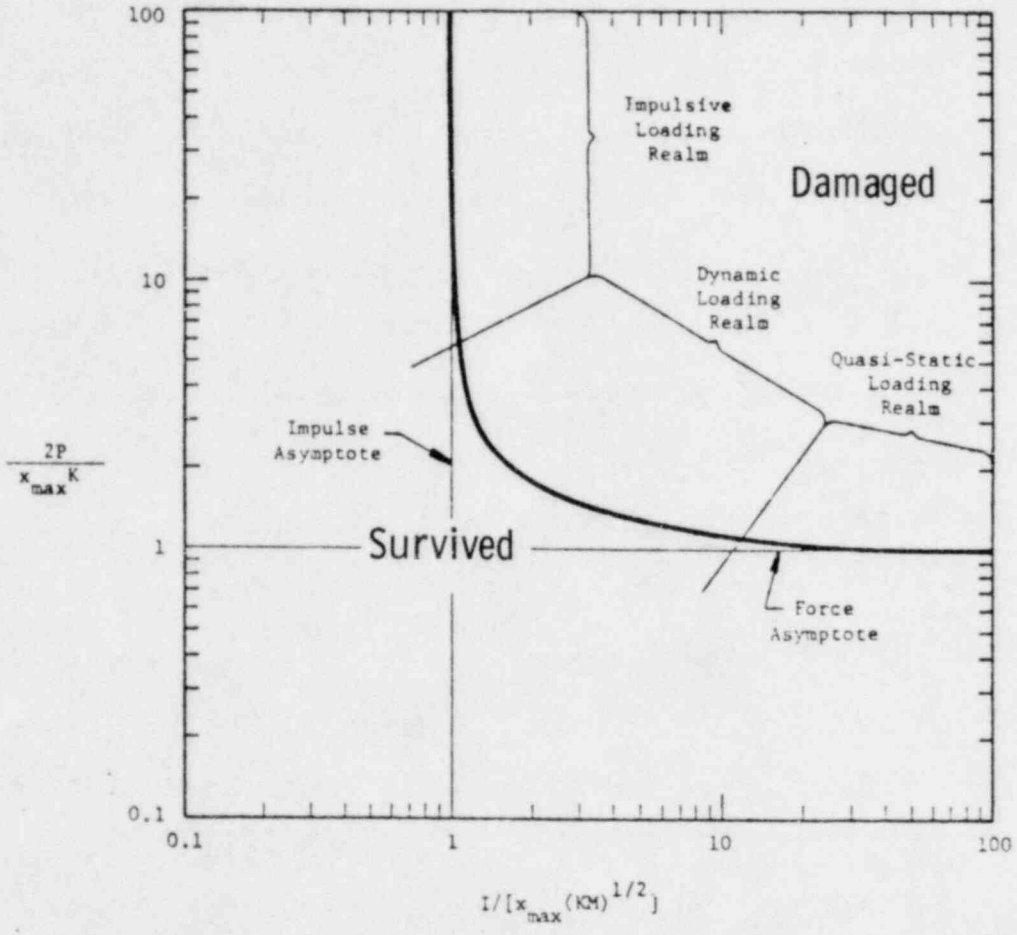

FIG. 19. PRESSURE-IMPULSE DIAGRAM FOR 70 BLAST LOADED ELASTIC OSCILLATOR

The main qualitative features of the above model apply when the particular load is replaced by other suddenly applied loads. We have a quasi-static limit, an impulsive limit and an intermediate region. For deflagrations in containment, both the rise and the fall in load will be of long duration compared to the period. For this case the deformation at each instant will correspond to the static deformation expected by the given load, ignoring transient effects.

For ductile materials such as steel, the material will plastically deform if loaded above the yield stress. The reinforcing steel in reinforced concrete containment structures will be expected to undergo plastic deformation before the structure fails completely. The analysis of a single degree of freedom system subject to a rapidly applied load can be extended to plastic behavior. Qualitatively, the results are similar. We again have an impulsive limit for short duration loads, a quasi-static limit for long duration loads and an intermediate region.

APPENDIX D

CHEMICAL REACTION RATES FOR HYDROGEN-OXYGEN COMBUSTION

The important chemical reactions involved in the combustion of hydrogen in oxygen or air are known, and the reaction rates are fairly well known. The combustion of hydrogen in oxygen or air is a branched chain reaction. The radicals H, O, and OH play a commanding role in the reaction. H_2O_2 and HO_2 can also play important roles. The current picture is that the chemistry starts with the formation of free radicals by endothermic dissociation. The concentration of radicals increases by chain branching reactions.

1) $H_2 + M \longrightarrow H + H + M$ (chain initiation, M is third body)

2) $H + O_2 \longrightarrow OH + O$ (two most important chain branching reactions)

3) $O + H_2 \longrightarrow OH + H$

4) $OH + H_2 \longrightarrow H_2O + H$ (chain reaction)

The most important recombination reaction can be the reverse of reaction 1. At low pressures in small containers, a major cause of radical removal can be the diffusion of HO_2 to the wall, and its subsequent reaction to stable species. HO_2 is formed by

5) $H + O_2 + M \longrightarrow HO_2 + M$

For the conditions of a nuclear reactor containment, the HO_2 will probably react and create new radicals, before reaching solid walls,

6) $HO_2 + H_2 \longrightarrow H_2O_2 + H$

The peroxide will quickly decompose into reactive radicals. An alternative chain initiation can occur through the formation of peroxide,

7) $H_2 + O_2 + M \longrightarrow H_2O_2 + M \longrightarrow 2OH + M$

In all there are less than 20 reactions that are believed to be of significance in determining the overall combustion rate.

The rate of reaction per unit volume for a given chemical reaction is expressed as the product of the concentration of the reactants and a rate coefficient, where the rate coefficient is a function of temperature. In most of the literature cgs metric units are used with energy expressed in kcal. The reaction rates are in units of moles/cm^3-sec, and the reactant concentrations in units of moles/cm^3.

The rate coefficient is usually expresed in the form

$$k = AT^n \exp(-E/RT)$$

where T is the absolute temperature in K, R is the universal gas constant, 1.998×10^{-3} kcal/mole-K, E is the activation energy in kcal, and A and n are constants. The units of the rate coefficient are cm^3/mole-s for two body reactions and cm^6/$mole^2$-s for three body reactions. However, in the table of rate coefficients presented in this Appendix, the units are cm^3/molecule-s for two body reactions and cm^6/$molecule^2$-s for three body reactions. These values can be converted into the more common form by multiplication by the Avogadro number, 6.023×10^{23} molecule/mole for two body reactions, and Avogadro number squared for three body reactions.

The table selected presents forward and backward reaction rates for many of the important reactions. This is a convenience that led to its selection. The backward rate coefficient k_b, is related to the forward rate coefficient, k_f, by the equilibrium constant, K,

$$K = k_f/k_b \quad .$$

Since the equilibrium constant can be determined from thermodynamics alone, without a knowledge of reaction rates, it is usually much more accurately known than either rate coefficient. Consequently, most of the tables of rate coefficients omit listing the backward rates.

The values of the rate coefficients presented by several of the references were compared for some of the important reactions. In all cases the agreement in the activation energies was excellent. Usually, but not always, the value of n was the same. When E and n were nearly the same, the rate coefficient values could be compared just by comparing the values of A. In many cases the agreement was excellent, but in a few the values differed by a factor of two. The uncertainties in the rates of the reactions involved in the hydrogen-oxygen are probably of less importance to hydrogen combustion than the uncertainties in the fluid mechanics.

TABLE 1[71]

Chemical Reaction Rates*

	Reactants	Products	Reaction rate constants $k = AT^B e^{C/T}$ A	B	C
1.	H + H + M	H_2 + M	1.80(-30)	-1.00	0.00
2.	H + O + M	OH + M	2.80(-32)	0.00	0.00
3.	H + OH	H_2 + O	1.40(-14)	1.00	-3.50(+03)
4.	H + OH + M	H_2O + M	6.20(-26)	-2.00	0.00
5.	H + H_2O	H_2 + OH	1.50(-10)	0.00	-1.03(+04)
6.	H + O_2	O + OH	3.70(-10)	0.00	-8.45(+03)
7.	H + O_2 + M	HO_2 + M	4.10(-33)	0.00	5.00(+02)
8.	H + HO_2	H_2 + O_2	4.20(-11)	0.00	-3.50(+02)
9.	H + HO_2	O + H_2O	8.30(-11)	0.00	-5.00(+02)
10.	H + HO_2	OH + OH	4.20(-10)	0.00	-9.50(+02)
11.	H + H_2O_2	H_2 + HO_2	2.80(-12)	0.00	-1.90(+03)
12.	H_2 + O	H + OH	3.00(-14)	1.00	-4.48(+03)
13.	H_2 + OH	H + H_2O	3.60(-11)	0.00	-2.59(+03)
14.	H_2 + O_2	H + HO_2	9.10(-11)	0.00	-2.91(+04)
15.	H_2 + O_2	OH + OH	2.80(-11)	0.00	-2.42(+04)
16.	H_2 + HO_2	H + H_2O_2	1.20(-12)	0.00	-9.40(+03)
17.	H_2 + HO_2	OH + H_2O	1.21(-12)	0.00	-9.41(+03)
18.	H_2 + M	H + H + M	3.70(-10)	0.00	-4.83(+04)
19.	O + O + M	O_2 + M	5.00(-35)	0.00	9.00(+02)
20.	O + OH	H + O_2	2.72(-12)	2.80(-01)	8.10(+01)
21.	O + OH + M	HO_2 + M	2.80(-31)	0.00	0.00
22.	O + H_2O	H + HO_2	1.75(-12)	4.50(-01)	-2.84(+04)
23.	O + H_2O	OH + OH	1.10(-10)	0.00	-9.24(+03)
24.	O + HO_2	OH + O_2	8.00(-11)	0.00	-5.00(+02)
25.	O + H_2O_2	OH + HO_2	1.40(-12)	0.00	-2.13(+03)
26.	OH + OH	H + HO_2	2.00(-11)	0.00	-2.02(+04)
27.	OH + OH	H_2 + O_2	1.09(-13)	2.60(-01)	-1.47(+04)
28.	OH + OH	O + H_2O	1.00(-11)	0.00	-5.50(+02)
29.	OH + OH + M	H_2O_2 + M	2.50(-33)	0.00	2.55(+03)
30.	OH + HO_2	H_2O + O_2	8.30(-11)	0.00	-5.00(+02)

TABLE 1 (cont)

Chemical Reaction Rates*

	Reactants	Products	Reaction rate constants $k = AT^B e^{C/T}$ A	B	C
31.	$OH + H_2O$	$H_2 + HO_2$	1.34(-14)	4.30(-01)	-3.62(+04)
32.	$OH + O_2$	$HO_2 + O$	2.20(-11)	1.80(-01)	-2.82(+04)
33.	$OH + H_2O_2$	$H_2O + HO_2$	1.70(-11)	0.00	-9.10(+02)
34.	$OH + M$	$H + O + M$	2.20(-08)	3.00(-02)	-5.14(+04)
35.	$H_2O + O_2$	$OH + HO_2$	2.38(-10)	1.70(-01)	-3.69(+04)
36.	$H_2O + HO_2$	$OH + H_2O_2$	4.70(-11)	0.00	-1.65(+04)
37.	$H_2O + M$	$H + OH + M$	5.80(-09)	0.00	-5.29(+04)
38.	$O_2 + H_2O_2$	$HO_2 + HO_2$	1.20(-13)	5.00(-01)	-2.11(+04)
39.	$O_2 + M$	$O + O + M$	3.00(-06)	-1.00	-5.94(+04)
40.	$HO_2 + HO_2$	$O_2 + H_2O_2$	3.00(-11)	0.00	-5.00(+02)
41.	$HO_2 + M$	$H + O_2 + M$	3.50(-09)	0.00	-2.30(+04)
42.	$HO_2 + M$	$O + OH + M$	1.13(-04)	-4.30(-01)	-3.22(+04)
43.	$H_2O_2 + M$	$OH + OH + M$	2.00(-07)	0.00	-2.29(+04)

*Rate constants are given in units of molecules^{-1} cm^3/sec,T in °K. Three body rates are in molecules^{-2} cm^6/sec where M is the third body. Read 1.80(-30) as 1.80 x 10^{-30}.

References

1. B. Lewis and G. von Elbe, Combustion, Flames and Explosions of Gases, 2nd, Ed., (New York: Academic Press, 1961)

2. A. A. Heckes, "Hydrogen Explosions," Core-Meltdown Experimental Review, SAND7 -0382 (Albuquerque: Sandia Laboratories, March 1977)

3. G. I. Shivashinsky, "Hydrodynamic theory of flame propagation in an enclosed volume," Acta Astron 5:631-645 (1978)

4. W. Murfin, Ed: Zion-Indian Point Study, SAND80-0617-1 (Albuquerque: Sandia Labortories, 1980)

5. A. L. Kuhl, M. M. Kameland, A. K. Oppenheim, "Pressure Waves Generated by Steady Flames," 14 Sym on Comb., Pittsburg, Combustion Institute, 1201-1215, (1973)

6. L. A. Lovachev, "Flammability limits a Review," Comb. Sci. & Tech. 20:209-224 (1979)

7. H. F. Coward and G. W. Jones, Limits of Flammability of Gases and Vapors, Bulletin 503, Bureau of Mines, U. S. Department of the Interior (1952)

8. M. G. Zabetakis, Flammability Characteristics of Combustible Gases and Vapors, Bulletin 627, Bureau of Mines, U. S. Department of the Interior (1965)

9. L. K. Parfenov, "Combustion of a Hydrogen-Oxygen Mixture Under Conditions of Weightlessness," Combustion, Explosion and Shock Waves, 14:412-4, (1 Jan 1979)

10. Z. M. Shapiro and T. R. Moffette, Hydrogen Flammability Data and Application to PWR Loss-of-Coolant Accident, WAPD-SC-545, Bettis Plant (September 1957)

11. "Appendix D, Noncondensible Gases" of Appendix VII, Physical Processes in Reactor Meltdown Accidents" to Reactor Safety Study, WASH-1400 (NUREG-75/014) U. S. Nuclear Regulatory Commission (October, 1975)

12. B. Bregeon, A. S. Gordon and F. A. Williams, "Near-Limit Downward Propagation of Hydrogen and Methane Flames in Oxygen-Nitrogen Mixtures," Comb. & Flame 33:33-45 (1978)

13. D. Burgess and M. Hertzberg, "The Flammability Limits of Lean Fuel-Air Mixtures-Thermodynamic Criteria For Explosion Hazards," ISA Trans., 14:129-136 (1975)

14. A. Macek, "Flammability Limits: A Re-examination," Comb. Sci. & Tech., 21:43-52 (1979)

References contd

15. A. L. Furno, E. B. Cook, J. M. Kuchta and D. S. Burgess, "Some Observations on Near-Limit Flames," 13 Sym. on Comb., (Pittsburg, Comb. Inst., 593-599, 1971)

16. B. C. Slifer and T. G. Peterson, "Hydrogen Flammability and Burning Characteristic in BWR Containments," NEDO-10812, 73NED49, General Electric (April, 1973)

17. M. P. aulson and J. O. Bradfute, "Pressure and Temperature Transients Resulting from Postulated Hydrogen Fires in Mark III Containments," EI 75-4, Energy, Inc.

18. G. W. Keilholtz, Hydrogen Considerations in Light-Water Power Reactors, ORNL-NSIC-120, (Oak Ridge National Laboratory, February 1976)

19. I. L. Drell and F. E. Belles, Survey of Hydrogen Combustion Properties,NACA R 1383, National Advisory Committee for Aeronautics, (1958)

20. R. A. Stehlow, Fundamentals of Combustion, (New York: R. E. Krieger Pub. Co., 1968)

21. G. E. Andrews and D. Bradley, "Determination of Burning Velocities: A Critical Review," Comb. & Flame, (18:133-149, 1972)

22. G. Jahn, "Der Zundvorgang in Gasemischen," Olderbourg, Berlin, 1934

23. T. G. Scholte and P. B. Vaags, "The Burning Velocity of Hydrogen-Air Mixtures and Mixtures of Some Hydrocarbons with Air," Comb. & Flame, (3:495-501, 1959)

24. H. Edmondson and M. P. Heap, "The Burning Velocity of Hydrogen-Air Flames," Comb. and Flame, (16:161-165, 1971)

25. G. Dixon-Lewis, "Flame Structure and Flame Reaction Kinerics I. Solution of Conservation Equations and Application to Rich Hydrogen-Air Flames," Proc. Roy Soc, Ser A (298:495-513, 1967)

26. G. Dixon-Lewis, "Flame Structure and Flame Reaction Kinetics II. Transport Phenomena in Multicomponent Systems," Pro Roy Soc, Ser A (307:111-135, 1968)

27. G. Dixon-Lewis and G. L. Isles, "Flame Structure and Flame Reaction Kinetics III. Measurement of Temperature Profiles in Flames at Atmospheric Pressure," Proc Roy Soc, Ser A, (308:517-536, 1969)

References contd

28. G. Dixon-Lewis, M. M. Sutton and A. Williams, "Flame Structure and Flame Reaction Kinetics IV. Experimental Investigations of a Fuel-Rich Hydrogen+Nit+Nitrogen+Oxygen Flame at Atmospheric Pressure," Proc. Roy Soc, Ser A (317. 227-234, 1970)

29. G. Dixon-Lewis, Flame Structure and Flame Reaction Kinetics V. Investigation of Reaction Mechanism in a Rich Hydrogen+Nitrogen+ Oxygen Flame by Solution of Conservation Equations," Proc Roy Soc, Ser A, (317:235-263, 1970)

30. J. Warnatz, "Calculation of the Structure of Laminar Flat Flames II: Flame Velocity and Structure of Freely Propagating Hydrogen-Oxygen and Hydrogen-Air Flames," Ber Bunsenges Phys Chem, (82:643-649, 1978)

31. D. K. Kuehl, "Effects of Water on the Burning Velocity of Hydrogen-Air Flames," ARS, (32:1724-1726, 1962)

32. A. Levy, "Effects of Water on Hydrogen Flames," AIAA J, (1:1239, 1963)

33. G. Dixon-Lewis and A. Williams, "Effects of Nitrogen, Excess Hydrogen and Water Additions on Hydrogen-Air Flames," AIAA J, (1, 2416-2417, 1963)

34. G. H. Markstein, Non-Steady Flame Propagation, Pergamon Press, 1964)

35. G. I. Shivashinsky, "On the Distorted Flame Front as a Hydro-Dynamic Discontinuity," Acta Astron, (3:889-918, 1976)

36. G. I. Shivashinsky, "Nonlinear Analysis of Hydrodynamic Instability in Laminar Flames-I. Derivation of the Basic Equations," Acta Astron, (4:1177 - 1206, 1977)

37. D. M. Michelson and G. I. Shivashinsky, "Nonlinear Analysis of Hydrodynamic Instability in Laminar Flames-II. Numerical Experiments," Acta Astron, (4:1207-1221, 1977)

38. G. I. Shivashinsky, "On Self-Turbulization of a Laminar Flame," Acta Astron, (5:569-591, 1978)

39. A. G. Istratov and V. B. Librovich, "On the Stability of Gas-Dynamic Discontinuities Associated with Chemical Reactions. The Case of the Spherical Flame," Acta Astron, (14:453-466, 1969)

40. W. G. Struck and H. W. Reichenbach, "Investigaticn of Freely Expanding Spherical Combustion Waves Using Methods of High Speed Photography," p. 677-682, 11 Sym on Comb. (Pittsburg: Comb. Inst. Pub. Co., 1967)

References contd

41. I. O. Moen, M. Donato, R. Knystaukas and J. H. Lee, "Turbulent Flame Propagation and Acceleration in the Presence of Obstacles," McGill Univ. 1979

42. J. Breton, Ann. Office Natl. Combustibles Liquides, (11:487, 1936) These Faculte des Sciences, Univ. Nancy, 1936

43. A. S. Sokolik, Self-Ignition, Flame, and Detonation in Gases, Translated from Russian by Israel Program for Scientific Translations for U. S. National Aeronautics and Jerusalem (1963) p. 321-413

44. J. G. Moore and E. V. Gilby, A Review of the Problems Arising From the Combustion of Hydrogen in a Water Reactor Containment, AHSB(s) R101, (U.K.A.E.A., 1966)

45. G. G. Bach, R. Knystaukas and J. H. Lee, "Direct Initiation of Spherical Detonations in Gaseous Explosives," 12th Sym on Comb. (Pittsburg, Comb. Inst: 853-864)

46. R. Knystaukas and J. H. Lee, "On the Effective Energy for Direct Initiation of Gaseous Detonations," Comb. & Flame, (27:221-228, 1976)

47. L. H. Cassutt, "Experimental Investigation of Detonation on Unconfined Gaseous Hydrogen-Oxygen-Nitrogen Mixtures," ARS J (31:1122-1128, 1961)

48. L. W. Carlson, R. M. Knight and J. O. Henrie, "Flame and Detonation Initiation and Propagation in Various Hydrogen-Air Mixtures, With and Without Water Spray," AI-73-29, Atom Int. Div., Rockwell Int. (May 1973)

49. F. E. Belles, "Detonability and Chemical Kinetics: Prediction of Limits of Detonability in Hydrogen," 7th Sym. on Comb. London, Butterworths:745-751, 1959)

50. A. K. Oppenheim and R. A. Stern, "On the Development of Gaseous Detonation-Analysis of Wave Phenomena," 7th Sym. on Comb. (London, Butterworths:837-850, 1959)

51. J. W. Meyer, P. M. Urtiew and A. K. Oppenheim, "On the Inadequacy of Gasdynamic Processes for Triggering the Transition to Detonation," Comb. & Flame,(14:13-20, 1970)

52. J. W. Meyer and A. K. Oppenheim, "On the Shock-Induced Ignition of Explosive Gases," 13th Sym. on Comb. (Pittsburg, Comb. Inst: 1153-1164, 1971)

53. W. Fickett and W. C. Davis, Detonation, (Berkeley: Univ. of Cal. Press, 1979)

References contd

54. N. Manson, C. Brochet, J. Brossard, and Y. Pujol, "Vibratory Phenomena and Instability of Self-Sustained Detonations in Gases," 9th Sym. on Comb., (N.Y Academic Press, 461-469, 1963)

55. R. A. Strehlow, R. Liaugminas, R. H. Watson, and J. R. Eyman, "Transverse Wave Structure in Detonations," 11th Sym. on Comb. (Pittsburg, Combustion Institute: 683-692, 1967)

56. R. A. Strehlow, "The Nature of Transverse Waves in Detonations," Acta Astron, 14:539-548, 1969

57. L. F. Henderson, "The Cellular Structure of Shock Waves and Detonation Waves," Acta Astron, 14:559-564, 1969

58. R. A. Strehlow, R. E. Mauer, and S. Rajan, "Transverse Waves in Detonations: I. Spacing in the Hydrogen-Oxygen System," AIAA J, 7:323-328, 1969

59. A. K. Macpherson, "On the Structure of Single Headed Spin Detonation," Acta Astron., 14:549-558, 1969

60. K. W. Chiu and J. H. Lee, "A Simplified Version of the Barthel Model for Transverse Wave "pacings in Gaseous Detonation," Comb. & Flame, 26:353-361, 1976

61. R. L. Panton, "Effects of Structure on Average Properties of Two-Dimensional Detonations," Comb. & Flame, 16:75-82, 1971

62. "Experimentelle Untersuchung der Wasserstoffvertieling im Containment eines Leichtwasserreactors nach einen Kuhlmittelverlust-Storfall," BF-R-63.363-3 Battelle-Inst. e.V. Frankfurt

63. G. J. E. Willcutt, Jr. and R. G. Gido, "Mixing of Radiolytic Hydrogen Generated Within a Containment Compartment Following a LOCA," NUREG/CR-0304, LA-7421-MS, Los Alamos, 1978

64. D. S. Trent, "Mixing of Bouyant Combustible Gases in BWR Containment Systems," BNWL-B-298, Battelle Pacific NW Lab, August 1973

65. M. E. Neer, "Autoignition of Flowing Hydrogen-Air Mixtures," AIAA J, (13:924-928, 1975)

66. R. W. Wierman and R. K. Hilliard, "Experimental Study of Hydrogen Formation and Recombination Under Postulated LMFBR Accident conditions," HEDL-TC-730, Hanford Eng. Dev. Lab. Westinghouse (Dec. 1976)

67. G. J. Van Wylan and R. E. Sonntag, Fundamentals of Classical Thermodynamics, SI Version 2E, (N. Y., J. Wiley & Sons, 1976)

68. I. Glassman, Combustion, (N. Y., Academic Press, 1977)

Reference Contd

69. W. D. Hayes, "The Basic Theory of Gasdynamic Discontinuities," Fundamentals of Cas Dynamics, H. W. Emmons, Ed. (Princeton, Princeton Univ. Press, 1958)

70. W. E. Baker, P. A. Cox, P. S. Westine, J. J. Kulesz, R. A. Strehlow, A Short Course on Explosion Hazards Evaluation (Southwest Research Inst., 1979)

71. E. Oran, T. Young, and J. Boris, "Application of Time Dependent Numerical Methods to the Description of Reactive Shocks," 17th Sym. on Comb. (Pittsburg, Comb. Inst.:43-53, 197)

72. C. K. Westbrook and F. Dryer, "Prediction of Laminar Flame Properties of Methanol-Air Mixtures," Comb. & Flame, (37:171-192, 1980)

73. J. A. Miller and R. J. Kee, "Chemical Nonequilibrium Effects in Hydrogen-Air Laminar Jet Diffusion Flames," J Chem. Phy., *81:253-2542 (1977)

74. C. K. Westbrook and J. Creighton, Jr., "A Numerical Model of Chemical Kinetics of Combustion in a Turbulent Flow Reactor," J Chem. Phy., (81:2542-25)

75. N. J. Brown, K. H. Eberius, R. M. Fristrom, K. H. Hoyermann and H. G. Wagner, "Low-Pressure Hydrogen/Oxygen Flame Studies," Comb. & Flame, 33:151-160 (1978)

76. W. C. Gardiner, Jr., Et al, "Elementary Reaction Rates from Post-Induction-Period Profiles in Shock-Initiated Combustion," 14th Sym. on Comb. (Pittsburg, Comb. Inst.:61-75, 1973)

77. T. Fujiwara, "Spherical Ignition of Oxyhydrogen Behind a Reflected Shock Wave," 15th Sym. on Comb. (Pittsburg, Comb. Inst.:1515-1524, 1974)

78. M. P. Moyle, R. B. Morrison, and S. W. Churchill, "Detonation Characteristics of Hydrogen-Oxygen Mixtures," AIChE Journal, Vol. 6:92-96 (1960)

IV. HYDROGEN RECOMBINERS

Post-LOCA hydrogen recombiners are examined from both system and component perspectives. First, the accident scenarios in which recombiners play a useful role are identified. For these accidents, recombiner operation with both atmospheric and inerted containments is discussed. Next, the three design concepts that have been used for post-LOCA containment recombiners are reviewed, and then a description of the currently available commercial products is given. Finally, possible improvements to recombiner technology and application are considered, and conclusions drawn.

THE RECOMBINER/CONTAINMENT SYSTEM

The recombiner - as the name implies - combines the hydrogen and oxygen present in a containment atmosphere. The process requires heat, is exothermic, and produces water vapor. Available devices have inlet flow rates not exceeding 200 scfm.

Current applications of recombiners are limited to containment atmospheres outside the flammability limits (less than 4 vol % hydrogen in the presence of 5 or more vol % oxygen). For such applications, the recombiners are provided to recombine hydrogen produced by radiolysis and corrosion.

For cases in which the containment atmosphere contains hydrogen in quantities greater than 4 vol %, recombiners are not used because they in fact constitute an ignition source. In these cases no control schemes currently exist, and the only way a recombiner may be of use is if the hydrogen concentration is reduced to less than 4 vol % by a burn which does not damage the containment. This, in fact, was what happened at TMI-2, and is shown by darkened lines in Figure 1.

A special variation of the typical recombiner application is that for inerted containments. Here the recombiner system is limited to operating only if the concentration of oxygen in the containment is below 5 vol % above upper flammability limit. This is because a Zirconium-steam reaction in such small containments will most likely result in a hydrogen concentration in excess of 4 vol %. The recombiners provided for these applications recombine oxygen generated from radiolysis, and keep its concentration below 5 vol %.

In inerted containments, if the gas flow to the recombiner contains hydrogen in excess of 4 vol %, a reduction in heat load is required. One method uses recirculation of the hydrogen free effluent to the inlet, diluting the hydrogen concentration there to below 4 vol %. Another method limits the temperature attained within the recombiner by controlling the rate of recombination through regulation of input power.

The recombiners used for inerted containments can also be used for containment recovery after an accident. For this application, when the oxygen level drops to below 2 vol % but hydrogen concentration is high (>>4 vol %) oxygen is added to the influent gas stream to raise the oxygen concentration to 2 vol %. This will allow a reduction in the hydrogen level to below 4 vol %.

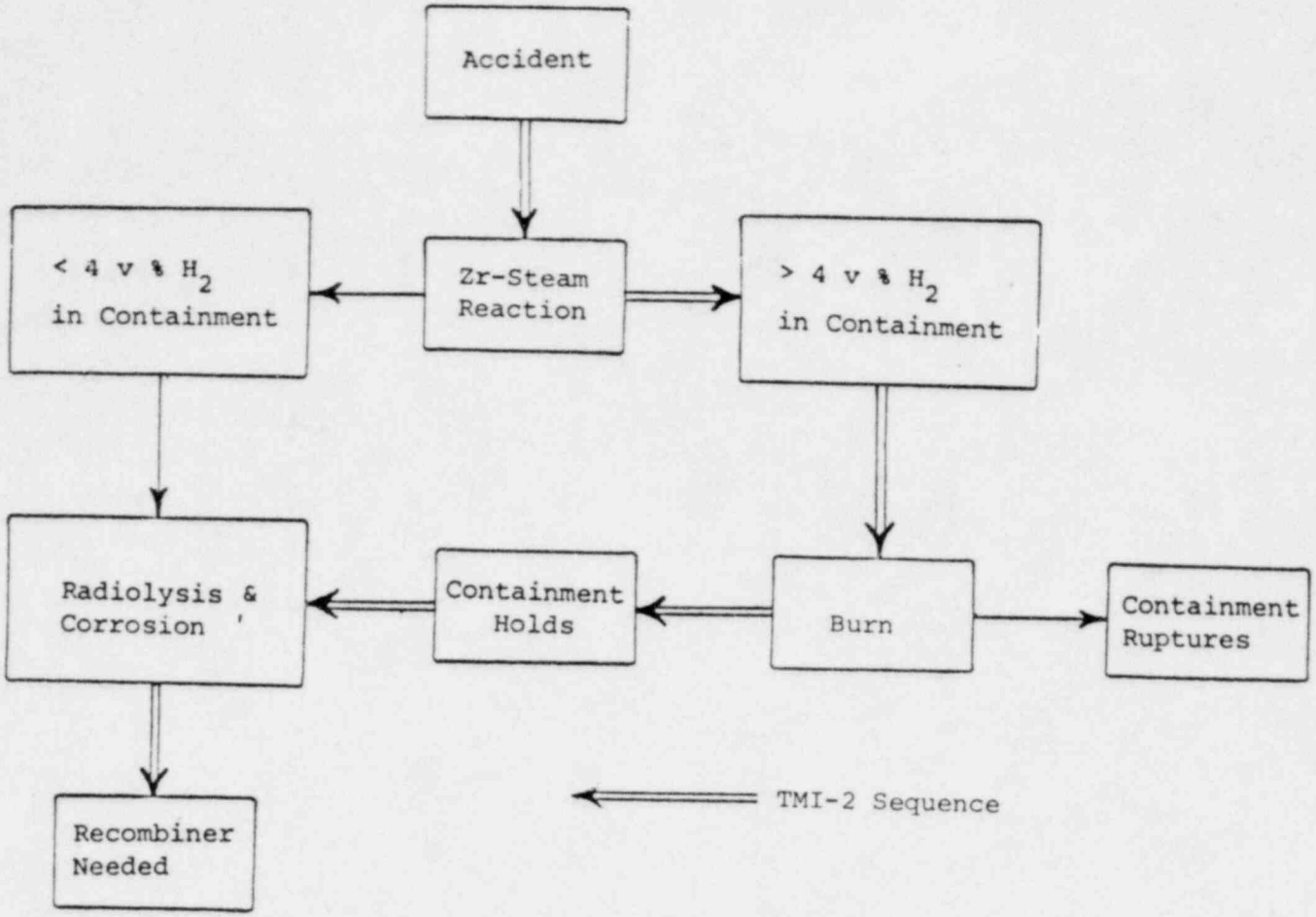

Figure 1 - Recombiner Use - Atmospheric Containments
(Normal oxygen concentration is 21 vol%)

Commercial Post-LOCA Recombiners

Recombiner designs have been classified as flame, thermal, and catalytic. Although the recombination of H_2 and O_2 is always exothermic, the thermal recombiner is distinguished from flame recombiners by using primarily radiant heat to bring about recombination. Flame recombiners depend on the exothermic combustion process being self-maintaining, while catalytic recombiners use a noble metal catalyst bed to promote recombination at relatively low temperatures.

The flame recombiner has the advantage of negligible heat input, but is more difficult to start than the other two types, and requires supplementary H_2 and O_2 for reliable ignition and flame control.[1] Also, the addition of H_2 and O_2 to the input stream makes flame arresters necessary.[1,2] This type of recombiner has found very limited use in containment applications.

The catalytic recombiner is widely used to recombine radiolytically generated off-gas during normal operation of boiling water reactors.[3] Extensive testing[4] has indicated that the catalytic recombiner can also be effective in the less predictable post-LOCA environment. Units for this purpose are being marketed.[5]

Two styles of thermal recombiners were undergoing generic qualification with the NRC by means of Topical Reports during the 1970's. One style[6] is for location inside containment, and uses convective gas flow which is regulated by the size of built-in orifices. The other style[7] is for location outside containment, and allows control over several operating parameters.

These thermal and catalytic designs will be described below.

Two Thermal Recombiners

The thermal (electric) recombiners described here are those manufactured and sold by the Westinghouse Electric Corporation (Nuclear Energy Systems), and by the Atomics International Division of Rockwell International. The Westinghouse recombiner was qualified with the NRC during the 1970's by means of a Topical Report series, numbered WCAP-7820. An improved version is now being produced. Its qualification was reported in WCAP 9347. The Atomics International unit was partially qualified by Topical Reports AI-72-61 and AI-73-27. Further qualification negotiations are continuing, based in part on reports AI-75-2 (Rev. 3) and AI-77-55.

As of 1980, there were no other thermal (electric) recombiners available in the U. S. for post-LOCA containment applications.

Description of Westinghouse Recombiner.[8]

The recombiner consists of a thermally insulated vertical metal duct with electric resistance metal sheathed heaters provided to heat a continuous flow of containment air (containing hydrogen) up to a temperature which is sufficient to cause a reaction between hydrogen and oxygen. The recombiner is provided with an outer enclosure to keep out containment spray water. The recombiner consists of an inlet preheater section, a heater-recombination section, and a discharge mixing chamber that lowers the exit temperature of the air (see Figs. 2&3).

The unit is manufactured of corrosion resistant, high temperature material except for the base which is carbon steel. The electric hydrogen recombiner uses commercial type electric resistance heaters sheathed with Incoloy-800 which is an excellent

corrosion resistant material for this service.

Air is drawn into the recombiner by natural convection and passes first through the preheater section. This section consists of a shroud placed around the central heater section to take advantage of heat conduction through the walls to preheat the incoming air. This accomplishes the dual functions of reducing heat losses from the recombiner and of preheating the air.

The warmed air passes through an orifice plate and then enters the electric heater section where it is heated to approximately 1150 to 1400°F causing recombination to occur. Tests have verified that the recombination is not a catalytic surface effect associated with the heaters but occurs due to the increased temperature of the process gases; therefore catalyst poisoning is not a problem. The heater section consists of five assemblies of electric heaters stacked vertically. Each assembly contains individual heating elements.

The power panel forthe recombiner is located in the auxiliary building, and contains an isolation transformer plus a semi-conductor controlled rectifier controller to regulate power into the recombiner. This equipment is not exposed to the post loss-of-coolant accident environment. The control panel is located in the control room. To control the recombination process, the correct power input which will bring the recombiner above the threshold temperature for recombination will be set on the controller. The correct power required for recombination depends upon containment atmosphere conditions and will be determined when recombiner operation is required. For equipment test and periodic checkout,

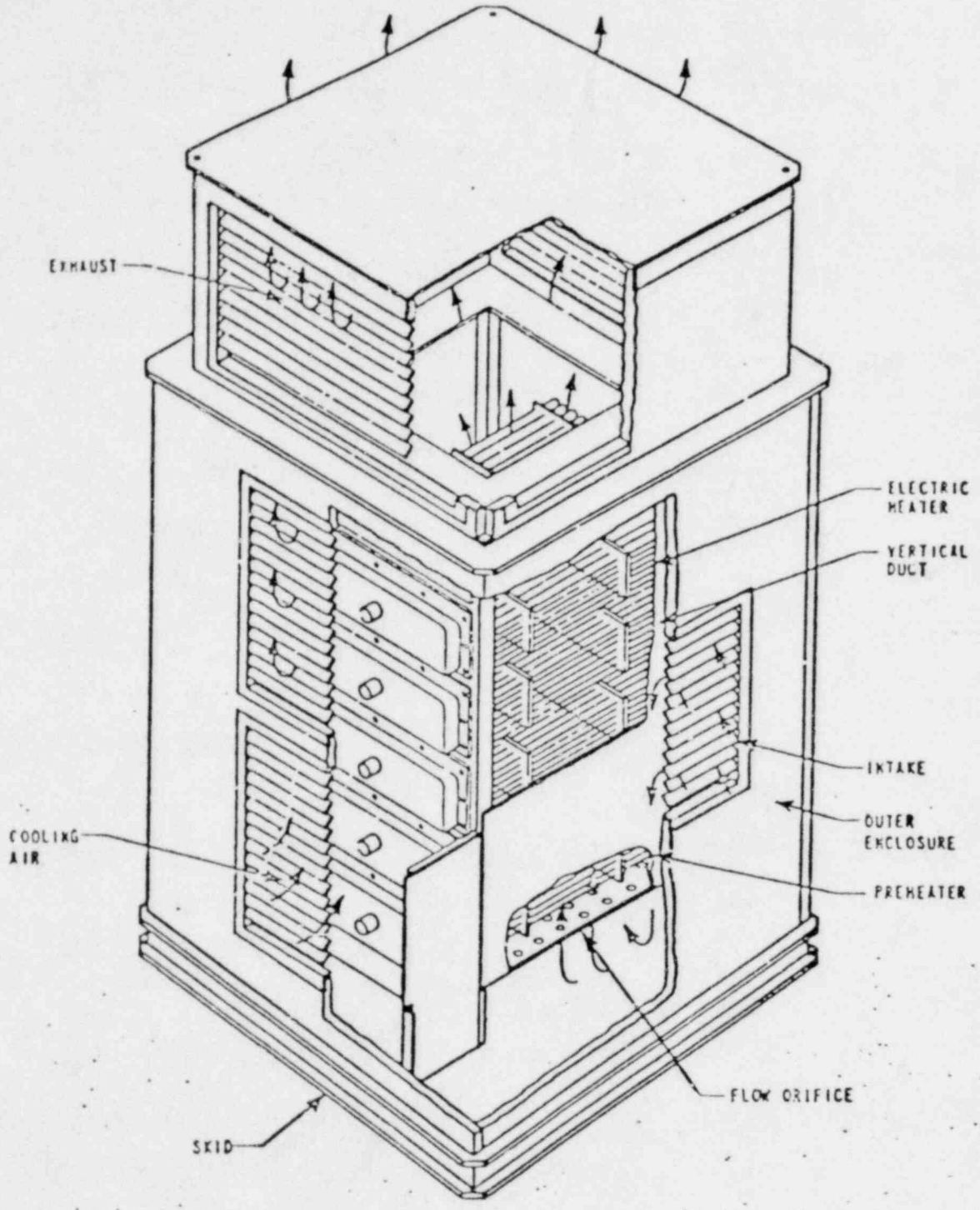

Westinghouse Electric Hydrogen Recombiner

Figure 2

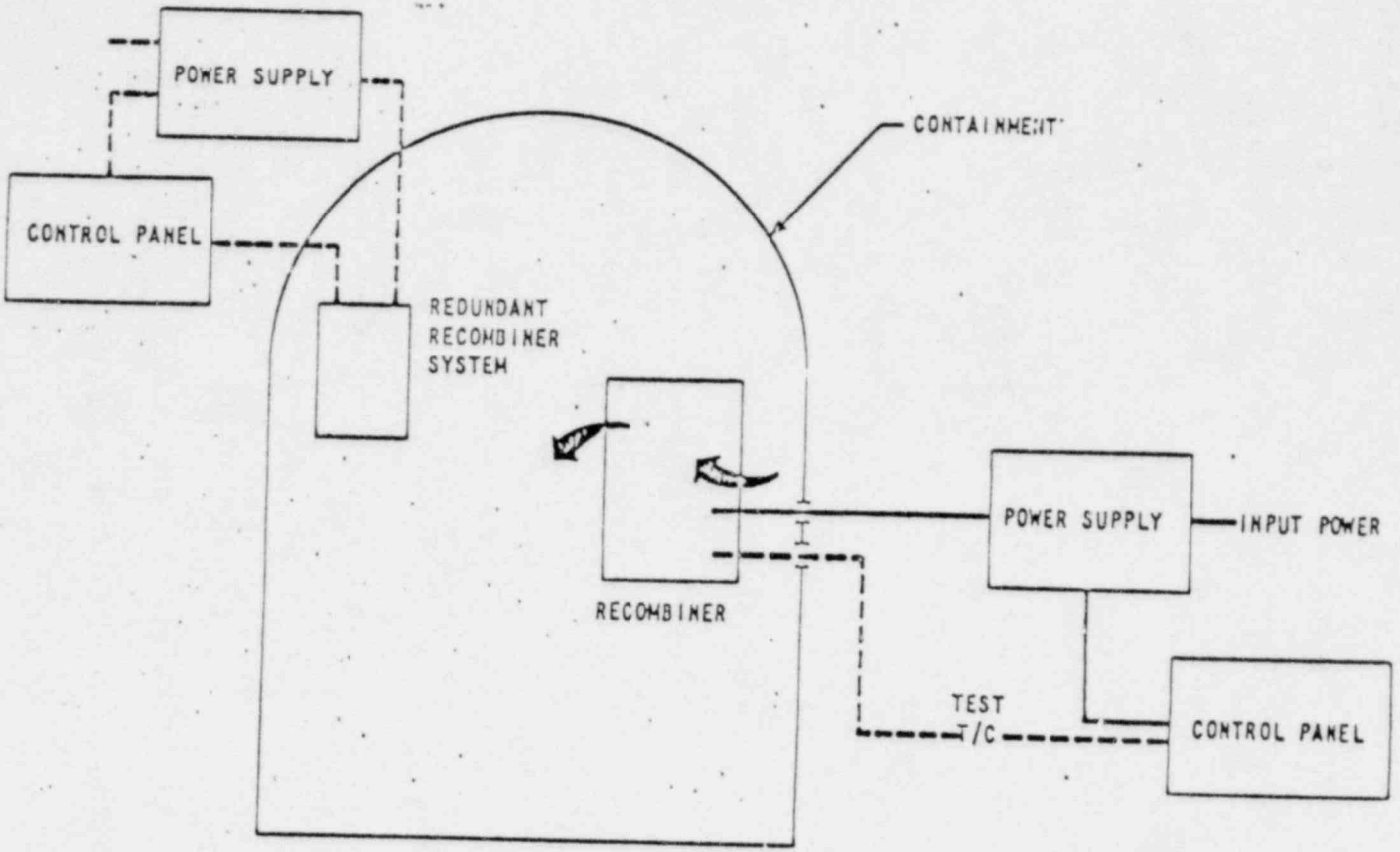

Schematic of Westinghouse Electric Recombiner System

Figure 3

a thermocouple readout instrument is also provided in the control panel for monitoring temperatures in the recombiner.

The recombiner units are located in the containment such that they process a flow of containment air containing hydrogen at a concentration which is generally typical of the average concentration throughout the containment.

Each electric recombiner is capable of continually processing a minimum of 100 cfm of containment atmosphere. The hydrogen contained in the processed atmosphere is converted to steam, thus reducing the overall containment hydrogen concentration.

The unit is designed to sustain all accident loads such as seismic loads and temperature and pressure transients from a loss-of-coolant accident. See Table 1 for a summary of recombiner parameters, and Table 2 for installation criteria.

The electric hydrogen recombiners have undergone extensive testing in the Westinghouse development program. These tests encompassed the initial analytical studies, laboratory proof-of-principal tests, full scale prototype testing and production model testing. The full scale prototype tests included the effects of:

1. Varying hydrogen concentrations
2. Alkaline spray atmosphere
3. Steam effects
4. Convection currents

TABLE 1

WESTINGHOUSE ELECTRIC HYDROGEN RECOMBINER TYPICAL PARAMETERS

Power (Maximum)	75 KW*
Capacity (Minimum)	100 scfm
Heaters	
Number	5
Heater Surface Area/Heater	35 ft^2
Maximum Heat Flux	2850 BTU/hr ft^2 or 5.8 Watts/in^2
Maximum Sheath Temperature	1550°F
Gas Temperature	
Inlet	80 to 155°F
In Heater Section	1150 to 1400°F
Materials	
Outer Structure	300-Series Stainless Steel
Inner Structure	Inconel-600
Heater Element Sheath	Incoloy-800
Dimensions	
Height	9 ft
Width	4.5 ft
Depth	5.5 ft
Weight	6200 lb

*Power can be controlled by a semiconductor controlled rectifier.

TABLE 2

WESTINGHOUSE ELECTRIC HYDROGEN RECOMBINER INSTALLATION CRITERIA

1. The recombiners must be located in the containment such that they process a flow of containment air containing hydrogen at a concentration which is generally typical of the average concentration throughout the containment.

2. The recombiners should be located away from high velocity air streams, such as could emanate from fan cooler exhaust ports, or they must be protected from direct impingement of high velocity air streams by suitable barriers such as walls or floors.

3. The recombiners should be located such that any incident effecting one unit will not effect the other one; thus maintaining an independent redundant system.

4. The recombiners should be located in an area of the containment such that they will be protected from high energy missiles or jet impingement from broken pipes.

5. The recombiners should be mounted on a substantial foundation with no ambient vibration.

6. The recombiners should be located in such a manner that there is adequate area around the unit for maintenance.

The recombiners do not require any instrumentation inside the containment for proper operation after a loss of coolant accident. The recombiners will be started manually after a loss of coolant accident.

The materials of construction for the electric recombiner are selected for their compatibility with the post loss-of-coolant accident environment.

The major structural components are manufactured from 300-Series stainless steel except for the base which is carbon steel. Incoloy-800 is used for the heater sheaths and Inconel-600 for other parts such as the heat duct, which operates at high temperature.

There are no radiolytic or pyrolytic decomposition products from these materials. The carbon steel base of the recombiner unit is coated with a paint that satisfies the requirements of ANSI 101.2 (1972), "Protective Coatings (Paints) for Light Water Nuclear Reactor Containment Facilities."

Description of AI Recombiner System[9]

A. System Description and Operation (see Fig. 4)

The thermal recombiner system consists of two portable, skid-mounted packages, the recombiner and the control cabinet. The recombiner, Figure 5 is a welded stainless-steel gas containment piping system made up of inlet pipe which connects to the containment piping, process gas cooler, and outlet piping returnign to containment. The recombiner and control console are connected by instrumentation and power cables.

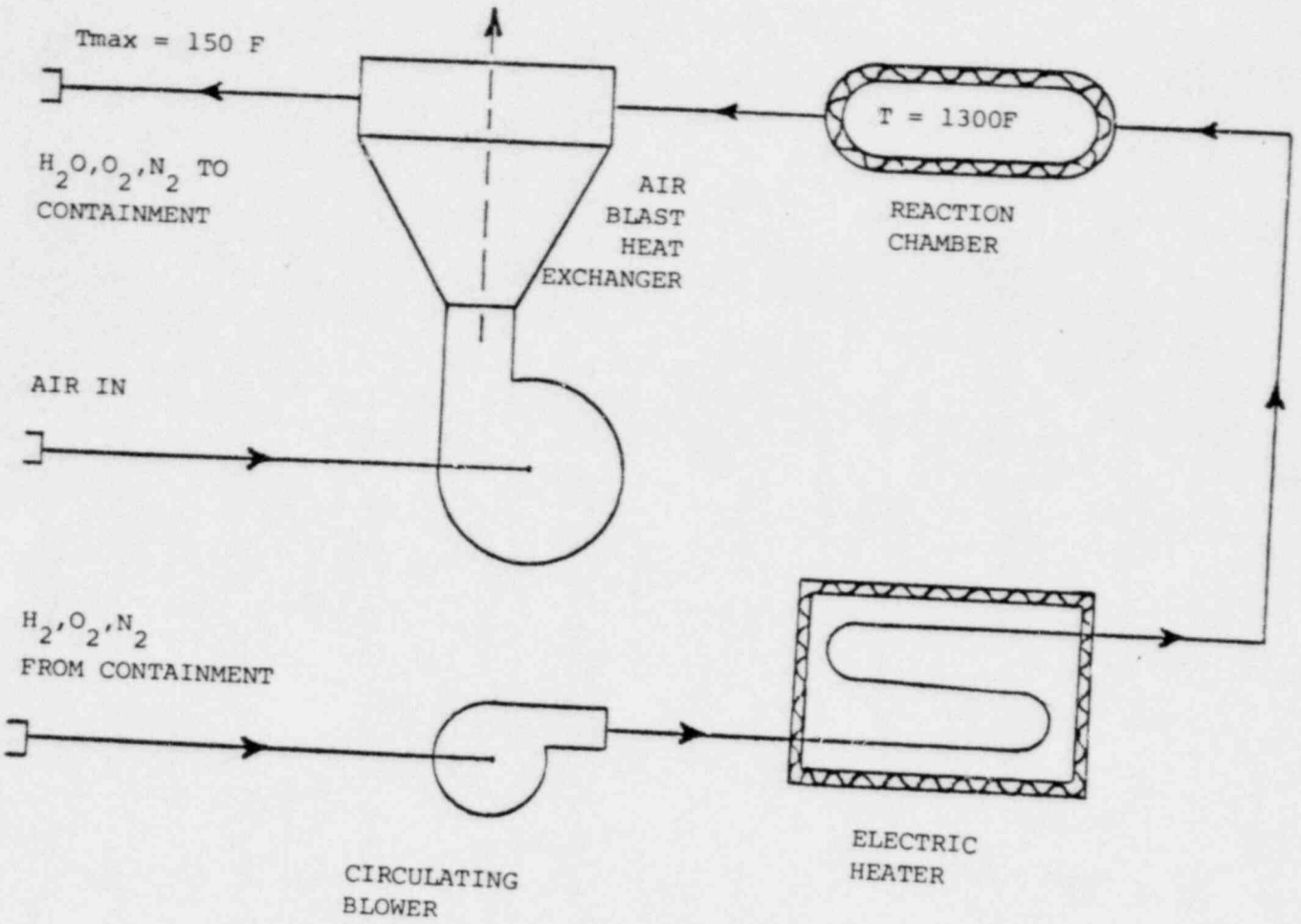

SCHEMATIC REPRESENTATION OF THE A.I. THERMAL RECOMBINER

FIGURE 4

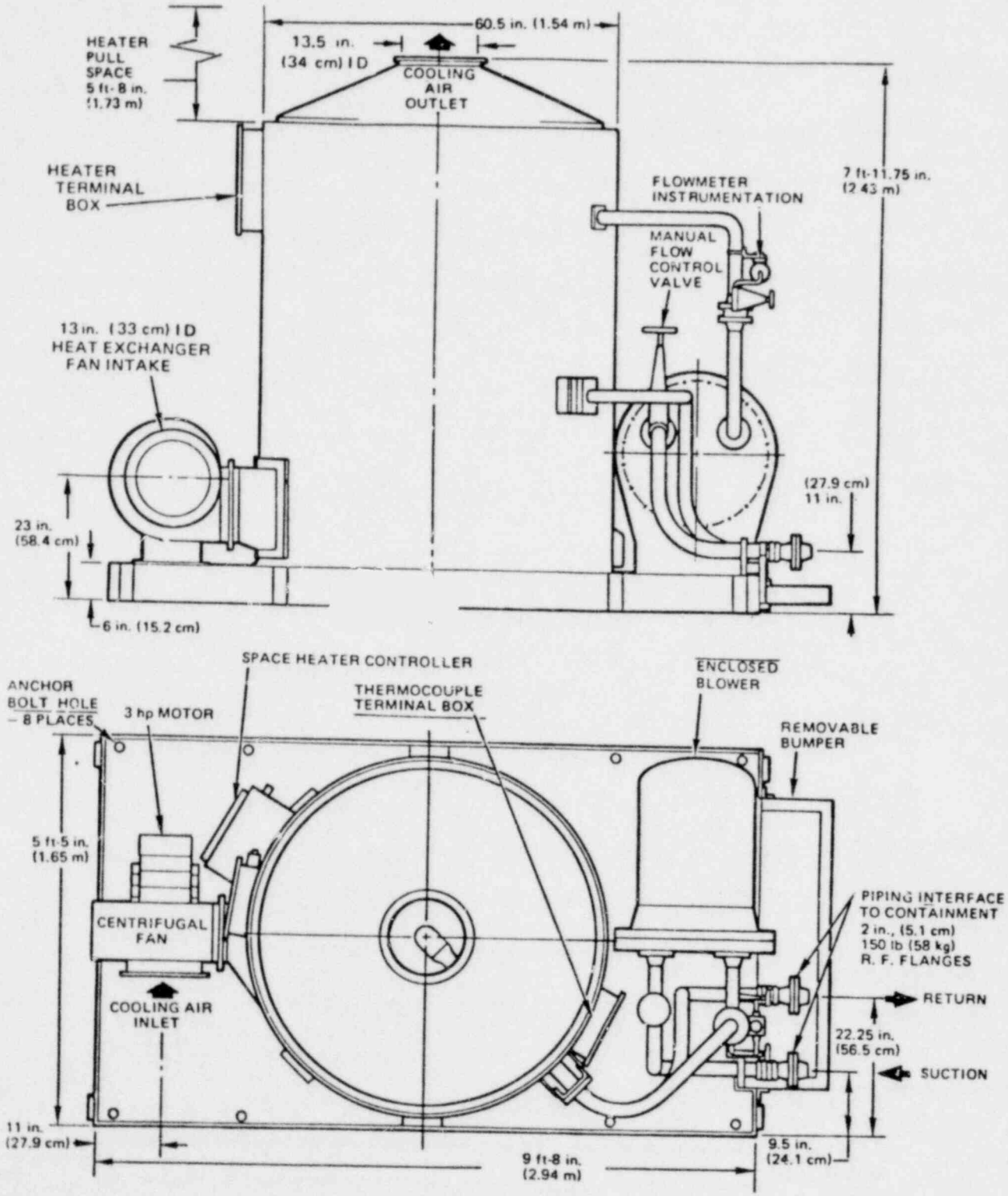

Typical Thermal Recombiner Package

Figure 5

The control console is a system of motor starters, circuit breakers, timers, relays, temperature controllers and indicators, thermal switches, and an annunciator. All of these components are integrated into a control system which activates, controls, and indicates the operation of the recombiner. The control console is connected to a 480-v, 3-phase, facility power source by a single cable. The distribution of electric power to motors, heaters, and instruments is accomplished through cables from the control console. A front and rear view of the control console is shown in Figure 6. See Table 3 for a summary of parameters.

B. Component description

1. Recombiner Package

a. Enclosed Blower

The process gas is drawn from the containment building into and through the recombiner system and back to containment by either a positive displacement or a regenerative blower direct driven by a totally enclosed, fan cooled, 3600-rpm, 480-v, 3-phase, 60-Hz induction motor. These components were selected because of their proven performance capabilities over many years of continuous duty operation in commercial applications.

The blower and motor are enclosed in a stainless-steel vessel. The internal components are mounted on a tray attached to a blind flange at one end of the vessel. The flange and attached components can be removed for inspection or maintenance.

b. Flowmeter

Flowrate of the containment gas through the system is measured by a Model T2B flow tube fabricated by the Flow Tube Division of the Bethleham Corporation. It is held in the pipe system between two pipe flanges in the line between the blower and heater. Connections are made to a differential-pressure transmitter through Type 304 stainless-steel tubes. An electric signal is transmitted through a cable to a flow indicator located in the control package.

c. Gas Heater

The gas being heated is contained in coiled, 2-in., Type 304 austenitic stainless-steel pipe. The array of radiant heater elements are individually positioned 2 in. or more away from the heater coil and insulation. The elements are free to radiate in all directions, either directly to the heater coil or to the insulation with subsequent reradiation to the coil. The spacing of the elements away from the process gas piping precludes the possibility of damaging the coil if a heater should fail.

d. Reactor Chamber

(Proprietary)

e. Gas Cooler

The gas cooler consists of a coiled 2-in. pipe which ducts the reacted gas from the reaction chamber to the return outlet. The cooler coil is located in an annular space between the heater shell and outer shell. A centrifugal fan forces about 3000 cfm of air past the coil,

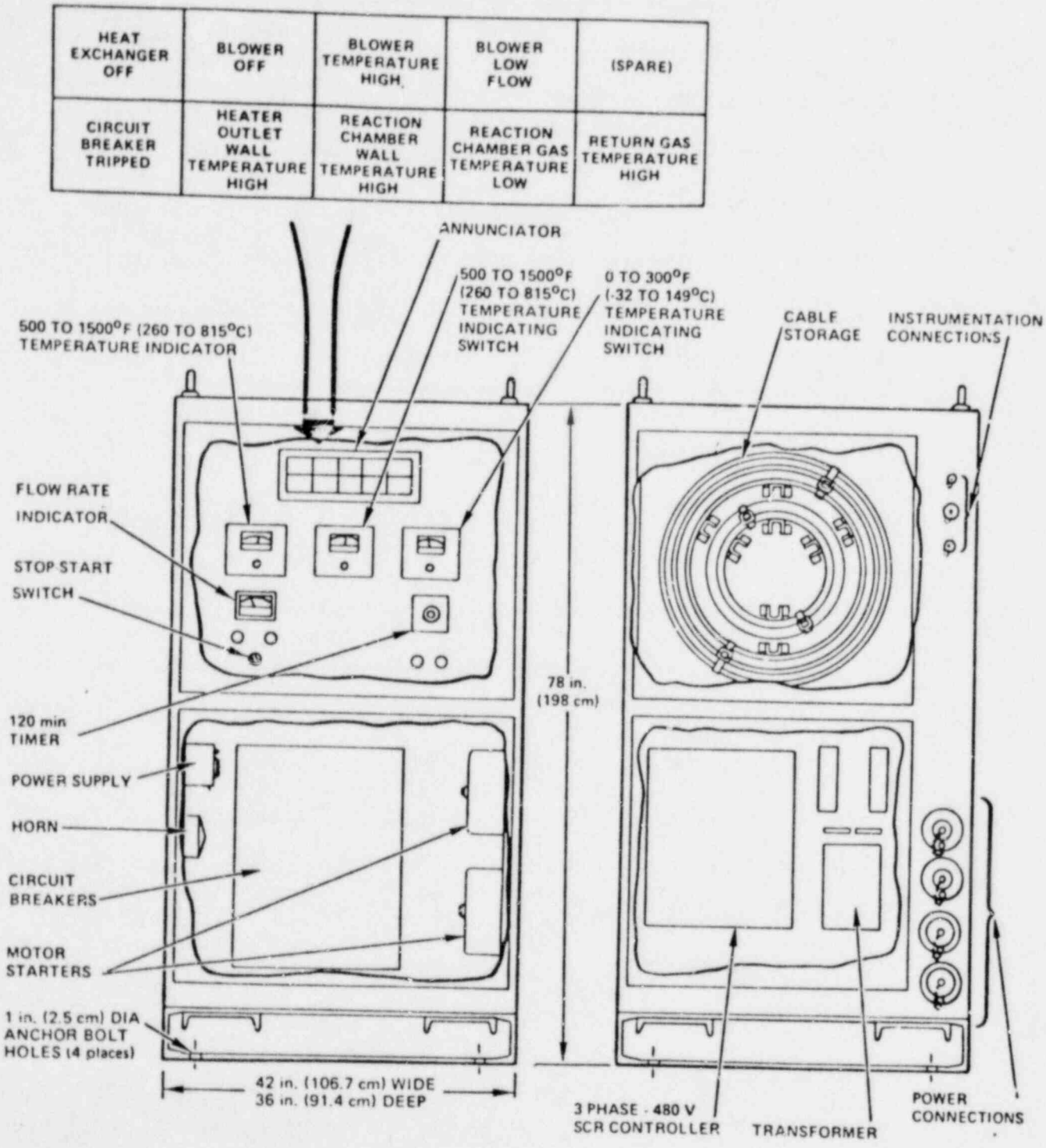

Front and Rear Views of the Power and Control Cabinet

Figure 6

TABLE 3

The AI recombiner system is designed to function within the parameter limits summarized below:

Pressure:	50 psig at Ambient Temperature - non operating 10 psig at Operating Temperatures
Temperature:	Inlet and Outlet: 150°F (maximum) Heater, Reaction Chamber and Cooler: 1400°F (maximum)
Flow Rate:	50 to 70 scfm (a 150 scfm is also available)
Hydrogen Concentration:	Up to 5½% in the Influent. Less than 0.1% in the Effluent.
Power Required:	Startup: 480 vac, 3-phase, 60 Hz, 45 kw (maximum) Steady-State: 480 vac, 3-phase, 60 Hz, 20 kw (approximate) Standby: 120 vac, 1-phase, 60 Hz, 400 w (maximum)
Cooling Air:	3000 cfm at 120°F maximum
Seismic Response:	System Operating (Hot) during a Safe Shutdown Earthquake at Resonant Frequencies of: ≤20 Hz; 6.8 g Horizontal, 3.7 g Vertical >20 Hz; 4.4 g Horizontal, 0.2 g Vertical

cooling the process gas to less than 150°F. The heat exchange rate at the 50 scfm design condition is 63,000 BTU/hr. The fan is driven by a 3-hp, totally enclosed, fan cooled, induction motor. The fan is mounted on the motor shaft which provides a fan system with the fewest possible parts. The component selection was based on proven long-life performance in commercial applications.

f. Materials

The material for the primary gas containment recombiner components is Type 304 austenitic stainless-steel, meeting the ASME Boiler and Pressure Vessel Code requirements for Section III, Class 2 components. This material provides the requisite structural integrity and corrosion resistance for the service environment and operating conditions. However, it is to be noted that periodic testing of the recombiner system, at its operating temperature, over the 40-year life, will subject the system to repetitive thermal cycling through the sensitizing temperature range of stainless-steel. To preclude the possibility of intergranular corrosion within the system, a low-power "trickle heater" is provided in the recombiner package to assure that the system remains dry during periods of non-use.

The process gas blower and motor are in contact with the process gas, but they are completely enclosed by a stainless-steel vessel. The blower and motor cases are carbon steel which have been painted. These materials provide the requisite structural integrity and corrosion resistance for the service environment and operating conditions.

The skid and heater enclosure structure are made of ASTM A-36 structural steel. The external surfaces are painted with a rust-inhibiting primer, and finish coats as specified by the customer.

g. Electrical

Recombiner package wiring and terminal blocks for the heaters, blower and fan motors, and thermocouples are protected in steel enclosures and conduit. Thermocouples are redundant at critical points of temperature measurement and are routed separately from power writing. Portable instrument and power cables, 50 ft long, are used to connect the recombiner package to the control console.

All electrical components in the system meet the requirements of ANSI C1 for NEMA 4 service, IEEE 308, IEEE 279, and IEEE 323.

h. Trickle Heater

During periods of non-operation, it is possible for moisture to accumulate in the gas containment piping. To preclude this and thereby inhibit corrosion, an auxiliary heater control system "trickle heater" is provided. The controller is connected between a 120-V facility power source and the heater receptacle. In this mode the heaters are operating continuously at about 400 W which will sustain the heated section temperatures at approximately 150°F.

i. Control and Power Equipment

All electrical control and instrumentation components are installed in a dual-access, 6 by 3 by 2 1/2 ft, NEMA 4 cabinet mounted on a 3-ft skid. Power connection to the panel is made through a 20-ft, 4-conductor, No. 4 portable cable to a 100-amp circuit breaker panel mounted in the back half of the cabinet at the bottom. In addition to the main 100-amp circuit breaker, additional breakers are provided for the blower and fan motors, the heaters, and the control console instruments. The top, back half of the cabinet is reserved for storage of the portable cables which connect to the recombiner package.

Control relays, a power supply, a Size 1 contactor, a 50-amp silicon control rectifier, and a control transformer are located in the bottom front of the panel with access through a half-door. The annunciator uses a two-color lamp system, showing on all-green board when the system is operating normally. Operation of all circuit breakers is manual, with overload trips and a shunt trip on the SCR breaker.

An adjustable 0 to 120 minute timer, nominally set for 1 hour, provides for a low-alarm cutout during startup. Interlocks are provided to turn off the heater in the event that heater or reaction gas temperature exceeds the normal control range. A low-flow blower and heater cutoff, which receives its signal from the gas flowmeter, completes the safety instrumentation for the system.

Separate instrumentation and power cables for each motor, the heaters, d/p transmitter and thermocouples are stored in the upper rear section of the control console. Each cable is 50 ft long and terminates with Crouse-Hinds receptacles. The receptacles are sized or keyed each different from the other, to preclude connecting the wrong cable to a circuit.

3. Facility Services

Electric power and cooling air in the following amounts are required to operate the recombiner system.

A. Post-LOCA operation or Test

1. A maximum of 45 kW of electric power, 480 VAC, 3-phase, 60 Hz. After a 1-hour startup period, the power demand is reduced to about 20 kW. Electrical cable, 20 ft long, is provided in the control console for this interface.
2. Ambient temperature air (120°F maximum) is circulated in the gas cooler at 3000 cfm. The air is taken from the room or ducting system into the centrifugal fan mounted on the recombiner package and exhausted through the top of the heater enclosure. Ducting (14 in. diameter) from enclosure to an air handling system or to the outside atmosphere is needed.

B. Standby Storage Operation

A maximum of 400 W of electric power, 120 VAC, single-phase, 60 Hz is required to power the trickle heater controller. The controller is mounted on the recombiner package. Twenty feet of power cable are provided to connect to the facility power source.

A Catalytic Recombiner

The only catalytic recombiner on the U. S. market in 1980 for post-LOCA containment applications was the model PPL-70 made by Air Products and Chemicals, inc. (APCI). A description of the model PPL-70 follows.

Description of APCI Recombiner[10]

System Description

The system presented here will treat 50 to 100 scfm of gas, with a hydrogen removal efficiency of essentially 100% at inlet hydrogen concentrations greater than 0.1% (see Fig. 7) Table 4 summarizes the recombiner parameters.

The Process Flowsheet (Figure 8) shows the system components, process flow path, instrumentation, and controls. The recombiner system is mounted on a skid of portable size, located outside the containment, with piping connections for withdrawal and return of containment atmosphere gas and cooling water. The system is started remotely with a single pushbutton to actuate the blower and preheater. Gas feed is continuous after startup with no temperature or flow adjustments made by the operator.

Entrained solid and liquid contaminants expected to be present in the gas stream entering the recombiner system are removed by a separator and the gas then enters the blower.

The blower withdraws containment gas, circulates it through the recombiner system and returns it to the containment. Model PPL-70 has a flow capacity of 50 to 100 SCFM and other models are designed to handle higher flow rates.

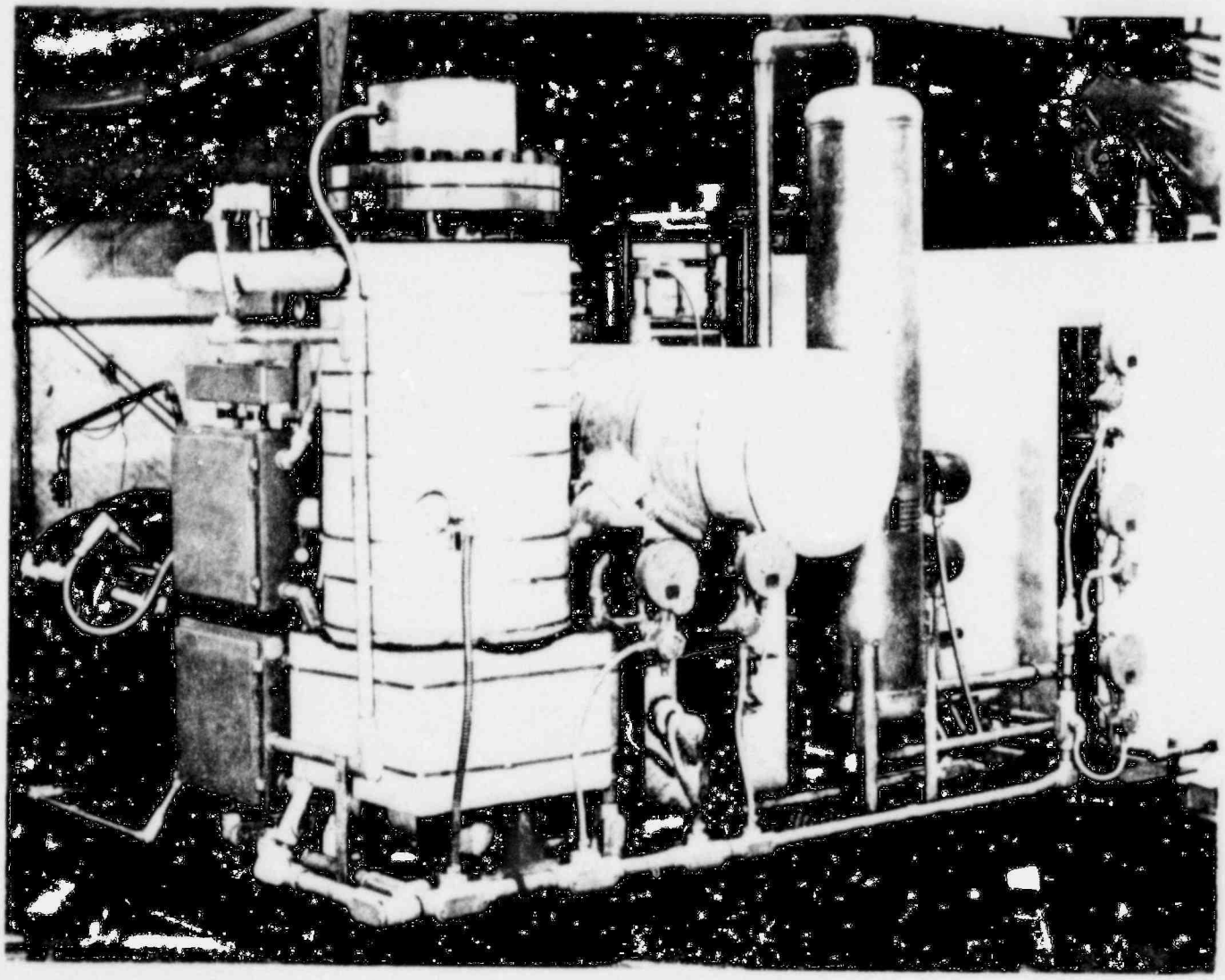

FIG. 7. AIR PRODUCTS POST LOCA HYDROGEN RECOMBINER PROCESS SKID

TABLE 4

SUMMARY OF APCI RECOMBINER PARAMETERS

POWER (MAX):	12.5 kW
FLOW:	50 TO 100 SCFM

HYDROGEN CONCENTRATION:

INLET: $\leq$ 4 v %

OUTLET: < 0.1 v %

GAS TEMPERATURE:

IN COMBINER: TIN + (145° F) (v % H_2)

OUTLET: 150°F (TYPICAL)

MATERIALS, PRESSURE RETAINING:

ASME SECTION III, CLASS 2

SEISMIC RESPONSE:

CATEGORY 1

HEAT RELEASE WITH AIR COOLING (ALTERNATE):

36 000 TO 116 000 BTU/HR

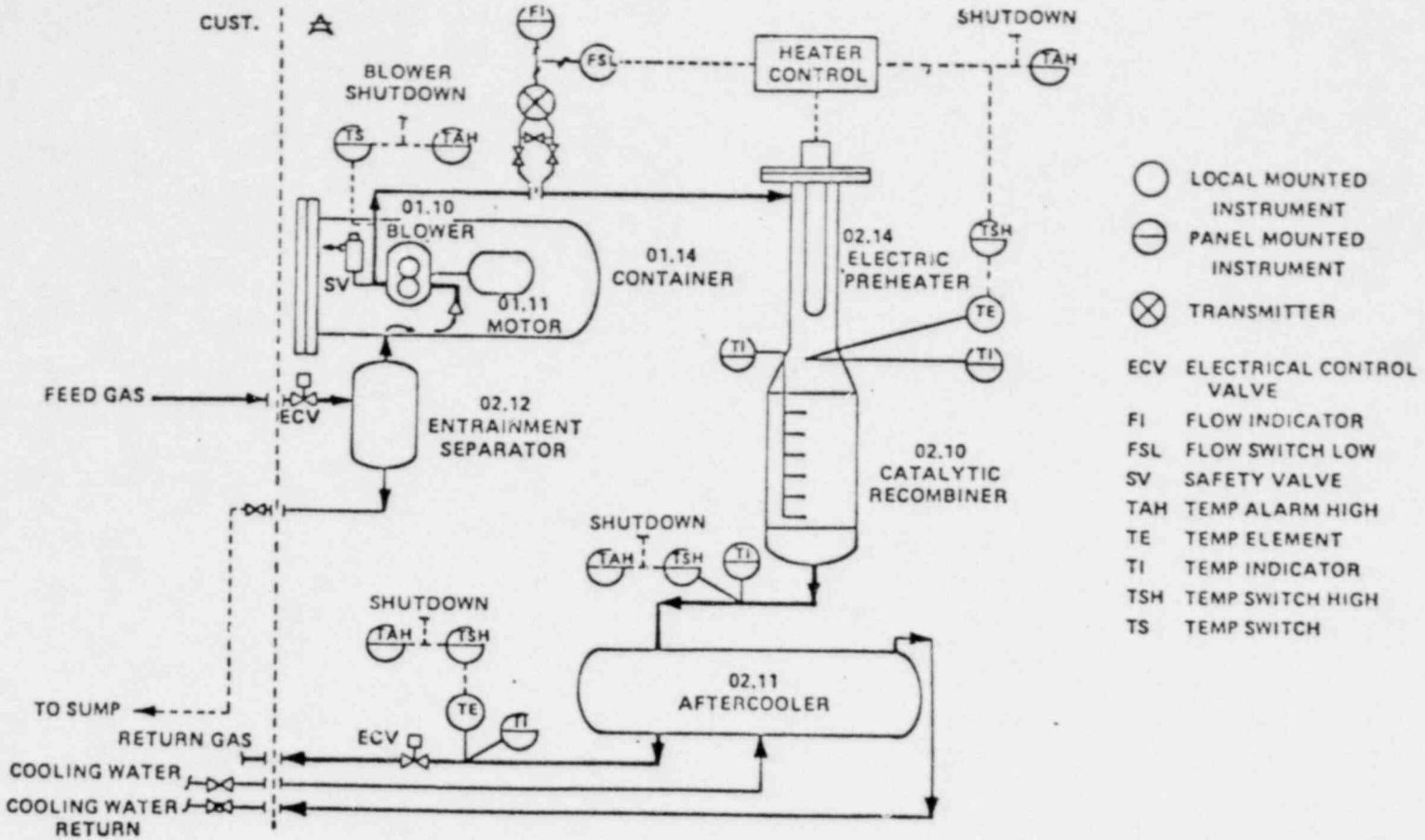

POST-LOCA HYDROGEN RECOMBINER SYSTEM

Model PPL-70

Figure 8

The blower is a single stage, rotary lobe unit, sized to provide required flow at the extremes of containment atmosphere pressure expected. Heat from the blower motor is rejected to the feed gas as this gas flows by the motor inside the sealed blower container.

The gas enters the preheater/recombiner vessel where the electric preheater boosts the gas temperature and thermostatically controls it to maintain a constant elevated recombiner inlet temperature. The warmed gas then passes into the catalytic recombiner catalyst bed where the hydrogen and oxygen from the containment atmosphere react to form water vapor. The exothermic heat of reaction and the preheat maintain the catalyst bed temperature sufficiently high to provide essentially 100% conversion efficienty and to prevent any reduction in catalyst efficiency due to atmospheric contaminants.

The hot recombiner effluent gas, free of hydrogen, is cooled in the gas aftercooler and returned to the containment, completing the treatment cycle by the recombiner unit. The unit is operated until the hydrogen content of the containment atmosphere is reduced to a minimal level and further generation is insignificant. The recombiner operates with the blower feeding gas continuously through the unit and with the preheater temperature thermostatically controlled. Multipoint temperature indication through the catalyst bed provides direct monitoring of the unit's effective hydrogen removal activity, since, due to the exothermic nature of this catalysis process, the bed temperature will rise approximately 145°F for every one percent hydrogen reacted. Safety

shutdown controls (with annunciators) operate when any of the following conditions are reached:

- Low feed gas flow
- High exit temperature from preheater
- High exit temperature from recombiner
- High exit temperature from aftercooler

Equipment description

The equipment components are pressure vessels, interconnecting piping, and valves, of stainless steel, installed as a skid-mounted system, with a separate instrument control panel. The pressure-retaining components are fabricated to ASME Section III, Class 2 standards with Seismic Category I design, as required for a safety class, emergency use system. Figure 9 shows a typical Skid Layout and Equipment Perspective view of the system. The components are listed and briefly described here.

Entrainment Separator

This component is a vertical separator vessel with a demister pad in the upper gas exit section, designed to remove any entrained liquid droplets or suspended particulates from the inlet gas stream. The separator provides reduced gas velocity for the feed stream, tangential gas flow, and a wetted surface on which entrained water droplets can impact and coalesce. The mechanism of inertial impaction also removes entrained solid particulates which will strike and adhere to this wetted surface. Small droplets will be removed by the demister pad. The separated liquid drains into the bottom of the vessel and through a discharge line to the containment.

Blower Package

The blower is a rotary lobe, positive displacement, direct driven gas pump designed to delivery constant volume against varying pressures.

Both the blower and motor are supported on a common base and housed in a horizontal, flanged head pressure vessel. The blower/motor assembly is on a rack fixed to the inside of the removable flanged head, permitting the entire assembly to be removed and replaced through the flanged end of the vessel. The gas convection in the can and cooling effect of ambient air outside the can allows the canned unit to operate without overheating.

Preheater/Recombiner

This preheater/recombiner is a common vertical pressure vessel housing the electrical preheater elements in the upper section and the catalyst bed in the low section. The preheater is an electrical resistance heated surface exchanger consisting of sheathed, immersion heater elements mounted inside the upper section of the vessel. The process gas is heated in this unit before it enters the recombiner section. Gas flows across the heater elements from the top to bottom and the outlet gas temperature is thermostatically controlled. The flanged pre heater assembly can be readily removed from the top flanged head of the vessel for inspection or maintenance. This also provides access to the catalyst bed below.

The CataGuard™ recombiner section, below the preheater, contains pelletized catalyst in a deep packed bed. The catalyst bed allows the feed stream hydrogen and oxygen to react to form

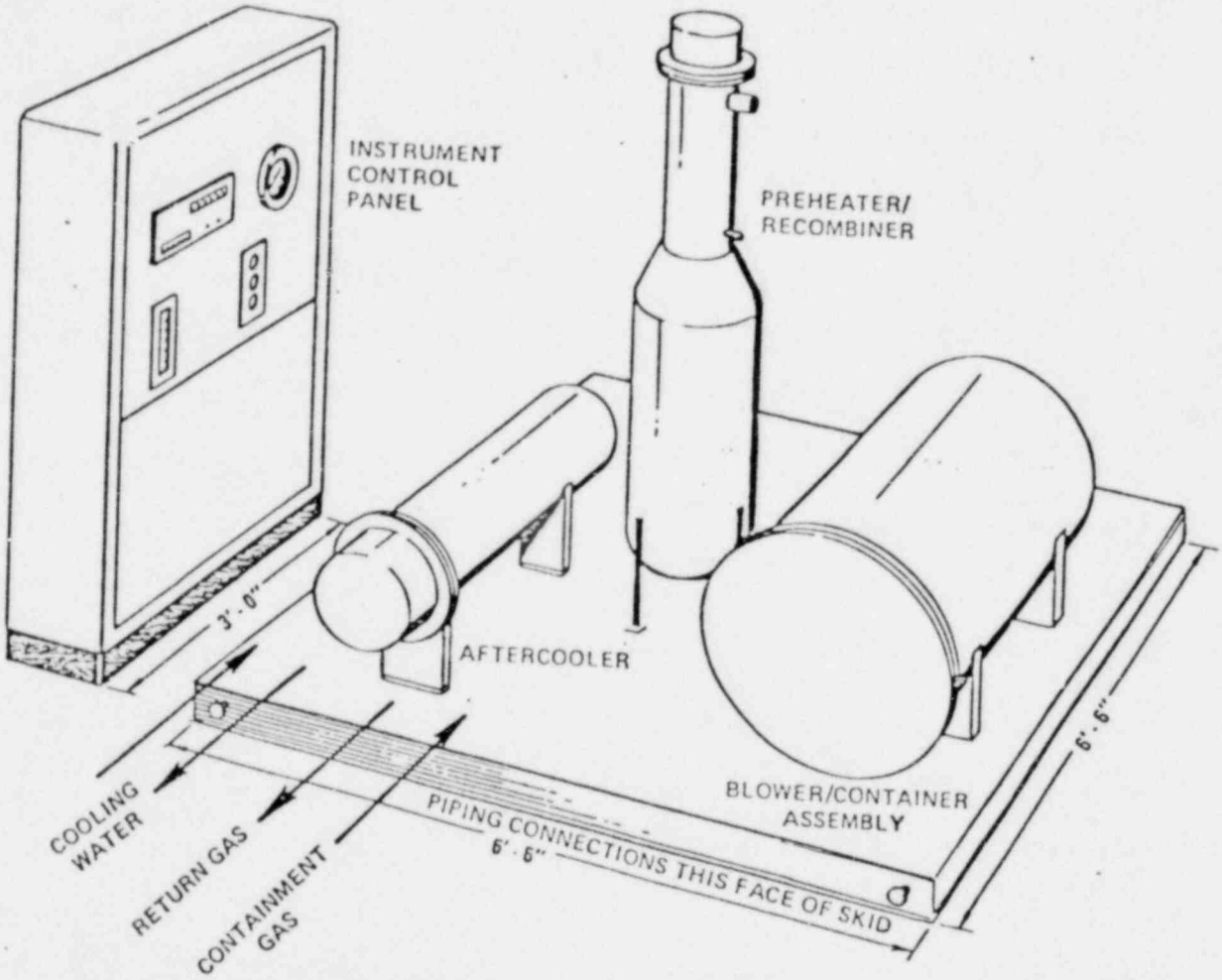

APCI

POST-LOCA HYDROGEN RECOMBINER SYSTEM

Model PPL-70

Perspective View: Skid

Figure 9

water (vapor) by heterogeneous catalysis on the surface of the pellets.

The catalyst pellets can be removed by a simple vacuum hose technique should replacement ever by necessary. However, the need to replace the catalyst is considered to be remote over the 40-year life of the unit. The noble metal on the ceramic pelletized base will not deteriorate in standby conditions or in operation. Vessel design, bed geometry, flow distribution, and catalyst selection are all based on Air Products' considerable experience in gas purification systems. Air Products has completed a significant test program on a pilot recombiner system simulating specific LOCA feed conditions. In this program a noble metal catalyst on a pelletized ceramic support, made by the Houdry Division of Air Products, was selected for its resistance to poisoning by trace contaminants such as halogens in the feed gas. The tests show that controlled bed temperature operation permits high reaction efficiency even with halogens present in the feed gas at well above postulated post-LOCA concentrations. The tests were long duration demonstrations of the resistance of the Cata-Guard™ catalyst bed to iodine and other halogens. This test information has been used in the design of the post-LOCA recombiner system with conservative design factors applied to insure an effective system. The results of these pilot plant tests were supported by tests carried out on full scale production units.

Water-Cooled Aftercooler

The cooler is a shell-and-tube exchanger with component cooling water in a cylindrical shell cooling the process gas in

the tubes. The cooler is designed to cool the recombiner effluent gas to a typical discharge temperature of 150°F.

Air-Cooled Gas Cooler (optional alternate to Water-Cooled Aftercooler)

Should ambient air cooling be preferable to the use of cooling water to the unit after cooler, an air cooler can be supplied.

The air cooler is a bank of vertical coiled tubes with common top inlet and bottom outlet horizontal manifold headers, designed to cool the recombiner effluent gas flowing in the tubes to approximately 150°F. Heat is rejected to ambient air by natural convection from the tube surfaces.

Instrumentation and Control

The hydrogen recombiner system is designed to operate automatically with varying gas concentration and containment conditions. Instruments included in a separate control panel are: a process gas flow indicator, blower and preheater controls, and a multipoint temperature indicator to monitor temperatures at the preheater outlet, inside the recombiner bed, and at the aftercooler outlet.

The process flowmeter is an orifice with pressure taps in the process line, with a transmitter to a flow indicator located on the control panel. A low flow switch and alarm is provided as part of the preheater control.

The blower has a motor starter and disconnect in the control panel along with a start/stop button common for the blower motor and preheater.

The electric preheater is thermostatically controlled to maintain recombiner feed temperature. The heater is protected from burnout by a high temperature switch and the low flow switch with alarm mentioned above.

Utility requirements

The only utilities required are electric power for the blower, heater, and instrumentation, and cooling water for the aftercooler.

The blower typically consumes 4 kW, the heater 8 kW, and the instrumentation less than 015 kW. The water-cooled aftercooler alternate requires 16 gpm of cooling water. The air-cooled aftercooler alternate will release 36,000 to 116,000 BTU's/hr to the room air.

CONCLUSIONS

The current limitations on recombiner performance - 200 scfm of input flow per unit, and 5 vol %/2.5 vol % concentration of H_2/O_2 - probably reflect a limit in cost/effectiveness.

It is now clear that no cost effective solution exists for using recombiners to cope with the hydrogen from an extensive zirconium-steam reaction in a LOCA. On the other hand, recombiners as they now exists are capable of dealing effectively with hydrogen and oxygen that result from radiolysis and corrosion, following a LOCA.

It is possible that recombiner technology could improve in the sense of offering existing performance at substantially lower cost; however such a development is not likely, considering the large amount of effort already spent in reaching current performance levels.

The question of recombining H_2 and O_2 at rates sufficient to cope with hydrogen from an extensive zirconium-steam reaction does not lie in the field of hydrogen recombiners, and is discussed elsewhere in this compendium.

Intentionally left blank

NOTES AND REFERENCES

1. Henry, J. O., F. E. Gregor, J. W. Honkala, Post-LOCA Hydrogen Recombiner System for LWR Nuclear Plants, V. 36 Proc. Amer. Power Conf., 1974, pp. 219-25.

2. NRC Regulatory Guide 1.7, p. 1.7-4.

3. Rogers, W. M., R. H. Lechelt, Nuc. Engr. Intl., Sept. 73, pp. 711-15.

4. SNE-100 (Southern Nuclear Engineering report; limited distribution); APCI-78-8 (Air Products & Chemicals, Inc. report).

5. Air Products & Chemicals, Inc. (Allentown, PA)

6. Westinghouse

7. Atomics Int'l (Rockwell)

8. This description was extracted from Westinghouse document WCAP-8660, Appendix A to RESAR-3S, Combustible Gas Control in Containment, Dec. 1975. With permission.

9. This description was extracted from Atomics Int'l document AI 75-2, Rev. 1, Thermal Hydrogen Recombiner System for Water Cooled Reactors, Feb. 75, except for Figs. 5 & 6, which were taken from AI document ESG-79-11 Hydrogen Recombiner System for Post-LOCA Application. With permission. (Revised, updated, and additional material on AI recombiners is available from the manufacturer (Canoga Park, CA), but was not obtained in time for use in this edition.)

10. This description was extracted from the APCI brochure CataGuard™ Hydrogen Recombiner Model PPL-70: Post-LOCA Hydrogen Control, July 1978. With permission.

V. LITERATURE REVIEW AND BIBLIOGRAPHY

The sequence of tasks comprising the literature review were performed in three phases. In the first phase, a descriptors list was determined, and was then submitted to the libraries at Sandia Laboratories and Energy Incorporated.

In phase two, the libraries performed computerized literature searches, accessing the following data bases:

1) Nuclear Science Abstracts
2) Energy Data Base
3) National Safety Information Center
4) National Technical Information Services
5) Compendex (Engineering Index)
6) INSPEC (Science Abstracts)
7) SCISEARCH (Science Citation Index)
8) Chemical Abstracts

The final phase of the review consisted of (1) screening the citation lists obtained from the literature searches, (2) submitting follow-up requests for specific reports, and (3) reading and collating the information obtained.

The bibliography that follows includes all materials identified in the literature search as likely to be of interest to readers of the Compedium, and also other similar materials known to both Sandia Laboratories and Energy Incorporated prior to the onset of this project.

The formats used for the bibliographical entries were obtained from the ISO Standards Handbook 1, first edition, 1977, a handbook on International Standards governing information transfer, compiled by the ISO Information Centre and sponsored by USESCO within its UNISIST program. Specifically, the following ISO (International Organization for Standardization) standards were used:

ISO 690-1975 Documentation - Bibliographic references - Essential and supplementary elements.

ISO 3388-1977 Patent documents - Bibliographic references - Essential and complementary elements.

ISO 3166-1974 Code for representation of names of countries.

Specifically, the following codes for the identification of countries of origin were used in the bibliographic entries for patent documents:

DE Germany, Federal Republic of

FR France (French Republic)

GB United Kingdom (of Great Britain and Northern Ireland)

US United States (of America)

METAL-WATER REACTION BIBLIOGRAPHY

ALLISON, W. W., A Preliminary Study of the Pyropheric Properties of Zirconium Machines and Standard Warning Labels for Zirconium, WAPD-TM-14, Washington D.C., U. S. Department of Commerce, 1956, 13 p.

BAKER, Louis Jr., and IVINS, Richard O., Analyzing the Effects of a Zirconium-Water Reaction. In: Nucleonics, 23(7) 1965: 70-74.

BAKER, Louis Jr., and JUST, Louis C., Studies of Metal-Water Reactions at High Temperatures III. Experimental and Theoretical Studies of the Zirconium-Water Reaction, ANL-6548, Argonne, Illinois, Argonne National Laboratory, 84 p.

BAKER, L., and LIMATAINEN, R. C., The Technology of Nuclear Reactor Safety (vol. 2). Chapter 17- Chemical Reactions, Agronne National Laboratory, 1973, avail. MIT Press, 104 p.

BALLINGER, W. G., et al., Oxidation Reaction Kinetics of Zircaloy-4 in an Unlimited Steam Environment. In: Journal of Nuclear Materials, 62 1976: 213-220 p.

BERMAN, R. M., et al., Properties of Zircaloy-4 Tubing, WAPD-TM-585, 1966, avail. NTIS, 220 p.

BITTEL, J. T., et al., Oxidation of 304 Stainless Steel by Steam and by Air. In: Corrosion, 25(1) 1969: 7-94

BRITTON, C. F., et al., Further Studies on the Inhibition by Boric Acid of the Oxidation of Zirconium in High Pressure Steam. In: Journal of Nuclear Materials, Amsterdam, 15(4) 1965: 263-277.

CATHCART, J. V., Quarterly Progress Report on the Zirconium Metal-Water Oxidation Kinetics Program Sponsored By The NRC Division of Reactor Safety Research for January-March 1977, ORNL/NUREG/TM-110, 1977, avail. NTIS, 27 p.

COMMONWEALTH EDISON COMPANY, Hydrogen Generation in a Boiling Water Reactor, 1970, avail. NTIS, 52 p.

DEMANT, J. T., and WANKLYN, J. N., The Effects of Contamination on the Oxidation of Zirconium in Steam, AERE-R4788, Harwell, Berkshire, Atomic Energy Research Establishment, 1965, 22 p.

FLETCHER, W. D., et al., Post LOCA Hydrogen Generation in PWR Containments, 1970, avail. Westinghouse Electric Corporation, NES-PWR Systems Division, 2 p.

GENCO, Joseph M., and RAINES, Gilbert E., Metal-Water Reactions During a Loss-of-Coolant Accident: The Zirconium-Steam Reaction. In: Amer. Nucl. Soc. 9(2), 1966: 555-556.

GROSSMAN, L. N., and ROONEY, D. M., Interfacial Reaction Between UO_2 and Zircaloy-2, GEAP-4679, San Jose, California, General Electric, 1965, 17 p.

HESSON, J. C., et al., Laboratory Simulations of Cladding-Steam Reactions Following Loss-of-Coolant Accidents in Water-Cooled Power Reactors, ANL-7609, Argonne National Laboratory, 1970, avail. NTIS, 39 p.

HEUZEL, N., and KLEINE, A., Experimental Investigation of Reactions Between Uranium Dioxide and Water Under Nonisothermal Quasi-Isobaric Conditions AEC-TR-6960, Battelle Institute, 1968, avail. Clearinghouse for Federal Scientific and Technical Information, 44 p.

HIGH-TEMPERATURE Materials Program Progress Report No. 52, Part A, GEMP-52A, Cincinnati, Ohio, General Electric, 1965, 55 p.

HIGH-TEMPERATURE Materials Program Progress Report No. 54, Part A, GEMP-59A, Cincinnati, Ohio, General Electric, 1965, 77 p.

HIGH-TEMPERATURE Materials Program Progress Report No. 58, Part A, GEMP-58A, Cincinnati, Ohio, General Electric, 1966, 67 p.

HOBSON, D.O. and RITTENHOUSE, P.L., Embrittlement of Zircaloy-Clad Fuel Rods by Steam During LOCA Transients, ORNL-4758, Oak Ridge, Tennessee, Oak Ridge National Laboratory, 40 p.

HOMA, K., et al. Behavior of the Zircaloy Cladding Tube in a Mixed Gas of Hydrogen and Steam, Japan Atomic Energy Research Inst., Tokai, 1977, Avail. NTIS, 24 p.

HYDROGEN Production in Light Water Reactors, NP-19937, Germany, Technische Univ., 1973, 253 p., in German.

IANNI, P.W. Metal-Water Reactions -- Effects on Core Cooling and Containment, APED-5454, Class 1 68APE6, San Jose, California, General Electric, 1968, 42 p.

JAHN, H. Hydrogen Production in Containment After a Loss-of-Coolant Accident in Light-Water Reactors, MRR-117, Germany, Technische Universitaet Muenchen, 1973, avail. NTIS, 58 p., in German.

JAHN, H.L. RALOC: A New Model for Calculation of Local Hydrogen Concentrations in Subdivided Containments Under LOCA, Aspects, CONF-770708--, Illinois, American Nuclear Society, 1977, pp. 629-641.

KAWASAKA, S. et al. Inner Surface Oxidation of a Fuel Cladding for LWR Under a LOCA, INIS-MF--3224, (1976), 21 p., in summary form only.

KILPATRICK, M. and LOTT, S. K. Reaction of Flowing Stream with Refractory Metals. In: Journal of Electrochemical Soc., 113(1), January 1966: 15-16.

LAWROSKI, Stephen. Chemical Engineering Division Summary Report July, August, September, 1962, ANL-6596, Argonne, Illinois, Argonne National Laboratory, 1962, 218 p.

LEISTIKOW, S. Behavior of LWR Cladding Material Under Loss-of-Coolant Conditions Zircaloy 4 - High Temperature Steam Oxidation, Karlsruhe, Germany, Gesellschaft fur Kernforschung m.b.H, 1975, 20 p.

LEISTIKOW, S., et al. Comparative Studies of Zircaloy 4/High Temperature Steam Oxidation Under Isothermal and Temperature-Transient Conditions, Germany, Kernforschungszentrum Karlsruhe, 27 p.

LUSTMAN, B. Zirconium-Water Reaction Data and Application to PWR Loss-of-Coolant Accident, WAPD-SC-543, Washington, D.C., Department of Commerce, 1957, 43 p.

MALANG, S. and Schanz, G. Description and Verification of SIMTRAN I - A Computer Code for the Calculation of the High Temperature Steam Oxidation of Zircaloy, Germany, Kernforschungszentrum Karlsruche, 18 p.

McLAIN, Howard A. Potential Metal-Water Reactions in Light-Water-Cooled Power Reactors, ORNL-NSIC-23, Tennessee, Oak Ridge National Lab., 1968, 201 p. Also in: Nuclear Safety, 10(5), Sep.-Oct. 69: 392-404

MORRISON, D.L., et al. An Evaluation of the Applicabili of Existing Data to the Analytical Description of Nuclear Reactor. Accident Core Meltdown Evaluat BMI-1910, 1971, avail. NTIS, 25 p.

PICKMAN, D.O. Properties of Zircaloy Cladding. In: Nuclear Engineering and Design, 21, 1972: 212-36.

POPESCU, E. et al. Aspects Concerning the Corrosion Behavior of Zirconium and Zirconium Alloys in Water at High Temperature. In: Rev. Coroz. Rumania, 2(2), 1972: 79-85.

REID, D.L. et al. Metal Reactions of Irradiated N-Reactor Fuels at 1025 to 1080°C, BNWL--1361, Richland WA, 43 p.

ROEDDER, P. and DANDER, W. Hydrogen-Generation By Metal-Water Corrosion During LOCA in a PWR of the "Muchlheim-Kaerlich"-Design. In German. In: Isu Mitt., 3, 1978: 167-171.

ROEDDER, P. and GEISER, H. Formation of Hydrogen During Core Melt Accidents in Nuclear Power Plants with Light Water Reactors. In German and English. In: Kerntechnik, Germany, 19(11), 1977: 473-477.

ROSA, C.J. Oxidation of Zirconium -- A Critical Review of Literature. In: J. Less-Common Metals, Netherlands, 16, 1968: 173-201.

SANDIA LABORATORIES. Core-Meltdown Experimental Review, UC-78b, Albuquerque, New Mexico, U.S. Department of Commerce, 1975, 470 p., bibliogr.

TECHNISCHE UNIV., Hydrogen Production in Light Water Reactors, NP-19937, Germany, 1973, avail. NTIS, 253 p., in German.

TOLKSDORF, E., The Transition Phenomenon. A Hypothesis Concerning the Behavior of Zr and its Alloy During Corrosion in Steam. In: Corrosion Science, Great Britain, 14, 1974: 565-573.

TUCKER, M.O. et al. Partitioning of Oxygen in Steam Oxidised Zircaloy.

UNITED STATES DEPARTMENT OF INTERIOR, Zirconium Hazards Research, Progress Report No. 2, September 1, 1957 to February 28, 1958, AECU-3682, United States Department of Interior, 1958, 25 p.

BANIC, V.F. Method for Estimating the Exposure Time and Temperature for Zircaloy Oxidation in Steam. In: Journal of Nuclear Materials, 59, 1976: 90-94.

D.R., et al. Hydrogen Monitor for Detecting s in LMFBR Steam Generators. In: Trans. Amer. Soc., 13, 1970: 96-7.

RADIOLYSIS BIBLIOGRAPHY

Patent 2,445,953 A, DE. 22 May 1975. Method of Hydrogen Production, Texas Gas Transmission Corp., U.S., GOMBER, H.J., 13 p., in German.

Patent 2, 604,974 A, DE. 19 Aug 1976. Chemical and Radiolytic Multi-Stage Method for the Production of Gas, Texas Gas Transmission Corp., U.S., O'NEAL, R.D., 17 p., in German.

Patent 7,601,343 A, NL. 10 Feb 1976. Multi-Step Chemical and Radiation Process for the Production of Gas, Texas Gas Transmission Corp., U.S., 8 p, in Dutch.

CEA CENTRE D'ETUDES NUCLEAIRES DE SACLAY. Radiolytic Yields in Water Reactors Systems and Influence of Dissolved Hydrogen and Nitrogen, CEA-CONF--4186, (France), 1977, 10 p.

Interscience Monographs on Physical Chemistry, 1968, 480 p.

ISRAEL ATOMIC ENERGY COMMISSION, Radiation Chemistry, IA--1128, pp. 78-96.

Matrix of Combustion-Relevant Properties and Classifications of Gases, Vapors, and Selected Solids, NMAB-353-1, National Materials Advisory Board (NRC), 1979, avail. NTIS, 99 p.

OAK RIDGE NATIONAL LAB. Irradiation Effects on Heterogeneous Systems, ORNL--4272, Tennessee, 218 p.

Radiolysis of Water Vapour at Very High Dose Rates. 2. Isotope Effects in the Hydrogen Yield from H_2O D_2O Mixtures. In: Can. J. Phys., 51(24), 1973: 4056-4061.

ANBAR, M., et al. Selected Specific Rates of Reactions of Transients from Water in Aqueous Solutions. II. Hydrogen Atom, 1975, 56 p.

ANDERSON, A.R. and WINTER, J.A. Radiolysis of Water Vapour. In: SILINI, G., Radiation Research, Amsterdam, North-Holland Publishing Co., 1967, pp. 167-78.

APPLEBY, A. and GAGNON, W.F. Scavenging of the Molecular Hydrogen Yield from Water Irradiated with Tritium β Particles. In: J. Phys. Chem., 75, 1971: 601-2.

APPLEBY, A. and SCHWARZ, H.A. Radical and Molecular Yields in Water Irradiated by Rays and Heavy Ions. In: J. Phys. Chem., 73, 1969: 1937-41.

BALMANNO, WILLIAM F. A Study of Detonation and Non-Stoichiometric Hydrogen-Oxygen-Diluent Mixtures: Master's Thesis, GAM/ME 72-4, Air Force Inst. of Technology Wright-Patterson AFB, Ohio School of Engineering, March 1972, avail. NTIS, 49 p.

BELL, M.J., et al. Investigation of Chemical Additives for Reactor Containment Sprays, WCAP-7153-A, Westinghouse Electric Corp., 1975, avail. NRC Public Document Room, 80 p.

BELLONI, J. and HAIESSINSKY, M. X-Radiolysis of Aqueous Hydrazine Solutions. In French. In: Int. J. Radiat. Phys. Chem., 1, 1969: 519-27.

BETTINALI, C. Hydrogen from Nuclear Wastes. In: Trans. Am. Nucl. Soc., Vol. 20, Paris, 1975, pp. 793-795.

BHASKARAN, K.A., et al. Shock Tube Study of the Effect of Unsymmetric Dimethyl Hydrazine on the Ignition Characteristics of Hydrogen-Air Mixtures. In: Combust. Flame, 21(1), Aug. 1973: 45-48.

BIBLER, N.E. Radiolysis of 0.4 M Sulfuric Acid Solutions with Fission Fragments from Dissolved Californium-252. Estimated Yields of Radical and Molecular Products that Escape Reactions in Fission Fragment Tracks. In: J. Phys. Chem., 79(19), 1975: 1991-1995.

BIBLER, N.E. Radiolytic Gas Production During Long-Term Storage of Nuclear Wastes, DP-MS--76-51, 1976, 25 p.

BLAIR, L.S. and GETZINGER, R.W. Shock Tube Study of Recombination in the Hydrogen-Oxygen Reaction Using Infrared Emission from Water Vapor. In: Combust. Flame, 14(1), Feb. 1970: 5-12.

BOYD, A.W., et al. Radiolysis of Water Vapour at Very High Dose Rates. 1. Hydrogen Yields from H_2O, H_2O--HCL, and H_2O--HBR Mixtures. In: Can. J. Phys. Canada, 51(24), 1973: 4048-4055.

BROKAW, R.S. Analytic Solutions to the Ignition Kinetics of the Hydrogen-Oxygen Reaction, NASA-TM-X-52003, National Aeronautics and Space Administration, 1964, avail. NTIS, 27 p.

BROKAW, R.S. Rate of Reaction Between Molecular Hydrogen and Molecular Oxygen, NASA-TM-X-2707; E-7195, NASA, Lewis Research Center, February 1973, avail. NTIS, 11 p.

BUGAENKO, L.T. Radiolysis of Liquid Inorganic Hydrogen Compounds. In German, Z. Chem., Moscow, 8, 1968: 51-9

BURNS, W.G. Suppression by Dissolved Hydrogen of the Radiolysis of Water by Mixed Radiation Fields, AERE-M-2702, URAEA Research Group, Atomic Energy Research Establishment, March 1975, avail. NTIS, 24 p.

BURNS, W.G. and MOORE, P.B. Water Radiolysis and Its Effect Upon In-Reactor Zircaloy Corrosion. In: Radiat. Eff., 30(4), 1976: 233-242.

BYAKOV, V.M. Nature of the Precursors of Radiolytic Molecular Hydrogen in Water, and the Mechanism of Positronium Formation in Liquids. In: Int. J. Radiat. Phys. Chem., 8(3), 1976: 283-288.

BYAKOV, V.M. and KALYAZIN, E.P. Mechanism of Formation of Products of the Radiolysis of Water. In: KHIM. VYS. Energ., Russia, 4, 1970: 255-9.

BYAKOV, V.M., et al. Effects of Various Factors on the Radiolytic Product Yields from Water, Budapest, Akademiai Kiado, 1967, pp. 87-94, Proceedings of the Second Tihany Symposium on Radiation Chemistry.

CATHCART, J.V. Zirconium Metal-Water Oxidation Kinetics Program Sponsored by the NRC Division of Reactor Safety Research. Quarterly Progress Report, January--March 1977, PC A03/MF A01, Oak Ridge National Lab., 28 April 1977, avail. NTIS, 26 p.

CERRAI, E., et al. Radiolysis of Steam--Water Mixtures: Effect of Steam Quality. In: Energ. Nucl., Milan, 16, 1969: 768-74.

CHOI, S.U. Effect of Additives on Gamma Radiolysis of Methanol. In: Daehan Hwahak Hwoejee, 14(3), 1970: 237-42.

CHRISTENSSEN, H. Consideration of Radiolysis of Ground Water, Kaernbraenslesaekerhet, 1978, avail. NTIS, 26 p. in Swedish.

COTTRELL, W.B. ORNL Nuclear Safety Research and Development Program Bimonthly Report for November--December 1969, ORNL-TM--2829, (Tennessee), Oak Ridge National Laboratory, 1970, 156 p.

COTTRELL, W.B. ORNL Nuclear Safety Research and Development Program Bimonthly Report for January--February 1971, ORNL-TM--3342, Tennessee, 1971, 127 p.

CUCCHIARA, ORLANDO, et al. Investigation of Hazardous Vapor Detection for Advanced Flight Vehicles, AO-487 447/5ST, Parametrics Inc., August 1966, avail. NTIS, 75 p.

DANIELS, M. and WIGG, E., Oxygen As a Primary Species in Radiolysis of Water. In: Science, Washington, D. C., 153, 1966: 1533-4

DAYAN, V. H., et al., Hydrogen Leak and Fire Detection a Survey, NASA-SP-5092, [California], [Rocketdyne], 1970, 88 p.

DI PIETRO, R., et al., Treatment of Water in a Nuclear Plant for the Testing of Fuel Elements, LIB/TRANS--35, Italy, 21 p.

DOLLE, L. and ROZENBERG, J., Radiolytic Yields in Water Reactor System and Influence of Dissolved Hydrogen and Nitrogen, CONF-7710187, [France], pp. 291-297.

DRAGANIC, I. G., et al., Radiolysis of HCOOH + O_2 at Ph 1.3 to 13 and the Yields of ^{2} Primary Products in Radiolysis of Water. In: J. Phys. Chem., 73, 1969: 2564-71.

DRAGANIC, Z. D. and DRAGANIC, I. G., On the Orgin of Primary Hydrogen Peroxide Yield in the Radiolysis of Water. In: J. Phys. Chem., 72, 1969: 2571-7.

DRAGANIC, Z. D. and DRAGANIC, I. G., Studies on the Formmation of Primary Yields of Hydrogen Peroxide and Molecular Hydrogen (G_{H2O2} and G_{H2}) in the Radiolysis of Neutral Aqueous Solutions. In: J. Phys. Chem., Belgrade, 75 (26), 1971: 3950-7.

DRAGANIC, Z. D. and DRAGANIC, I. G., Studies on the Formation of Primary Hydrogen Atom Yield G_H in the Radiolysis of Water. In: J. Phys. Chem., Belgrade, 76 (19), 1972: 2733-7.

EDWARDS, R. K., et al., Solid Solution Equilibra in the Ternary System, Zirconium-Oxygen-Hydrogen, AD-017 926/7ST, Illinois Inst. of Tech. Chicago, 1953, avail. NTIS, 37 p.

ERIKSEN, T. E., Gamma Radiolysis of Aqueous Solutions of Sulphur Dioxide. In: Radiochem. Radioanal. Lett., Sweden, 16(3), 1974: 147-153.

FINDEISEN, A., Hydrogen Gas Studies in the WNR-S(M) Research Reactor. In: Kernenergie, Germany, 14(9), 1971: 286-9.

FIRESTONE, R. E., Kinetic Isotope Effects in the Radiolysis of Water Vapor and the Reactions of Hydrogen Atoms with Water Vapor. Technical Progress Report, Part 11A, September 1, 1971--July 23, 1972, COO--1116-20 (Pt. 2), 1972, 19 p.

FLETCHER, W. D., et al., Post LOCA Hydrogen Generation in PWR Containments, CONF-700608--12, [Pittsburgh, PA], 26 p.

FRANK, H., Hydrogen-Oxygen Electrolytic Regenerative Fuel Cells, NASA-CR 57663; EOS-4110-M-7, Electro-optical Systems, Inc., 10 April 1964, avail. NTIS, 3 p.

GARDINER, JR., E. C., and WAKEFIELD, C. B., Influence of Gasdynamic Processes on the Chemical Kinetics of the Hydrogen-Oxygen Explosion at Temperatures Near 1000 K and Pressures of Several Atmospheres. In: Astronaut Acta, 15(5-6), Nov. 1970: 399-409.

GAWLOWSKI, J. and NIEDZIELSKI, J., Evidence for the Formation of Methane By the Dissociation of Excited Butyl Ions in the Radiolysis of Ethylene. In: Radiochem. Radioanal. Lett., Warsaw, 6(6), 1971: 345-50.

GRUBER, C. L., Thin Film Atomic Hydrogen Detectors, NASA-CR-152605, South Dakota School of Mines and Technology, June 1977, avail. NTIS, 33 p.

HART, E. J., Radiation Chemistry of Aqueous Solutions. In: Radiat. Res. Rev., vol. 3(4), 1972, pp. 285-304.

HAYON, E., Primary Radicals Yields in the Radiation Chemistry of Water and Aqueous Solutions. In: GABRIEL, Stein, Radiation Chemistry of Aqueous Systems, New York, John Wiley and sons, Inc., 1968, pp. 157-209.

HENTZ, R. R., et al., -Radiolysis of Liquids at High Pressures. I. Aqueous Solutions of Ferrous Sulfate, COO-38-516. In: J. Chem. Phys., 46, 1967: 2995-3000.

HENTZ, R. R., et al., -Radiolysis of Liquids at High Pressures. IV Primary Yields in Neutral Aqueous Solutions, COO-38-528. In: J. Chem. Phys. 47, 1967: 4865-7.

HENTZ, R. R. and KNIGHT, R. J., -Radiolysis of Liquids at High Pressures. VIII Primary Yields at 8.7 KBAR and Reactions of the Hydrated Electron with H_2O and H_3O. In: J. Chem. Phys., 52, 1970: 2456-9.

HOPKINS, H., et al., Simulation Experiments Using Hydrogen/Oxygen Gas Mixtures in a High Pressure Detonation Tube. Final Report, NASA-CR-12855, MSC-05836, Ohio, Cincinnati University Research Dept., May 1973, avail. NTIS, 155 p.

IWATA, S., et al., Radionuclides and Hydrogen Peroxide Detected in the Primary Cooling Water of Kyoto University Reactor. In. Annu. Rep. Res. Reactor Inst., Kyoto Univ., 2, 1969: 97-100.

JENKS, G. H., Prediction of Radiation Effects on Reactor Water and Solutions. In: Trans. Amer. Nucl. Soc., 9, 1966: 382.

JOHNSON, G. R. A. and SIMIC, M., Excitation and Ionization in the Radiolysis of Water Vapour. H/D Isotope Effect in the Formation of Hydrogen Atoms. In: Chemistry of Ionisation and Excitation, JOHNSON, G.R.A. and SCHOLES, G., London, Taylor and Francis, 1967, pp. 211-16.

JOSIMOVIC, J. and DRAGANIC, I., Radiolysis of Acetic Acid in Aqueous Solutions and Acetic Acid-Water Mixtures. In: Int. J. Radiat. Phys. Chem., Belgrade, 5(6), 1973: 505-512.

KABAKCHI, S. H., et al., Radiolysis of Water Containing Hydrogen Peroxide, Hydrogen and Oxygen. In Russian. In: KHIM. VYS. ENERG. 2, 1968: 40-5.

KESTEN, A. S., Study of Catalytic Reactors for Hydrogen-Oxygen Ignition Final Progress Report, 28 August 1968-28 May 1969, NASA-CR-72567; UARL-H-910721, United Aircraft Corp., July 1969, avail. NTIS, 78 p.

KISS, I. and SCHILLER, R., Some Considerations on the Structure and Radiation Chemistry of Water, NASA-TT-F-11366, National Aeronautics and Space Administration, December 1967, avail. NTIS, 10 p.

KOIKE, M., et al., Gamma-Radiolysis of Aqueous Boric Acid Solution. In: J. Nucl. Sci. Technol., Tokyo, 6, 1969: 163-9.

KOIKE, M., et al., Gamma Radiolysis of Water Using a Specially Designed Gamma-Irradiation Loop. In: J. Nucl. Sci. Technol., Tokyo, 10(2), 1973: 111-117.

KOT, A. A., et al., Water control and the Prevention of Water and Steam Radiolysis at the Beloyarsk Nuclear Power Station, AERE-TRANS-1112. In: Elek. Sta., 39(1), 1968: 39-41.

KULES, I. and SCHILLER, R., Radiation Chemistry of Supercooked Water. In: J. Phys. Chem., Budapest, 75(19), 1971: 2997-9.

LABELLE, D. W., Post-Accident Hydrogen Generation and Control. In: Nucl. Technol., 10, 1971: 454-9.

LADERMAN, A. J., Study of Detonation of Mixtures of Gaseous Hydrogen and Gaseous Oxygen Final Report, June 1, 1962-February 18, 1965, NASA-CR-64032, California University, April 1965, avail. NTIS, 267 p.

LEMAIRE, G. and FERRADINI, C., Yield of Hydrogen Peroxide in Aerated Acidified Water Exposed to Tritium Rays. In: Radiochem. Radionanal. Lett., Paris, 5, 1970: 175-8.

LEMAIRE, G., et al., Radiolysis of Water by Tritium Rays: Scavenging of Hydrogen Peroxide Precursors. In: J. Phys. Chem., France, 76(11), 1972: 1542-6.

MAHLMAN, H. A. and SWORSKI, T. J., Nature of the Precursor of Molecular Hydrogen in the Radiolysis of Water. In: JOHNSON, G.R.A. and SCHOLES, G., Chemistry of Ionisation and Excitation, London, Taylor and Francis, 1967, pp. 259-67.

MAIBORODA, V. D., et al., Mechanism of the Radiolysis of Water in the Presence of H_2O_2, H_2, O_2. In: Vestsi Akod. Navuk Belarus. SSR, Ser. Fiz.-Energ. Navuk, Minsk, Russia, 1973(1): 32-36.

MAJBORODA, V. D., et al., On Decomposition Mechanism of Hydrogen Peroxide Water Solutions When Influenced by Different Decomposition Initiators. In: Vestsi Akad. NAvuk Belarus. SSR Serv. Fiz.- Energ. Navuk, Russia, 1973(3), 50-53.

MATSUDA, KATASUHIKO, et al., Dissolution of Hydrogen Gas in Aqueous Solutions. In: J. Min. Metall. Inst., Japan, 93(1078), Dec. 1977: 969-974.

MATSUDA, KATSUHIKO, et al., Dissolution Behavior of Hydrogen Gas in Aqueous Solutions Containing Strong Electrolytes--2. Studies on the Gaseous Reduction of Metals from Aqueous Solutions. In: J. Min. Metall. Inst., Japan, 94(1079), Jan. 1978: 44-48.

METZLER, A. J., and GAUGLER, R. E., High-Response On-Line Gas Analysis System for Hydrogen-Reaction Combustion Products, NASA-TM-X-3123; E-8014, NASA-Lewis Research Center, October 1974, avail. NTIS, 16 p.

MOORTHY, P. N. and RAO, K. N., Hydrogen Peroxide Yield in Gamma-Irradiated Air-Saturated Ice at 77°K. In: Radiat. Eff., India, 14(1-2), 1972: 113-17.

MOREAU, M. and SUTTON J., Influence of Ph on Yield of Hydrogen Atoms in Radiolysis of Aqueous Solutions. In: Trans. Faraday Soc., 65, 1969: 380-9.

MULLER, J. C. et al., High-Intensity Radiolysis of Water, I. Formation of Hydrogen Peroxide in Deaerated Acidic Solutions. In: Int. J. Radiat. Phys. Chem., Paris, 7(5), 1975: 635-641.

NICHIPOROV, F. G. and BYAKOV, V. M., Radiation-Chemical Yields of Molecular Hydrogen in Aqueous H_2O_2 Solutions, and the Nature of Its Precursors. In: High Energy Chem., USSR, 9(2), 1975: 151-152.

ORAN, E. S., et al., Time Dependent Studies of Reactive Shocks in the Gas Phase, NRL-MR-3889, Naval Research Lab., 16 November 1978, avail. NTIS, 42 p.

PAOLI, O. and ROZENBERG, J., Generation of Hydrogen by Radiolytic Decomposition of Sprinkling Solutions Capable of Absorbing Fission Iodine. Influence of Certain Additives (in French). France, CEA Centre D'Etudes Nucleaires de Saclay, 1975, avail. NTIS, 18 p.

PIKAEV, A. K. and ERSHOV, B. G., Primary Products of the Radiolysis of Water and Their Creativity, FSTC-HT-23-136-68, Army Foreign Science and Technology Center, 1968, avail. NTIS, 56 p.

PELED, E. and CZAPSKI, G., Studies on the Molecular Hydrogen Formation G_{H_2} in the Radiation Chemistry of Aqueous Solutions. In: J. Phys. Chem., 74, 1970: 2903-11.

PESTANER, J. F., The Radiolysis of Seawater, USNRDL-TR-44, Naval Radiological Defense Lab., 3 April 1967, avail. NTIS, 24 p.

PIEPER, H., The Radiolysis of Water Under the Influence of Ionizing Radiation in Water Cooled Nuclear Reactors, Germany, VGB Feedwater Conference, 1970, 5 p., in German.

PRISTUPA, A. I., et al., Low-Temperature Radiolysis of Aqueous Alkaline Solutions. In Russian. In: IZV. AKAD. NAUK SSSR, SER. KHIM., Russia, 1970(2), 488-9.

RAICHEVSKII, G., Influence of Ph on the Stationary Concentrations of Molecular Radiolysis Products of Water. In: High Energy Chem., USSR, 6(6), 1972: 464-469.

RAJESHNARI, A. R., Radiation Effects on Organic Compounds, INIS-MF--706, India, 1972.

RANDRIANARIVO, P., et al., Gamma Radiolysis of the Water Vapor--Ammonia--Oxygen System. In: Radiochim. Acta, Paris, 1894), 1973: 178-180.

SASSE, RONALD A., Hydrogen and Hydrogen Peroxide Produced by Gamma Radiolysis of Oxygen-Saturated Water, NDL-TR-122, Army Nuclear Defense Lab., June 1969, avail. NTIS, 38 p.

SAUER, M. C., et al., Measurement of the Hydrogen Yield in the Radiolysis of Water by Dissolved Fission Products, ANL--76-46, Illinois, Argonne National Lab, 1976, 16 p.

SCHMIDT, K. H. and ANDER, S. M., Formation and Recombination of H_3O^+ and Hydroxide in Irradiated Water. In: J. Phys. Chem., 73, 1969: 2846-52.

SCHWARZ, H. A., Applications of the Spur Diffusion Model to the Radiation Chemistry of Aqueous Solutions. In: J. Phys. Chem., 73, 1969: 1928-37.

SEHESTED, K., et al., Primary Species Yields in the ^{60}CO Gamma Ray Radiolysis of Aqueous Solutions of H_2SO_4 Between Ph7 and 0.46. In: Radiat. Res., Denmark, 56(2), 1973: 385-399.

SHUMAR, J. W. and POWELL, J. D., Hydrogen Detection Study, Final Report Jan.-30 Sep. 1974, NASA-CR-137563; LSI-ER-170-85, Life Systems, Inc., September 1974, avail. NTIS, 49 p.

SUTTON, J. and MOREAU, M., Origin of the Yield of Primary Hydrogen Atoms in Water Radiolysis, Budapest, Akademiai Kiado, 1967, pp. 95-103, Proceedings of the Second Tihany Symposium on Radiation Chemistry.

SWAN, T., A Review of the Reaction of Carbon with Water Vapour and Hydrogen, RD/B/M--1297, [England], 1969, 31 p.

SWORSKI, T. J., Solvated Electron. Advances in Chemistry, Series 50, Conf-6509101--, Washington, D.C., Amer. Chem. Soc., 1965, pp. 263-78.

SZYMANSKI, E., et al., Radiation Stability Increase of Poly (vinyl chloride). I. Radiation Yield of Hydrogen Chloride in Pure Poly (Vinyl Chlorides) Irradiated ^{60}Co. In: Nukleonika, Poland, 19(4), 1974: 323-328.

SZYMANSKI, W. and SMIETANSKA, G., Radiation Yield of Hydrogen Chloride in the Poly (Vinyl Chloride) Foils Irradiated by Accelerated Electrons. In: J. Appl. Polym. Sci., 19(7), 1975: 1955-1958.

TECHNISCHE UNIV., Hydrogen Formation in Light-Water Reactors, IRS-SB--2, Germany, 1973, 243 p.

TURNER, S. E., Radiolytic Decomposition of Water in Water-Moderated Reactors Under Accident Conditions. In: Reactor and Fuel-Processing Technology, 12(1), 1969: 68-79.

VAN METER, R. A., et al., Hydrogen Safety, Annual Report for the Period January 1--December 31, 1964, (Progress Report No. 4), PC EO3/MFA01, Bureau of Mines, January 1965, avail. NTIS, 48 p.

VARTAK, D. G., et al., Radiolytic Decomposition of Coolant Water in Cirus Reactor, INIS-MF--1147. In: Symposium on Nuclear Science and Engineering, Bombay, 1973.

VLADIMIROVA, M. V., et al., Alpha- and Beta-Radiolysis of Aqueous Solutions of Light and Heavy Water. In Russian. In: Radiokhimiya, Russia, 8, 1966: 226-32.

VUKMIROVIC, Z. B., Hydrogen Isotope Effects in the Radiolysis of Water. In: Israel J. Chem., Israel, 5, 1967: 75-87.

WALTON, G. N., Underlying Mechanism in the Water Chemistry of Nuclear Reactor Systems. Proceedings of an International Conference Organized by the British Nuclear Energy Society, Bournemouth, 24-27 October 1977, CONF-7701087--, London, Thomas Telford for BNES, 1978, pp. 275-279.

WIERMAN, R. W. and HILLARD, R. K., Experimental Study of Hydrogen Formation and Recombination under Postulated LMFBR Accident Conditions, PC A04/MF A01, Energy Research and Development Administration, 1 December 1976, avail. NTIS, 58 p.

WILLCUTT, G. J. E. JR., and GIDO, R. G., Mixing of Radiolytic Hydrogen Generated within a Containment Compartment Following a LOCA, LA-7421-MS, Los Alamos Scientific Lab., July 1978, avail. NTIS, 61 p.

WILLIS, C., et al., Experimental and Calculated Yields in the Radiolysis of Water at Very High Dose Rates. In: Int. J. Radiat. Phys. Chem., 1, 1969: 373-81.

ZERMIZOGLOU, R., et al., Recombination of Radiolytic Gases Dissolved in Water on a Fixed Catalyst Bed. In French. In: La Chimica Dell'Acqua Nei Reattori Nucleari, Rome, Comitato Nazionale Energia Nucleare, 1966, pp. 269-91.

ZHABROVA, G. M., et al., Electronic Mechanisms of Catalytic and Chemisorption Processes Induced by Ionizing Radiation. [Berlin], Water De Gruyter and Co., 1969, from Symposium on Electronic Phenomena in Chemisorption and Catalysis on Semiconductors, held in Moscow, July 2-4, 1968, pp. 231-43.

ZITTEL, H. E., Radiolytic Hydrogen Generation After Loss-of-Coolant Accidents in Water-Cooled Power Reactors. In: Nucl. Safety, 13(6), 1972: 459-67.

ZITTEL. H. E. and ROW, T. H., Radiation and Thermal Stability of Spray Solutions. In: Nuclear Technology, 10(4), April 1971: 436-443.

CORE-CONCRETE INTERACTIONS

The following bibliography is intended to guide the interested reader to further details concerning subjects treated in section I-5. Capsule descriptions of the references are included to aid the reader's selection. The bibliography is a listing of works that will be of use in gaining an understanding of gas generation during melt interactions with concrete. The bibliography should provide a starting place for those interested in pursuing the subject in greater depth.

CONCRETE CHEMISTRY BIBLIOGRAPHY

BRUNAUER, S. and COPELAND, L. E., "The Chemistry of Concrete," Scientific American 210 81 (April 1964).

A readable account for the non-specialist of the chemistry of conventional and more exotic concretes.

TAYLOR, H. F. W. (ed.) The Chemistry of Cements, Academic Press, (1964).

A collection of monographs on various features of concrete chemistry. Especially detailed on chemical species. The treatments of pore structure and texture are weaker.

KALOUSEK, G. L., DAVIS, Jr., C. W., and SCHMERTZ, W. E., "An Investigation of Hydrating Cements and Related Hydrous Solids by Differential Thermal Analysis," Proc. Amer. Conc. Institute, 45 693 (1949).

A classic study of the thermal decomposition of cementitious phases of concrete.

KANTRO, D. L. and COPELAND, L. E., "The Stoichiometry of the Hydration of Portland Cement," Chemistry of Cement, Proc. 4th Int'l Symp., Natl. Bur. Stds. Monograph 43 Vol 1, p. 430 (1960).

Hydration and water in concrete are described.

BAZANT, Z. P., "Review of Literature on High Temperature Behavior of Concrete," Appendix I in Evaluation of Structural Integrity of LMFBR Equipment Cell Liners - Results of Preliminary Investigations, W. J. McAfee and W. K. Sartory, ORNL-TM-5154, Oak Ridge National Laboratory, Oak Ridge, TN, January 1976.

Bazant presents a noncritical listing of some of the literature on concrete. The emphasis is on mechanical behavior of heated concrete. The discussions on gas release are not extensive.

THERMAL DECOMPOSITION OF CONCRETE

FORRESTER, J. A., "The Determination of Calcium Oxide, Calcium Hydroxide and Carbon Dioxide by Thermogravimetry," Analysis of Calcareous Materials Comprising Compilation of Basic Methods of Analysis and Papers. Monograph 18, p. 407 Society of Chemical Industry, London.

Effects of aging and heat treatment on the stoichiometry of weight loss from concrete. The results can only be qualitatively extrapolated to other concretes.

HARMATHY, T. Z., "Determining the Temperature History of Concrete Constructions Following Fire Exposure," J. Am. Conc. Inst. 65 959 (1968).

A qualitative description of water loss from concrete during heat treatment. Of principal interest to those concerned with changes in concrete rather than gas generation.

HARMATHY, T. Z. "Thermal Properties of Concrete at Elevated Temperatures," J. Materials 5 47 (1970).

An attempt to quantitatively describe the variation in the properties of concrete with temperatures.

POWERS, D. A., "Empirical Model for the Thermal Decomposition of Concrete," Trans. Amer. Nucl. Society 26 400 (1977).

This is the presentation of a kinetic approach to the quantitative description of microscopic processes of concrete decomposition at high temperatures. The formalism considered in this work could be used to describe most structural concrete decompositions.

HANCOX, N. L., "The diffusion of Water in Concretes," AEEW-R482 Atomic Energy Establishment at Winfrith, England, 1966.

The drying of a concrete sphere is treated in the conventional diffusion manner. The strong dependence on temperature of diffusion coefficients determined in the study reflect the fundamental inapplicability of simple diffusion theory to water migration.

BAZANT, Z. P. and Majjar, J. J., "Nonlinear Water Diffusion in Nonsaturated Concrete," Materiaux et Constructions, 5 3 (1972).

PIHLAJAVAARA, S. E. and TIUSANEN, K., "A Preliminary Study on Thermal Moisure Transfer in Concrete," Paper 34-47 Concrete for Nuclear Reactors Special Publication SP-34, American Concrete Institute, Detroit, Michigan, 1972.

Nonlinear diffusion is used to explain moisture migration. The descriptions in these papers of the texture and pore structure of cementitious concrete is useful. The models of moisture migration are outdated.

McCORMAK, J. D., POSTMA, A. K. and SCHUR, J. A., Water Evolution from Heated Concrete, HEDL-TME-78-87, Hanford Engineering and Development Laboratory, Richland, WA, February 1979.

This document describes the WATRE computer code for predicting water loss from heated concrete. The treatment is strongly biased toward non-calcareous concretes.

BAZANT, Z. P. and THONGUTHAI, W., "Pore Pressure and Drying of Concrete at High Temperatures," ASCE J. Eng. Mech. Div. 104 1059 (1978).

Despite the title, the model described in this paper is best applied to analysis of water loss at temperatures less than 150°C.

DYAN, A., COWAR-2 User's Manual - Thermohydraulic Behavior of Heated Concrete, GE-FBRD-GEFR-00090(L), General Electric Corp., May 1977.

A description of a model of water release from heated concrete during reactor accidents.

BECK, J. V. and KNIGHT, R. L., User's Manual for USINT - A Program for Calculating Heat and Mass Transfer in Concrete Subjected to High Heat Fluxes" NUREG/CR-1375 SAND79-1694, Sandia National Laboratories, Albuquerque, NM, May 1980.

This document describes a model to predict both water and CO_2 release from heated concrete at temperatures that might be encountered in reactor accidents.

GLUEKER, E. L. and DAYAN, A., "Concrete Failure Modes at Elevated Temperatures," Proc. 3rd Post Accident Heat Removal Information Exchange. Argonne National Laboratories, 2-4 Nov. 1977, ANL-78-10, p. 233.

Primarily a discussion of mechanical failure by spallation of concrete. Shows a comparison of COWAR-2 predictions of pressure in concrete with experimental data.

KNIGHT, R. L. and BECK, J. V., "Model and Computer Code for Energy and Mass Transport in Decomposing Concrete and Related Materials," Proc. Int'l. Mtg. on Fast Reactor

Safety Tech., Seattle, WA, Aug. 19-23, 1979. Vol. IV, p. 2113, Am. Nucl. Soc., LaGrange Park, IL.

The article provides a capsule view of the USINT model and a comparison of predicted and experimental results.

FISCHER, R., "Uber das Verhalten von Zementmortel u. Betonbei Hoheren Temperaturen," Deutscher Ausschuss fur Stahlbeton, Heft 214, W. Ernst u. Sohn, Berlin 1970.

Fisher presents data from extensive investigations of various concretes. The data are useful for showing the range of concrete properties and their dependence on temperature. Correlations to apply results to particular concretes are not available. Unfortunately, the article is in German. A translation to English has not appeared yet.

MOISTURE MIGRATION IN CONCRETE

POWERS, T. C. and BROWNYARD, T. L., "Studies of the Physical Properties of Hardened Portland Cement Paste," J. Am. Conc. Inst. 18 249 (1946).

One of the earliest studies of the physical properties of concrete and classification of the various types of water in concrete.

YUAN, R. L., HILSDORF, H. K. and KESLER, C. E., "The Effect of Temperature on the Drying of Concrete," Paper SP 34-46

Concrete for Nuclear Reports, Special Publication SP-34. American Concrete Institute, Detroit, Michigan, 1972.

Isotherms for the adsorption of physically bound water in concrete for temperatures up to 60°C.

ENGLAND, G. L. and SHARP, T. J., "Migration of Moisture and Pore Pressure in Heated Concrete," Paper H 2/4, Proc. First Int'l Conf. Struct. Mech. in Reactor Tech., Berlin, Germany, Sept. 20-24, 1971.

A classic paper on the development of high pressures within concrete heated on one surface.

HARMATHY, T. Z., "Simultaneous Moisture and Heat Transfer in Porous Systems with Particular Reference to Drying," Ind. Eng. Chem. 8(1) 92(1969).

An approach to moisture migration during heating of concrete that works best when bulk porosity does not change dramatically and thermal gradients are small.

HARMATHY, T. Z. and ALLEN, L. W., "Thermal Properties of Selected Unit Concretes," J. Am. Conc. Inst. 70, 132 (1973).

A collection of data on various concretes that is of use in gaining appreciation for the range of concrete thermal properties. The data can only be used as guides to the properties of specific concretes.

ENGLAND, G. L. and SKIPPER, M. E., "On the Prediction of Moisture Movement in Heated Concrete," 2nd Int'l Conf. on Struct. Mech. in React. Tech., Berlin, 10-14 Sept. 1973, V. 3.

A qualitative description of moisture migration in concrete at temperatures to 150°C.

VOS, B. H., "Moisture Migration in Concrete," Paper H 2/5, Proc. 1st Int'l Conf. Struct. Mech. in Reactor Tech., Berlin, Sept. 20-24, 1971.

An analytic treatment of moisture migration in concrete at low temperatures that raises the issue of capillary action neglected in some treatments.

SULLIVAN, P. J. E. and ZAMAN, A. A. A., "Explosive Spallation of Concrete Exposed to High Temperatures," Proc. 1st Int'l Conf. on Struct. Mech. in Reactor Tech., Berlin, 20-24 September 1972, Vol. 4, Paper H 1/5.

An account of catastrophic failure of heated concrete.

METAL GAS REACTIONS

ELLIOT, J. F. and GLEISER, M., Thermochemistry for Steelmaking, Addison Wesley Publ. Co., Inc., Reading, MA, 1960.

A classic reference dealing in part with the subject of gas-melt equilibria. See also BOF Steelmaking Vol. 2 Theory, Chapter 4, E. T. Turkdogan, "Physical Chemistry of Oxygen Steelmaking, Thermochemistry and Thermodynamics," AIME (1975).

FLORIDIS, T. P. and CHIPMAN, J., "Activity of Oxygen in Liquid Iron Alloys," Trans. Met. Soc. AIME 212 54g (1958).
Data on the solution effects on oxygen activity in liquid steels are presented.

CHEN, H. M. and CHIPMAN, J., "The Chromium-Oxygen Equilibrium," Trans. Am. Soc. Metals, 38 70 (1947).
Equilibrium in the reaction of H_2O with chromium dissolved in iron is discussed.

CHIPMAN, J., GERO, J. B. and WINKLER, T. B., "The Manganese Equilibrium under Simple Oxide Slags," Trans. AIME 188 341 (1950).
Equilibrium of manganese-MnO system is discussed.

ORR, R. L. and CHIPMAN, J., Trans. Met. Soc. AIME 239 630 (1967).
Thermodynamic functions are presented for liquid iron alloys.

RICHARDSON, F. D., Physical Chemistry of Melts in Metallurgy, Vol. 2, Academic Press, London and New York, (1974).
Chapter 10 of this book has a brief discussion of some of the kinetic aspects of gas-melt reactions.

BICKERMAN, Foams: Theory and Industrial Applications, Reinhold Press, New York, 1953, Especially Sections 3-7.

A review of the formation of bubbles at sites below a liquid. See also Silberman p 263-284 Proc. 5th Midwestern Conf. on Fluid Mech., University of Michigan Press, Ann Arbor, Michigan, 1957 for a discussion of flow regimes.

HELSBY and TUSON, Research, London 8 270 (1955).
Discusses coalescence of gas bubbles formed at multiple sites.

HABERMAN and MORTON, Report 802, David W. Taylor Model Basin, Washington, DC, 1953.
Bubble velocities in liquids discussed theoretically and experimentally.

HYDROGENATION AND COKING

EMMETT, P. H., Catalysis Vol. IV Hydrogenation, Reinhold Publ. Co., 1956. Especially -

Chapter 1, R. B. Anderson, "The Thermodynamics of Hydrogenation of CO and Related Reactions."

Chapter 2, R. B. Anderson, "Catalyst for the Fisher-Tropsch Synthesis."

Chapter 4, L. J. E. Hofer, "Crystalline Phases and Their Relation to Fischer-Tropsch Catalysis."

Chapter 6, M. Greyson, "Methanation."

These chapters will provide background on possible reactions that could occur in gases produced during melt/concrete interactions.

STORCH, H. H., "The Fischer-Tropsch and Related Processes for Synthesis of Hydrocarbons by Hydrogenation of Carbon Monoxide," Advances in Catalysis, Vol. 1, Academic Press, 1948.

This article provides further perspective on the formation of hydrocarbons in H_2/CO mixtures. The emphasis is on controlled synthesis and the role of catalysts such as iron and nickel.

BURNING OF CO AND H_2

DIXON-LEWIS, G. and WILLIAMS, D. J., "The Oxidation of Hydrogen and Carbon Monoxide," and R. T. Pollard, "Hydrocarbons," Chapters 1 and 2 in Comprehensive Chemical Kinetics Vol. 17 - Gas Phase Combustion, C. H. Bamford and C. F. H. Tripper eds., Elsevier Scientific Publishing Co., 1977.

These works present a thorough review of combustion and explosion limits of gases important during core meltdown accidents.

NOUGHTON, J. J., Geochemica et Cosmochimica Acta 37 1163 (1973).

Flammability limits of diffusional hydrogen flames are determined in experiments with hydrogen/helium mixtures.

MELT/CONCRETE INTERACTIONS

POWERS, D. A., DAHLGREN, D. A., MUIR, J. F. and MURFIN. W. D., Exploratory Study of Molten Core Material/Concrete Interactions, July 1975-March 1977, SAND77-2042, Sandia Laboratories, Albuquerque, NM, February 1978.

Qualitative features of melt interactions with concrete are described.

PEEHS, M. et al., Untersuchung der Wechselwirkung von Kernschmelze under Reaktorbeton, BMFT RS 154 RE 23/017/78 Kvaftwerk Union Erlangen, Fed. Rep. of Germany.

Account of research on melt/concrete interactions conducted by the German reactor vendor on behalf of the German regulatory authorities. Some attempts at real-time identification of gases given off during the interaction are described.

BAKER, Jr., L. et al., Post Accident Heat Removal Technology, ANL/RAS 77-2, Argonne National Laboratory, January 1977.

Chapter VII reviews some small-scale studies of melt/concrete interactions. Emphasis is on erosion processes and temperatures within the concrete.

POWERS, D. A., "Sustained Molten Steel/Concrete Interactions Tests," Proc. Post Accident Heat Removal Informaton

Exchange Nov. 2-4, 1977, Argonne National Laboratory ANL-78-10, p. 433.

Tests of 200-kg melts of stainless steel interacting with concrete are described. Gas flow rates and gas composition data are presented.

POWERS, D. A., "Influence of Gas Generation on Melt/Concrete Interactions," IAEA Symposium on the Thermodynamics of Nuclear Materials, Julich, Fed. Rep. of Germany, 1979.

Review of the chemical and mechanical features of gas generation during melt/concrete interactions.

BAUKAL, W., NIXDORF, J., SKOUTAJAN, R. and WINTER, H., Investigation of the Relevancy and the Feasibility of Measurements of Chemical Reactions During Core Meltdown on the Integral Heat Content of Molten Cores, BMFT-RS-197, Battelle Institut, e.v. Frankfurt am Main. Fed. Rep. of Germany, June 1977. English Trans. NUREG/TR-0047, October 1978.

Heat produced by the reaction of CO_2 and H_2O with metallic constituents of a core melt is shown to be comparable to the fission-product decay heat.

MURFIN, W. B., A Preliminary Model for Core/Concrete Interactions, SAND77-0370, Sandia Laboratories, Albuquerque, NM, July 1977.

The INTER Model of melt/concrete interactions is described. The model is most useful for sensitivity studies to identify processes that have the greatest impact on the interaction.

REIMANN, M. and MURFIN, W. B., "Calculations for the Decomposition of Concrete Structures by a Molten Pool," Proc. Post Accident Heat Removal Information Exchange Meeting, Ispra, Italy, October 10-12, 1978.

The WECHSL Model of melt/concrete interactions developed at the Kernforschungszentrum Karlsruhe, Fed. Rep. of Germany is described. This model is far more comprehensive than the INTER Model, but it still underestimates the rate of gas generation.

KUMAS, R., BAKER, Jr., J. and CHASANOV, M. G., Ex-Vessel Considerations in Post Accident Heat Removal, Chapter 5, ANL/RAS 74-29, Argonne National Laboratory, Argonne, IL, October 1974.

This is a description of the GROWS code that has been used for the analysis of metal/concrete interactions.

MUIR, J. F. and BENJAMIN, A., "Modelling of Molten Fuel/Concrete Interactions," Proc. ANS/ENS Topical Meeting Thermal Reactor Safety, 7-11 April 1980, Knoxville, TN.

This paper briefly outlines the CORCON model of melt/concrete interactions and a possible model of the rate of heat transfer from the melt to concrete.

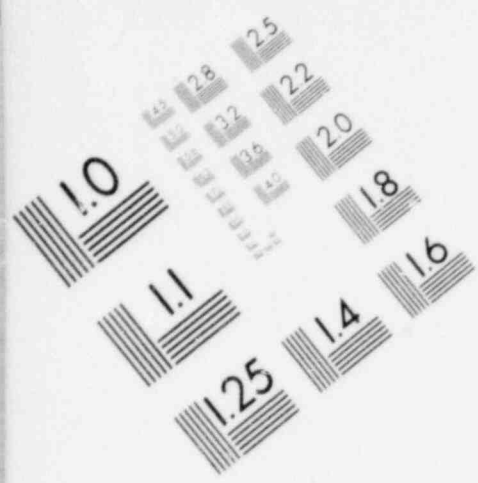

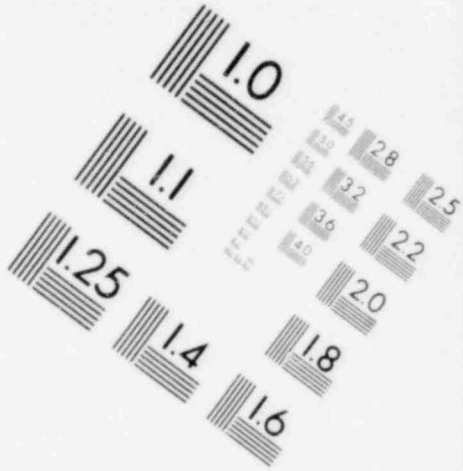

IMAGE EVALUATION
TEST TARGET (MT-3)

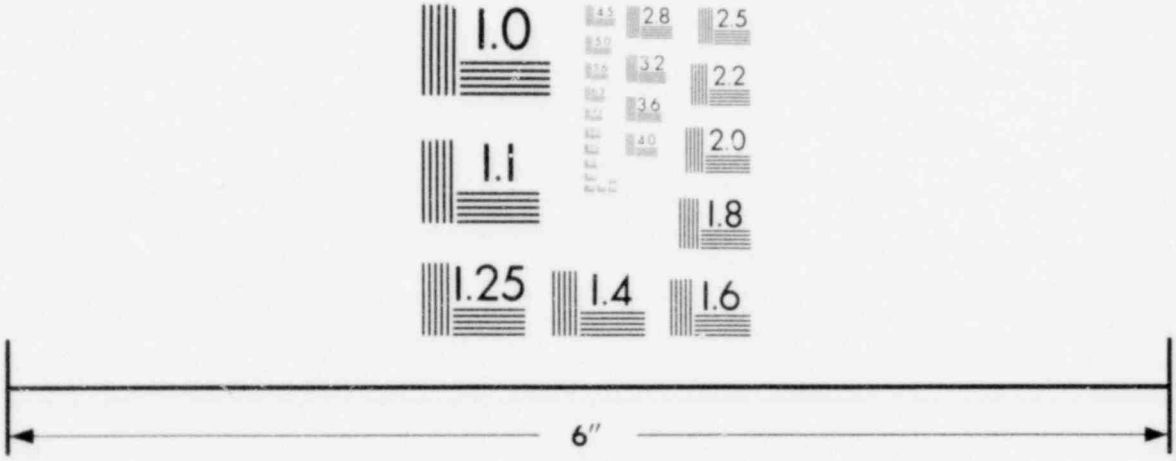

MICROCOPY RESOLUTION TEST CHART

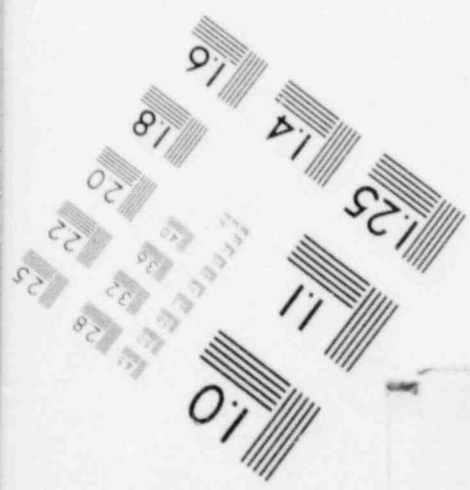

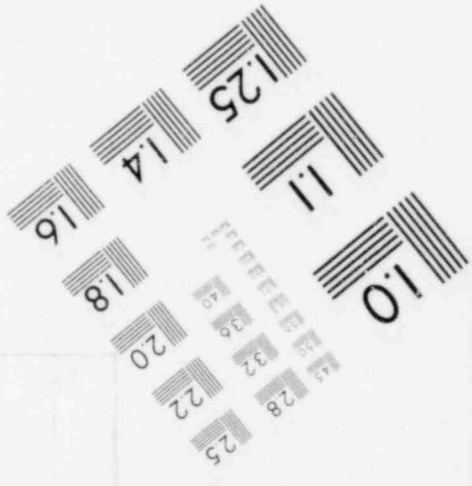

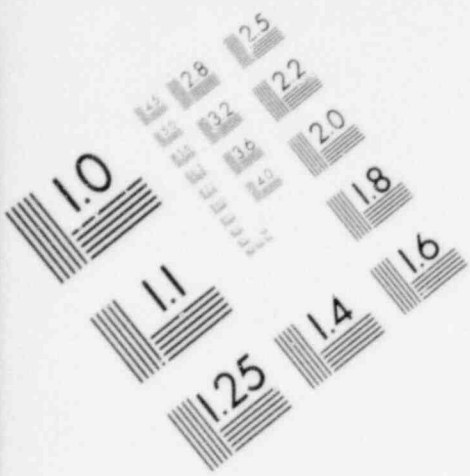

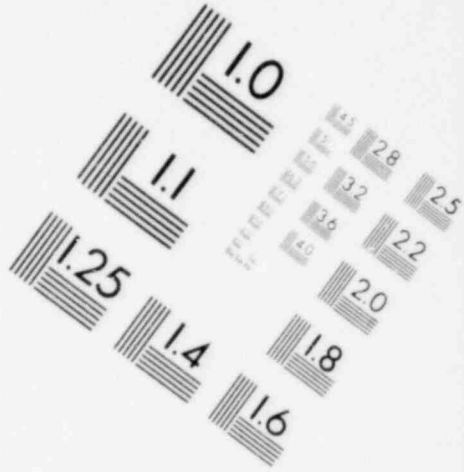

IMAGE EVALUATION
TEST TARGET (MT-3)

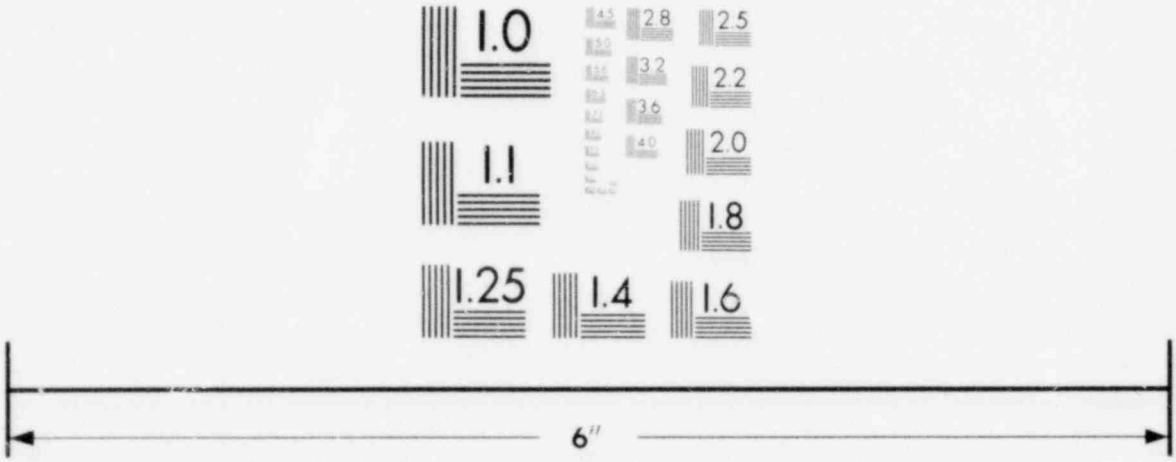

MICROCOPY RESOLUTION TEST CHART

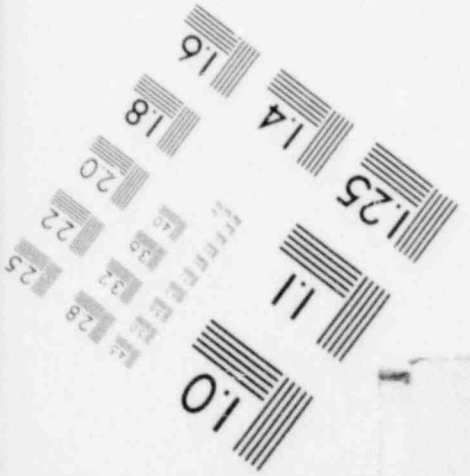

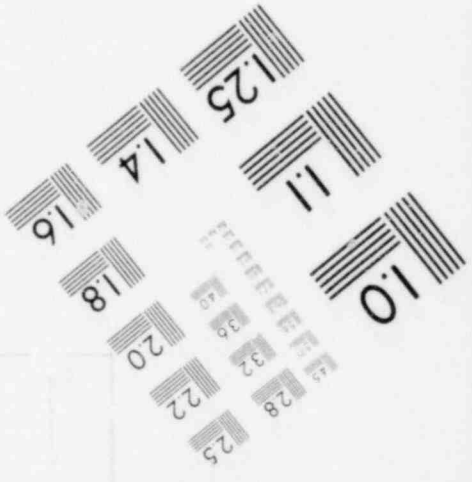

SOLUBILITY BIBLIOGRAPHY

ANDERSON, T. S., Correlation of Solubility Data for Hydrogen and Nitrogen in Water. In: Trans. Amer. Nucl. Soc., 10, 1967: 507-8.

GORDON, LOUIS I., et al., The Solubility of Molecular Hydrogen in Seawater, 77-19, Oregon State University, School of Oceanography, 22 April 1976, avail. NTIS, 7 p.

JOSE, C. J., et al., Apparatus for the Determination of Dissolved Gases in Nuclear Reactor Coolants (Water), BARC-361, Bhabha Atomic Research Centre, 1968, avail. NTIS, 19 p.

KATAYAMA, TAKASHI and NITTA, TOMOSHIGE, Solubilities of Hydrogen and Nitrogen in Alcohols and n-Hexane. In: J. Chem. Eng. Data, 21(2), Apr. 1976: 194-196.

PIEROTTI, ROBERT A. and LIABASTRE, ALBERT, A., The Structure and Properties of Water Solutions: Completion Report, ERC-0572, Georgia Institute of Technology, Environmental Resources Center, June 1972, avail. NTIS, 113 p.

VARTAK, D. G., et al., Apparatus for the Determination of Dissolved Gases in Nuclear Reactor Coolants (Water), BARC--361, 1968, 17 p.

SAMPLING BIBLIOGRAPHY

Patent 2,245,942 E, FR. 27 September 1974. A Gas Conditioning and Analysis System, General Electric Co., U.S., BUSCH, F. R., 22 p., in French.

Patent 3,472,629, U.S. 14 October 1969. Hydrogen Leak Detection Device, [NASA], [U.S.], ROMMEL, MARJORIE A.

Patent 3,849,539, U.S. 19 November 1974. Method of Oxygen Detection and Removal, Atomic Energy Commission, U.S., COLEMAN, JOHN H., 3 p.

BIRAULT, J., et al., Detection of Small Leaks by Hydrogen Measurements in a Sodium-Heated Steam Generator, ANL--7520(Pt.1), [France], pp.345-73.

BYRON, D. B., Post Ignition Hydrogen Detection System, Phase 2. NASA-CR-98131; R-568-31, Nassau Instrument Co., 31 May 1968, avail. NTIS, 44 p.

CUCCHIARA, O., et al., Kryptonate Hydrogen Detection System. Final Report, NYO--3735-1, 1968, 35 p.

FIKE, R. S., and FRANK, C. W., In-Flame Gas-Solid Interactions for Simultaneous Determination of Iodide and Bromide on the Parts-per-Billion Level. In: Anal. Chem., 50(11), 1978: 1446-1449.

KRUGER, G. B., et al., Leak Detection System Design and Operating Considerations for the US-CRBRP, Energy Research and Development Administration, 1976, avail. NTIS, 23 p.

LEVINE, R. J., A Hydrogen Air Detector Suitable for Use Aboard Spacecraft Final Report, NASA-CR-61536, Nassau Instrument Co., December 1967, NTIS, 58 p.

MACINTYRE, J. R. and NEPPEL, N. C., Gaseous Hydrogen Detection System Final Report, NASA-CR-102608; DOC-70HV031, General Electric Co., 6 April 1970, avail. NTIS, 81 p.

MCPHEETERS, C. C., et al., Design and Performance of Hydrogen Meters for Detecting Water-to-Sodium Leaks in LMFBR Steam Generators, 1971, avail. Argonne National Laboratory, 1 pg.

TRUMBLE, T. M., Description and Analysis of Prototype of a Portable Hydrogen Fire Detector, AFAPL-TR-65-75, Air Force AERO Propulsion Lab, Wright-Patterson AFB, December 1965, avail. NTIS, 49 p.

VISSERS, D. R., A Hydrogen Monitor for Detecting Leaks in LMFBR Steam Generators, 1970, avail. Argonne National Laboratory, 2 p.

WALKER, J. A., and CAMPION, P., A Continuous Monitor for Hydrogen in Gases, TRG-Report-1046, Risley, United Kingdom Atomic Energy Authority, 1965, 6 p.

COMBUSTION BIBLIOGRAPHY

Patent 1, 648, 909 C, DE. 3 February 1977. Gas Detector and Method for Its Fabrication, General Electric Co., U.S., LOH, J.C.Y., 6 p., in German.

Hydrogen-Oxygen Reaction Studies First Quarterly Progress Report, NASA-CR-59415, General Dynamics/Astronautics, October 1964, avail. NTIS, 9 p.

NRC Moves to Make LWR 'Inerting' A Requirement, In: Nuclear News, 19 (15), December 1976: 36.

Research and Technologic Work on Explosives, Explosions, and Flames: Fiscal Year 1967; Information Circular, IC-8387, Bureau of Mines, August 1968, avail. NTIS, 28 p.

ADOMETI, G., Ignition of Gases at Hot Surfaces under Non-steady-state Conditions, Conf-640824--, Pittsburgh, Combustion Institute, 1965, pp. 237-243, International Symnposium on Combustion.

ANDREWS, G. E. and BRADLEY, D., Determination of Burning Velocity by Double Ignition in a Closed Vessel. In: Combust. Flame, 20(1), Feb. 1973: 77-89.

ANTHONY, EDWARD J. and POWELL, MARGARET F., Peak Flammability Limits of Hydrogen Sulfide, Carbon Dioxide, and Air for Upward Propagation. In: Ind. Eng. Chem. Fundam., 18(3), Aug. 1979: 238-240.

AZATYAN, V. V., et al. Combustion and Explosion Physics. Volume 3 Number 1, 1967 (Selected Articles), FTD-HT-23-776-68, Foreign Technology Division Wright-Patterson, 3 February 1979, avail. NTIS, 31 p.

BABUSHOK, V. I., et al. Chain Ignition of Hydrogen at High Degress of Burnup. In: Combust. Explos. Shock Waves, 11(5), Sept.-Oct. 1975: 584-586.

BAEV, V. K., et al. Calculation of Ignition and Combustion of a Hydrogen Jet in Air with Finite Chemical Reaction Rates. In: Acta Astronaut, Russia, U.S.S.R. Acad. of Sci., Novosibirsk, 1(9-10), Sept.-Oct. 1974: 1227-1238.

BAKER, L. A., JR. and FERRARD, C. Jr., Combustible Gas Detection in High-Energy Research Operations, BNL-11620, New York, 12 p.

BALDWIN, R. R., et al., The Self-Inhibition of Gaseous Explosions, AD-614 884, Hull University, 1962, avail. NTIS, 2 p.

BALDWIN, R. R., Kinetics of Hydrogen-Oxygen and Hydrocarbon-Oxygen Reactions; Final Rept., October 61-October 62, AD-640 169, Hull University, October 1962, avail. NTIS, 2 p.

BASCOMBE, K. N., Calculation of Ignition Delays in the Hydrogen-Air System, ERDE-offprint-67/9, Explosives Research and Development Establishment, 1967, avail. NTIS, 12 p.

BEHRENS, K. and SCHNEIDER, H., Initiation of Detonation of Hydrogen-Air Mixtures and Propagation of Shock Waves in the Environment, RS-102-06-6, Ernst-Mach-Institut, 1977, avail. NTIS, 37 p., in German.

BENJAMIN, B. M. and ISBIN, H. S., Recombination of Hydrogen and Oxygen in the Presence of Water Vapor under the Influence of Radiation; Final Report. C00-1032-1, Minnesota University, July 1965, avail. NTIS, 36 p.

BENNETT, J. E. and BLACKMORE, D. R., Rates of Gas-Phase Hydrogen-Atom Recombination at Room Temperature in the Presence of Added Gases, CONF-700870--, Pittsburgh, Combustion Institute, 1971, pp. 51-59, International Symposium on Combustion.

BENOIT, A., Properties of Chapman-Jouquet Detonations in Stoichiometric Hydrogen-Oxygen Mixtures Diluted with Helium and Hydrogen, Interium Technical Report, UTIAS-TN-104; ARL-67,0019, Toronto University, January 1967, avail. NTIS, 141 p.

BLACKMORE, R. D., et al., Inhibition of the Thermal Reaction Between Hydrogen and Oxygen; Final Scientific report, AD-621 216, Manchester College of Science and Technology, 1 March 1965, avail. NTIS, 2 p.

BROSSARD, J., et al., Experimental Study of the Overpressure Generated by the Detonation of Spherical Air-Hydrogen Gaseous Mixtures, FRR SR-155, 1978, avail. NTIS 15 p.

BULEWICZ, E. M. and PADLEY, P. J., Catalytic Effect of Metal Additives on Free Radical Recombination Rates in $H_2 + O_2 + N_2$ Flames, CONF-700870--, Pittsburgh Combustion Institute, 1971, pp. 73-80, International Symposium on Combustion.

CARLSON, L. W., et al., Flame and Detonation Initiation and Propagation in Various Hydrogen-Air Mixtures, With and Without Water Spray, AI-73-29, 1973, avail. NTIS, 45 p.

CHIU, K., et al., A Simplified Version of the Barthel Model for Transverse Wave Spacings in Gaseous Detonation. In: Combustion and Flame, 26, 1976: 353-361, avail. NTIS.

COHEN, A., and LARSEN, J., Explosive Mechanism of the H_2O_2 Reaction Near the Second Ignition Limit, BRL-1386, Ballistic Research Labs, December 1967, avail. NTIS, 35 p.

DALGARNO, A., et al., Recombination Rates of H+ and H-; Final Report. 1 October 65-26, November 1968, GCA-TR-69-1-A, Gca Corp., Gca Technology Division, April 1969, avail. NTIS, 18 p.

D'ARCY, G. P., and CLARK, R. O., Simulation of Air Shocks with Detonation Waves, AD-478-706/5ST, New Mexico University, February 1966, avail. NTIS, 129 p.

DETROIT EDISON CO., Enrico Fermi Atomic Power Plant, Unit 2. Post-LOCA Hydrogen Control System, Docket 50341--77, 1973, 21 p.

DIXON-LEWIS, G., Flame Structure and Flame Reaction Kinetics. VII. Reactions of Traces of Heavy Water, Deuterium, and Carbon Dioxide Added to Rich Hydrogen + Nitrogen + Oxygen Flames, England, University of Leeds, 1972, 26 p.

DIXON-LEWIS, G., and SHEPHERD, I.G., Some Aspects of Ignition by Localized Sources, and of Cylindrical and Spherical Flames, Symp. on Combust., 15th Int. Proc., Tokyo, Jpn, Aug. 25-31, 1974, Pittsburgh, Combust. Inst., 1975, pp. 1483-1492.

DORFMAN, L. M., Combination of Hydrogen Isotopes and Oxygen Initiated by Tritium Beta-Radiation, CONF-540802, New York, Reinhold Publishing Corp., 1955, pp. 578-582, International Symposium on Combustion.

DORR, V. A., and SCHREINDER, H. R., Region of Noncombustion Flammability Limits of Hydrogen-Oxygen Mixtures, Full Scale Combustion and Extinguishing Tests and Screening of Flame-Resistant Materials, Summary report, No. 2, 31 March 67-1, AD-651 583, Ocean Systems Inc., 1 May 1979, avail. NTIS, 211 p.

DOVE, J. E., et al., Computer Studies of Reaction Profiles in Gas Detonations. In: Astronautica Acta, 14, 1969: 521-531, avail. NTIS.

DOVE, J. E., et al., Velocity Deficits and Detonability Limits of Hydrogen-Oxygen Detonations. In: Acta Astronaut, [Russia], 1(3-4), Mar-Apr 1974: 345-359.

EDSE, R. and LAWRENCE, L. R., JR., Detonation Induction Phenomena and Flame Propagation Rates in Low Temperature Hydrogen-Oxygen Mixtures. In: Combustion and Flame, 13(5), October 1969: 479-486, avail. NTIS.

EDSE, RUDOLPH, Ingition, Combustion, Detonation and Quenching of Reactive Mixtures, AD-A024 343/6ST, Ohio State University Research Foundation, November 1975, 125 p.

EDSE, RUDOLPH, et al., Ignition, Combustion, Detonation, and Quenching of Reactive Mixtures, AD-A035 486/OST, Ohio State University Research Foundation, September 1976, avail. NTIS, 80 p.

EGERTON, A. C., Limits of Inflammability, CONF-520901--, Baltimore, Williams and Wilkins Co., 1953, pp. 4-13, International Symposium on Combustion.

FENIMORE, C. P., and JONES, G. W., Radical Recombination and Heat Evolution in H_2O_2 Flames, Pittsburgh, Combustion Institute, 1965, pp. 489-494.

FUJIWARA, T., Spherical Ignition of Oxyhydrogen Behind a Reflected Shock Wave, Symp. on Combust., 15th Int., Aug. 25-31, 1974, Combust. Inst., Pittsburgh, 1975, pp. 1515-1524.

GARDINER, W. C., et al., Elementary Reaction Rates from Post-Induction-Period Profiles in Shock-Initiated Combustion, CONF-720811--, Pittsburgh, Combustion Inst., 1973, pp. 61-75, International Symnposium on Combustion.

GETZINGER, R. W., Shock-Wave Study of Recombination in Near-Stoichiometric Hydrogen--Oxygen Mixtures, CONF-6600802--, Pittsburgh, Combustion Institute, 1967, pp. 117-124, International Symposium on Combustion.

GRACIE, P. S., Strength of Metals Under Rapid Loading: A Survey in Relation to the DIDO 4H5 Liquid-Hydrogen Loop Containment Vessel, AERE-M--1471, 1965, 17 p.

GREER, J. S. and RANKIN, R. L., Limits of Hydrogen-Oxygen-Nitrogen-Steam Mixtures, MSAR-68-109, MSA Research Corp., 1968, avail. NTIS, 43 p.

GRUMER, J., et al., Hydrogen Flare Stalk Diffusion Flames: Low and High Flow Instabilities, Burning Rates, Dilution Limits, Temperatures, and Wind Effects; Report of Investigations, BM-RI-7457, Bureau of Mines, December 1970, avail. NTIS, 39 p.

GUDKOV, V. I., and PONOMAREV, I. A., Nomogram of the Explosiveness of Complex Gas--Air Mixtures. In Russian. In: UGOL, 45(7), 1970: 64-66.

HALSTEAD, C. J., and JENKINS, D. R., Radical Recombination in Rich Premixed Hydrogen/Oxygen Flames, CONF-680701--, Pittsburgh, Combustion Inst., 1969, pp. 979-987, International Symposium (12th) on Combustion, France, July 14-20, 1968.

HEYMACH, G. J., Catalyzed Hydrogen-Air Combustion at Ambient Temperatures: Technical Report, ECOM-3556, Army Electronics Command, March 1972, avail. NTIS, 21 p.

HICKEL, B., Radiolysis of Concentrated Nitrate and Formate Solutions, CEA-R--4046, Paris, Thesis, 1970, in French, 64 p.

HOLMSTEDT, G. S., Upper Limit of Flammability of Hydrogen in Air, Oxygen, and Oxygen-Invert Mixtures at Elevated Pressures. In: Combust. Flame, 17(3), Dec. 1971: 295-301.

HORD, J., How Safe is Hydrogen, CONF-780748--, Chicago, Institute of Gas Technology, 1979, pp. 613-643.

HOWARD, J. B., et al., Kinetics of Carbon Monoxide Oxidation in Post-flame GHases, CONF-720811--, Pittsburgh, Combustion Inst., 1973, pp. 975-986, International Symposium on Combustion.

HOWSON, A. C. and SIMMONS, R. F., First Limit of the Hydrogen + Oxygen Reaction in Vessels Coated with Barium Bromide. In: Transactions of the Faraday Society, 63(534) P+ 6, June 1967: 1385-93, avail. NTIS.

HURLE, I. E., Measurements of Hydrogen-Atom Recombination Rates Behind Shock Waves, CONF-660802--, Pittsburgh, Combustion Institute, 1967, pp. 827-836, International Symposium on Combustion.

JENSEN, D. E., and PADLEY, P. J., Kinetic Studies of Ionization and Recombination Processes of Metallic Addivities in Flames, CONF-660802--, Pittsburgh, Combustion Institute, 1967, pp. 351-358, International Symposium on Combustion.

JOHNSON. J. E., JR., H_2-O_2-NO_x Flammability and Explosibility--a Literature Survey, ICP-1002, Allied Chemical Corp., October 1971, avail. NTIS, 27 p.

KAHN, J. E., et al., Effects of Explosion-Generated Shock Waves in Ducts, Oak Ridge National Lab., 1976, avail. Oak Ridge National Lab., 10 p.

KARIM, G. A., et al., Analytical Study of the Compression Ignition Characteristics of H_2-O_2-N_2 Mixtures in a Reciprocating Engine. In: J. Mech. Eng. Sci., 16(2), Apr. 1974: 88-94.

KARIM, G. A., et al., Investigation of the Ignition Characteristics of H_2-O_2-N_2 Mixtures, Hydrogen Econ. Miami Energy (THEME) Conf., Miami Beach, FL, Mar. 18-20, 1974, New York, 1975, pp. 697-715.

KERKAM, B. F. and DABORA, E. K., The Influence of Water Vapor Addition on Hydrogen-Oxygen Detonations; Technical Rept. no. 1, 06996-1-T, Michigan University, April 1965, avail. NTIS, 2 p.

KERKAN, B. F. and DABORA, E. K., Effect of Water Vapor on H_2-O_2 Detonations; Revised ed., AD-638 313, Michigan Univ., 18 January 1966, avail. NTIS, 2 p.

KRUPININ, V.G. and RUTOVSKLL, V.B., Ignition Conditions for Gases That Are Being Mixed. In Russian. In: Tr. Mosk. Aviats, Inst., SB. Statei, [Russia], 329, 1975: 34-41.

KURZIUS, SHELBY CLARKE. Kinetics of the Branching Step in the Reaction of Hydrogen with Oxygen; Doctoral thesis, AD-635 159, Princeton University, December 1964, avail. NTIS, 2 p.

LEVITT, B. and HORNIG, D.F., The Structure of the Discontinuity in Detonation Waves, TR-2, Princeton University, 15 March 1961, avail. NTIS, 36 p.

LINNETT, J. W. and TOOTAL, C.P., Production of Hydrogen Peroxide in Reacting Mixtures of Hydrogen and Oxygen, CONF-580801--, New York, Academic Press, 1958, pp. 23-26, International Symposium on Combustion.

LITCHFIELD, ELTON L., Freely Expanding Gaseous Detonation Waves Initiated by Electrical Discharges, TR-BUM-32-PBUM-32-P, Princeton Univ. N. J. James Forrestal Research Center, January 1961, avail. NTIS, 6 p.

LOVACHEV, L. A., et al., Kinetics of Hydrogen Oxidation 2. Hydrogen Bromide Both as Inhibitor and Catalyst of Self-Ignition. In: Conbust. Sci. Technol. Moscow, Inst. of Chem. Phys., Acad. of Sci. of the U. S. S. R., 17(3-4), 1977: 143-151.

MACEK, ANDRE J., Flammability Limits: Thermodynamics and Kinetics, NBSIR-76-1076, National Bureau of Standards, Center for Fire Research, May 1976, avail. NTIS, 28 p.

MACPHERSON, A. K., A Preliminary Study of Spherical Detonation-Wave Symmetry in Stoichiometric Hydrogen-Oxygen Mixtures; Technical Note, UTIAS-TN-54, Toronto University, February 1970, avail. NTIS, 15 p.

MARTIN, F. E., Thermal Radiation From Burning Hydrogen Plume, LA-DC-7313 + CONF-651002-6, Los Alamos Scientific Laboratory, 1965, avail. Instrument Society of America, 5 p.

MATHEWS, R. L., Explosion and Detonation Limits for and Oxygen--Hydrogen--Water--Vapor System, KAPL-M--6564, 1966, 54 p.

MELLISH, C. E. and LINNETT, J. W., Influence of Inert Gases on Some Flame Phenonmena, CONF-52091--, Baltimore, Williams and Wilkins, 1953, pp. 407-420, International Symposium on Combustion.

MCELWAIN, D. L. S. and PRICHARD, H. O., Temperature of Diatomic Dissociation and Recombination Reactions, CONF-700870--, Pittsburgh, Combustion Institute, 1971, pp. 37-49; International Symposium on Combustion.

MOORE, J. G., Shock Waves and Transient Loading from Chemical Reactions, EUR--4101, 75-88 pp.

MOORE, J. G. and GILBY, E. V., A Review of the Problems Arising From the Combustion of Hydrogen in a Water Reactor Containment, AHSB(S)R-101, United Kingdom Atomic Energy Authority, Safeguards Division, 1966, avail. Clearinghouse for Federal Scientific and Technical Information, 48 p.

MUZYCZUK, J., Improved Graphical Method for Determination of Explosibility Parameters of Gas Mixtures. In: Pr. Gl. Inst. Gorn., Komun., [Poland], 653, 1975, in Polish.

NEER, MICHAEL, E., Autiognition of Flowing Hydrogen-Air Mixtures. In: AIAA J., 13(7), Jul. 1975: 924-928.

NETTLETON, M.A. and YOUNG, D.M., Propagation of Flames in Gases in Large Diameter Pipes. In: Combust. Inst. Eur. Symp., Pap., Univ. of Sheffield, Engl., Sept. 16-21, 1973, New York, Acad. Press Inc., 1973: 717-722.

NORTHERN INDIANA PUBLIC SERVICE COMPANY, Response to Question 5.3-1 Containment Building Air Mixing, 1971, avail. NTIS. Docket 50-367-15.

NORTHRUP, C. JM., et al., Considerations When Designing, Assembling, and Operating a Gaseous Hydrogen Pressure System, SC-DR--720593, Albuquerque, NM, Sandia Labs, 1972, 34 p.

OLSEN, H. L., et al., Propagation of Incipient Spark-Ignited Flames in Hydrogen--Air and Propane--Air Mixtures, CONF-52091--, Baltimore, Williams and Wilkins, 1953, pp. 144-148, International Symposium on Combustion.

OMATA, I., Analysis of Gas Layering and Flammability in the Containment Vessel of a High-Temperature Gas-Cooled Reactor Following Depressurization. BNL-NUREG-50622, Energy Research and Development Administration, March 1977, avail NTIS, 73 p.

PADLEY, P.J., and SUGDEN, T. M., Some Observations on the Production and Recombination of Ions and Electrons from Metallic Additives in Hydrogen and Hydrocarbon Flames, pp. 164-179, International Symposium on Combustion.

PAWEL, D., et al., The Influence of Initial Temperature on the Limits of Detonability, Final Report. 1 June 67-30 June 1969, Goettingen University, 30 June 1969, avail. NTIS, 71 p.

PENLAND, J. R., Explosion Suppression By Room Inerting, LA-DC-8592 + CONF-670201-2, Los Alamos Scientific Lab., 1967, avail. Clearinghouse for Federal Scientific and Technical Information, 5 p.

PETERSEN, PRISCILLA, C., et al., The Ignition, Combustion and Radiant Intensity of Spherical Clouds of Hydrogen, ARAP-291, Aeronautical Research Associates of Princeton, Inc., April 1977, avail. NTIS, 38 p.

POPTER, J. B., Analysis of Hydrogen Explosion Hazards, DP-1295, Du Pont De Nemours (E.I.) and Co., July 1972, avail. NTIS, 39 p.

ROBERTS, R. W., et al., Investigation of Catalytic Ignition of Oxygen/Hydrogen Systems; Final Report, 15 June 64-15, October 1965, Rocketdyne, December 1965, avail. NTIS, 217 p.

SAL MANDRA, G. D., Formation of the Gas Flow Before the Flame Front, FTD-HT-23-1233-67, Foreign Technology Division Wright-Patterson AFB Ohio, 14 December 1967, avail. NTIS, 10 p.

SAMUEL, W. A., and GREER, J. S., Investigation of Methods for Arresting Detonations in Gas Mixtures, MSAR-67-187, MSA Research Corp., 1967, avail. NTIS, 61 p.

SCHOTT, G. L., Detonation Spin in Driven Shock Waves in a Dilute Exothermic Mixture, LA-DC-8814, New Mexico, 6 p.

SCHOTT, G. L., Chain Branching and Initiation Rates Measured by Spatially Integrated Light Emission During Reflected Shock Wave Ignition, LA-DC--9245, New Mexico, 22 p.

SCHOTT, G. L., and BIRD, P. F., Kinetic Studies of Hydroxyl Radicals in Shock Waves. IV. Recombination Rates in Rich Hydrogen--Oxygen Mixtures. In: Am. Chem. Soc. Div. Fuel Chem., Prepr., 8(2), 1964: 113-121.

SCHUSTER, F., Air/oxygen Content and Ignitability of (gas + Air + Inert Gas) Mixtures. In German. In: Gas-Wasserfach, gas-Erdgas, 120(1), 1979: 44-48.

SHAPIRO, Z. M., and MOFFETTE, T. R., Hydrogen Flammability Data and Application to PWR Loss-of-Coolant Accident, WAPD-SC-545, Westinghouse Electric Corp., 1957, 23 p.

SHUI, VEN H., and APPLETON, JOHN P., Gas Phase Recombination of Hydrogen. A Comparison Between Theory and Experiment, PUB-71-4, AD-735-996, Massachusetts Institute of Technology, February 1971, avail. NTIS, 26 p.

SHUI, V. H., et al., Three-body Recombination and Dissociation of Diatomic Molecules: A Comparison Between Theory and Experiment, CONF-700870--, Pittsburgh, Combustion Institute, 1971, pp. 21-35, International Symposium on Combustion.

SHUI, VLN H., Thermal Dissociation and Recombination of Hydrogen According to the Reactions H_2 + H + H + H + H. In: Massachusetts Institute of Technology, 72-11, Oct. 1972, 48 p.

SIEGLER, M., and MOORE, G. E., Flame Recombination of Oxygen and Hydrogen, General Electric Company. In: Chem. Eng. Progr., Symp. Series, 66(104), 1970: 1-11.

SLACK, M., and GRILLO, A., Investigation of Hydrogen-Air Ignition sensitized by Nitric Oxide and by Nitrogen Dioxide, Final Report, N78-10233/2ST, Grumman Aerospace Corp., October 1977, avail. NTIS, 43 p.

SKINNER, G. B., et al., Chemical Inhibition of the Hydrogen-Oxygen Reaction, ASD-TDR- 62-1042, Wright-Patterson Air Force Base, 1962, NTIS, 104 p.

SMITH, E. J., and KESTEN, A. S., Computer Program Manual Transient Model of Hydrogen/Oxygen Reactor, NASA-CR-120800, United Aircraft Corp., February 1971, avail. NTIS, 108 p.

STRAUSS, W. A. and SCOTT, JAMES N., Experimental Investigation of the Detonation Properties of Hydrogen-Oxygen and Hydrogen-Nitric Oxide Mixtures at Initial Pressures up to 40 Atmospheres. In: Combustion and Flame, 19, 1972: 141-143, avail. NTIS.

SURETTE, ROBERT GEORGE, and GERSTEIN, MELVIN. Unsteady Shock Wave Initiation of a Detonation Wave in a Compressible Gas Mixture, AD-A024 358/4ST, University of Southern California. Department of Mechanical Engineering, December 1975, avail. NTIS, 216 p.

TERAO, KUNIO, Explosion Limits of Hydrogen-Oxygen Mixture As A Stochastic Phenomenon. In: Jpn. J. Appl. Phys., Japan, 16(1), Jan. 1977: 29-38.

TRENT, D. S., Mixing of Buoyant Combustible Gases in BWR Containment Systems, BNWL-B-298, Battelle Pacific Northwest Labs., 1973, avail. NTIS, 24 p.

URTIEW, P. A., et al., Dynamics of The Generation of Pressure Waves by Accelerating Flames, CONF-640824--, Pittsburgh, Combustion Institute, 1965, pp. 797-804, International Symposium on Combustion.

VAN METER, R. A., et al., Hydrogen Safety. Annual Report for the Period January 1-- December 31, 1964 (Progress Report No. 4), TID/SNA-- 1636, NTIS, 1965, 48 pp.

VASUDEVAN, B., Pressure Measurements at the Focus of Combustion-Driven Implosions, UTIAS-TN-209: CN-ISSN-0082-5263, Toronto Univ. Inst. for Aerospace Studies, April 1977, avail. NTIS, 9[illegible] p.

WALKER, DARRELL, et al., Investigation of the Ignition Properties of Flowing Combustible Gas Mixtures, AD-863 260/6ST, Ohio State University Columbus Aeronautical and Astronautical Research lab., September 1969, avail. NTIS, 60 p.

WAKEFIELD, C. B., et al., Chemical Kinetics of The Shock-Integrated Combustion of Hydrogen at High Pressure and Low Temperatures. In: Jnl. of Chemical Physics, 50(1), 1 January 1969: 325-332, avail. NTIS.

WIERMAN, R. W., Experimental Study of Hydrogen Jet Ignition and Extinguishment, HEDL-TME 78-80, 1979, Hanford Engineering Development Lab., 1979, avail. NTIS, 104 p.

WHITTINGHAM, A. C., Review of Previous Work on the Liquid Sodium--Hydrogen--Oxygen Systems, CFR/BMWP/P-(73) 135, Central Electricity Generating Board, February 1973, avail. NTIS, 32 p.

WHITE, D. R., and MOORE, G. E., Structures of Gaseous Detonation. IV. Induction Zone Studies in H_2O_2 and CO--O_2 Mixtures, Pittsburgh, Combustion Institute, 1965, pp. 785-795.

WISE, H., and ROSSER, W. A., Homogeneous and Heterogeneous Reactions of Flame Intermediates, New York, Academic Press, Inc., 1963, pp. 733-746.

WOLFSON, BERNARD, T., The Influence of Inert and Chemically Reactive Additives on the Mechanism of Detonation in Gaseous Mixtures over Wide Ranges of Initial Pressure and Additive Concentration, AD-450801/6ST, Office of Aerospace Research, 1964, avail. NTIS, 69 p.

ZALOSH, R. G., Comparative Analysis of Hydrogen Fire and Explosion Incidents. Quarterly Report No. 1, September 1, 1977--November 30, 1977, COO/4442-1, Factory Mutual Research Corp., December 1977, avail. NTIS, 35 p.

ZALOSH, R. G. and SHORT, T. P., Comparative Analysis of Hydrogen Fire and Explosion Incidents: Quarterly Report No. 2, December 1, 1977--February 28, 1978, ERDA/080500, Factory Mutual Research Corp., March 1978, avail. NTIS, 34 p.

ZALOSH, R. G. and SHORT, T. P., Comparative Analysis of Hydrogen Fire and Explosion Incidents. Progress Report No. 3, March 1, 1978-June 30, 1978. Factory Mutual Research Corp., July 1978, avail. NTIS, 36 p.

RECOMBINER BIBLIOGRAPHY

Patent 2,008,218 C, DE. 30 September 1976. Equipment for Catalytic Recombination to Water of Hydrogen and Oxygen Gases Produced During the Operation of Electric Accumulators, Accumulatorenwerk Hoppecke Carl Zoellner und Sohn, DE, SASSMANNSCHAUSEN, G. and LAHME, N., 4 p., in German.

Patent 2,363,844 A, DE. 26 June 1975. System Reduce the Possible Dangers of a Reactor Core Meltdown, Geselschaft Fuer Kernforschung MBH, DE, 7 p., in German

Patent 2,451,438 A, DE. 6 May 1976. Recombinator of Hydrogen and Oxygen, DEcatox G.M.B.H., DE STEJSKAL, J., et al., 7 p., in German.

Patent 2,455,744 A, DE. 26 May 1976. Equipment for the Catalytic Recombination of Hydrogen and Oxygen Gases Produced in Accumulators, Accumulatorenfabriken Wilhelm Hagen A. G., DE, NANN, E., 17 p., in German.

Patent 1971-07,581, JP. 25 Feb. 1971. Catalyst for the Reaction of Hydrogen and Oxygen, Japan Storage Battery Co., Ltd., JP TSUBOTA, S., 3 p.

Patent 1975-30,000 A, JP. 31 May 1973. Device for Recombining Degasses Gases in Nuclear Reactor, Nippon Koran K.K. [JP], MIZUNO, A. et al., 5 p., in Japanese.

Patent 3,755,075, U.S. 28 Aug. 1973. Condenser-Type Gas Combiner, North American Rockwell Corp., U.S., HENRIE, J. O.

Patent 4,119,706, U.S. 10 Oct. 1978. Method of Catalytically Recombining Radiolytic Hydrogen and Radiolytic Oxyten, Engelhard Minerals and Chemicals Corp., U.S., ROGERS, W. M., 10 p.

Appendix A to Resar-35: Combustible Gas Control in Containment, WCAP-8660, Westinghouse Electric Corp., 1975, avail. NRC Public Document Room, 33 p.

LATEST LITERATURE ON HYDROGEN TECHNOLOGY, Japan, 1975, pp. 163-235, in Japanese.

WESTINGHOUSE ELECTRIC CORP., Appendix A to Resar-35: Combustible Gas control in Containment, WCAP-8660, 1975, avail. NRC Public Document Room, 33 p.

ARMSTRONG, W. E., et al., Development of Hydrogen-Oxygen Catalysts Final Report, Aug. 1965-July 1966, NASA-CR-7211, Shell Development Co., July 1966, avail. NTIS, 67 p.

BROWN, GILBERT M., et al., Investigation of Catalytic Recombination of Radiolytic Oxygen and Hydrogen; Quarterly Progress Report No. 1, October-December 1963, EURAEC-991, General Nuclear Engineering Corp., 10 January 1964, avail. NTIS, 54 p.

BROWN, GILBERT M. and SAWYER, THOMAS C., Investigation of Catalytic Recombination of Radiolytic Oxygen and Hydrogen; Quarterly Report, July-September 1964, EURAEC-1233, Combustion Engineering, Inc., 1964, avail. NTIS, 37 p.

HENRIE, J. O. and STONE, L. R., Thermal Hydrogen Recombiner System for Water-Cooled Reactors, AI-75-2 (Rev. 1), Atomics International, 1975, avail. NRC Public Document Room, 52 p.

HENRIE, J. O., et al., Post-LOCA Hydrogen Recombiner System for LWR Nuclear Plants In: Proc. Am. Power Conf., Vol. 36, Chicago, American Power Conference, 1974, pp. 219-225.

HOMSY, R. V. and GLATRON, C. A., Review of Literature on Catalytic Recombination of Hydrogen--Oxygen, ORNL/MIT--55, 1968, 25 p.

ITOH, H. and FUNAKOSHI, T., Radioactive Gaseous Waste Processing Package in Nuclear Power Plants. Catalytic Hydrogen Recombiner. In Japanese. In: Mitsubishi Juko Giho, 13(3), 1976: 404-413.

JAHN, H., Hydrogen Production in Containment After a Loss-of-Coolant Accident in Light-Water Reactors, MRR-117, Technische Universitaet Meunchen, March 1973, avail. NTIS, 58 p., in German.

JOHNSON, R. J., Hydrogen-Oxygen Catalytic Ignition and Thruster Investigation, Volume 1 Catalytic Ignition and Low Pressure Thruster Evaluations; Final Report, June 1970-December 1971, NASA-CR-120869; TRW-14549-6001-RO-00, TRW Systems Group, November 1972, avail. NTIS, 214 p.

JOHNSON, R. J., et al., Hydrogen-Oxygen Catalytic Ignition and Thruster Investigation. Volume 2 High Pressure Thruster Evaluations. Final Report, March-December 1971, NASA-CR-120870; TRW-14549-6001-RO-00, TRW Systems Corp., 1972, avail. NTIS, 176 p.

LOPATA, JAMES R., Control of Containment H_2 Levels Evolved from Zinc Primers During a LOCA. In: Power Eng. Illinois, 78(11), Nov. 1974: 48-51.

MIZUNO, A. and TANI, J., Catalytic Recombination for Oxygen and Hydrogen in Off-Gas of Nuclear Power Plants. In: Koatsu Gasu, 9(2), April 1972: 486-492.

O'MARA, R. L., Hydrogen Recycle. In: Trans. Amer. Nucl. Soc., [Boston], 13, 1970: 20-1.

ROEDDER, PETER and GEISER, HEINZ, Formation of Hydrogen During Core Melt Accidents in Nuclear Power Plants with Light Water Reactors (Wasserstoffentstehung Bei Coreschmelzunfaellen in Kernkraft-Werken Mit Leichtwasserreaktoren). In: Kerntechnik, Germany, 19(11), Nov. 1977: 473-477.

ROGERS, W. M. and LECHELT, R. H., Catalytic Recombiners for Boiling Water Reactors. In: Nucl. Eng. Int., 18(208), 1973: 711-715.

SCHUTTE, A., et al., Recombination of Atomic Hydrogen on Low Temperature Surfaces. In: J. Chem. Phys., 64(10), 1976: 4135-4142.

WIERMAN, R. W., Hydrogen Jet Recombination under Postulated LMFBR Accident Conditions, CONF-770611-27, Energy Research and Development Administration, 1977, avail. NTIS, 11 p.

WILSON, J. F., Electrical Hydrogen Recombiner for Water Reactor Containments, WCAP-7820, Westinghouse Nuclear Energy Systems, 1971, avail. NRC Public Document Room, 25 p.

WILSON, J. F., Electric Hydrogen Recombiner for PWR Containments, WCAP-7820 (Suppl. 1), Westinghouse Nuclear Energy Systems, 1972, NRC Public Document Room, 50 p.

WILSON, J. F., Electric Hydrogen Recombiner for PWR Containments-Equipment Qualification Report, WCAP-7820 (Suppl. 2), Westinghouse Electric Corporation, 1973, avail. NRC Public Document Room, 50 p.

WILSON, J. F., Electric Hydrogen Recombiner for PWR Containments WCAP-7920 (Suppl. 4), Westinghouse Electric Corporation, 1974, avail. NRC Public Document room, 12 p.

WILSON, J. F., Electric Hydrogen Recombiner Special Tests, WCAP-7820, Suppl. 5, Westinghouse Electric Corp., 1975, avail. NRC Public Document room, 50 p.

WILSON, J. F., Electric Hydrogen Recombiners, IEEE 323-1974 Qualification, WCAP-7820 (Supp. 6), Westinghouse Electric Corp., 1976, avail. NRC Public Document Room, 10 p.

WILSON, J. F., Electric Hydrogen Recombiner LWR Containments Supplemental Test Number 2, WCAP-7820 (Supp. 7), Westinghouse Electric Corp., 1977, avail. NRC Public Document Room, 18 p.

MISCELLANEOUS

Patent 2,633,113 A, DE. 26 January 1978. Method of Avoiding Hazards Resulting from Accidents in Nuclear Reactors, Kernforschungszentrum, Karlsruhe G.M.B.H., DE, DORNER, S. et al., 7 p., in German.

Utility Model, 2,146,346, DE. 22 March 1973. Hydrogen Diffusion Seal for Nuclear Reactor Fuel Rods. Siemens, A. G., Berlin and Meunchen, DE.

Patent 668,994, FR. 31 Dec. 1928, Hydrogen, Imperial Chemical Industries, Ltd.

Patent 311,299 GB. 31 January 1928. Purifying Hydrogen, Imperial Chemical Industries, Ltd., GORDON, K.

Patent 3,630,778, U.S. 28 Dec. 1971. Recombining Hydrogen and Oxygen in a Sealed Battery and Controlling Recombination of Catalytic Surfaces, Koehler Manufacturing Co., U.S., KREIDEL, E. L., and SHOOTER, D., 12 p.

Patent 3,691,084, U.S., 12 September 1972. Improved Base-Borate Reactor Safety Spray Solution for Radiolytic Hydrogen Suppression, ZITTEL, H. E., et al., avail. U. S. Patent Office.

AEC Fuels and Materials Development Program Progress Report No. 71, General Electric, 1967, 143 p.

ARGONNE NATIONAL LABORATORY, Chemical and Associated Energy-Transfer Problems in Reactor Safety, ANL-7115, 1965, 3 p.

BATTELLE-NORTHWEST. Sodium Analyses, BNWL--1200-1, Richland, WA, Pacific Northwest Lab., 4. 1-30 p.

BATTELLE PACIFIC NORTHWEST LABS., AEC Reactor Development and Technology Programs. Technical Activities Quarterly Report, April--June 1971. BNWL--1522-3, Richland, WA, 1971, 61 p.

COMMONWEALTH EDISON COMPANY, Hydrogen Flammability Control System in a Boiling Water Reactor (Special Report 14, Dresden 3), 1971, avail. NRC Public Document Room, 47 p.

ASTY, M. and LEMARIE, P. H., Quenching Effect in Gadolinium: Influence of Hydrogen. In: Phys. Status Solidi (4), France, 2192), 1974: 457-461.

ATKINS, D. F., Hydrogen In SNAP Systems, NAA-SR--11164, 1965, 82 p.

BAKER, L., et al., U.S. Reactor Containment Experience-A Handbook of Current Practice and Analysis, Design, Construction, Test, and Operation. Chapter 5--Energy Sources, ORNL-NSIC-5, Oak Ridge National Laboratory, Argonne Natonal Laboratory, 1965, 145 p.

CARAS, GUS J., Hazards Due to Hydrogen Aboard A Space Vehicle, RSIC-291, Redstone Scientific Information Center, September 1964, avail. NTIS, 26 p.

CARAS, C. J., Prevention Detection, and Suppression of Hydrogen Explosions in Aerospace Vehicles, RSIC-486, Redstone Scientific Information Center, 31 March 1966, avail. NTIS, 2 p.

COTTRELL, WM. B., ORNL Nuclear Safety Research and Development Program Bimonthly Report for July-August 1970, ORNL-TM-3122, Oak Ridge National Lab., October 1970, NTIS, 152 p.

CREWE, ALBERT V., Reactor Development Program Progress Report September 1964, ANL-6944, Argonne, Illinois, Argonne National Laboratory, 1964, 89 p.

CREWE, ALBERT V., Reactor Development Program Progress Report November 1964, ANL-6977, Argonne, Illinois, Argonne National Laboratory, 1964, 93 p.

DANNO, A., Chemical Nuclear Reactor and Economy of Hydrogen. In: Kagaku Keizai, Japan, 21(9), 1974: 40-49.

DEACKOFF, L. P., et al. Post LOCA-DBA Containment Hydrogen Generation, Methods for Calculating and Controlling Hydrogen Accumulation, Stone and Webster Engineering Corporation, 1970, avail. L. P. Deackoff, Stone and Webster Engineering Corporation, 2 p.

DIETZ, K. A., Quarterly Technical Report Step Project April 1965-June 1965, IDO-17145, TID-4500, Idaho, U.S. Atomic Energy Commission, 1966, 104 p.

FLETCHER, W. D., et al., Post-LOCA Hydrogen Generation in PWR Containments. In: Nuclear Technology, 10(4), April 1971: 420-427.

HITCHCOCK, D. R., et al., Sulfur Isotope Studies of Biogenic Sulfur Emissions at Wallops Island, Virginia. ERT-P-2058, Washington, DC, [National Science Foundation], 1978, 204 p.

KAZANJIAN, A. R., Radiation Stability of a Hydrogen Getter Material (DPPEE), ERDA/360605, Energy Research and Development Administration, 18 October 1976, avail. NTIS, 8 p.

KUBASCHEWSKI, O., 4. Diffusion. Vienna, IAEA, 1976, pp. 263-268.

LITCHFIELD, E. G., and PERLEE, H. E., Fire and Explosion Hazards of Flight Vehicle Combustibles; Final Report for 2 January 64-2 January 1965, AD-614 694, Bureau of Mines, March 1965, avail. NTIS, 2 p.

LOPATA, J. R., Control of Containment H2 Levels Evolved from Zinc Primers During a LOCA. In: Power Engineering, 78(11), November 1974: 48-51.

MORRISON, D. L., et al., An Evaluation of the Applicability of Existing Data to the Analytical Description of a Nuclear Reactor, BMI-1910, Battelle Columbus Labs., 1971, avail. NTIS, 25 p.

NORTHRUP, C. J. M. JR., Thermodynamics of the Uranium , , Phases-Hydrogen System, Amsterdam, North-Holland, 1976, pp. 109-114, International Conference on Plutonium and Other Actinides.

POMEROY, B. D., et al., Comparative Study and Evaluation of Advanced-Cycle Systems. Final Report. New York, General Electric Co., Feb. 1978, 231 p.

PREUSS, H. J., Reactor Safety Estimation of the H_2 Evolution From the Reacton Between Concrete and Core Melt, BMFT RS 237 + GERR SR-271, Kraftwerk Union, 1978, avail. NTIS, 175 p., in German.

REPKE, W., Nuclear Power Stations - Technology and Insurance. 7th Allianz Technical Colloquium on the 4th December, 1973 in Munich, AED-CONF--73-687-005, Germany, Allianz, 1974, 33-38 p.

TSINMAN, A. I., et al., Corrosion-Electrochemical Behavior of Metals and Alloys in Acetic Acid Solution and in Concentrated Acetic Acid at Increased Temperatures; In: Prot. Met., USSR, 10(6), 1974: 617-622.

TAXELIUS, T. G., Spert Project. annual Report, October 1968--September 1969, IN--1370, [Idaho Falls], 1970, 211 p.

VOGEL, R. C., et al., Chemical Engineering Division. Semiannual Report January-June 1964, ANL-6900, Argonne Illinois, Argonne National Laboratory, 1064, 269 p.

ZALOSH, R. G., and SHORT, T. P., Compilation and Analysis of Hydrogen Accident Reports, COO-4442-4, Factory Mutual Research Corp., 1978, avail. NTIS, 135 p.

Distribution:

US Nuclear Regulatory Commission
(400 copies for R3)
Division of Document Control
Distribution Services Branch
7920 Norfolk Avenue
Bethesda, MD 20014

US Nuclear Regulatory Commission (26)
Office of Nuclear Regulatory Research
Washington, DC 20555
Attn: R. DiSalvo
S. Fabic
D. A. Hcatson (20)
C. E. Johnson
C. Z. Serpan
R. R. Sherry
L. H. Sullivan

US Nuclear Regulatory Commission (11)
Office of Nuclear Reactor Regulation
Washington, DC 20555
Attn: W. R. Butler
C. Tinkler
S. S. Hanauer
N. Lauben
J. K. Long
A. R. Marchese
R. J. Mattson
J. F. Meyer
W. C. Milstead
D. F. Ross
T. P. Speis

Loren B. Thompson
EPRI
3412 Hillview Ave.
Palo Alto, CA 94303

Larry E. Hochreiter
Westinghouse Corp.
Nuclear Energy Systems
P. O. Box 350
Pittsburgh, PA 15230

Ed Forest
GPU Service Corp.
100 Interpace Parkway
Parsipanny, NY 07054

Robert A. Bari
Brookhaven National Laboratory
Upton, NY 11973

Peter Cybulskis
Battelle Columbus Laboratories
505 King Ave.
Columbus, Ohio 43201

Nancy B. Willoughby
Bechtel Power Corp.
15740 Shady Grove Rd.
Gaithersburg, MD 20760

D. H. Walker
Offshore Power System
8000 Arlington Expressway
Box 8000
Jacksonville, FL 32211

P. B. Bieniarz and
O. R. Green (2)
Energy, Inc.
300 San Mateo NE
Albuquerque, NM 87108

K. Niyogi
United Engineers
30 S. 17th St.
Philadelphia, PA 19101

J. J. Wilder
Tennessee Valley Authority
503 Power Bldg.
Chattanooga, TENN 37401

M. L. Stevenson
Los Alamos Scientific Laboratory
P. O. Box 1663
Los Alamos, NM 87545

Dr. M. Peehs/Dr. K. Hassmann (2)
Kraftwerk Union
Hammerbacherstrasse 12+14
Postfach 3220
D-3520 Erlangen 2
Federal Republic of Germany

Dr. J. P. Hosemann/
Dr. S. Hagen (2)
Gesellschaft für Kernforschung
75 Karlsruhe
Postfach 3640
Federal Republic of Germany

Mr. Richard Owen
Westinghouse Hanford Co.
Building 221T-HE
200 West Area
Richland, Washington 99352

Dr. H. Karwat
Technische Universitaet Muenchen
D-8046 Garching
Federal Republic of Germany

Prof. F. Mayinger
Technische Universitaet Hannover
3000 Hannover 1
Federal Republic of Germany

Eric Ahlstroem/Wiktor Frid
Swedish State Power Board
El-Och Vaermeteknik
Sweden

Dr. M. V. Banaschik
Gesellschaft fuer Reaktorsicherheit (GRS)
Postfach 101650
Glockengasse 2
5000 Koeln 1
Federal Republic of Germany

400 C. Winter
2165 J. E. Gover
2510 D. H. Anderson
2513 J. E. Kennedy
2513 P. L. Stanton
2514 B. H. VanDomelen
2514 D. E. Mitchell
2516 W. G. Perkins
4210 J. B. Gerardo
4218 J. K. Rice
4400 A. W. Snyder
4410 D. J. McCloskey
4414 A. S. Benjamin
4414 W. B. Murfin
4420 J. V. Walker
4421 R. L. Coats
4422 D. A. Powers
4440 G. R. Otey
4441 M. Berman (30)
4441 R. K. Cole
4441 M. L. Corradini
4441 J. C. Cummings
4441 J. F. Muir
4441 M. P. Sherman
4441 G. G. Weigand
4442 W. A. VonRiesemann
4443 D. A. Dahlgren
4443 J. L. Sprung
4444 S. L. Thompson
4444 L. D. Buxton
4444 R. K. Byers
4445 L. O. Cropp
5130 G. A. Samara
5131 B. Morosin
5131 W. B. Benedick
5510 D. B. Hayes
5512 M. R. Baer
5513 D. W. Larson
5520 T. B. Lane
5521 L. W. Davison
5810 R. G. Kepler
5811 L. A. Harrah
5820 R. E. Whan
5830 M. J. Davis
5836 J. L. Ledman
5840 N. J. Magnani
5846 E. K. Beauchamp
8300 B. F. Murphey
8310 D. M. Shuster
8320 R. Rinne
8331 R. J. Kee
8340 W. Bauer
8350 D. Hartley
8266 E. A. Aas
3141 T. L. Werner (5)
3151 W. L. Garner (3)
3154-3 R. P. Campbell (25)
(For NRC distribution to NTIS)